

SYNTHESIS, ELECTROCHEMICAL CHARACTERIZATION  
AND APPLICATIONS OF ELECTROACTIVE POLYMERS

by

Peter Phung Minh Hoang

B.Eng., Tokyo Institute of Technology (Japan), 1977

M.Eng., Tokyo Institute of Technology (Japan), 1979

A THESIS SUBMITTED IN PARTIAL FULFILLMENT  
OF THE REQUIREMENTS FOR THE DEGREE OF  
DOCTOR OF PHILOSOPHY  
in the Department  
of  
Chemistry

© Peter Phung Minh Hoang  
SIMON FRASER UNIVERSITY

July 1985

All rights reserved. This thesis may not be  
reproduced in whole or in part, by photocopy  
or other means, without permission of the author.

APPROVAL

Name: Peter Phung Minh Hoang  
Degree: Doctor of Philosophy  
Title of Thesis: Synthesis, Electrochemical Characterization  
and Applications of Electroactive Polymers

Examining Committee:

Chairman: Dr. F.W.B. Einstein

Dr. B.L. Funt  
Senior Supervisor

Dr. Y.L. Chow

Dr. W.R. Richards

Dr. A.G. Sherwood

Dr. M.M. Baizer  
External Examiner  
Professor,  
Department of Chemistry,  
University of California at Santa Barbara  
California

Date Approved: July 30, 1985

PARTIAL COPYRIGHT LICENSE

I hereby grant to Simon Fraser University the right to lend my thesis, project or extended essay (the title of which is shown below) to users of the Simon Fraser University Library, and to make partial or single copies only for such users or in response to a request from the library of any other university, or other educational institution, on its own behalf or for one of its users. I further agree that permission for multiple copying of this work for scholarly purposes may be granted by me or the Dean of Graduate Studies. It is understood that copying or publication of this work for financial gain shall not be allowed without my written permission.

Title of Thesis/Project/Extended Essay

"Synthesis, Electrochemical Characterization and Applications of

Electroactive Polymers"

---

---

---

Author:

(signature)

Peter Phung M. Hoang

(name)

Aug. 9, 1985

(date)

ABSTRACT

Substituent groups which are easily oxidized or reduced can be incorporated into a polymer chain to form an electroactive polymer. The chain imposes a geometrical limitation to the movement of these groups and provides a locus for neighboring group interactions. This work explores the effect of chain constraint on the ability of individual substituent groups to undergo electrochemical change in solution and in thin films.

The electrochemical behavior of several electroactive polymer systems in solution was investigated. The effect of chain length and of neighboring group interactions was determined by controlling the composition of copolymers with pendant electroactive groups. For these studies, poly[p-(9,10-anthraquinone-2-carbonyl)styrene]-co-styrene (PAQ), poly(4-vinylbenzophenone) (PVBP), poly(vinyl-p-benzoquinone) (PVBQ) and copolymers with styrene (PVBP-St and PVBQ-St) were synthesized. Voltammetric studies of polymer solutions revealed that in the benzophenone and anthraquinone polymer systems, the electroactive groups behaved independently and the current was limited only by the low diffusion rate of the polymer molecules. Diffusion parameters were evaluated from voltammetric curves and agreed with values obtained by viscometry. A correlation between the limiting current and molecular weight was derived and verified, indicating a method of determining polymer molecular weights by voltammetric techniques. In the PVBQ polymers, reversible behavior was found only when the electroactive groups

were separated by several styrene units on the chain.

The electroactive polymers were coated onto Pt electrodes to form polymer-modified electrodes and the electrocatalytic properties of these were investigated. The homogeneous electrocatalytic reduction of polychlorinated benzenes and biphenyls, with and without benzophenone and anthracene as mediators, was selected as a model system for the corresponding heterogeneous reaction on modified electrodes. The efficiency of the catalytic reduction was related to the difference in redox potential of substrates and mediators.

The modified electrodes exhibit electrochemical response analogous to that found in the solution studies. The effect of film thickness and scan rate, and the kinetics of charge transport in the coatings were investigated. A profound effect of solvent on the properties of the film is attributed to a variation in permeability due to changes in chain configuration. The application of PVBP films in electrocatalytic reduction of polychlorinated compounds, and of PAQ films in the reduction of oxygen is described.

TO MY PARENTS.

## ACKNOWLEDGEMENTS

I wish to offer my thanks to Dr. B. L. Funt for his supervision throughout the course of this work.

Thanks are also due to Drs. L. C. Hsu and J. P. Martenot, and Mr. J. V. Landa for helpful comments and discussions.

I would like to express my deep appreciation to Messrs. S. V. Lowen, G. H. Fritzke, S. Holdcroft and W. P. Kastelic, and Ms. D. L. Darling for assistance in various tasks such as computation, experimental work and proofreading the thesis.

The friendship and help of various members of the Department of Chemistry, and the technical assistance of the personnel of the Glassblowing, Electronics, Machine and Physics Shops are gratefully acknowledged.

I am also grateful to Simon Fraser University for providing me with scholarships for financial support.

Finally, I would like to thank my sister, Thu Hoang, who endured the typing of the manuscript.

ABBREVIATIONS AND GLOSSARY OF FREQUENTLY-USED TERMS

BP	Benzophenone
PVBP	Polyvinylbenzophenone
PVBP-St	Polyvinylbenzophenone-co-Styrene
BQ	p-Benzoquinone
PVBQ	Poly(p-Vinylbenzoquinone)
PVBQ-St	Poly(p-Vinylbenzoquinone)-co-Styrene
MeBQ	Methyl-1,4-Benzoquinone
VBEH	Vinylbis(1-Ethoxyethyl)hydroquinone
EBAQ	2-(p-Ethylbenzoyl)-9,10-Anthraquinone
PAQ	Poly-[p-(9,10-Anthraquinone-2-Carbonyl)styrene]-co-Styrene
PCB's	Polychlorinated Biphenyls
DMSO	Dimethylsulfoxide
DMF	Dimethylformamide
TEAP	Tetraethylammonium Perchlorate
RDE	Rotating Disk Electrode
$\bar{M}_n$	Number Average Molecular Weight
$\overline{DP}_n$	Number Average Degree of Polymerization
$E_{pc}$	Cathodic Peak Potential
$E_{pa}$	Anodic Peak Potential
$\Delta E$	1) Peak Separation Potential 2) Difference in Peak Potentials of Mediators and Substrates
$E^{\circ'}$	Formal Potential
$E_{1/2}$	Half-Wave Potential



$i_{pc}$	Cathodic Peak Current
$i_{pa}$	Anodic Peak Current
$i_l$	Limiting Current
$n$	Number of Electrons Transferred per Molecule
$F$	Faraday Number
$R$	Gas Constant
$T$	Temperature
$A$	Electrode Area
$D$	Diffusion Coefficient of Dissolved Species
$D_{CT}$	Charge Transport Coefficient
$\nu$	Kinematic Viscosity
$[\eta]$	Limiting Viscosity Number
$\omega$	Rotation Rate
$v$	Scan Rate
$C_o$	Bulk Concentration of Electroactive Species in Oxidized Form
$C_r$	Bulk Concentration of Electroactive Species in Reduced Form
$C_o^e$	Concentration of Electroactive Species in Oxidized Form at Electrode Surface
$C_r^e$	Concentration of Electroactive Species in Reduced Form at Electrode Surface
$\Gamma_{obs}$	Observed Surface Coverage
$\Gamma_{cal}$	Calculated Surface Coverage
$\delta$	Peak Width at Half-height
$l$	Film Thickness
$R^*$	Catalytic Enhancement Factor

TABLE OF CONTENTS

	PAGE
APPROVAL	ii
ABSTRACT	iii
DEDICATION	v
ACKNOWLEDGEMENTS	vi
ABBREVIATIONS AND GLOSSARY	vii
TABLE OF CONTENTS	ix
LIST OF TABLES	xiv
LIST OF FIGURES	xvi
GENERAL INTRODUCTION	1
CHAPTER I      SYNTHESIS OF ELECTROACTIVE POLYMERS AND STUDIES OF THEIR ELECTROCHEMICAL BEHAVIOR IN SOLUTION	
I.1. INTRODUCTION	3
I.1.1. Electrochemical Studies of Electroactive Polymers	3
I.1.2. Electroanalytical Techniques	9
a) Cyclic Voltammetry	11
b) Rotating Disk Electrode Voltammetry	16
I.1.3. Electrochemical Determination of Diffusion Coefficient of Polymers	21
I.1.4. Relationship Between Diffusion Coefficient and Molecular Weight	23

I.1.5. Relationship Between Limiting Viscosity Number and Molecular Weight	25
I.2. EXPERIMENTAL	28
I.2.1. Chemicals	28
I.2.2. Measurement of Limiting Viscosity Number	31
I.2.3. Determination of Molecular Weight	32
I.2.4. Electrochemical Experiments	32
a) Rotating Disk Electrode Voltammetry	32
b) Cyclic Voltammetry	34
I.3. RESULTS AND DISCUSSION	36
I.3.1. Electrochemical Studies of Polyvinylbenzophenone and Its Copolymers With Styrene	36
a) Synthesis of Polymers	36
b) Voltammetric Studies	38
c) Determination of Diffusion Coefficient	48
d) Relationship Between Diffusion Coefficient and Molecular Weight	49
e) Relationship Between Limiting Current and Molecular Weight	52
I.3.2. Electrochemical Studies of Poly(vinyl-p- benzoquinone) and Its Copolymers With Styrene	56
a) Synthesis of Polymers	56
b) Voltammetric Studies	58
I.3.3. Electrochemical Studies of Poly[p-(9,10- anthraquinone-2-carbonyl)styrene]-co-styrene	66
a) Synthesis of Polymers	66

b) Voltammetric Studies	67
c) Determination of Diffusion Coefficient	74
I.3.4. Conclusion	80
CHAPTER II	HOMOGENEOUS ELECTROCATALYTIC REDUCTION OF
	POLYCHLORINATED BENZENES AND -BIPHENYLS
	82
II.1. INTRODUCTION	82
II.1.1. General Remarks	82
II.1.2. Studies of Homogeneous Electrocatalysis	85
II.2. EXPERIMENTAL	94
II.2.1. Chemicals	94
II.2.2. Electrochemistry	94
a) Cyclic Voltammetry	94
b) Preparative Electrolysis	94
II.3. RESULTS AND DISCUSSION	99
II.3.1. Direct Reduction of Chlorobenzene, p-Dichlorobenzene, 1,2,4-Trichlorobenzene, 1,2,4,5-Tetrachlorobenzene, p-Chlobiphenyl and Polychlorinated Biphenyls	99
II.3.2. Electrocatalytic Reduction of Polychlorinated Benzenes and -Biphenyls	105
a) Benzophenone as Mediator	105
i) Voltammetric Studies	105
ii) Mechanism of Catalytic Reactions	113
iii) Preparative Electrolysis	116

iv) Reaction of Benzophenone Radical Anions with $C_6H_2Cl_4$	117
b) Anthracene as Mediator	119
II.3.3. Conclusion	122
CHAPTER III ELECTROCHEMICAL STUDIES OF POLYMER- MODIFIED ELECTRODES	126
III.1. INTRODUCTION	126
III.1.1. General Remarks	126
III.1.2. Methods of Modifying Electrodes	128
III.1.3. Studies of Polymer-Modified Electrodes	130
a) Early Works	130
b) Studies of Polymer-Modified Electrodes	133
i) Type of Polymer Films	133
ii) Theoretical Studies	136
iii) Electrochemical Studies	147
iv) Charge Transport	148
III.2 EXPERIMENTAL	150
III.2.1. Chemicals	150
III.2.2. Film Preparation	150
III.2.3. Electrochemistry	150
III.2.4. Spectroelectrochemistry	151
III.3. RESULTS AND DISCUSSION	153
III.3.1. Studies of Electrodes Modified With Polyvinylbenzophenone	153

a) Stability of Polymer Films	153
b) Voltammetric Studies	159
c) Electrocatalytic Reduction of $C_6H_2Cl_4$ by PVBP Films	165
d) Conclusion	166
III.3.2. Studies of Electrodes Modified With Poly(vinyl-p-benzoquinone) and Its Copolymers With Styrene	169
a) Film Stability	169
b) Voltammetric Studies of Electrodes Coated With PVBQ-St Films	172
c) Comparative Voltammetric Studies of PVBQ-St Films and PVBQ Films	177
d) Effect of Solvent	177
e) Conclusion	184
III.3.3. Studies of Electrodes Modified With Poly[p-(9,10- antraquinone-2-carbonyl)styrene]-co-styrene	185
a) Film Stability	185
b) Voltammetric Studies	187
c) Determination of Charge-Transport Coefficient	197
d) Effect of Anthraquinone Content	201
e) Effect of Solvent	205
f) Spectroelectrochemistry	214
g) Electrocatalytic Reduction of Oxygen	220
h) Conclusion	231

LIST OF TABLES

	PAGE
Table 1 Reduction Potentials of Various Oligomeric 1,4-Benzoquinones.	5
Table 2 Composition, Molecular Weight and Molecular Distribution of PVBP and PVBP-St.	37
Table 3 Voltammetric Characteristics of BP Species in Solution.	38
Table 4 Diffusion Coefficients of Polyvinylbenzophenone and Its Copolymers with Styrene.	50
Table 5 Composition, Molecular Weight and Molecular Distribution of PVBQ and PVBQ-St.	57
Table 6 Cyclic Voltammetry of Quinone Species in Solution.	60
Table 7 Composition, Molecular Weight and Molecular Distribution of PAQ.	66
Table 8 Voltammetric Characteristics of Anthraquinone Species in Solution.	69
Table 9 Diffusion Coefficients of EBAQ and PAQ.	75
Table 10 Catalytic Oxidation of 2-Octanol.	92
Table 11 Retention Time and Relative Responses of Chlorobenzenes, Benzophenone, Anthracene and Durene.	98
Table 12 Peak Potentials of Mediators and Substrates.	102
Table 13 Preparative Electrocatalytic Reduction of $C_6H_2Cl_4$ .	117
Table 14 Preparative Electrocatalytic Reduction of $C_6H_3Cl_3$ .	121
Table 15 Difference in Peak Potentials of Mediators and Substrates, and Catalytic Enhancement Factors.	125
Table 16 Ionic Redox Polymers.	136
Table 17 Voltammetric Characteristics of PVBP in Solution and Coated on an Electrode Surface.	158
Table 18 Voltammetric Characteristics of PVBP Films.	161
Table 19 Voltammetric Characteristics of PVBQ-St Films.	174

Table 20	Voltammetric Characteristics of a EBAQ Solution and of a PAQ-Coated Electrode.	185
Table 21	Voltammetric Characteristics of PAQ Films.	189
Table 22	Effect of AQ Content on Voltammetric Characteristics of PAQ Films.	202



LIST OF FIGURES

	PAGE
Figure 1 Structures of Polymers.	10
Figure 2 Cyclic Voltammetry.	12
Figure 3 Rotating Disk Electrode.	17
Figure 4 Rotating Disk Electrode Voltammetry.	19
Figure 5 Electrochemical Cell.	33
Figure 6 Cyclic Voltammograms of BP and PVBP.	39
Figure 7 Rotating Disk Electrode Voltammograms of BP and PVBP-St.	42
Figure 8 Nernstian Plots of BP and PVBP-St	43
Figure 9 Effect of Varying Spacing of Electroactive Centers for Three Values of DP <sub>n</sub> in Solution of 2.8 mM VBP.	46
Figure 10 Relationship Between Diffusion Coefficient and Molecular Weight for PVBP-St.	51
Figure 11 Relationship Between Limiting Viscosity Number and Molecular Weight for PVBP-St.	53
Figure 12 Relationship Between Limiting Current and Molecular Weight for PVBP-St.	55
Figure 13 Cyclic Voltammograms of 3 mM Solutions of a) BQ, b) MeBQ, c) PVBQ, d) PVBQ-St.	59
Figure 14 Cyclic Voltammograms of PVBQ-St of Various VBQ Contents.	63
Figure 15 Cyclic Voltammograms of Solutions of a) MeBQ, b) PVBQ-St (VBQ% = 10.7), c) PVBQ.	64
Figure 16 Cyclic Voltammetry in 0.3M TEAP/Py-DMF (2/1, v/v) of a) EBAQ, b) PAQ.	68
Figure 17 Cyclic Voltammetry at Various Scan Rates of a) EBAQ, b) PAQ.	70
Figure 18 Plots of Cathodic Peak Current against (Scan Rate) for 1 mM Anthraquinone Residues.	73
Figure 19 Dependence of Diffusion Coefficient on Molecular Weight of PAQ Copolymers and EBAQ.	76

Figure 20	Limiting Viscosity Number-Molecular Weight Relationship for PAQ.	78
Figure 21	Dependence of Peak Current at a Scan Rate of $0.05 \text{ Vs}^{-1}$ on Molecular Weight of PAQ Copolymers and of EBAQ.	79
Figure 22	Profile at an Electrode Surface for an Electrocatalytic Reduction Reaction.	83
Figure 23	Electrochemical Cell for Preparative Electrolysis.	95
Figure 24	Cyclic Voltammetry of 3 mM Solutions of a) PhCl, b) 1,4- $\text{C}_6\text{H}_4\text{Cl}_2$ , c) 1,2,4- $\text{C}_6\text{H}_3\text{Cl}_3$ , d) 1,2,4,5- $\text{C}_6\text{H}_2\text{Cl}_4$ .	101
Figure 25	Cyclic Voltammetry of 3 mM Solutions of a) Biphenyl, b) p-Chlorobiphenyl, c) PCB's.	104
Figure 26	Cyclic Voltammetry of a) 3mM Benzophenone, b) 3mM Benzophenone + 3mM $\text{C}_6\text{H}_2\text{Cl}_4$ .	107
Figure 27	Cyclic Voltammetry of 3mM BP + 3mM $\text{C}_6\text{H}_2\text{Cl}_4$ at Various Scan Rates.	108
Figure 28	Cyclic Voltammetry of a) 3mM $\text{C}_6\text{H}_2\text{Cl}_4$ , b) 3mM BP, c) 3mM BP + 3mM $\text{C}_6\text{H}_2\text{Cl}_4$ .	110
Figure 29	Cyclic Voltammetry of a) 3mM BP, b) 3mM BP + PCB's.	111
Figure 30	Cyclic Voltammetry of a) 3mM PCB's, b) 3mM BP, c) 3mM BP + 3mM PCB's.	112
Figure 31	Cyclic Voltammetry of a) 3mM $\text{C}_6\text{H}_3\text{Cl}_3$ , b) 3mM Anthracene, c) 3mM Anthracene + 3mM $\text{C}_6\text{H}_3\text{Cl}_3$ .	120
Figure 32	Cyclic Voltammetry of a) 3mM Anthracene, b) 3mM Anthracene + 3mM p-Chlorobiphenyl.	123
Figure 33	Cyclic Voltammetry of a) 3mM PCB's, b) 3mM Anthracene, c) 3mM Anthracene + 3mM PCB's.	124
Figure 34	Cyclic Voltammogram of a Reversible Monolayer Coating	138
Figure 35	A Multi-Layer Model.	140
Figure 36	Theoretical Voltammograms and Concentration-Distance Plots for Oxidized Sites for a Redox Polymer Film with Fast Electron-Transfer with an Electrode.	143

Figure 37	Theoretical Voltammograms for Redox Polymer Films of Various Thicknesses (Fast Electron-Transfer with an Electrode).	145
Figure 38	Theoretical Voltammograms for a Redox Polymer Film with a Quasi-Reversible Electron-Transfer with an Electrode.	146
Figure 39	Spectroelectrochemical Cell.	152
Figure 40	Cyclic Voltammetry in 0.1M TEAP/DMF on Successive Scans of Electrodes Coated with a) a Non-Irradiated PVBP Film, b) an Irradiated PVBP Film.	154
Figure 41	Cyclic Voltammetry of PVBP Films in 0.1M TEAP/CH <sub>3</sub> CN: a) a Non-irradiated film, b) an Irradiated Film.	157
Figure 42	Effect of Time of U.V. Irradiation on the Cathodic Peak Current of PVBP-Coated Electrodes.	160
Figure 43	Cathodic Peak Current vs. Scan Rate Plot for PVBP Films.	163
Figure 44	Cyclic Voltammetry of a) 3mM C <sub>6</sub> H <sub>2</sub> Cl <sub>4</sub> at a Bare Electrode, b) a PVBP Coated Electrode, c) 3mM C <sub>6</sub> H <sub>2</sub> Cl <sub>4</sub> at the Same Coated Electrode in b), First Scan, d) as c) but Second Scan.	167
Figure 45	Cyclic Voltammetry in 0.1M TEAP/DMSO of a 5000 Å PVBQ-St Film (VBQ% = 24.5) on Successive Scans.	170
Figure 46	Cyclic Voltammetry in 0.1M TEAP/DMSO of a 1000 Å 1000 Å PVBQ-St Film (VBQ% = 24.5) at Various Scan Rates.	173
Figure 47	Cyclic Voltammetry in 0.1M TEAP/DMSO of a PVBQ-St Film (VBQ% = 24.5) at Various Rotation Rates.	175
Figure 48	Cyclic Voltammetry in 0.1M TEAP/DMSO of a Pt Electrode Coated with a) PVBQ, b) PVBQ-St (VBQ% = 24.5).	178
Figure 49	Cyclic Voltammogram of a PVBQ-St (VBQ% = 24.5) Coated Electrode a) in 0.1M TEAP/DMSO, b) the Same Electrode in 0.1M TEAP/H <sub>2</sub> O, c) the Same Electrode in 0.1M TEAP/DMSO again.	179
Figure 50	Cyclic Voltammograms of a PVBQ-St (VBQ% = 24.5) Coated Electrode in 0.1M TEAP/CH <sub>3</sub> CN: a) on Successive Scans, b) 15 min. after the Last Scan	

Figure 51	Cyclic Voltammograms in 0.1M TEAP/DMSO of a) EBAQ in Solution, b) Unirradiated PAQ-Coated Electrode, c) Irradiated PAQ-Coated Electrode.	186
Figure 52	Effect of Time of U.V. Irradiation on The Cathodic Peak Current of PAQ 200(2)-Coated Electrodes.	188
Figure 53	Cyclic Voltammograms of PAQ 200(2) Films of Differing Thickness.	190
Figure 54	Effect of Scan Rate for Films of PAQ 200(2) of Various Thicknesses.	192
Figure 55	A Proposed Structure for PAQ Films.	196
Figure 56	Chronoamperometry of a 1000 Å 200(2) Film in 0.1M TEAP/DMSO. a) Current-Time Plot b) Cottrell Plot	198
Figure 57	Cyclic Voltammetry of PAQ Films of Various AQ Contents.	203
Figure 58	Cyclic Voltammetry of PAQ 200(2) Films in a) 0.1M TEAP/DMSO, b) 0.1M TEAP/DMF, c) 0.1M TEAP/H <sub>2</sub> O, d) 0.1M TEAP/CH <sub>3</sub> CN	206
Figure 59	Dependence of Peak Potentials on Scan Rate for a PAQ Film in 0.1M TEAP/CH <sub>3</sub> CN.	208
Figure 60	Voltammograms in 0.1M TEAP/DMSO of a) 1mM Benzoquinone Solution at a Bare Electrode, b) an Electrode Coated with a 1000 Å PAQ 200(2) Film, c) as a) but at The Coated Electrode.	210
Figure 61	Voltammograms in 0.1M TEAP/H <sub>2</sub> O of a) 1mM Benzoquinone Solution at a Bare Electrode, b) as a) but at an Electrode Coated with a 1000 Å PAQ 200(2) Film.	212
Figure 62	Voltammograms in 0.1M TEAP/CH <sub>3</sub> CN of a) 1mM Benzoquinone Solution at a Bare Electrode, b) an Electrode Coated with a 1000 Å PAQ 200(2) Film, c) as a) but at the Coated Electrode.	213
Figure 63	Spectroelectrochemistry of a PAQ 200(2) Film in 0.1M TEAP/DMSO.	216
Figure 64	Potential Dependence of Absorbances of a PAQ Film in 0.1M TEAP/DMSO at a) 595 nm, b) 690 nm.	217
Figure 65	Nernstian Plots for Absorbances of a PAQ Film in 0.1M TEAP/DMSO at a) 595 nm (First Reduction),	

	b) 690 nm (Second Reduction).	219
Figure 66	Reduction of $O_2$ . a) Pt Electrode under $N_2$ , b) as a) but $O_2$ Saturated, c) PAQ 200(2)- Coated Electrode (Film Thickness 100 Å), $N_2$ Saturated, d) as c) But $O_2$ Saturated.	222
Figure 67	Voltammetry of a $O_2$ Saturated Solution in 0.1M TEAP/DMSO at Various Scan Rates at A) a PAQ 200(2)-Coated Electrode (Film Thickness 100 Å, B) a Bare Pt Electrode.	225
Figure 68	RDE Voltammograms of $O_2$ at a Bare Electrode (----) and at a PAQ-Coated Electrode (Film Thickness 100 Å) (——) at Various Rotation Rates in 0.1M TEAP/DMSO.	226
Figure 69	Nernstian Plots for Reduction of $O_2$ at a) a Bare Electrode, b) a PAQ-Coated Electrode (Film Thickness 100 Å)	228
Figure 70	RDE Voltammetry of a $O_2$ Saturated Solution at Electrodes Coated with PAQ Films of Differing Thicknesses.	229

## GENERAL INTRODUCTION

In recent years, there has been considerable interest in the synthesis and electrochemical characterization of electroactive polymers (1-15). These molecules can be reversibly oxidized and reduced at an electrode, and can exchange electrons with ambient medium. These characteristics, coupled with the light weight, the corrosion resistance, the flexibility and the processibility of macromolecules have made these polymers potentially useful for applications in electrochemical devices, solar-energy conversion, storage batteries and electrocatalysis (4-19).

The electrochemical investigation of electroactive polymers is of fundamental and practical importance. Most applications of electroactive polymers depend on the electrochemical properties of active groups incorporated in a polymer chain. These groups may behave independently as their monomeric analogues, or their properties may be influenced by the macromolecular structure (1, 24-30). An understanding of the electrochemical behavior of these groups is thus vital for successful applications of polymers. By comparing the behavior of polymers with that of the corresponding monomeric compound, information on the "polymer effect" can be obtained. This may be used to characterize and design polymers.

Some of the most important applications of electroactive polymers involve the formation of polymer films directly on an electrode surface (4-19). The effect of electrode modification is to produce an electrode surface whose chemical, optical and electrochemical characteristics are governed by the immobilized molecules. With thoughtful selection of electroactive centers,

electrodes with new and interesting properties may be obtained which may form the basis for new applications of electrochemistry and novel devices. This technique also provides a new method of electrochemically characterizing polymers. The effects of the macromolecular environment on the electrochemical behavior of active centers in a polymer film can be examined through a comparison of voltammetric data with theoretical models. The electrochemistry of polymer films is unique in that there is no mass transfer of reactants and products to and from the electrode. Fundamental studies of such modified electrodes will provide a better insight into the nature of charge transfer and charge transport processes in polymer films.

Homogeneous electrocatalysis is of current interest in electroorganic chemistry (20-23). In this reaction, a soluble, reversible redox couple is utilized to mediate the electrolysis of compounds in solution. The technique reduces overpotential and enhances the rate of electrochemical reactions of substrates. The recent development of modified electrodes, in which catalytic species are attached on the electrode surface, has increased the scope of electrocatalytic reactions.

This thesis is concerned with these current topics and is divided into three chapters. The first chapter describes the synthesis of a number of electroactive polymers, and the investigation of their electrochemical behavior in solution; the second deals with the study of homogeneous electrocatalytic reactions and the third concerns the study of polymer-modified electrodes.

## CHAPTER I

### SYNTHESIS OF ELECTROACTIVE POLYMERS AND STUDIES OF THEIR ELECTROCHEMICAL BEHAVIOR IN SOLUTION.

#### I.1. INTRODUCTION

##### I.1.1. Electrochemical Studies of Electroactive Polymers

Electroactive polymers contain groups which can undergo electron transfer reactions at an electrode. For reversible electron transfer, the polymers are classified as electron transfer type or redox polymers.

Electrochemically active groups may have their properties altered when incorporated in a polymer matrix. Neighboring interaction, and induction effects from the substituents may exert an influence on the redox potentials of the active residues. Electrostatic interactions can lead to changes in electron donor-acceptor ability as neighboring groups acquire charges. The active centers may be buried in a polymer network and be shielded from direct access to the locus of reaction. The high concentration of active centers in a polymer coil may lead to a difference in the extent of ion-pairing or solvation within monomeric vs. macromolecular systems.

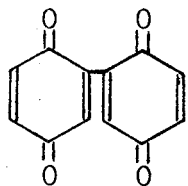
The studies of electrochemical behavior of electroactive groups incorporated in a polymeric structure are important from both theoretical and practical view points. The presence of the polymeric structure may confer new, distinctive and sometimes



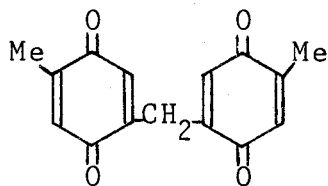
unusual properties on the functional groups and on the molecule. The multi-electron transfer process may provide information of fundamental importance in polymer chemistry and electrochemistry. Factors which affect the electroactivities of the incorporated redox groups may be diagnosed through the voltammetric examination of the polymer solutions in comparison with monomeric model compounds. Information can be obtained on the process of electron transfer between active centers and on the conformation of the polymer. The electrochemical data may serve to probe the polymer structure, or may be used to characterize the polymers. An understanding of the behavior of polymers in solution may be used to screen polymeric systems for possible utilization in polymer modified electrodes, the study of which has recently attracted unusual interest.

There have been several investigations of the electrochemical behavior of molecules bearing multiple, reducible (or oxidizable) centers, but the majority dealt with electroactive oligomers (24-28). The poor solubility of polymers in many of the solvents used in electrochemical experiments is presumably the reason for the limited studies of these compounds.

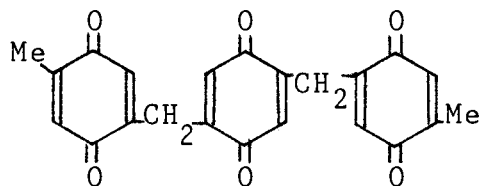
Lindsey and coworkers (24,25) examined a number of dimeric and trimeric quinones in which the redox centers were either directly linked together or separated by a methylene bridge. Polarographic studies in protic and aprotic solvents showed that each quinone center was reduced at characteristic potentials, which were different from those found for the monomeric model compounds (Table 1). For example, the dimer (I) possesses a redox



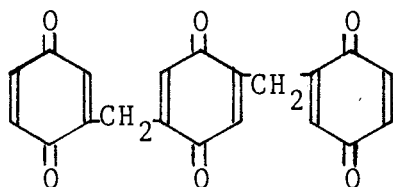
(I)



(II)



(III)



(IV)

Table 1: Half-wave Potentials of Various Oligomeric 1,4-Benzoquinones

Quinones	$-E_{1/2}$ (V vs. SCE)		
1,4-Benzoquinone	0.51		
Phenyl-1,4-benzoquinone	0.50		
Methyl-1,4-benzoquinone	0.58		
I	0.35	0.65	
II	0.55	0.72	
III	0.49	0.65	0.73

in 0.1M  $\text{Et}_4\text{NClO}_4/\text{CH}_3\text{CN}$

potential 0.16 V more positive than phenyl-1,4- benzoquinone for the first reduction reaction. This was ascribed to the strong, electronegative, inductive effect of the quinone "substituent". This effect was greatly reduced when the redox centers were separated by a methylene bridge. The fact that the reduction of each quinone center of the dimer (I) occurred at distinct potentials indicated that the electroactivity of the redox residues was dependent on the reduction state of their neighbors. In other words, the reduction of one quinone group had influenced the subsequent reduction of the other.

Rausch et al. studied the behavior of 1,1'-ferrocene oligomers and found that the redox groups were oxidized successively at potentials separated by hundreds of millivolts (26,27). It was reported that these potentials could be predicted on the basis of ferrocenyl substituent effects.

Morrison et al. examined the voltammetric characteristics of several biferrocene compounds, using stationary and rotating electrodes (28). For molecules in which the redox centers are separated by  $-C(CH_3)_2C(CH_3)_2-$ ,  $-Hg-$  and  $-CH=CHCH_2C_6H_4CH=CH-$ , a single two-electron wave was observed whereas non-bridged and methylene-bridged ferrocenes showed two one-electron waves, corresponding to two successive oxidation processes.

The first example of the study of electrochemical behavior of electroactive polymers was reported by Smith et al. (1). They investigated a series of polyvinylferrocenes of differing chain lengths at a rotating disk electrode. It was shown that the polymers produced voltammograms with shape and half-wave

potential similar to those found for ferrocene. However, the diffusion coefficients of the polymers, which were determined from the voltammetric currents were considerably lower than those calculated theoretically. This led them to suggest that only "isolated" ferrocene groups on a polymer chain were actually oxidized at the electrode. It was found that the fraction of oxidizable ferrocene residues decreased with increasing polymer chain lengths. For example, one in every 1.5 ferrocene groups was oxidized for polymers with molecular weight ( $\bar{M}_n$ ) of  $1 \times 10^3$ , one in three for  $\bar{M}_n = 5 \times 10^3$  and one in four for  $\bar{M}_n = 1.6 - 2.6 \times 10^4$ . The authors attributed the failure to oxidize all ferrocene centers on a chain to the inaccessibility of the active groups to the electrode.

Bard and co-workers investigated poly(2-vinylnaphthalene) and poly(9-vinylanthracene) by cyclic voltammetry and coulometry (2). It was shown that the shape and the peak potentials of the voltammetric response of the polymers were similar to those of the monomeric model compounds. The number of reduced groups per chain was calculated and was found to correspond closely to the degree of polymerization. It was concluded that there was no interference between electroactive centers. The group further formulated a theory for electron transfer for reactants with multiple, noninteracting centers (3). The results showed that such molecules produce current-potential responses having a shape identical to that obtained with the corresponding molecule containing a single center.

Yap and Dust developed a theoretical analysis of the effects

of nearest neighbor interaction in order to quantify the current-potential relationship as a function of interaction parameters and chain lengths (29). They predicted that the voltammetry of polymers containing interacting groups would exhibit current-potential responses with multi-wave shape in contrast to the simple shape found for molecules containing non-interacting centers.

Recently, Morishima et al. examined the oxidative behavior of polymers containing N-methylphenothiazine groups (polyMPT) (30). They found that although polyMPT and its copolymers with methylmethacrylate exhibited voltammograms with peak shapes similar to those for the monomeric analogue, a slight difference in half-wave potential from that of the model compound was observed for the homopolymers. This led them to conclude that a weak interaction existed between MPT groups in polyMPT and was eliminated when MPT centers were separated by non-active units. However, unlike the homopolymers, the copolymers could not be completely oxidized. It was suggested that close proximity of electroactive groups was essential for electron self-exchange within the polymer chain and for the occurrence of complete oxidation.

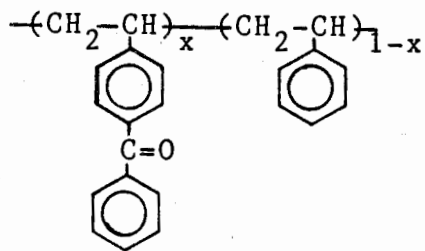
In view of the limited research and limited knowledge of the electrochemical behavior of electroactive polymers, this work was directed towards a fundamental study of the nature of the electrochemical and physicochemical changes occurring in a polymer chain. Experiments were devised to examine the possible interference effects attributable to the neighboring group

interactions and to the macromolecular environments. For these studies, polyvinylbenzophenone, polyvinylbenzoquinone, poly(p-(9,10-anthraquinone-2-carbonyl)styrene-co-styrene and copolymers with styrene were utilized. The structures of the polymers are shown in Figure 1. These polymers were chosen because the respective redox groups are known to undergo a simple, reversible, one-electron transfer reaction and the procedure of synthesizing the polymers has been well established (31-34). This research demonstrates that an understanding of the behavior of polymers is necessary to apply successfully electrochemical techniques as quantitative analytical tools for polymer systems.

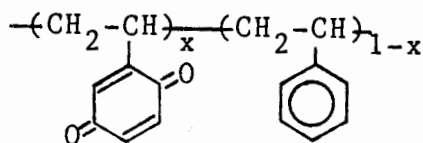
#### I.1.2. Electroanalytical Techniques

The study of the electrochemistry of a new redox species requires experiments which provide much information on the electrode reaction. Cyclic voltammetry and rotating disk electrode voltammetry are useful and versatile electrochemical techniques for such studies. The current-potential responses can be used for qualitative and quantitative analysis, for determining thermodynamic and kinetic criteria for the mechanistic study of chemical reactions coupled with the electrochemical process. Other advantages include the simplicity of the experiments and the relative ease of interpreting the data. Because these two techniques were employed in this work, a brief description of fundamental concepts is presented. The complete theoretical background has been documented in several reviews (35,36).

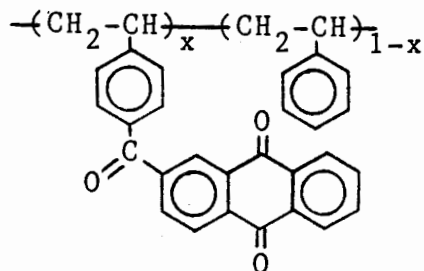
Figure 1: STRUCTURES OF POLYMERS.



Polyvinylbenzophenone (PVBP,  $x=1$ ) &  
Copolymers with Styrene (PVBP-St,  $x<1$ )



Poly(vinyl-p-benzoquinone) (PVBQ,  $x=1$ ) &  
Copolymers with Styrene (PVBQ-St,  $x<1$ )



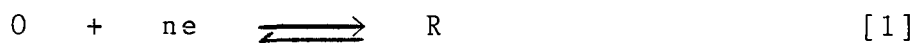
Poly[p-(9,10-anthraquinone-2-carbonyl)styrene]-co-styrene (PAQ,  
 $x<1$ )



a) Cyclic Voltammetry

In this technique, the potential of a small electrode in a quiescent solution containing supporting electrolyte is varied linearly with time, from a value where no electrode reaction occurs to a value higher than the point where the reaction of interest takes place. The direction of the scan is then reversed and the electrolysis of the products may occur on this scan.

Consider the reduction of a species O in solution:



If the reaction [1] is electrochemically reversible, i.e. both O and R species rapidly exchange electrons with the electrode, the Nernstian equation gives a relation between the electrode potential E and the solution composition in the vicinity of the electrode surface:

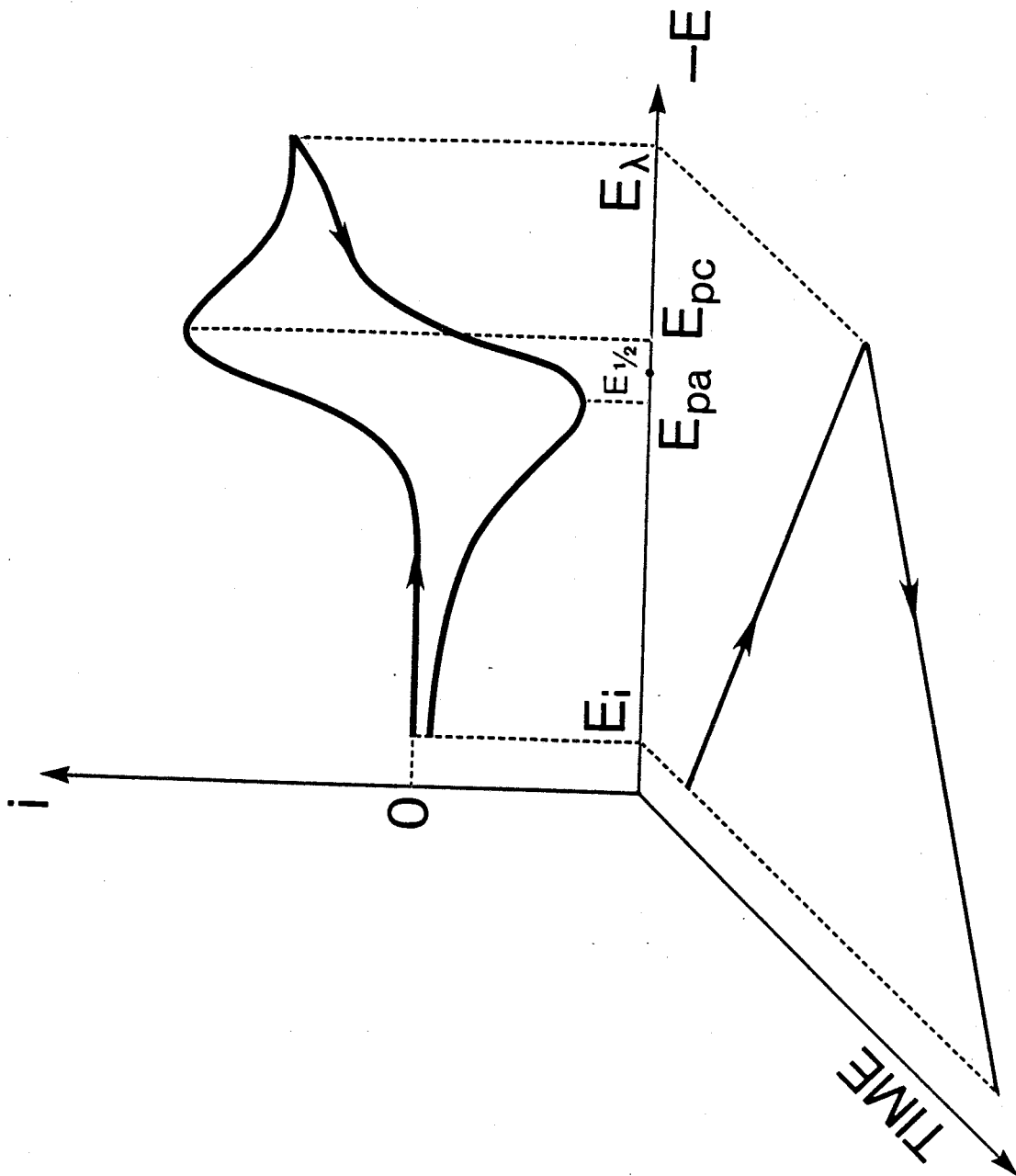
$$E = E^{o'} + \frac{RT}{nF} \ln(C_o^e/C_r^e) \quad [2]$$

$E^{o'}$  is the formal potential of the O/R redox couple, R is the gas constant, T is temperature, n is the number of electrons involved in reaction [1], and  $C_o^e$  and  $C_r^e$  are the concentrations at the electrode surface of O and R, respectively. For  $T=25^\circ\text{C}$  eq. [2] can be rewritten as:

$$E = E^{o'} + 0.059 \log(C_o^e/C_r^e) \quad [3]$$

A typical cyclic voltammogram of a reversible system is shown in Figure 2. At the beginning of the scan, no current flows until the electrode potential approaches  $E^{o'}$ . The current then

Figure 2: CYCLIC VOLTAMMETRY.



rises rapidly because the rate of electrode reaction is accelerated by increasing potentials. As the reaction proceeds, the region in the vicinity of the electrode becomes depleted of reactant. A concentration gradient is established which causes the reactant to diffuse from the bulk of solution to the electrode surface. The solution layer close to the electrode surface within which a concentration gradient exists is called diffusion layer. Since the solution is unstirred, the thickness of this layer increases with time. A peak potential is reached where the increase in the reaction rate is balanced by the diffusion rate of the reactant. Beyond the peak, the current decays because the diffusion rate decreases as the diffusion layer becomes thicker. On the reverse scan, the product formed in the forward scan is reoxidized and an anodic peak is observed.

Important parameters of a cyclic voltammogram are the magnitudes of the cathodic ( $i_{pc}$ ) and anodic ( $i_{pa}$ ) peak currents, and the potentials at which the peaks occur ( $E_{pc}$  and  $E_{pa}$ ). The peak current  $i_{pc}$  is related to the experimental parameters by the Randles-Sevcik equation (37,38):

$$i_{pc} = 2.69 \times 10^5 n^{3/2} A D_o^{1/2} C_o v^{1/2} \quad [4]$$

where A is the electrode area,  $C_o$  the bulk concentration of species O,  $D_o$  its diffusion coefficient and v the potential scan rate. The diffusion coefficient is defined as the proportionality between the diffusion rate f of a substance and its concentration gradient:

$$f = AD \left( \frac{\partial C}{\partial x} \right)_{x=0} \quad [5]$$

The positions of the cathodic and anodic peaks, relative to the formal potential  $E^{0'}$ , were calculated by Nicholson and Shain and are given by (39):

$$E_{pc} = E_{1/2} - 28.5/n \text{ mV (at } 25^{\circ}\text{C)} \quad [6]$$

$$E_{pa} = E_{1/2} + 28.5/n \text{ mV} \quad [7]$$

where

$$E_{1/2} = E^{0'} + 0.059 \log(D_r/D_o)^{1/2} \quad [8]$$

$E_{1/2}$  is the half-wave potential which corresponds to the value on a polarographic curve where the current is equal to one-half of the limiting current.  $D_r$  is the diffusion coefficient of species R. Usually,  $D_o \approx D_r$  and therefore,  $E_{1/2} \approx E^{0'}$ .

The half-wave potential  $E_{1/2}$  of a redox couple thus can be determined from a voltammogram.  $E_{1/2}$  is significant because it is characteristic for a given substance and may be used in qualitative identification. Furthermore,  $E_{1/2}$  is very close to  $E^{0'}$  so that thermodynamic data may be obtained from voltammetric measurements.

Equations [4], [6] and [7] imply that for an electrochemically reversible, one-electron transfer system where the species O and R are stable, the peak potentials are independent of scan rate, the peak separation is  $59/n$  mV, the peak currents are proportional to the square root of scan rate and the ratio of the anodic and cathodic peak currents is unity.

For systems where the electron exchange between the electrode and the redox species is slow relative to the experimental time scale, the electrode reaction is unable to maintain the equilibrium conditions as the potential changes. The

ratio of the concentrations of species O and R at the electrode surface calculated from the Nernstian equation (eq. [3]) differs significantly from the actual ratio. The current-potential and  $E_p - E_{1/2}$  relationships contain terms relating to the electron transfer characteristics of the electrode reaction. It was shown that peak currents are smaller than those expected for a reversible system and the peaks are more separated. As the scan rate increases, the reduction peak shifts cathodically, the oxidation peak shifts anodically and the peak separation increases (40).

Cyclic voltammetry can also be employed to obtain information on chemical reactions involving the redox species. For example, if the species R is unstable and undergoes an irreversible chemical reaction (eq. [9]), a fraction of R will



not be available for the reoxidation on the reverse scan and  $i_{pa}$  becomes smaller than  $i_{pc}$ . The variation of the  $i_{pa}/i_{pc}$  ratio is dependent on the rate of reaction [9] and on the scan rate. At higher scan rates, the time gap between the reduction and reoxidation reactions is short, less R is deactivated by the succeeding reaction and  $i_{pa}/i_{pc}$  will increase. Thus the kinetics of the reaction following the electron transfer process can be studied from the voltammetry at various scan rates.

Compared to the well-known, dropping Hg polarographic technique, cyclic voltammetry has the advantages of fast scan

rate and better resolution. Because the electrode is stationary, a variety of materials other than Hg can be utilized as working electrode and therefore, a wider range of potential can be used. The reversal of the potential sweep may allow the examination of the fate of products and the mechanism of chemical reactions associated with the electron transfer process.

b) Rotating Disk Electrode Voltammetry

A rotating disk electrode consists of a flat end of a conducting cylinder set into an insulating tube. As the electrode is rotated, solution is brought up to the electrode surface and then spins out radially towards the edges as shown in figure 3.

According to Nernst, a thin diffusion layer  $\delta$  exists in the vicinity of the electrode surface during the electrolysis. Within this layer, the solution is considered to be motionless, and the diffusion is the only means of mass transport. At the boundary of the diffusion layer, the concentration of the reactant is maintained at the value of the bulk concentration by the forced convection. The concentration within  $\delta$  is considered to be linear and the current for a reduction process is given by:

$$i = nFAD(\partial C/\partial x)_{x=0} \quad [10]$$

$$= nFAD \frac{C_o - C_o^e}{\delta} \quad [11]$$

where  $C_o^e$  is the concentration of the reactant at the electrode surface. The thickness of the diffusion layer  $\delta$  was derived by Levich from the principles of hydrodynamics (41):

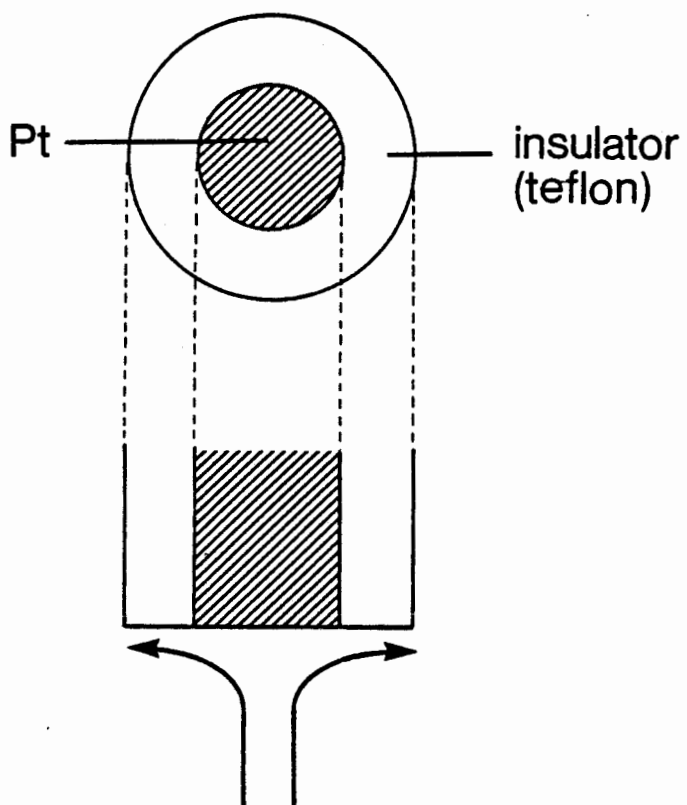


Figure 3: ROTATING DISK ELECTRODE.



$$\delta = 1.61 D^{1/3} \nu^{1/6} \omega^{-1/2} \quad [12]$$

where  $\omega$  is the angular velocity of the disk and  $\nu$  is the kinematic viscosity of the solution which is defined as the ratio of solution viscosity and density.

Substituting [12] into [11] yields:

$$i = 0.62nFAD^{2/3}\nu^{-1/6}\omega^{1/2}(C_o - C_o^e) \quad [13]$$

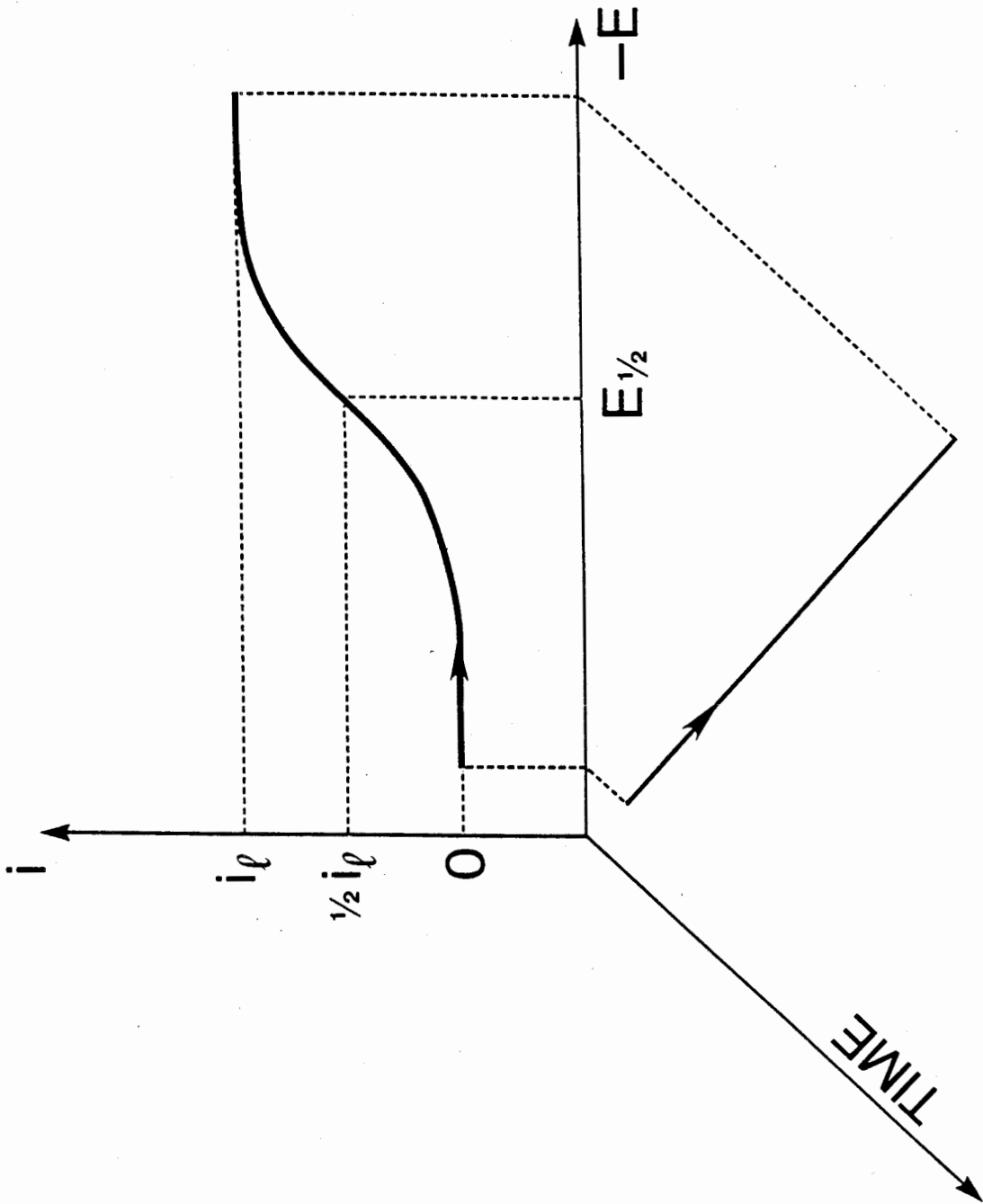
At potentials sufficiently negative so that  $C_o^e=0$ , a limiting current is observed and is given by the Levich equation:

$$i_1 = 0.62nFAC_oD^{2/3}\nu^{-1/6}\omega^{1/2} \quad [14]$$

A RDE voltammogram is shown in Figure 4. The curve has a S shape in contrast to a peaked shape found for experiments in a quiescent solution. In RDE technique, the thickness of the diffusion layer is independent of potential and time (eq. [12]) and is thus constant during the electrolysis. In the potential region where  $C_o^e=0$ , the diffusion rate of the reactant reaches a constant, maximum value and therefore, the limiting current becomes constant on the plateau of the wave.

RDE can be used to determine the half-wave potential and to examine the reversibility of an electrode reaction. For a reversible system, the Nernst equation (eq. [3]) applies at the electrode surface. Combining eq. [3], [13] and [14] with:

Figure 4: ROTATING DISK ELECTRODE VOLTAMMETRY.



$$C_o = C_o^e + C_r^e \quad [15]$$

gives an expression which relates the current with the electrode potential:

$$E = E_{1/2} - 0.059 \log\left(\frac{i_1 - i}{i}\right) \quad [16]$$

$E_{1/2}$  is taken as the potential where the current is one half of the limiting value. A plot of  $E$  vs.  $\log\left(\frac{i_1 - i}{i}\right)$  should yield a straight line with a slope of  $-0.059/n$  V and an intercept equal to  $E_{1/2}$ .

RDE has some advantages over voltammetry at a stationary electrode. A steady-state is quickly attained and the measurement of current can be made with high precision. The rates of mass transport by forced convection are much larger than the those of diffusion and therefore, the relative contribution of natural mass transfer to electron transfer kinetics is small. Natural mass transfer may arise from changes in temperature and in electrolyte density as a result of the electrode reaction. The limiting current obtained at a rotating electrode is much larger than the peak current in cyclic voltammetry at equal concentration of electroactive substance. The RDE is therefore capable of responding to considerably lower concentrations of electroactive material. Thus it is advantageous to use the RDE technique for quantitative analysis but it has no advantage over cyclic voltammetry for qualitative work.

### I.1.3. Electrochemical Determination of Diffusion Coefficient of Polymers

An electrochemical process generally consists of three individual steps: transport of reactants to the electrode surface, electrochemical reaction and transport of products away from the electrode. There are three modes of mass transport: migration, convection and diffusion. Migration is the movement of a charged body under the influence of an electric field. In most electrochemical experiments, migration effects serve no useful purpose and this transport mode is minimized by using a large excess of supporting electrolyte. Convection is the mode of mass transport by hydrodynamic forces and is important in stirred solutions. On the other hand, diffusion exists whenever concentration differences are established. Since a concentration gradient develops as soon as electrolysis is initiated, diffusion plays a part in every electrode reaction.

The diffusion coefficient of a solution species can be determined by various techniques. Non-electrochemical methods include isotopic tracers, centrifugation, optical and laser light spectroscopy. Common electrochemical techniques are chronoamperometry, and linear sweep voltammetry at a stationary and at a rotating disk electrode (42).

For linear sweep voltammetry at a stationary electrode, the relationship between current and diffusion coefficient is given by the Randles-Sevcik equation:

$$i_{pc} = 2.69 \times 10^5 n^{3/2} A D^{1/2} C v^{1/2} \quad [4]$$

Thus the diffusion coefficient can be determined from a single voltammetric measurement if other parameters are known.

Practically, to obtain a more accurate value, the diffusion coefficient is usually calculated from the slope of current vs. (scan rates)<sup>1/2</sup> or current vs. concentration plot.

Similarly, the diffusion coefficient D can be determined from the RDE technique, using the Levich equation which relates the measured limiting current to D:

$$i_1 = 0.62nFAC_0 D^{2/3} \nu^{-1/6} \omega^{1/2} \quad [14]$$

A plot of  $i_1$  vs.  $\omega^{1/2}$  will give a straight line from the slope of which D can be determined.

While electrochemical methods are more popular for determining diffusion constant of small, electroactive molecules, non-electrochemical techniques are more often employed for polymers (43). The use of electrochemical techniques for macromolecular systems has received little attention. The only studies are those of Drushel, who suggested a method to estimate the diffusion coefficient of aliphatic sulfides in petroleum by polarography (44), and of Smith who studied the electrooxidation of polyvinylferrocene at a rotating disk electrode (1). However, in Smith's work, the D values estimated were considerably lower than those calculated theoretically. The results were attributed to the inaccessibility of some electroactive residues to the electrode surface due to interferences from neighboring groups. However, it is believed that the use of electrochemical

techniques in determining diffusion coefficients of small molecules can also be applied to polymers containing active centers which behave independently of each other and thus will provide a new means of characterizing polymers.

#### I.1.4. Relationship Between Diffusion Coefficient and Molecular Weight

The diffusion coefficient  $D$  of a suspended or dissolved, spherical particle is related to its radius  $r$  by the Stokes-Einstein equation (45):

$$D = RT/6\pi\eta rN \quad [17]$$

where  $\eta$  is the viscosity of solvent and  $N$  the Avogadro number.

If  $M$  is the molecular weight of the particle and  $\bar{v}$  its specific volume, then:

$$4\pi r^3/3 = M\bar{v}/N \quad [18]$$

By substituting [18] into [17],  $D$  can be rewritten as:

$$D = RT(4\pi N/3M\bar{v})^{1/3}/6\pi\eta N \quad [19]$$

Thus for a spherical molecule, the diffusion coefficient is proportional to the cube root of the molecular weight.

While a small molecule has a relatively well-defined radius, a flexible polymer chain in a dilute solution changes its shape continuously. Consequently, the dimension of a polymer molecule is usually evaluated as an average over many possible

conformations of the chain. One of the commonly used averages is the average radius of gyration  $R_G$ , which is a measure of the average distance of a mass element on the chain to the center of mass.  $R_G$  is related to the polymer molecular weight by:

$$R_G^2 = \frac{\alpha^2 \beta^2 M}{6 M_0} \quad [20]$$

The parameter  $\alpha$  is related to the conformation of the polymer chain and therefore, is dependent on the polymer molecular weight and solvent,  $\beta$  is a constant for a given type of polymer and is independent of molecular weight, and  $M_0$  is the molecular weight of the repeating unit.

When a polymer molecule is considered as a sphere, the radius  $R_e$  of this equivalent sphere is:

$$R_e = \xi_f R_G \quad [21]$$

where  $\xi_f$  is a universal constant equal to 0.665.

By combining [17], [20] and [21], a relationship between the diffusion coefficient and the molecular weight of a polymer is obtained:

$$D = \frac{R T M_0^{1/2}}{6^{1/2} \pi N \eta \alpha \beta \xi_f M^{1/2}} \quad [22]$$

It was shown that  $\alpha$  varies approximately from 1 to  $M^{0.05}$  from a poor to a good solvent and therefore,  $D$  varies as  $M^{-0.50}$  in a poor solvent and as  $M^{-0.55}$  in a good solvent. By



letting

$$\alpha = M^x \quad [23]$$

D can be expressed in a more general form:

$$D = K_T M^{-b} \quad [24]$$

where 
$$K_T = RTM_o^{1/2} (6^{1/2} \pi N \eta \beta \xi_f)^{-1}$$

and 
$$b = x + 1/2 \quad [25]$$

b thus has values between 0.50 and 0.55. This prediction was confirmed by the study of Meyerhoff and Schulz on polymethyl methacrylate in acetone (46).

#### I.1.5. Relationship Between Limiting Viscosity Number and Molecular Weight

Einstein derived a relationship between the viscosity  $\eta$  of a solution of spherical particles, their volume fraction  $\phi$  and the viscosity of the pure solvent  $\eta_o$  (47):

$$\begin{aligned} \eta_{sp} &= \frac{\eta}{\eta_o} - 1 \\ &= 2.5\phi \end{aligned} \quad [26]$$

$\eta_{sp}$  is called specific viscosity. Since  $\eta_{sp}$  is dependent on the concentration C of the solute, it is more convenient to use the quantity  $\eta_{sp}/C$  at the limit of zero concentration. This

limiting value is called limiting viscosity number  $\{\eta\}$ , and is independent of concentration:

$$\{\eta\} = \left\{ \eta_{sp}/C \right\}_{C \rightarrow 0} \quad [27]$$

If  $v_h$  is the hydrodynamic volume of a dissolved macromolecule,  $C$  is the concentration, then:

$$\phi = NCv_h/M \quad [28]$$

and  $\{\eta\}$  becomes:

$$\{\eta\} = 2.5Nv_h/M \quad [29]$$

For flexible polymers which behave as spheres of radius  $R_e = \xi_f R_G$ , the hydrodynamic volume of a polymer chain is:

$$\begin{aligned} v_h &= \frac{4}{3} \pi R_e^3 \\ &= \frac{4}{3} \pi \xi_f^3 R_G^3 \\ &= \frac{4}{3} \frac{\pi \xi_f^3 \alpha^3 \beta^3 M^{3/2}}{(6 M_0)^{3/2}} \end{aligned} \quad [30]$$

Introducing [30] into [29] leads to the relation between the intrinsic viscosity and molecular weight of polymers:

$$[\eta] = \frac{10}{3} \frac{\pi N \alpha^3 \beta^3 \xi_f^3 M^{1/2}}{(6 M_0)^{3/2}} \quad [31]$$

or  $\{ \eta \} = KM^a$  [32]

where  $K = \frac{10 \pi N \beta^3 \xi_f^3}{3(6M_o)^{3/2}}$  [33]

and  $a = 3x + 1/2$  [34]

where x is defined by equation [23].

The exponent a can be related to the parameter b in the diffusion coefficient-molecular weight relationship by comparing eqs. [25] and [34]. The result is:

$$b = (1 + a)/3$$
 [35]

Eq. [35] implies that the parameter a (or b) can be determined independently from the  $\{ \eta \}$  vs. M or D vs. M relationship. Thus the validity of determining diffusion constants of polymers by voltammetric techniques can be evaluated by comparing the a value deduced electrochemically with that estimated viscometrically. Any discrepancy between these two results is indicative of the inaccuracy of the diffusion coefficients thus obtained and this may be attributed to the interaction between attached active groups which has altered their electroactivities.

## I.2. EXPERIMENTAL

### I.2.1. Chemicals

Benzophenone (BP), p-benzoquinone (BQ) and methyl-p-benzoquinone (MeBQ) were purified by sublimation and stored in the dark.

Bromohydroquinone and 2-anthraquinone carboxylic acid were used as received.

N,N-Dimethylformamide (DMF) was purified by stirring over barium oxide overnight, followed by distillation at reduced pressure.

Dimethyl sulfoxide (DMSO) was fractionally distilled at reduced pressure.

Pyridine (Py) (BDH, analytical grade) was used without further purification.

All solvents were stored under nitrogen atmosphere in the presence of molecular sieve type 4A, which had been activated by drying in vacuum at 300°C for several days.

Tetraethylammonium perchlorate (TEAP) was recrystallized twice from distilled water and dried in vacuum for several days.

### Synthesis of Polyvinylbenzophenone (PVBP) and Poly(vinylbenzophenone-co-styrene) (PVBP-St)

Polystyrene with narrow molecular weight distribution was prepared by anionic polymerization of styrene with either n-butyl lithium in benzene or with sodium naphthalene in tetrahydrofuran.

Polyvinylbenzophenone and its copolymers with styrene were obtained by reaction of polystyrene with benzoyl chloride

and aluminum chloride in nitrobenzene as described in the literature (32). The benzophenone content of the polymers was controlled by the stoichiometric ratio of the reactants. The products were purified by repetitive precipitation in methanol from benzene solution and finally freeze-dried. The polymers were stored in the dark, as exposure to ambient light greatly reduced their electrochemical reactivity.

The benzophenone content of the copolymers was determined by infrared spectroscopy performed on a Perkin Elmer 599B. A calibration curve was constructed from the spectra of blends of PVBP and PSt of known compositions, using absorbances of the vinylbenzophenone unit at  $1655\text{ cm}^{-1}$  and of the styrene unit at  $1490\text{ cm}^{-1}$ . The copolymer composition was also determined by ultraviolet spectroscopy (Unicam SP 8000), using the calibrated absorbance of PVBP at 343 nm in benzene. The results obtained from these two spectroscopic methods were in good agreement.

Synthesis of Poly(vinyl-p-benzoquinone) (PVBQ) and Poly(vinyl-p-benzoquinone)-co-styrene (PVBQ-St)

PVBQ was prepared by radical polymerization of vinylbis(1-ethoxyethyl)hydroquinone (VBEH) (monomer 13.9 mmol, bis-azoisobutyronitrile 0.122 mmol, benzene 5 ml,  $60^{\circ}\text{C}$ , 92 h.), followed by the hydrolysis and oxidation of the product (34).

PVBQ-St was obtained by copolymerization of VBEH with styrene by a procedure similar to that for PVBQ. The loading of VBQ in a copolymer chain was controlled by adjusting the molar ratio of the monomers. The copolymer composition was determined

by infrared spectroscopy of the VBEH-St copolymers, using a calibrated ratio of absorbances of the VBEH unit at  $945\text{ cm}^{-1}$  and of the styrene unit at  $705\text{ cm}^{-1}$ . The results were confirmed by elemental analysis.

The homo- and co-polymers had the yellow coloration characteristic of p-benzoquinone, with  $\lambda_{\text{max}}$  at 255 nm in dioxane/90% aq. MeOH (4/1, v/v) (literature value: 254 nm (34)). Their IR spectra show an absorption peak at  $1655\text{ cm}^{-1}$ , which is characteristic of the quinone group. The polymers were found to be photosensitive, as prolonged exposure to ambient light produced insoluble materials.

#### Synthesis of 2-(p-ethylbenzoyl)-9,10-anthraquinone (EBAQ)

2-Anthraquinone carbonylchloride was prepared from 2-anthraquinone carboxylic acid and thionyl chloride by a standard procedure (48). EBAQ was synthesized by reaction of 2-anthraquinone carbonylchloride (18.8 mmol) and aluminum chloride (22.5 mmol) with ethyl benzene (200 ml) at room temperature for 3 days. After recrystallization from methanol, the product was obtained as yellow crystals, yield 35%, m.p.  $125-6^{\circ}\text{C}$ . Elemental analysis: calcd. C 81.18, H 4.71; found C 80.68, H 4.83. Mass spectrum m/e (%): 342 ( $\text{M}^{+}+2$ , 1.5), 341 ( $\text{M}^{+}+1$ , 10.5), 340 ( $\text{M}^{+}$ , 35), 235 (9.5), 151 (17.1), 133 (100).

The IR spectrum showed a strong absorption of a quinone group at  $1675\text{ cm}^{-1}$ , a  $\beta$ -carbonyl group at  $1650\text{ cm}^{-1}$ , an ethyl group at  $2970\text{ cm}^{-1}$ ,  $2930\text{ cm}^{-1}$  and  $2880\text{ cm}^{-1}$ , and a phenyl group at  $700\text{ cm}^{-1}$ .

Synthesis of Poly[p-(9,10-anthraquinone-2-carbonyl)styrene]-co-styrene (PAQ)

PAQ was synthesized by reacting polystyrene with 2-anthraquinone carbonylchloride and aluminum chloride in dry nitrobenzene at room temperature for 3 days. Polymers of different anthraquinone loading were prepared by changing the relative amounts of 2-anthraquinonecarbonylchloride and polystyrene. The product was purified by repeated precipitation in methanol and finally freeze-dried in vacuum. The IR spectrum showed a quinone band at  $1675\text{ cm}^{-1}$ , a  $\beta$ -carbonyl band at  $1650\text{ cm}^{-1}$ , a methylene band at  $2920\text{ cm}^{-1}$  and a phenyl band at  $700\text{ cm}^{-1}$ . Copolymer compositions were determined by infrared spectroscopy. A calibration curve was constructed from the spectra of blends of polystyrene and EBAQ of known compositions, using absorbances of the anthraquinone unit at  $1170\text{ cm}^{-1}$  and of the styrene unit at  $3020\text{ cm}^{-1}$ . The results were consistent with those obtained from elemental analysis.

I.2.2. Measurement of Limiting Viscosity Numbers of Polymers

The limiting viscosity numbers  $\{ \eta \}$  of polymers were measured with an Ubbelohde viscometer for solutions of the composition utilized in the electrochemical measurements, i.e., PVBP/0.1 M TEAP/DMF and PAQ/0.3 M TEAP/Py-DMF (2/1 v/v). The measurements were performed at  $25^{\circ}\text{C}$  at four dilute concentrations of polymers and extrapolated to zero concentration. The limiting viscosity number was calculated according to the Huggins equation

$$\eta_{sp}/C = \{ \eta \} + K' \{ \eta \}^2 C \quad [36]$$

where  $\eta_{sp}$  is the specific viscosity, C the polymer concentration and K' is a constant.

### I.2.3. Determination of Polymer Molecular Weights

The molecular weights and polydispersities of the electron-transfer polymers were determined by gel permeation chromatography of the parent polymers. A Waters Associate Model GPC/ALC 301 equipped with five  $\mu$ -styragel columns with pore sizes of  $10^6$ ,  $10^5$ ,  $10^5$ ,  $10^4$ ,  $10^3$  Å was employed, with tetrahydrofuran as solvent. A series of N.B.S. polystyrene standards was used to construct the calibration curve. The calculation was performed with the aid of the University of Waterloo MDI computer program.

### 1.2.4. Electrochemical Experiments

#### a) Rotating Disk Electrode (RDE) Voltammetry

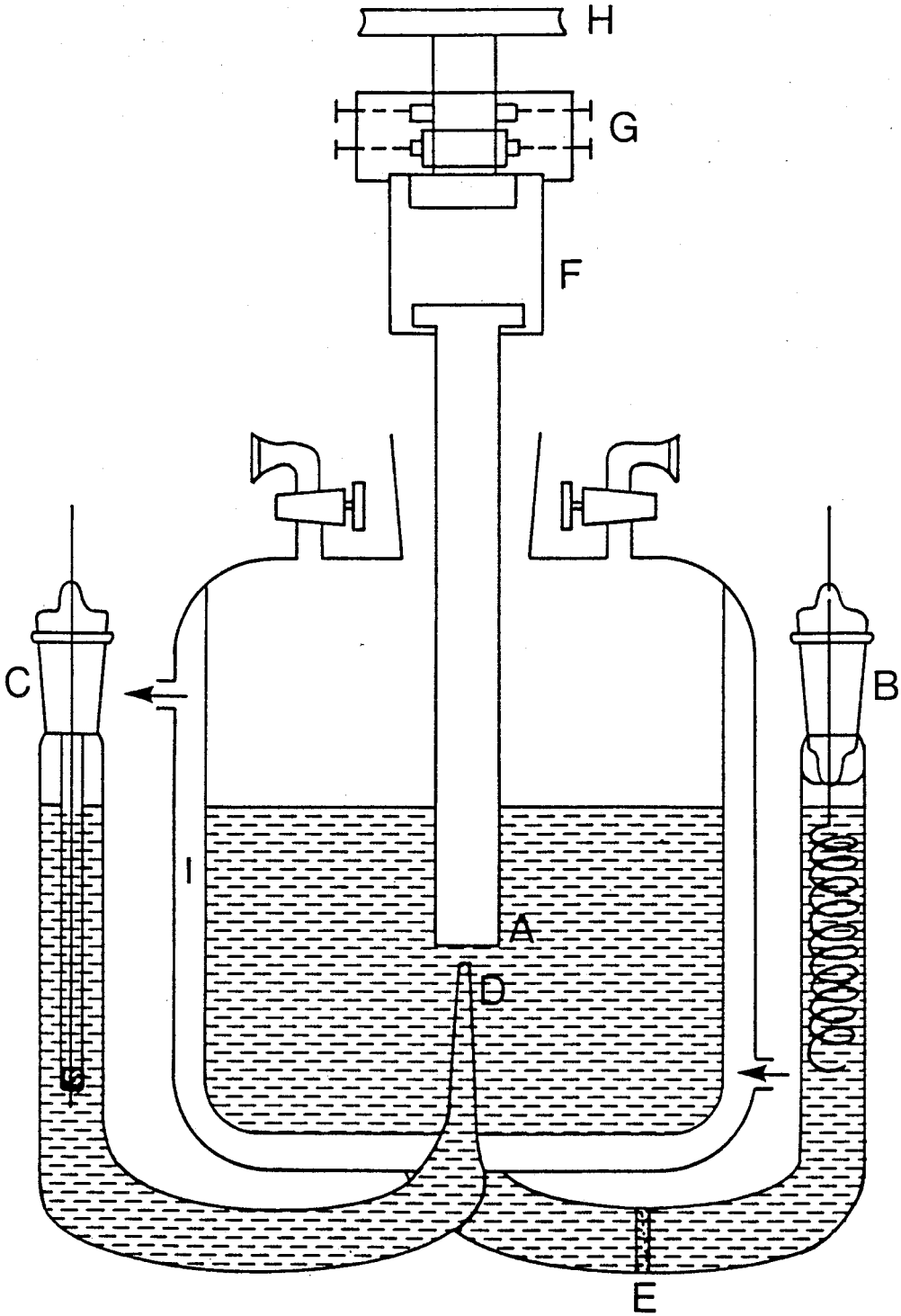
Experiments were performed in a three compartment cell, which was equipped with a water jacket to maintain the test solution at a constant temperature. A Luggin capillary connecting the reference and the working compartment was positioned near the working electrode to minimize the IR drop. The diagram of the cell is shown in Figure 5.

The working electrode was a 7.66 mm diameter, mirror-polished, Pt disk surrounded by a cylindrical Teflon collar of 5.27 mm thickness (Pine Instrument Co.). The electrode area was determined by chronoamperometry of the  $K_4Fe(CN)_6/0.1M$  KCl/ $H_2O$  standard system (42). A good agreement between the experimentally



Figure 5: ELECTROCHEMICAL CELL.

- A) Working Electrode
- B) Counter Electrode
- C) Reference Electrode
- D) Luggin Capillary
- E) Fritted Disk
- F) Bearing Assembly
- G) Brushes
- H) Speed Control Pulley
- I) Water Jacket



estimated value and the geometric area was obtained, which indicated that the Pt surface was adequately smooth. Before each experiment, the electrode was dipped sequentially in concentrated  $\text{HNO}_3$ , then saturated  $\text{FeSO}_4$  in  $2\text{M H}_2\text{SO}_4$  and finally rinsed thoroughly with distilled water. This procedure provided a consistent electrode surface, as judged by the reproducibility of the results. The speed of rotation was controlled to within 1% by a Carter motor tachometer. A Cole-Parmer Instrument stroboscope was employed to measure the rate of rotation.

A Pt wire spiral was used as counter electrode. The reference electrode was a Ag wire in a solution of  $0.01\text{M AgNO}_3/0.1\text{M TEAP/DMF}$ . However, for convenience of comparison, the results are reported with respect to the saturated calomel electrode (SCE).

The sample solutions were flushed thoroughly with oxygen-free  $\text{N}_2$ , and a  $\text{N}_2$  or Ar atmosphere was maintained throughout the voltammetric measurements. All experiments were carried out at  $25^\circ\text{C}$ .

A potentiostat built by the University Electronics Shop was employed. A Hewlett-Packard 3300 A function generator was used to sweep the electrode potential. Electrical responses were recorded on a Hewlett-Packard T0464A X-Y/Y' recorder.

#### b) Cyclic Voltammetry

The cell, the counter electrode and the reference for cyclic voltammetry were similar to those for RDE experiments. The working electrode was a 1.7 mm diameter highly polished Pt disk sealed in Kel F (Bioanalytical Systems, Co.). The procedure for

the electrode pretreatment and the determination of the surface area was the same as described above.

Experiments were performed at 25°C in cells maintained under a positive pressure of purified nitrogen or argon. A Princeton Applied Research Model 170 Electrochemical System with IR compensation was employed.

### I.3 RESULTS AND DISCUSSION

This section describes the studies of polyvinylbenzophenone (PVBP), poly(vinyl-p-benzoquinone) (PVBQ), poly{p-(9,10-anthraquinone-2-carbonyl)styrene-co-styrene} (PAQ) and copolymers with styrene. The electrochemical behavior of the polymers was examined by cyclic voltammetry and RDE technique and compared to that of the corresponding monomeric analogues. The electroreduction of polymers of differing spacings between active centers was compared in order to examine the interference effects attributable to the neighboring groups. The effect of macromolecular environment was studied with polymers of differing chain lengths. For polymers containing non-interacting redox centers, their diffusion coefficients were estimated from electrochemical data, and a relationship between voltammetric current and polymer molecular weight was derived. Detailed studies of each polymer are presented in separate sections.

#### I.3.1. Electrochemical Studies of Polyvinylbenzophenone (PVBP) and Its Copolymers with Styrene (PVBP-St)

##### a) Synthesis of Polymers

PVBP and PVBP-St were prepared by Friedel-Crafts reaction of polystyrene with benzoylchloride as shown in reaction [37].

The molecular weight and the composition of polymers are presented in table 2.

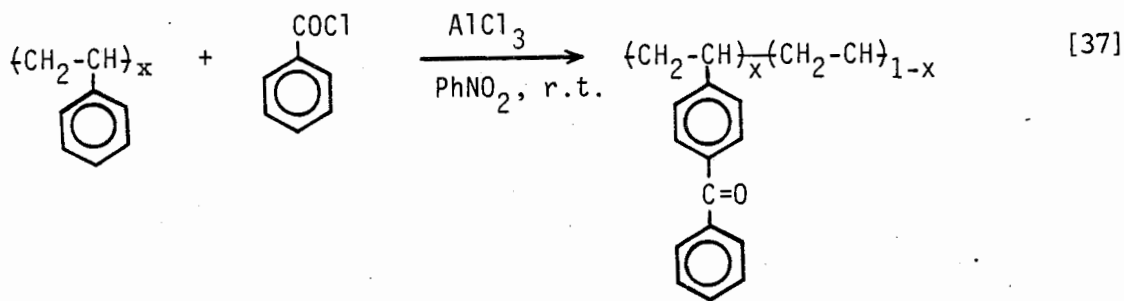


Table 2: Composition, Molecular Weight and Molecular Weight Distribution of PVBP and PVBP-St

Polymers	VBP %	$\overline{DP}_n$	$\overline{M}_n \times 10^{-4}$	$\overline{M}_w/\overline{M}_n$
P2A	37.4	22.5	0.32	1.16
P2C	100		0.47	
P5A	36.7	52	0.74	1.20
P5B	73		0.93	
P8A	30.8	72	0.98	1.22
P8B	77		1.33	
P8C	89		1.42	
P12A	30.7	108	1.46	1.14
P12B	61		1.80	
P12C	89		2.11	
P40A	22.5	414	5.27	1.16
P40B	52		6.52	
P40C	100		8.62	
P200A	32.5	2170	30.0	1.35
P200B	57		35.5	
P200C	100		45.2	
P300A	22.5	2740	34.9	1.12
P300B	76		50.2	

b) Voltammetric Studies

Figure 6 presents the cyclic voltammograms of benzophenone (BP) and PVBP in 0.1M TEAP/DMF solution and the data are summarized in table 3. When the potential scan was limited at

Table 3: Voltammetric Characteristics of Benzophenone Species in Solution<sup>a)</sup>

Compounds	$E_{pc}^1$ (V)	$E_{pa}^1$ (V)	$E_{1/2}$ (V)	$\Delta E$ (mV)	$E_{pc}^2$ (V)
BP	-1.80	-1.73	-1.77	65	-2.44
PVBP	-1.82	-1.74	-1.78	67	-2.43

a) 0.1M TEAP/DMF, 0.05 Vs<sup>-1</sup>, SCE.

-2.05 V, the voltammetry of the BP solution produced a reversible, one-electron wave with a cathodic peak potential at -1.80 V. This corresponds to the reduction of BP to BP radical anion. Within the range of scan rate investigated, ie. 0.01-0.5 Vs<sup>-1</sup>, the cathodic and anodic peak potentials were independent of scan rate  $v$ , the peak height was proportional to  $v^{1/2}$ ,  $i_{pa}/i_{pc}$  was unity and the peak-to-peak separation was about 65 mV, which is in good agreement with a value of 60 mV expected for a reversible species. These characteristics are indicative of the

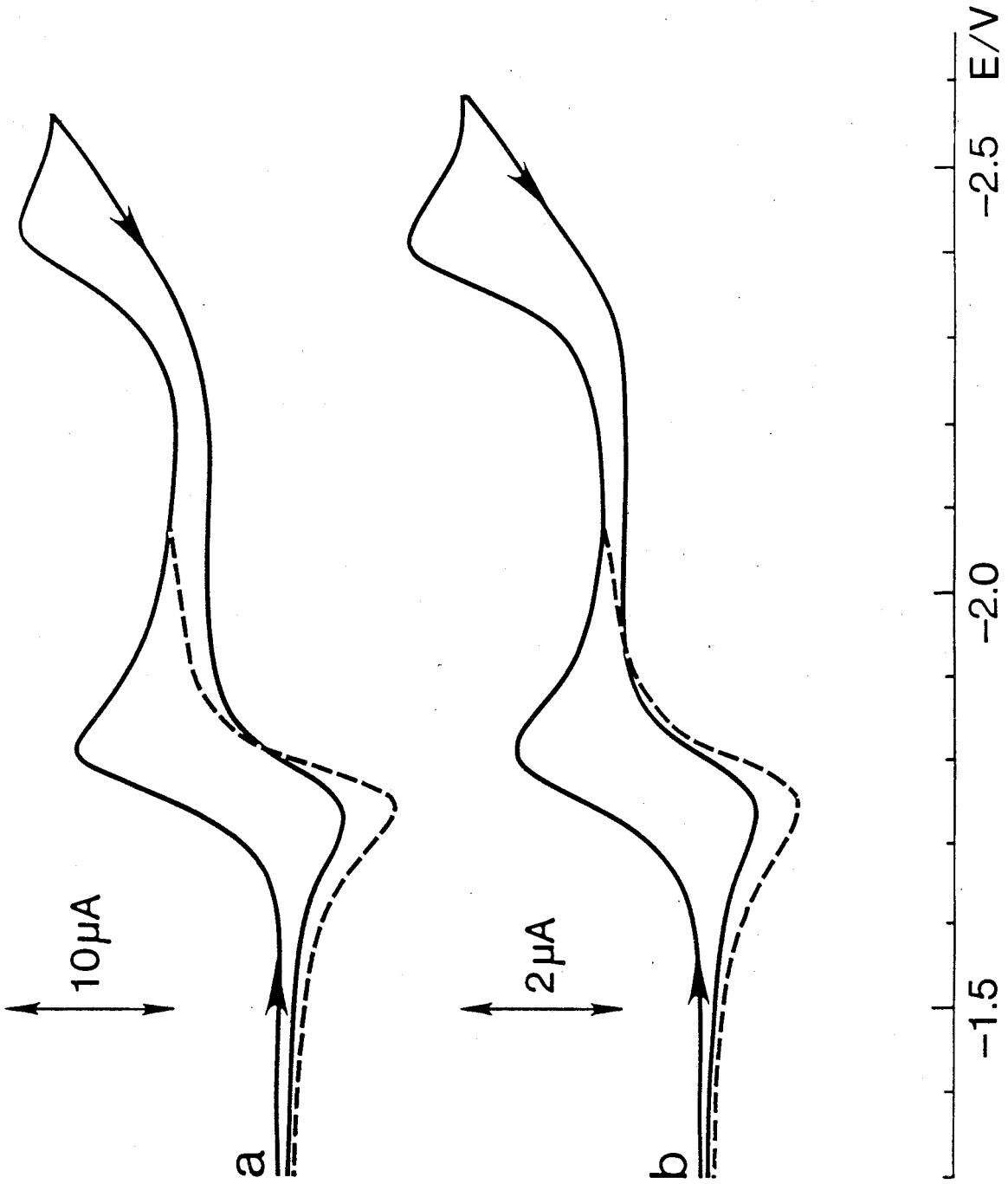
Figure 6: CYCLIC VOLTAMMOGRAMS OF BP AND PVBP:

a) BP 3mM

b) PVBP 12C (BP residues 2mM)

Scan rate  $0.05 \text{ Vs}^{-1}$ , 0.1M TEAP/DMF.

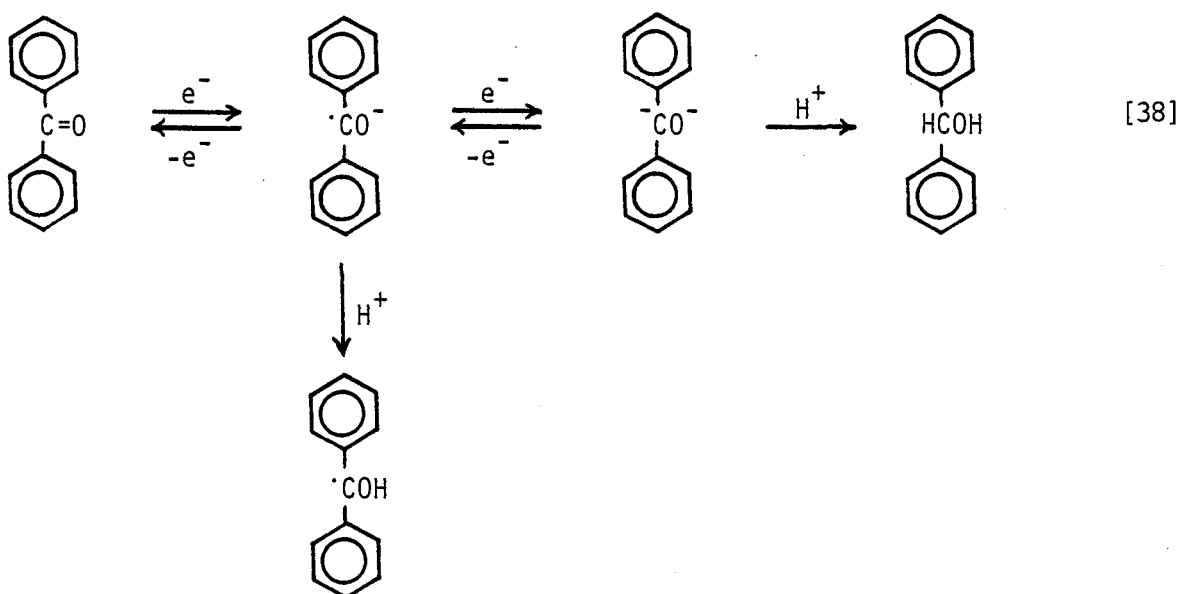




Nernstian behavior of BP/BP<sup>-</sup> couple.

When the potential was extended to -2.55 V, a second reduction wave due to the reduction of BP radical anion to BP dianion was observed. However, on the reverse scan, no anodic wave corresponding to the reoxidation of the dianion was obtained. This is due to the protonation of BP dianions by impurities, most likely the residual water, to form an unoxidizable product.

The second reduction peak is somewhat smaller than the first one. Presumably, a fraction of BP radical anions formed had reacted with impurities before the former could be further reduced. This intervening reaction may also be responsible for a decrease in the peak current of the anodic wave at -1.73 V, when the switching potential was extended to a more negative value. The overall reaction can be presented in the following scheme:



The cyclic voltammetry of a PVBP solution ( BP%=100,  $\bar{M}_n=2.11 \times 10^4$ ) is similar to that of BP, despite the fact that the polymers require the transfer of a large number of electrons per molecule. The voltammogram of the polymer consists of two reduction waves; both occur at potentials almost identical to those for BP. The first reduction is reversible and has characteristics of a Nernstian process whereas the second reaction does not produce a reoxidation peak. Similar features were also observed for polymers with different molecular weights and BP contents. However, in polymer systems, the peak current is much smaller compared to that obtained with a BP solution. This is due to the smaller diffusion rate of the polymer molecules, as the current is related to the diffusion coefficient of the electroactive species.

The similarity in the electrochemical properties of the molecular BP and of attached BP groups is also evident in the voltammetry at a rotating electrode. As seen from figure 7, the current-potential responses of both monomeric and polymeric compounds consist of two well-defined waves, which correspond to the formation of radical anions and dianions. Again, the half-wave potential and the shape of the RDE voltammogram of the polymers are almost identical to those of BP. A further examination of the reversibility of BP and PVBP can be made from the  $(E - E^{1/2})$  vs.  $\log \left( \frac{i_1 - i}{i} \right)$  plot. Theoretically, a reversible species should yield a straight line with a slope of  $59/n$  mV, in accordance with the following equation:

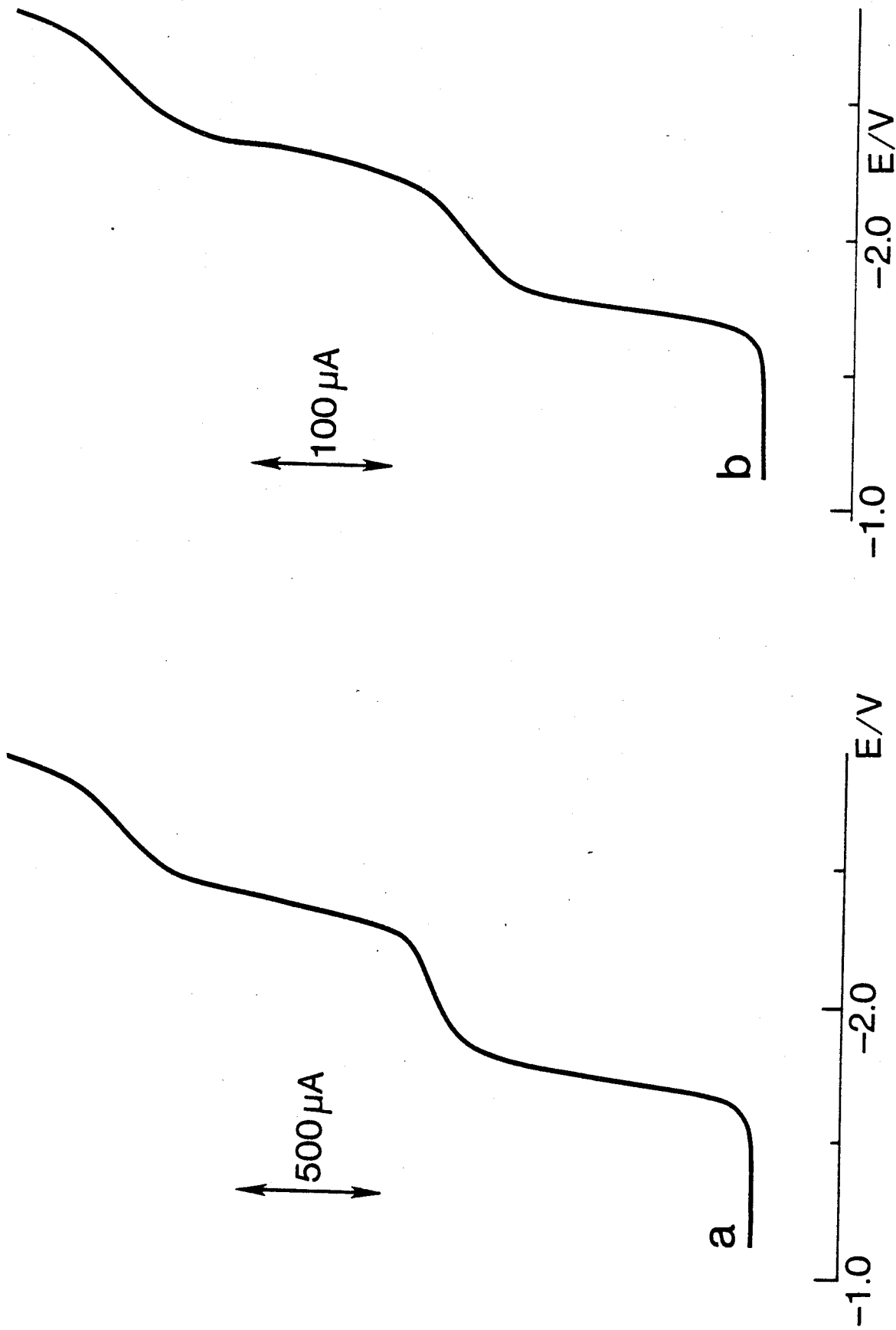
$$E = E_{1/2} - 0.059 \log \left( \frac{i_1 - i}{i} \right) \quad [16]$$

Figure 7: ROTATING DISK ELECTRODE VOLTAMMOGRAMS OF:

a) Benzophenone 2.9 mM

b) Polyvinylbenzophenone (3 mM benzophenone residues,  $\bar{M}_n = 1.8 \times 10^4$ , VBP% = 61)

Rotation rate =  $148 \text{ rads}^{-1}$ , 0.1M TEAP/DMF.



Indeed, the data for BP and PVBP shown in figure 8 indicate the expected reversible behavior. The plots are linear with the slopes estimated to be 62 and 67 mV for BP and PVBP, respectively. The results are thus consistent with data obtained from cyclic voltammetry and indicate that the electrochemical characteristics of BP moieties in a polymer chain are unchanged from that of BP molecule.

Flanagan et al. developed a theory for molecules containing multiple, identical, non-interacting centers (3). The results showed that such compounds would exhibit a current-potential curve with the half-wave potential and the overall shape identical to those of a molecule with a single center. However, in the study of polyvinylferrocenes, Smith et al. found that although the polymers produced voltammograms with the shape and potential similar to that of the ferrocene molecule, only a fraction of active centers on the chain was actually oxidized (1). This led them to suggest that field and proximity effects had lowered the number of residues accessible for the oxidation at the electrode. Recently, Morishima and co-workers studied the electrochemical behavior of polymers containing 10-methyl phenothiazine groups (30). The results revealed that the active residues in the homopolymers could be oxidized quantitatively whereas in copolymers, 20 ~ 30% of redox centers remained unoxidized. They concluded that the process of electron self-exchange between neighboring groups in a homopolymer chain had facilitated the exhaustive oxidation.

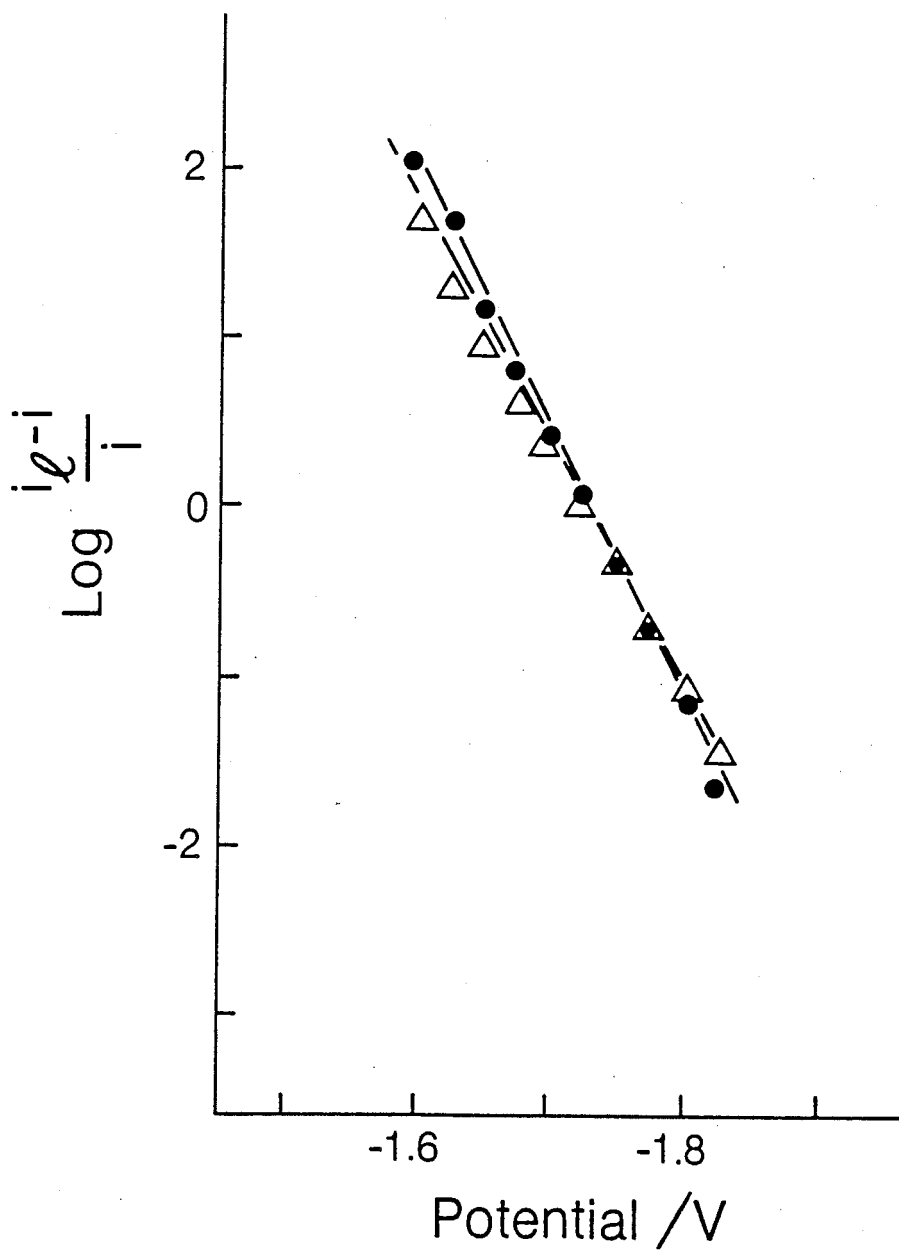


Figure 8: NERNSTIAN PLOTS OF BP AND PVBP-ST

● 2mM BP

△ 2 mM PVBP-St

In the present work, it was shown that PVBP polymers exhibit voltammograms with shape and peak potentials similar to those found for a BP molecule. This does not imply absence of interference from neighboring groups. For example, the reduction of a particular group on a chain may conceivably shield its neighbors from the subsequent reduction. To examine if such effects occur in the PVBP system, a series of polymers was studied with the same backbone chain length but with differing amounts of BP attached to a polymer chain. It was expected that if each active center behaved independently, solutions of polymers of similar chain length but with varying BP contents should yield similar voltammetric currents, when the concentrations of BP moieties are maintained constant. Otherwise, a variation in the currents will be observed when the spacing between BP sites changes.

The RDE technique was employed for this study and the data were analysed on the basis of the Levich equation:

$$i_1 = 0.62nFACD^{2/3}v^{-1/6}\omega^{1/2} \quad [14]$$

Figure 9 compares the limiting currents obtained with PVBP 2A and PVBP 2C samples, whose degrees of polymerization are identical but whose BP contents are 37% and 100%, respectively. The total number of electroactive groups was maintained at an equal value by adjusting the polymer concentration in the solution. Thus, the solution of PVBP 2A had a higher polymer concentration than the PVBP 2C.

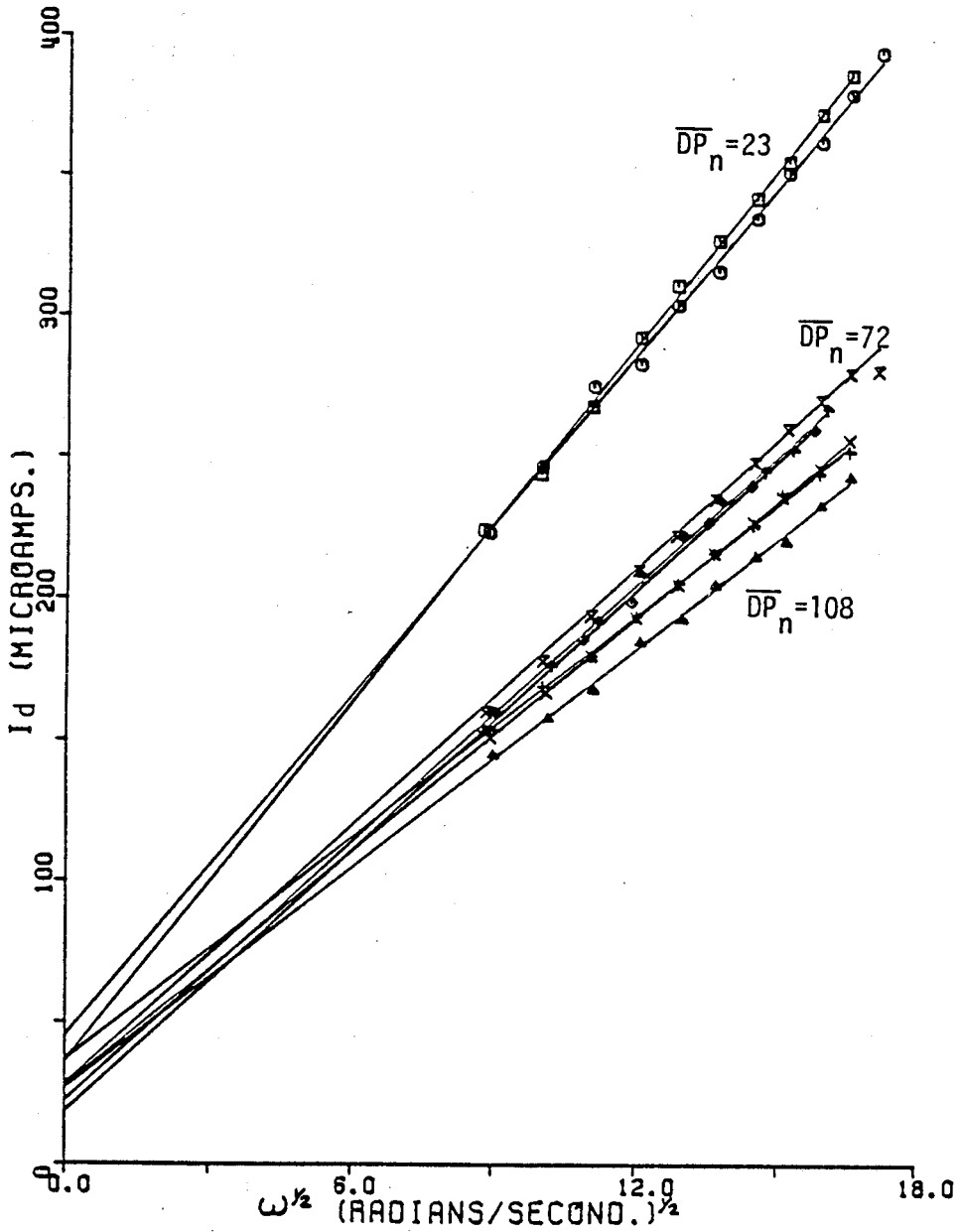


Figure 9: EFFECT OF VARYING SPACING OF ELECTROACTIVE CENTERS FOR THREE VALUES OF  $\overline{DP}_n$  IN SOLUTION OF 2.8 mM VBP

$\overline{DP}_n = 23$ ,  $\square$  % VBP = 37,  $\odot$  % VBP = 100

$\overline{DP}_n = 72$ ,  $\times$  % VBP = 31,  $\diamond$  % VBP = 77,  $\uparrow$  % VBP = 89

$\overline{DP}_n = 108$ ,  $\times$  % VBP = 31,  $+$  % VBP = 61,  $\triangle$  % VBP = 89



If the postulates of Smith were generally applicable, a three fold variation in  $i_1$  would be observed. On the other hand, if the process of electron self-exchange between adjacent groups occurred in the PVBP homopolymers and not in copolymers as proposed by Morishima et al., the PVBP 2A solution should produced much smaller currents than the PVBP 2C. Instead, the data are almost identical for the two polymers. The absence of appreciable interaction is thus demonstrated quite clearly. The pendant BP groups act independently in the electrochemical reduction of PVBP polymers.

To further examine the effect of chain length on the electroactivity of pendant groups, experiments were also performed on polymers with greater backbone chain length. Samples of  $\overline{DP}_n = 72$  and  $\overline{DP}_n = 108$  were chosen and polymers with 30%, 60% and 90% of repeating units with attached BP were examined. The data are shown in Figure 9 and again indicate no significant change in  $i_1$  for equal concentrations of BP centers. All the electroactive groups attached to the backbone were reducible at the electrode.

The results presented here thus provide strong evidence that active moieties on a PVBP chain behave as non-interacting centers. Pendant BP groups retain all the electrochemical characteristics of the BP molecule so that the voltammetric peaks of polymers appear at the same potentials, have the same shape and show the same reversibility found for molecular BP. Quantitative analysis of the voltammetric currents further indicates that each active group on a chain is accessible to the

reduction at the electrode.

c) Determination of Diffusion Coefficient of PVBP

Polymers

The Levich equation relates the limiting current  $i_1$ , measured at a rotating disk electrode, to the diffusion rate, the concentration of electroactive entities, the number of electrons transferred per group, the kinematic viscosity of the solution, the rotation rate and the area of the electrode. Thus, the diffusion coefficient  $D$  can be determined by measuring  $i_1$  at various rotation rates. A plot of  $i_1$  vs.  $\omega^{1/2}$  should yield a straight line with a slope of  $0.62nFACD^{2/3}\nu^{-1/6}$ , from which the value of  $D$  can be calculated.

However, the evaluation of the diffusion constants by this method is accurate only if the "real concentration" of the electroactive species is known. The "real concentration" reflects the number of redox species which actually get involved in the electrode reaction. For a monomeric system without the complication of adsorption or intervening chemical reaction, generally this concentration can be taken as the bulk concentration of active species. However, for a polymer system, such a treatment may cause considerable errors as some active residues on a chain may not be electrolyzed. This is exemplified by vinylferrocene polymers.

In the present work, it has been shown that each BP center in a polymer chain behaves independently and is accessible to reduction at the electrode. Thus, it is possible to utilize the bulk concentration of BP residues for the concentration term in

the Levich equation. Diffusion coefficients thus determined are listed in table 4. The D value decreases as the polymer molecular weight increases. The results thus indicate that the pendant BP groups retain their individuality and electrochemical characteristics, but their rate of transport is determined by the kinetic movement of the chain to which they are attached.

d) Relationship Between Diffusion Coefficient and Molecular Weight

The diffusion coefficient D can also be determined from solution properties of polymers. For flexible polymer molecules in a dilute solution, it was shown that the diffusion coefficient is related to the molecular weight by (43):

$$D = K_T M^{-b} \quad [39]$$

$K_T$  is a constant and the value of the exponent b varies from 0.50 for a poor solvent to 0.55 for a good solvent. The variation in b results from the changes in chain conformation which occur as the chains coil or become extended in the solvent. An approximate value of 0.55 was utilized by Bard and co-workers in their studies of polyvinylferrocene, poly(vinyl-2-naphthalene) and poly(vinyl-9-anthracene) in THF to estimate the diffusion coefficient of the polymers.

According to equation [39], a double logarithmic plot of D vs. M yields a straight line with an intercept  $K_T$  and a slope of -b. This plot is shown in figure 10 for polymers containing an average of 30% BP. As predicted, the plot is linear and a b

Table 4: Diffusion Coefficients of Benzophenone,  
Polyvinylbenzophenone and Its Copolymers with Styrene.

---

Electroactive Compounds	$\bar{M}_n \times 10^{-4}$	$D \times 10^7$ ( $\text{cm}^2 \text{s}^{-1}$ )
BP	0.0182	89.6
P2A	0.32	14.8
P2C	0.47	14.1
P5A	0.74	11.3
P5B	0.93	10.7
P8A	0.98	9.29
P8B	1.33	8.65
P8C	1.42	8.69
P12A	1.46	7.33
P12C	2.11	6.46
P40A	5.27	3.98
P200A	30.0	1.76

---

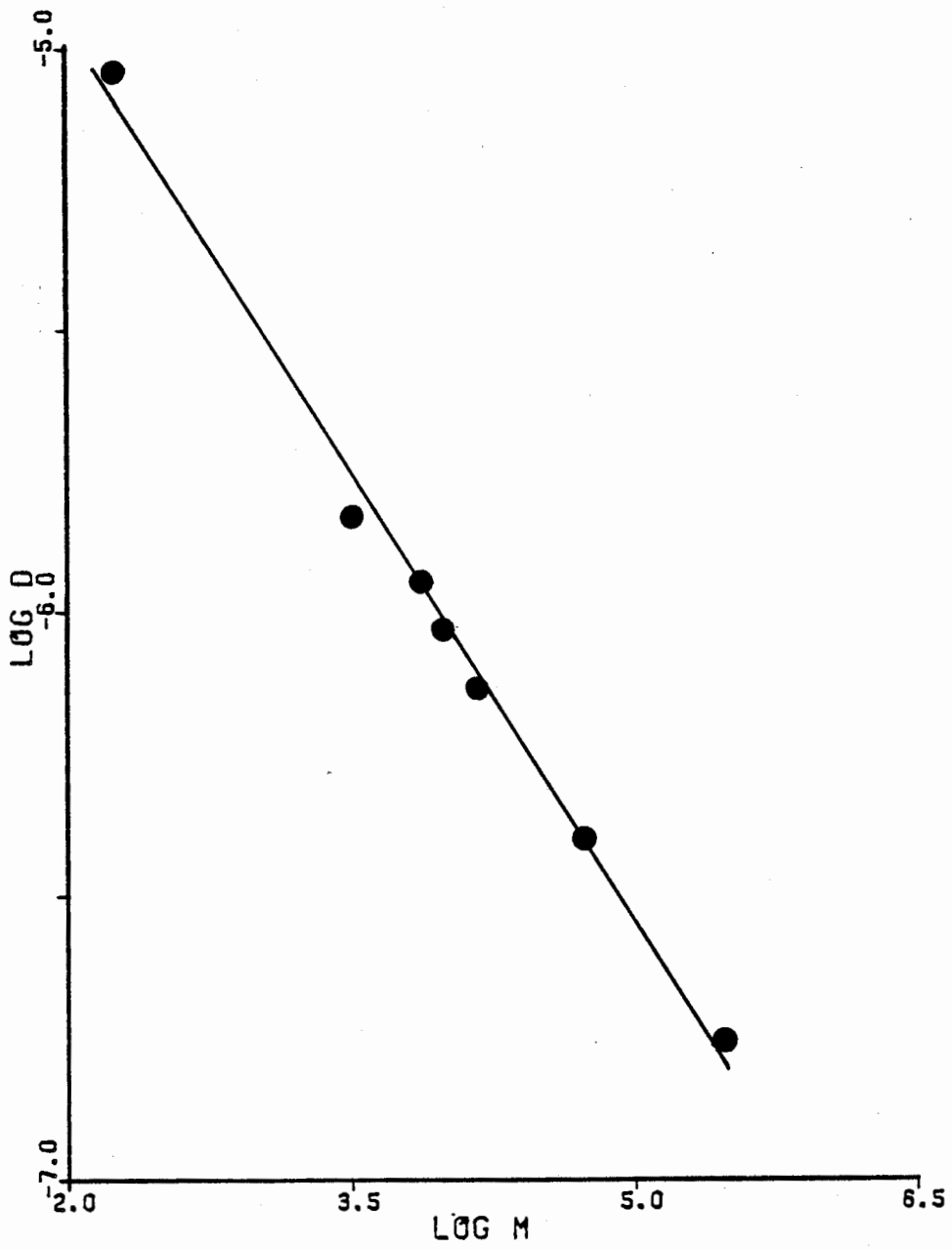


Figure 10: RELATIONSHIP BETWEEN DIFFUSION COEFFICIENT AND MOLECULAR WEIGHT FOR PVBP-ST

value of 0.53 was obtained. The b value indicates that DMF is an intermediate solvent for the PVBP-St copolymers.

The parameter b can also be determined by viscosity measurements, because b is related to the exponent a of the Mark-Houwink equation for the limiting viscosity number (see Section I.1.5.):

$$[\eta] = KM^a \quad (K=\text{constant}) \quad [32]$$

where  $b = (1 + a)/3$  [35]

The limiting viscosity numbers  $[\eta]$  of PVBP-St copolymers in 0.1M TEAP/DMF solution were measured and are listed in table 4. From the  $\log([\eta])$  vs.  $\log \bar{M}_n$  plot shown in figure 11, a and K were estimated to be 0.58 and  $3.39 \times 10^{-4}$ , respectively. The a value determined viscometrically is in good agreement with the value of 0.59 obtained electrochemically. The results thus confirm the independent, non-interacting characteristics of pendant BP groups in a polymer chain, and indicate the validity of estimating the diffusion coefficient of polymers by the rotating disk electrode technique.

e) Relationship Between Limiting Current and Molecular Weight

Since both the limiting current  $i_1$  and the polymer molecular weight M are related to the diffusion coefficient, a relationship between  $i_1$  and M can be derived. This suggests a new method of determining molecular weights by electrochemical techniques.

Substituting equation [39] into the Levich equation gives:



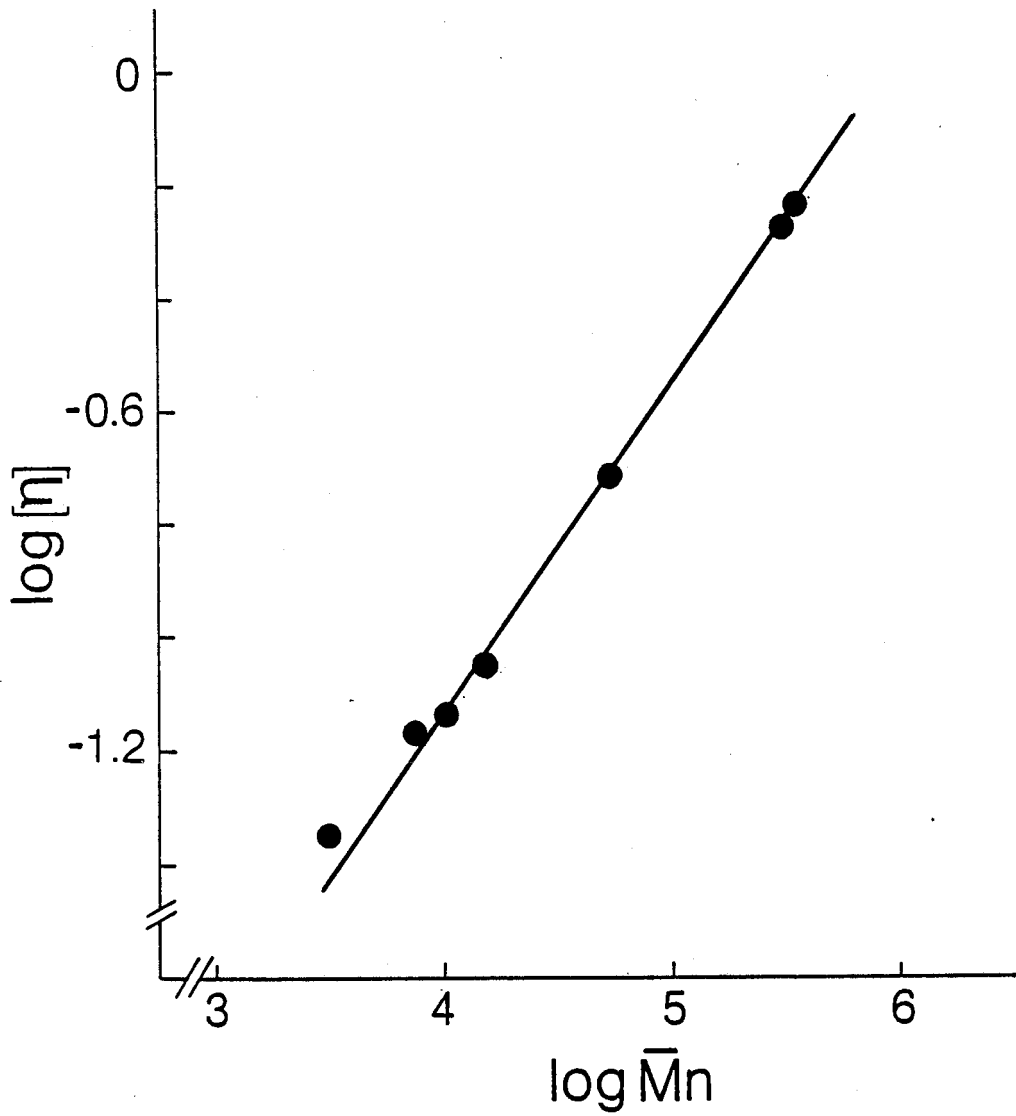


Figure 11: RELATIONSHIP BETWEEN LIMITING VISCOSITY NUMBER AND MOLECULAR WEIGHT FOR PVBP-ST

$$i_1 = kM^{-h} \quad [40]$$

where

$$k = 0.62nFACv^{-1/6}D^{2/3}\omega^{1/2}K_T^{2/3} \quad [41]$$

and

$$h = 2b/3 \quad [42]$$

A plot of  $\log i_1$  vs.  $\log \bar{M}_n$  for PVBP-St polymers is shown in figure 12 and a linear relationship is observed. This indicates the feasibility of determining polymer molecular weights from voltammetric measurements. However, one should keep in mind that the success of such an application requires conditions of ideality in the electrochemical behavior of polymers. The electroactivity of active centers should not be influenced by the presence of their neighboring groups nor by the macromolecular environment, and all active sites should be available for an electrode reaction.

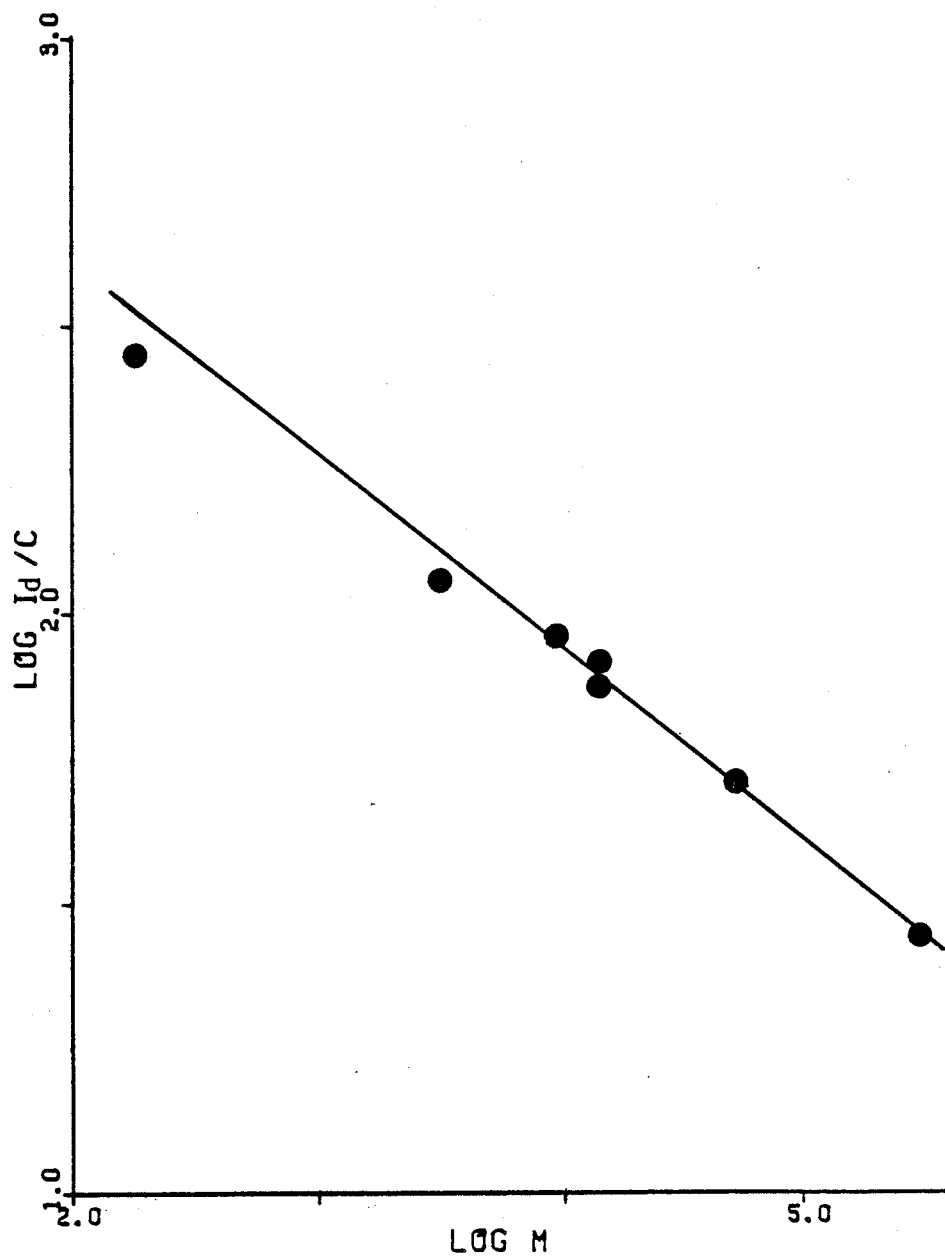
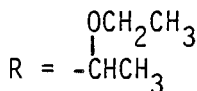
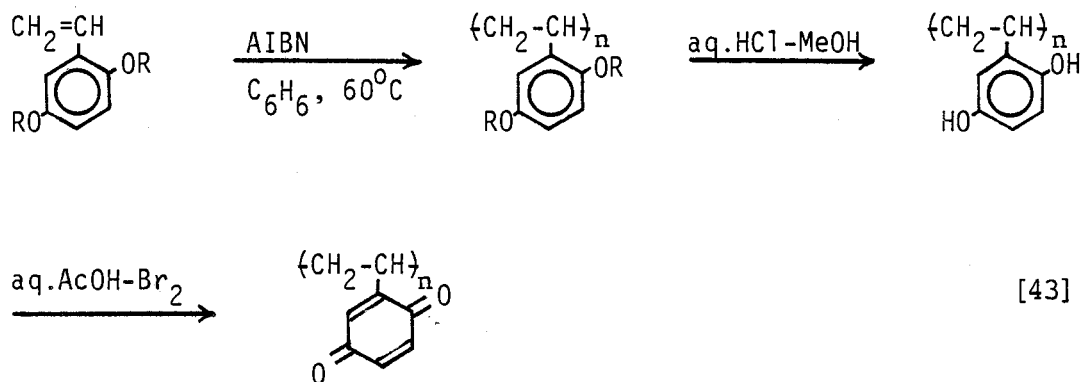


Figure 12: RELATIONSHIP BETWEEN LIMITING CURRENT AND MOLECULAR WEIGHT FOR PVBP-ST

I.3.2. Electrochemical Studies of Poly(vinyl-p-benzoquinone) (PVBQ) and Its Copolymers with Styrene (PVBQ-St)

a) Synthesis of Polymers

PVBQ and PVBQ-St were prepared by a procedure described by Cassidy et al. (34). The reaction scheme for synthesizing PVBQ is shown as follows:



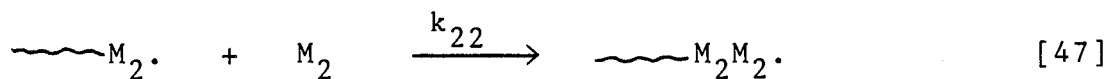
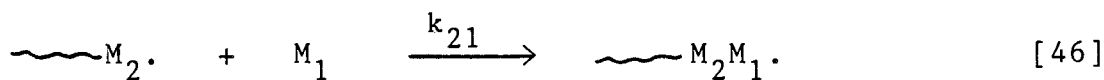
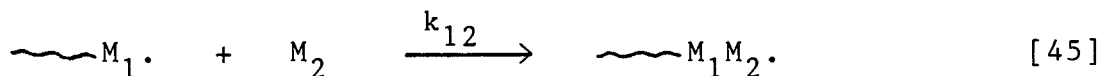
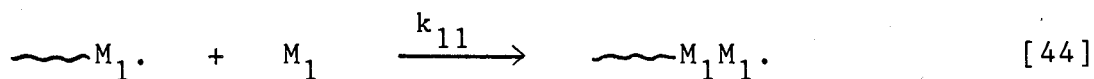
The molecular weight and composition of polymers are shown in table 5.

Since PVBQ-St polymers were obtained by a copolymerization reaction, they may have a block, random or alternating structure. The purpose of copolymerization was to vary the spacing between active centers and therefore, it is instructive to examine the distribution of comonomer units in a chain. This can be

Table 5: Composition, Molecular Weight and Molecular Weight Distribution of PVBQ and PVBQ-St

Polymers	VBQ %	$\bar{M}_n \times 10^{-5}$	$\bar{M}_w/\bar{M}_n$
PVBQ	100	2.82	6.3
PVBQ-St 1	70.6	8.7	8.0
PVBQ-St 2	58.1	5.5	8.5
PVBQ-St 3	52.9	1.15	4.5
PVBQ-St 4	36.8	1.05	4.0
PVBQ-St 5	24.5	1.35	4.3
PVBQ-St 6	10.7	1.05	2.5

calculated from the copolymerization reactivities of the monomers. Copolymerization reactivities  $r_1$ ,  $r_2$  for monomers  $M_1$  and  $M_2$ , respectively, are defined in the following equations, where eqs. [44]-[47] represent four possible propagation steps of a radical copolymerization process:



$$r_1 = k_{11}/k_{12} \quad [48]$$

$$r_2 = k_{22}/k_{21} \quad [49]$$

Copolymerization reactivities of VBEH ( $r_1$ ) and styrene ( $r_2$ ) in the same experimental conditions have been determined by Cassidy et al. , and were reported to be  $r_1=0.5$  and  $r_2=0.9$ , respectively (49). That  $r_1 < 1$ , ie.  $k_{11} < k_{12}$ , implies that during the course of copolymerization, the VBEH radical reacts more readily with styrene than with the VBEH monomer. In other words, in a VBEH-St copolymer chain, VBEH groups tend to be separated by styrene units rather than forming blocks.

#### b) Voltammetric Studies

The electrochemical behavior of solutions of p-benzoquinone (BQ), methyl-p-benzoquinone (MeBQ), PVBQ and PVBQ-St (VBQ=24.5%) in 0.1M TEAP/DMSO is compared in Table 6 and Figure 13. MeBQ was selected as a model of the base unit in the PVBQ polymer chain. Its reduction occurred at a potential 90 mV more negative than for BQ. This was considered due to the inductive effect of the substituent group. Very little shift was observed in the peaks positions between MeBQ and the polymers with pendant quinone groups. This indicates that the polymer backbone and the substituting methyl group exerted the same effect on the reduction of benzoquinone.

In contrast to the reversible behavior found for BQ and MeBQ, the PVBQ homopolymer produced a voltammogram with the anodic peak greatly suppressed. This implies that the pendant

Figure 13: CYCLIC VOLTAMMOGRAMS OF SOLUTIONS OF

a) BQ

b) MeBQ

c) PVBQ

d) PVBQ-St (VBQ% = 24.5)

Scan rate  $0.05 \text{ Vs}^{-1}$ , in 0.1M TEAP/DMSO.

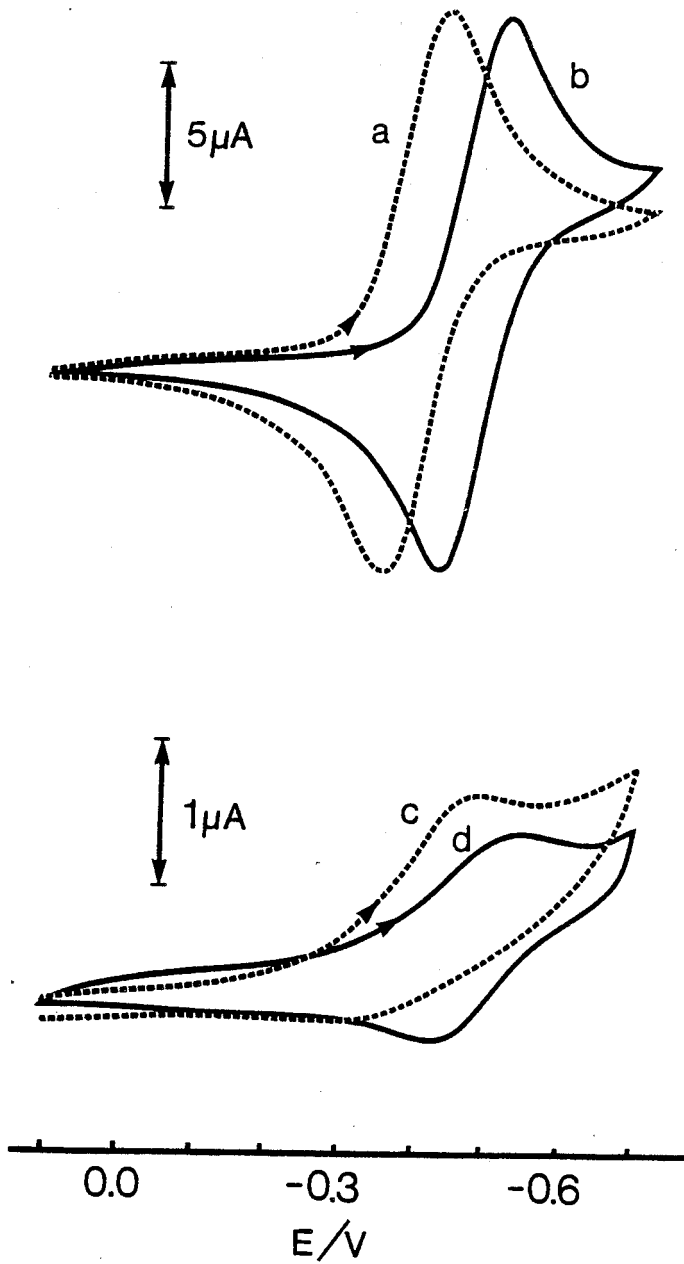




Table 6: Cyclic Voltammetry of Quinone Species in Solution<sup>a)</sup>

Compounds	$E_{pc}/V$	$E_{pa}/V$	$E_{1/2}/V$	$\Delta E/mV$
BQ	-0.41	-0.31	-0.38	74
MeBQ	-0.50	-0.43	-0.47	74
PVBQ	-0.49	-	-	-
PVBQ-St	-0.53	-0.47	-0.51	71

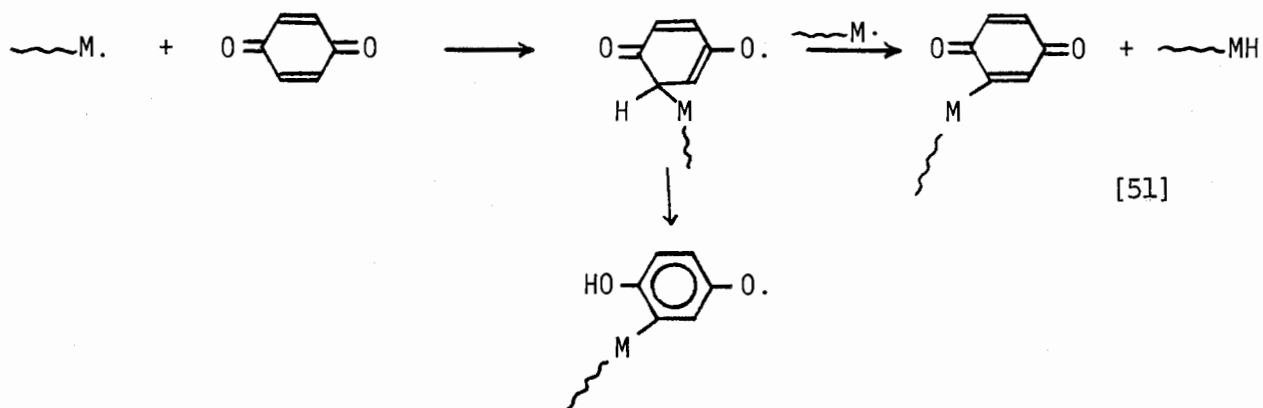
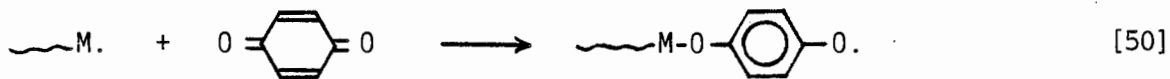
a) 0.1M TEAP/DMSO, 0.05 Vs<sup>-1</sup>, SCE.

benzoquinone radical anions formed in the forward scan were rapidly deactivated so that they could not be reoxidized.

However, the voltammetry of a PVBQ-St copolymer with 24.5% VBQ content yielded a reversible, one-electron transfer wave similar to that of the MeBQ model compound. Thus, the absence of an oxidation peak in the voltammogram of the PVBQ homopolymer must be associated with the increasing proximity between active centers. A possible explanation is the occurrence of an irreversible chemical reaction involving pendant semiquinones with their neighboring groups. In a copolymer chain, the BQ centers are separated by styrene units and the interaction is reduced.

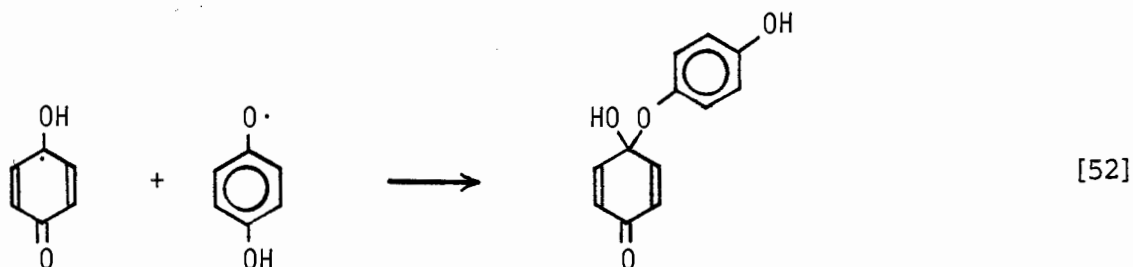
Benzoquinone is known to be reactive to radicals. Indeed, this compound has often been used as an inhibitor for radical

polymerization (50). Yassin and Risk reported that a propagating radical may attack at either a C or O atom of a quinone as shown in the following schemes (51,52):

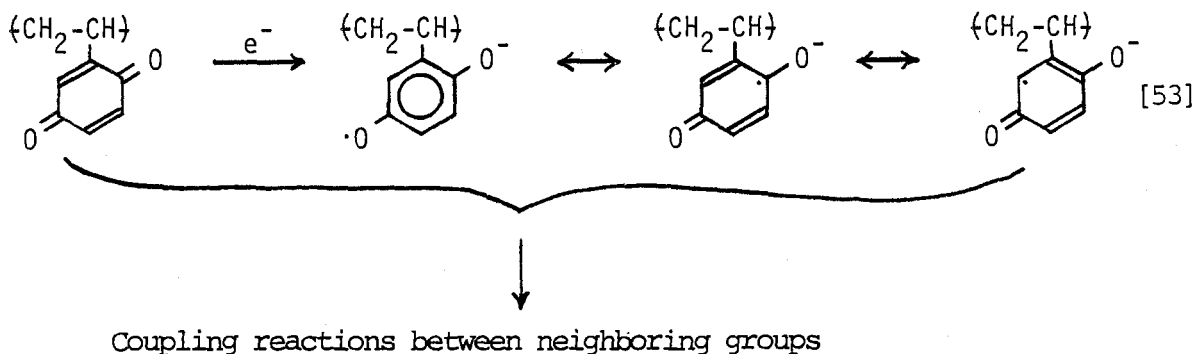


The resulting aryloxy radical may be terminated by coupling and/or disproportionation with another propagating radical or add monomer.

Chambers et al. studied the voltammetric reduction of p-benzoquinone in an acidic solution and reported that the protonated quinone radicals can combine to form a dimer (53):



On the basis of these references, it is suggested that the chemical interaction in PVBQ homopolymers may occur via the coupling of two adjacent radical anions, or via the reaction of semiquinone groups with their neighboring, unreduced centers:



The near-neighbor interaction is further evident from the comparison of the cyclic voltammograms of PVBQ-St copolymers of differing VBQ contents. As seen from Figure 14, the  $i$ -E response is irreversible for a copolymer with 70.6% VBQ content, and the reversibility increases as the VBQ content decreases. An almost reversible behavior is observed for a copolymer with VBQ content of 10.7%.

The occurrence of a chemical reaction between a semiquinone with a neighboring active center is also shown in the peak height of the second wave corresponding to the further reduction to dianion (Figure 15). For this reduction, MeBQ produced a wave with the characteristics of a reversible, one-electron transfer process. A similar pattern was found for the PVBQ-St 6 copolymer (VBQ= 10.7%). In contrast, the voltammogram of the PVBQ polymer

Figure 14: CYCLIC VOLTAMMOGRAMS OF PVBQ-ST OF VARIOUS  
VBQ CONTENTS.

VBQ % :

a) 70.6

b) 58.1

c) 52.9

d) 36.8

e) 10.7

Scan rate  $0.05 \text{ Vs}^{-1}$ , 0.1M TEAP/DMF

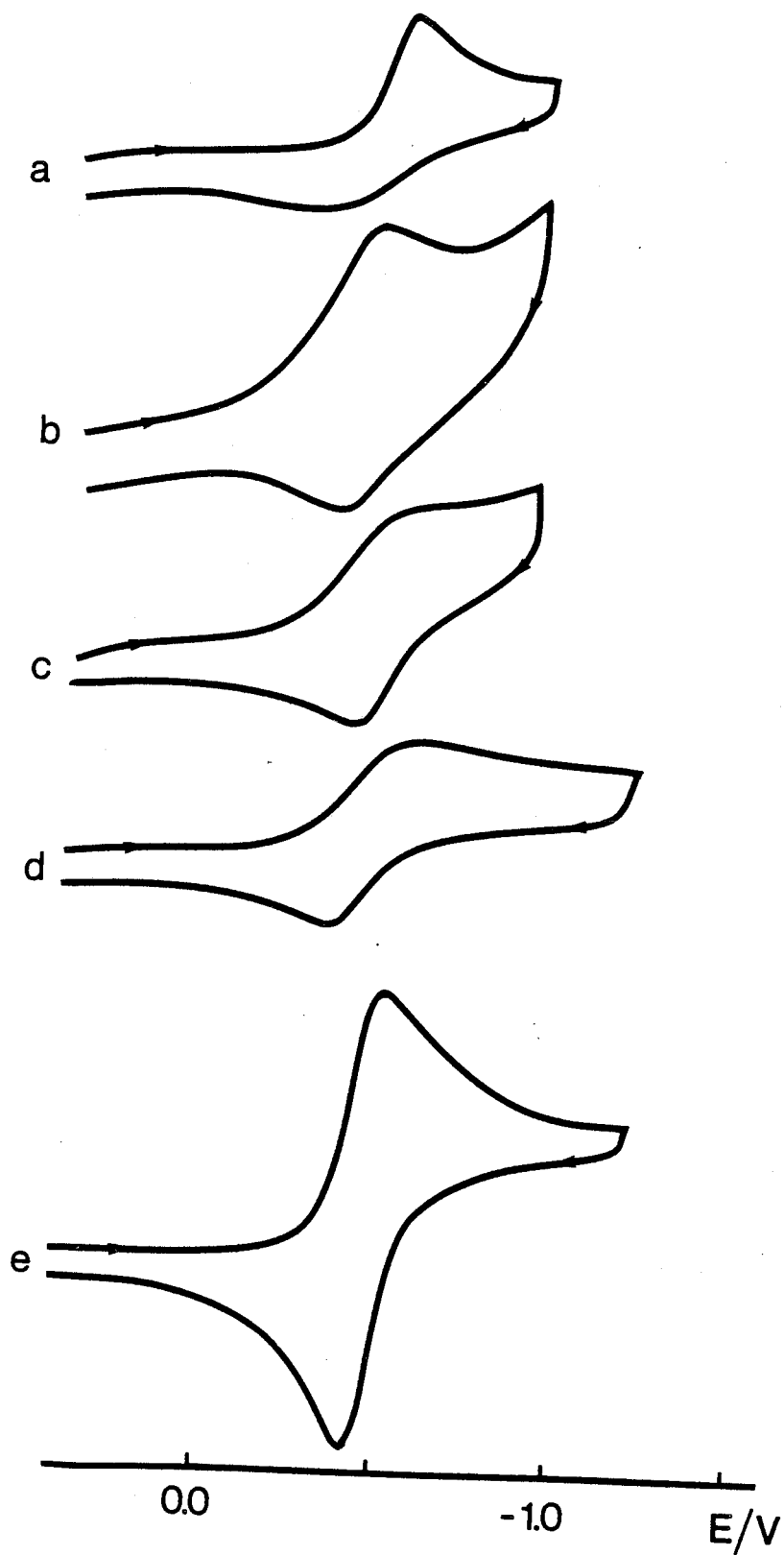


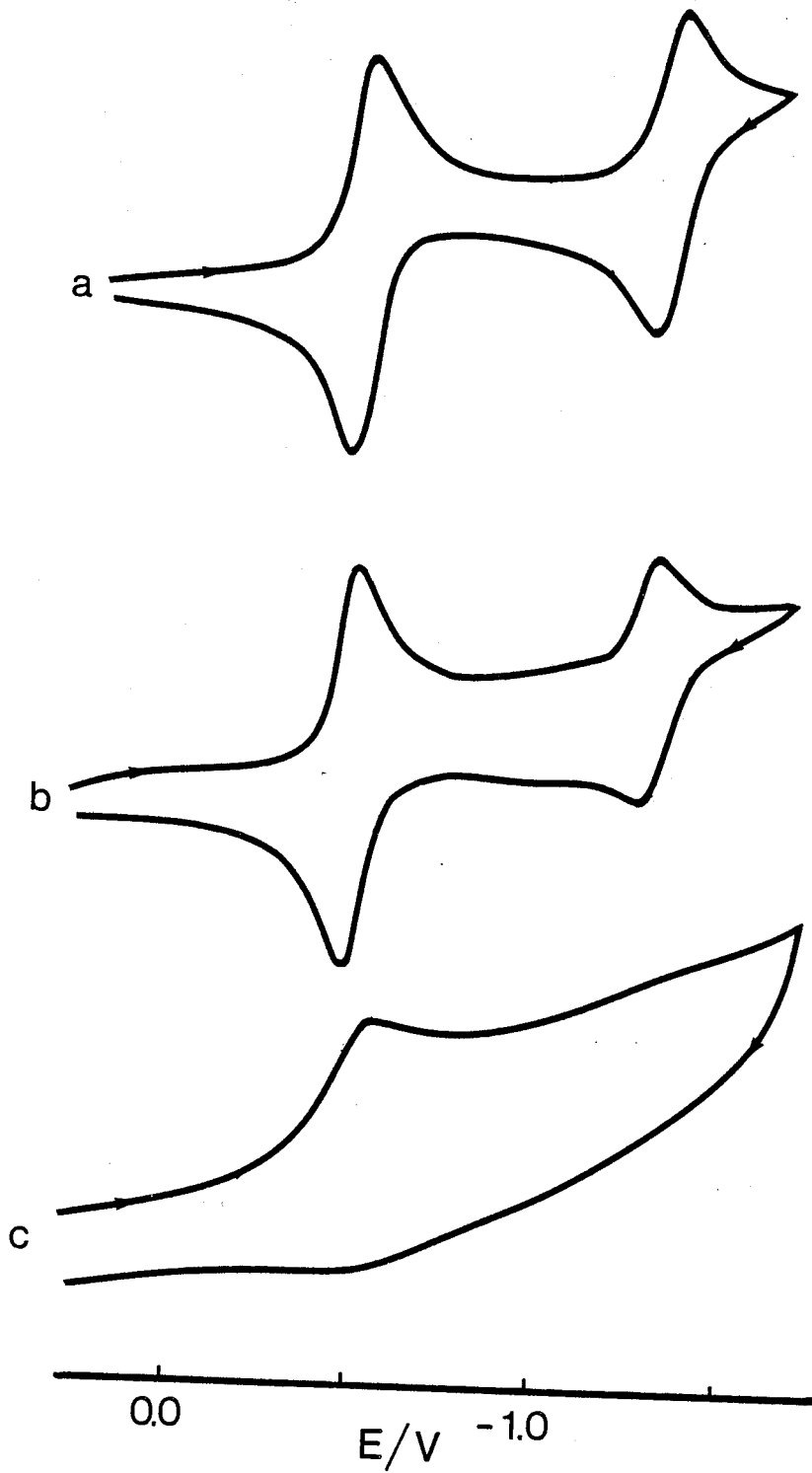
Figure 15: CYCLIC VOLTAMMOGRAMS OF SOLUTIONS OF

a) MEBQ

b) PVBQ-St (VBQ% = 10.7)

c) PVBQ

Scan Rate  $0.05 \text{ Vs}^{-1}$ , 0.1M TEAP/DMSO.



does not exhibit a second reduction peak. This implies that the  $PVBQ^{\cdot-}$  intermediate, which was formed in the reduction of PVBQ, could not be reduced further to the dianion. The results are thus consistent with the view that  $BQ^{\cdot-}$  moieties in a homopolymer chain reacted rapidly with their adjacent centers.

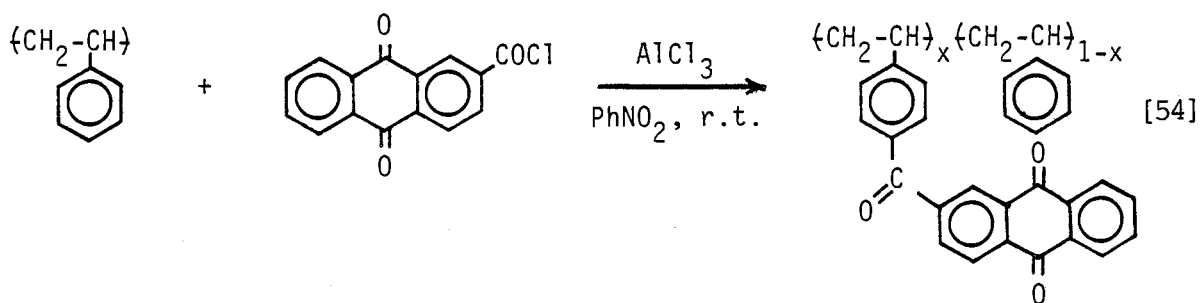
In summary, the electrochemical behavior of benzoquinone containing polymers has been examined, and the use of electrochemical techniques to probe the chemical interaction in a polymer chain has been demonstrated. In a copolymer chain where the BQ groups are sufficiently separated, the attached quinone moieties behave similarly to the model compound. The copolymer produced voltammograms with peak shape and potentials similar to those found for MeBQ. However, a chemical interaction occurred in a homopolymer chain, where the redox centers are adjacent to each other. The BQ radical anions produced in the reduction scan rapidly reacted with neighboring center and this resulted in a rapid deactivation of the electrochemical activity of the polymer.



I.3.3. Electrochemical Studies of Poly[p-(9,10-anthraquinone-2-carbonyl)styrene]-co-styrene (PAQ)

a) Synthesis of Polymers

PAQ was obtained by reacting polystyrene with 2-anthraquinone carbonylchloride with  $AlCl_3$  as catalyst as shown in the following reaction:



The molecular weight and composition of polymers are given in table 7.

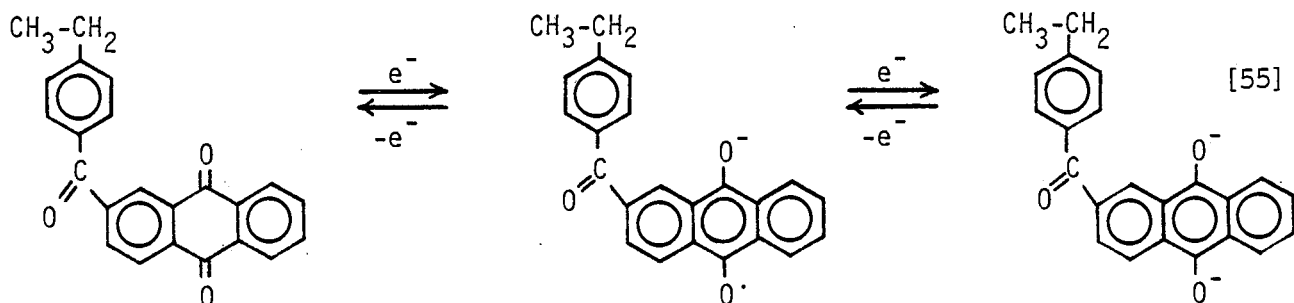
Table 7: Composition, Molecular Weight and Molecular Weight Distribution of PAQ

Polymers	AQ %	$\overline{DP}_n$	$\overline{M}_n \times 10^4$	$\overline{M}_w/\overline{M}_n$
PAQ 5(1)	19.3	} 52	0.78	} 1.2
PAQ 5(2)	41.3		1.04	
PAQ 5(3)	48.9		1.13	
PAQ 8	21.6	72	1.12	1.22
PAQ 12	23.1	108	1.71	1.14
PAQ 40	18.0	414	6.06	1.16
PAQ 200(1)	19.5	} 2170	32.6	} 1.35
PAQ 200(2)	28.0		36.9	
PAQ 200(3)	47.4		46.8	

b) Voltammetric Characteristics of Polymers

The electrochemistry of the model compound EBAQ and PAQ polymers was examined in 0.3M TEAP/Py-DMF (2/1 v/v) solution. This solvent system was chosen because of the poor solubility of the polymers in conventional solvents.

Cyclic voltammograms of EBAQ and of PAQ polymers are shown in figure 16 and the data are summarized in table 8. Between 0.0 V and -1.7 V (vs. SCE), the voltammetry of EBAQ produced two reversible waves with half-wave potentials of -0.74 V and -1.29 V, respectively (Figure 16a). For both waves, the difference between the anodic and cathodic peak potentials is ~60 mV and  $i_{pa}/i_{pc}$  is unity. These are characteristics of a reversible, one-electron transfer process. The first wave is due to the reduction of EBAQ to its radical anion, and the second to the further reduction to  $EBAQ^{2-}$  as shown in the following scheme:



The voltammogram of a PAQ 40 sample consists of two reduction waves at potentials similar to those of EBAQ (figure

Figure 16: CYCLIC VOLTAMMETRY OF SOLUTIONS OF

a) EBAQ (1.29 mM)

b) PAQ 40 (1.55 mM anthraquinone residues).

Scan rate  $0.05 \text{ Vs}^{-1}$ , 0.3M TEAP/Py-DMF (2/1, v/v)

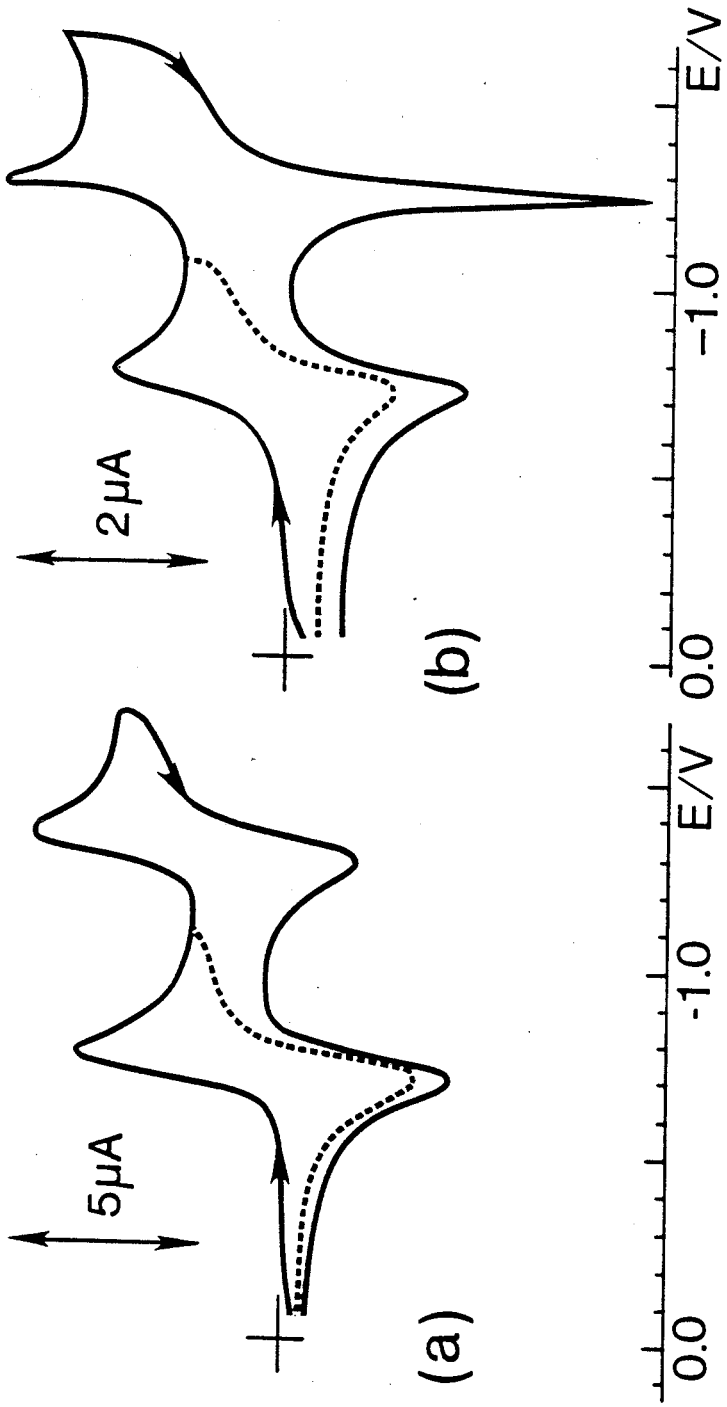


Table 8: Voltammetric Characteristics of Anthraquinone Species in Solution.<sup>a)</sup>

Compounds	$E_{1/2}^1$ (V)	$\Delta E^1$ (mV)	$E_{1/2}^2$ (V)	$\Delta E^2$ (mV)
EBAQ	-0.74	61	-1.29	70
PAQ 200(1)	-0.76	60	-1.27	24

a) 0.3M TEAP/Py-DMF (2/1, v/v), 0.05 Vs<sup>-1</sup>, SCE.

16 b). For the first electrochemical process, the polymer shows characteristics of a dissolved, reversible redox couple whereas the second reaction yielded a sharp, anionic peak indicative of the adsorption of the PAQ<sup>2-</sup> polymer on the electrode surface. Polymers with a high AQ content such as PAQ 5(3) and PAQ 200(3) gave evidence of adsorption of the PAQ and of the PAQ<sup>-</sup> polymers. These samples were excluded from further study, and the investigation of the remaining samples was confined to the first reduction step to the radical anions and of their reoxidation.

To examine further the reversibility of the first reduction process of EBAQ and PAQ, the voltammograms were recorded at various potential sweep rates. The results are presented in figure 17. For both monomeric and polymeric compounds, peak

Figure 17: CYCLIC VOLTAMMETRY OF SOLUTIONS OF

a) EBAQ (1.29 mM)

b) PAQ 40 (1.55 mM anthraquinone residues).

Scan rate:

1)  $0.50 \text{ Vs}^{-1}$

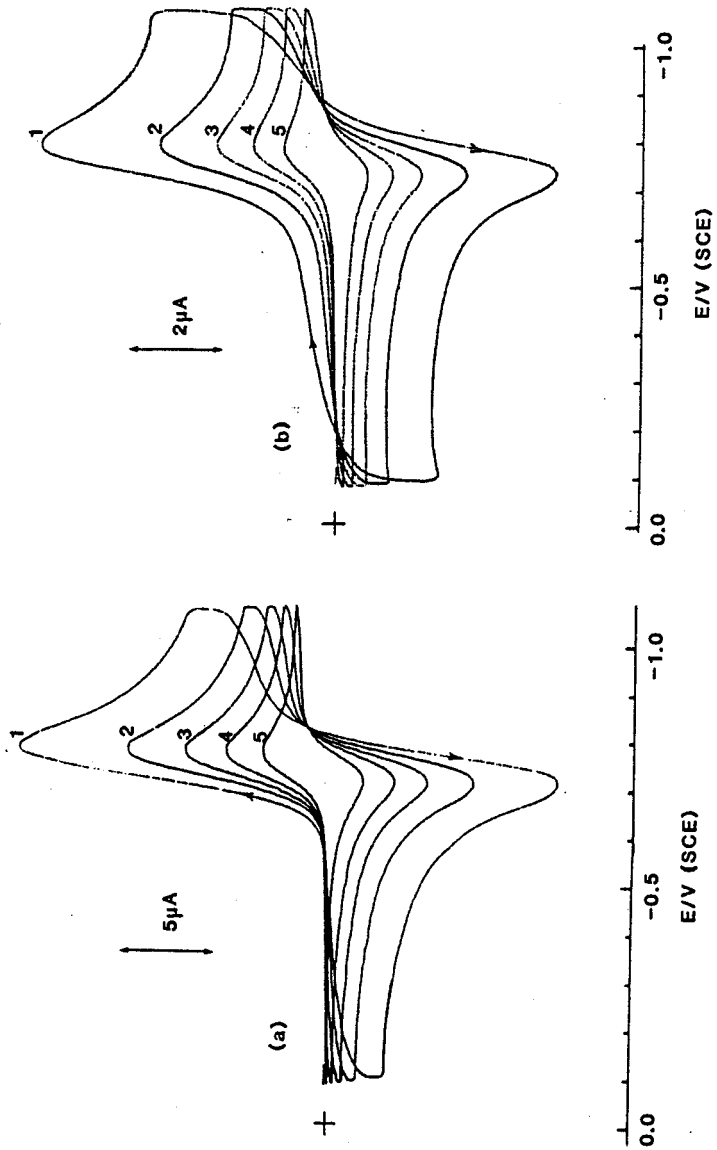
2)  $0.20 \text{ Vs}^{-1}$

3)  $0.10 \text{ Vs}^{-1}$

4)  $0.05 \text{ Vs}^{-1}$

5)  $0.02 \text{ Vs}^{-1}$

in 0.3M TEAP/Py-DMF (2/1, v/v)



potentials are independent of scan rate  $v$  for  $v \leq 0.5 \text{ Vs}^{-1}$  and peak currents are proportional to  $v^{1/2}$ . These characteristics suggest that the reduction of EBAQ and of PAQ polymers can be considered as a Nernstian process. The fact that the reduction of PAQ polymers produced voltammograms with the shape and peak potentials similar to those obtained with EBAQ indicates that the incorporation of AQ groups into a polymer chain does not have a significant effect on the electroactivity of the active centers.

As mentioned in section I.3.1.a), interactions between active centers may result in an inability to reduce certain groups in a polymer chain. To examine the possibility of such interactions, the voltammetry of polymers of the same chain length but with differing AQ contents was examined and the current magnitudes compared, in analogy to the study of PVBP polymers. The use of a RDE was attempted for this study but the method was unsuitable. The adsorption of  $\text{PAQ}^{2-}$  polymers on the electrode surface caused a dip in current after a current plateau and this made it difficult to determine accurately the limiting current of the first reduction wave. For this reason, the voltammetry was performed at a stationary electrode, and the data were analyzed on the basis of the Randles-Sevcik equation (37,38)

$$i_p = 2.69 \times 10^5 n^{3/2} A D^{1/2} C v^{1/2} \quad [4]$$

Eq. [4] implies that a plot of  $i_{pc}$  vs.  $v^{1/2}$  should give a straight line whose slope is proportional to  $D^{1/2}C$ . Thus, if the concentration of AQ moieties is maintained constant,



solutions of polymers of identical chain length should yield similar slopes. Failure to observe this is attributed to the shielding effects of neighboring groups and to the inability to reduce all the active centers.

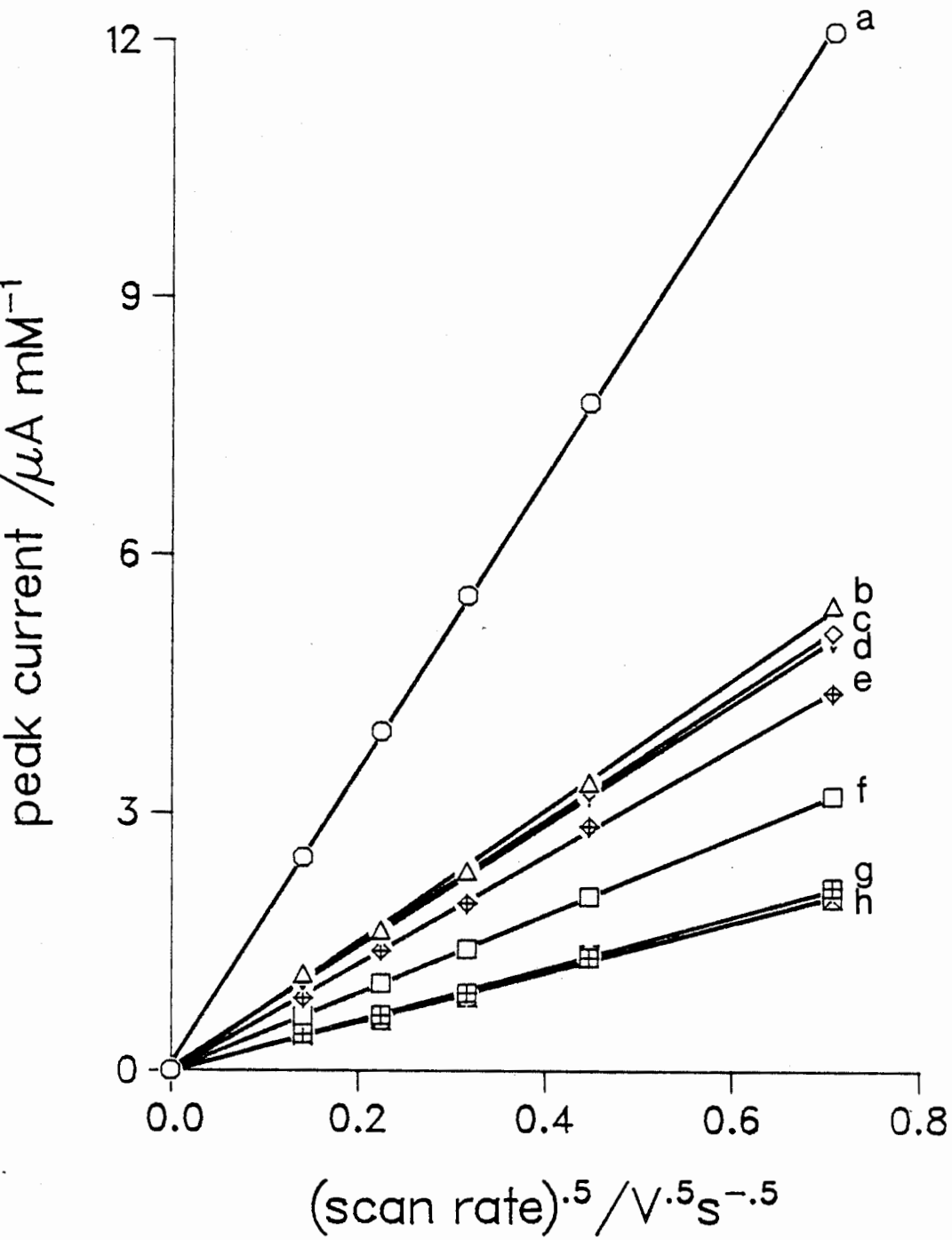
Plots of  $i_{pc}$  (normalized for the concentration of AQ residues) vs.  $v^{1/2}$  for a range of polymer chain lengths and for various spacings between electroactive groups are shown in figure 18. As predicted by the Randles-Sevcik equation, a linear relationship with zero intercept is obtained for all samples investigated. The slope decreases as the polymer chain length increases, but for samples of the same degree of polymerization, the currents are essentially independent of the number of electroactive groups on the chain. For example, PAQ 5(1) and PAQ 5(2) each have an average of 51.9 repeat units in the chain but have 19.3% and 41.3%, respectively, of pendant AQ groups. Despite this difference, the data are almost identical for these two samples. A similar pattern is also observed with PAQ 200(1) and PAQ 200(2), whose AQ contents are 19.5% and 28.0%, respectively.

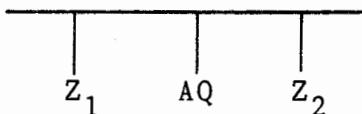
Since the AQ contents of polymers were less than 50%, one may think that in these molecules, the active centers were separated by at least one styrene unit along the chain. Therefore, one may expect an identical magnitude of current for polymers of identical chain length but differing AQ loadings. However, assuming the distribution of redox groups along the chain is random, the following calculation shows that the number of AQ sites, which are adjacent to one another on a chain, greatly varies with the AQ content of polymers.

Figure 18: PLOTS OF CATHODIC PEAK CURRENT AGAINST (SCAN RATES)<sup>1/2</sup> FOR 1 mM ANTHRAQUINONE RESIDUES.

- a) EBAQ
- b) PAQ 5(1)
- c) PAQ 5(2)
- d) PAQ 8
- e) PAQ 12
- f) PAQ 40
- g) PAQ 200(1)
- h) PAQ 200(2)

in 0.3M TEAP/Py-DMF (2/1, v/v)





Consider an AQ moieties and its two neighboring groups  $Z_1, Z_2$  on a copolymer chain. Let  $X$  be the fraction of AQ groups in the polymer, and  $(1-X)$  the fraction of styrene groups. The probability for structures such as AQ-AQ-AQ is  $X^2$ , AQ-AQ-St is  $2X(1-X)$  and St-AQ-St is  $(1-X)^2$ . Hence, the probability of an AQ group being adjacent to another AQ group is:

$$\begin{aligned}
 P &= X^2 + 2X(1-X) \\
 &= X(2-X) \qquad [56]
 \end{aligned}$$

The  $P$  value was calculated for each polymer and the results are listed in table 9. For PAQ 5(1) and PAQ 5(2) copolymers, 34.9% and 65.5%, respectively, of the AQ groups in the chain are expected to be adjacent to another AQ group. Thus, the opportunity for neighboring interaction is much higher in PAQ 5(2) than in PAQ 5(1). Despite this, almost identical voltammetric data were obtained for these polymers.

c) Determination of Diffusion Coefficient

The diffusion coefficient of polymers can be determined from the slope of  $i_{pc}$  vs.  $v^{1/2}$  plots, which reflects the product  $D^{1/2}C$ .  $C$  is the concentration of electroactive species, which were actually reduced at the electrode. For PAQ polymers,  $C$  can be taken as the bulk concentration of AQ moieties in solution because it has been shown that the electroactivity of the pendant

Table 9: Diffusion Coefficients of EBAQ and PAQ.

Polymers	AQ%	$\bar{M}_n \times 10^{-4}$	$p^a)$ (%)	$D \times 10^7$ ( $\text{cm}^2 \text{s}^{-1}$ )
EBAQ		0.0338		78.7
PAQ 5(1)	19.3	0.78	34.9	15.6
PAQ 5(2)	41.3	1.04	65.5	14.2
PAQ 8	21.6	1.12	38.5	13.4
PAQ 12	23.1	1.71	40.9	10.9
PAQ 40	18.0	6.06	32.8	5.84
PAQ 200(1)	19.5	32.6	35.2	2.29
PAQ 200(2)	28.0	36.9	48.2	2.00

a) P is defined by eq. [56]

groups is not affected by the macromolecular environment and that each AQ group is reducible at the electrode. The diffusion coefficients thus calculated are presented in Table 9.

In analogy to the study of PVBP polymers, the validity of determining the diffusion coefficient of PAQ polymers by cyclic voltammetry was examined. The D values obtained from the electrochemical data were plotted against the polymer molecular weight ( $\bar{M}_n$ ) estimated from gel permeation chromatography, on a double logarithmic scale. As seen from Figure 19, a straight line whose slope yielded  $b=0.52$  was obtained, in accordance with the following diffusion coefficient-molecular weight relationship:

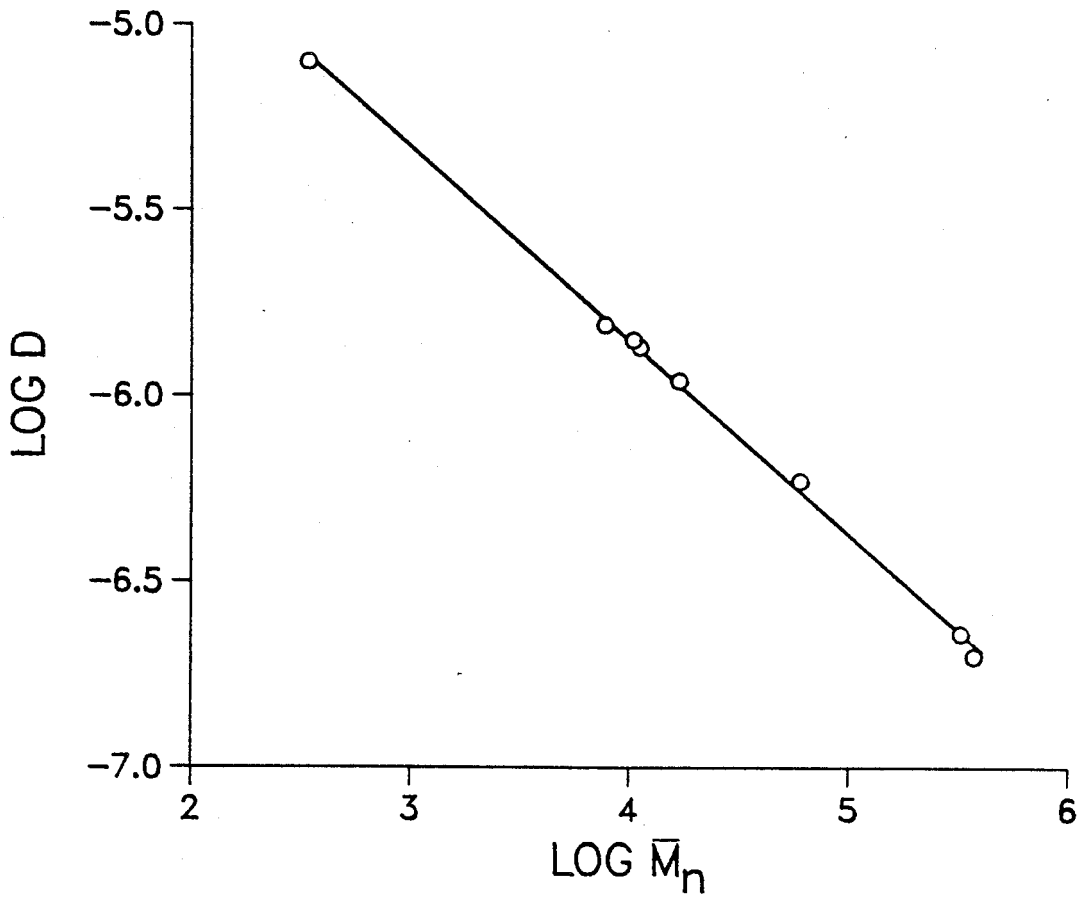


Figure 19: DEPENDENCE OF DIFFUSION COEFFICIENT ON MOLECULAR WEIGHT OF PAQ COPOLYMERS AND OF EBAQ.

$$D = K_T M^{-b} \quad [24]$$

$K_T$  is a constant and the exponent  $b$  is related to the limiting viscosity number  $\{\eta\}$  of polymers by:

$$\{\eta\} = KM^a \quad [32]$$

$$b = (1 + a)/3 \quad [35]$$

A value of  $a=0.56$  was obtained from eq. [35].

The viscosities of each of the polymer samples were measured and plotted against  $\bar{M}_n$  of polymers on a double logarithmic scale. The data in figure 20 yield  $a=0.57$  and  $K=3.27 \times 10^{-4}$ . This is in remarkable agreement with  $a=0.56$  obtained from the voltammetric data.

The non-interacting characteristics of attached AQ groups imply that the molecular weights of polymers can be determined by voltammetric techniques in a similar manner with PVBP. By substituting eq. [24] into eq. [4], the Randles-Sevcik equation can be rewritten in a form which relates the peak current to the molecular weight:

$$i_p = 2.69 \times 10^5 n^{3/2} A v^{1/2} C K_T^{1/2} M^{-b/2} \quad [57]$$

A plot of  $\log i_{pc}$  vs.  $\log \bar{M}_n$  is shown in figure 21 and a linear relationship is obtained. This again illustrates the feasibility of determining by voltammetric measurements of polymers containing non-interacting, Nernstian, electroactive centers.

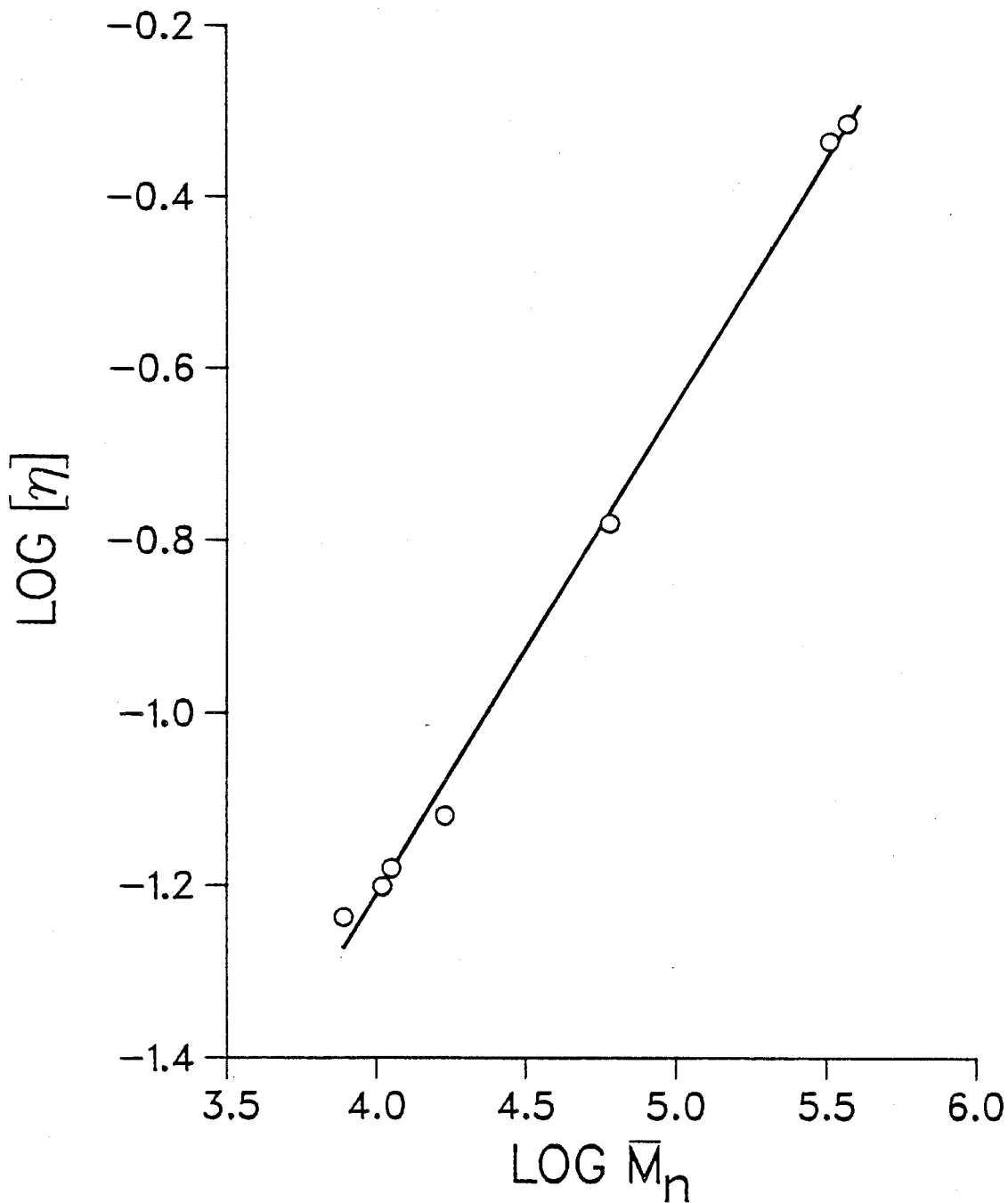


Figure 20: LIMITING VISCOSITY NUMBER-MOLECULAR RELATIONSHIP FOR PAQ.



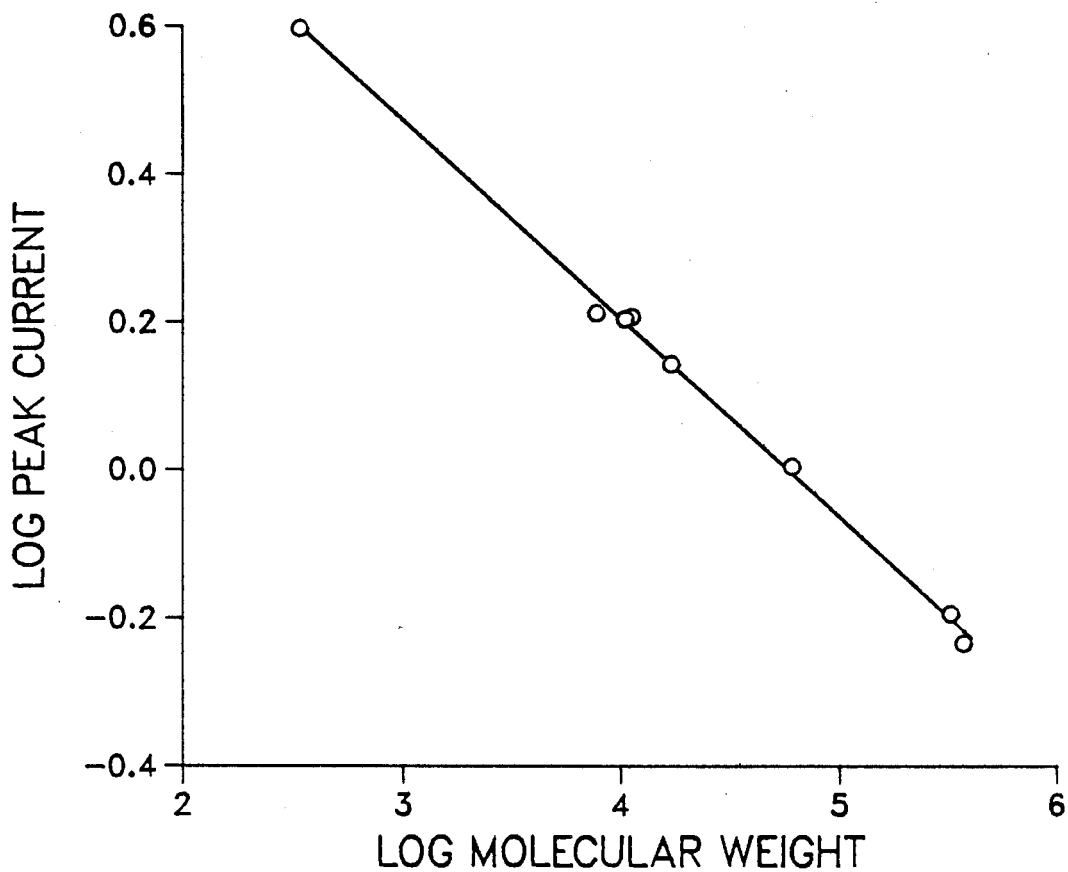


Figure 21: DEPENDENCE OF PEAK CURRENT AT A SCAN RATE OF  $0.05 \text{ Vs}^{-1}$  ON MOLECULAR WEIGHT OF PAQ COPOLYMERS AND OF EBAQ.

#### I.3.4. Conclusion

The electrochemical behavior of solutions of polymers containing benzophenone, benzoquinone and anthraquinone groups has been examined. For benzoquinone polymers, the active centers are reduced at potentials similar to those of the MeBQ model compound. However, a chemical reaction appears to occur between neighboring active centers on a polymer chain during the electroreduction process. This interaction is effectively reduced by separating active centers with styrene units.

For benzophenone and anthraquinone polymers, the electroactive groups act as independent entities despite the fact that they are constrained to a polymer chain. The peak potentials and the electrochemical reversibility of attached centers are essentially identical to those of the free, monomeric analogues, and each center is available for the reduction at the electrode. The solution behavior of these polymers is so close to ideality that the polymer diffusion coefficients and molecular weights obtained from voltammetric measurements are in good agreement within experimental errors with those determined by independent, conventional measurements of solution properties. This implies the potential use of voltammetric techniques in determining diffusion coefficients and molecular weights of electroactive polymers exhibiting an ideal behavior.

The ability to oxidize and reduce a large number of active centers on a polymer chain points to several applications of the electrochemistry of polymers. The pendant groups in the charged form are expected to undergo chemical reactions similar to those

of the corresponding monomeric analogs. Electrochemical techniques thus can be used to generate chemically active sites on a polymer chain which are useful for the modification of polymer structure, in analogy to the photolytic activation of photoactive centers of a polymer (54). Indeed, by exploiting the ability of BP radical anion to initiate the polymerization of methyl methacrylate (MMA) and acrylonitrile (AN), Funt and Hsu successfully grafted polyMMA and polyAN on a PVBP chain by electrochemical techniques (55). Furthermore, the adsorption of electroactive polymers on an electrode surface may alter the electrochemistry of the electrode and provides a new means of electrode modification.

CHAPTER II

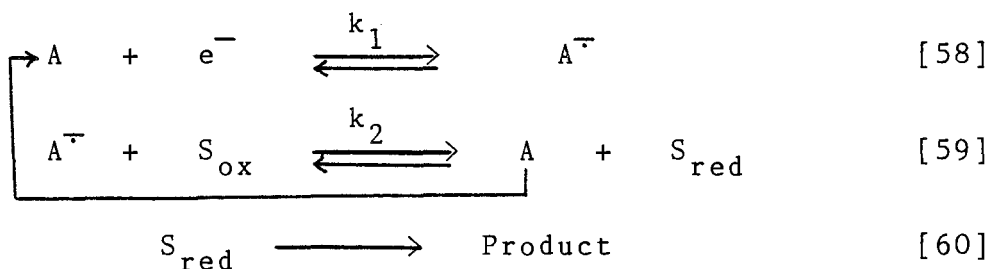
HOMOGENEOUS ELECTROCATALYTIC REDUCTION OF POLYCHLORINATED  
BENZENES AND BIPHENYLS

II.1. INTRODUCTION

II.1.1 General remarks

Homogeneous electrocatalysis is an electrochemical process, in which a soluble redox couple is used to mediate the electron transfer between an electrode and substrates. In principle, the mediator, which has a redox potential less negative than that of the substrate (consider an indirect reduction reaction) is first reduced at the electrode forming an intermediate having strong reducing properties. This species, in turn, reduces the substrate in solution, and the electron carrier is regenerated to its original oxidation state. The net result is that the substrate is reduced at the reduction potential of the mediator.

Equations [58] - [60] represent a general mechanism for a catalytic reduction process where  $A/A^-$  stands for the catalytic couple and  $S_{ox}$  and  $S_{red}$  are the oxidized and reduced substrates, respectively. The profile at the electrode surface is illustrated in Figure 22.



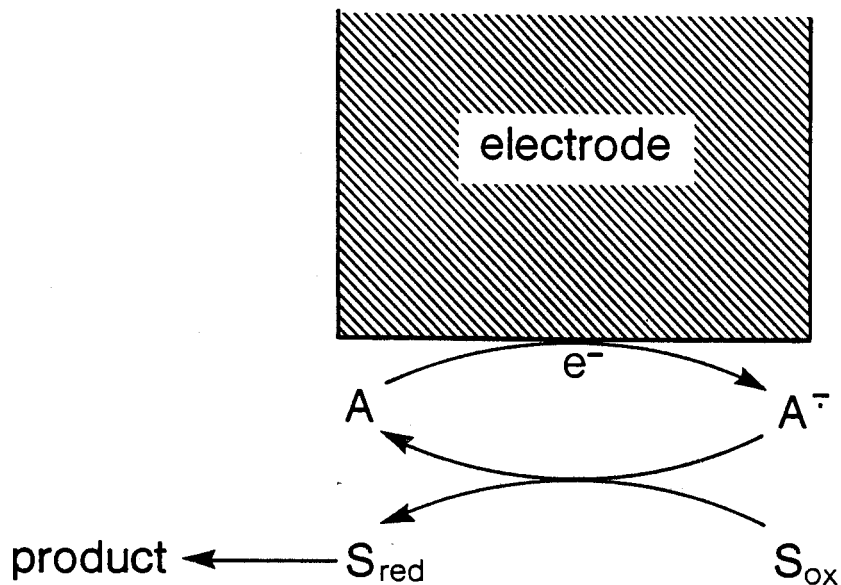


Figure 22: PROFILE AT AN ELECTRODE SURFACE FOR AN ELECTROCATALYTIC REDUCTION REACTION.

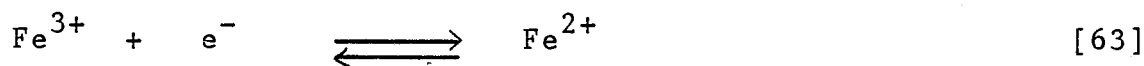
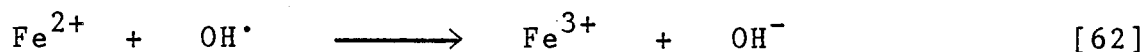
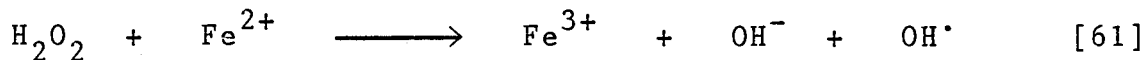
The transfer of an electron from  $A^{\bar{v}}$  to  $S_{ox}$  is not thermodynamically favored. However, the reaction is driven by the constant reduction of A to  $A^{\bar{v}}$ , and often by a fast and irreversible subsequent reaction involving the reduced substrate  $S_{red}$  (eq. [60]).

Since the catalyst is regenerated, the electrode senses a higher concentration of species A than that which corresponds to the analytical concentration. This produces an enhancement of the cathodic current of the catalyst when a substrate is added. The extent of the increase can thus be used to evaluate the catalytic efficiency of a mediator.

A major advantage of homogenous electrocatalysis over direct electrochemical reaction is the possibility of performing electrolyses at a potential less negative than that for the direct reduction. This means the overpotential of the direct reduction is decreased and the electrolysis may be facilitated of some species, which are not readily reduced at an electrode. Recently, the scope of electrocatalytic reactions has been widened by the development of electrodes modified with catalytic species. The immobilization of catalytic molecules on an electrode surface eliminates the subsequent separation of catalyst from products, and may allow the use of a small quantity of mediator.

### II.1.2. Studies of Homogeneous Electrolysis

Electrocatalysis using inorganic mediators has been known for several decades. As early as 1937, Brdicka and Tropp found that the reduction of  $H_2O_2$  shifted to more positive potentials upon the addition of hemoglobin (56). Initially, it was thought that the hemoglobin was activating the hydrogen peroxide, but later, it was shown that the potential shift was due to the catalytic reduction of  $H_2O_2$  by the iron compounds (57):



There are now numerous examples of electrocatalytic reactions using inorganic mediators (22,23,58,59). Most of the catalysts employed have been metal ions such as  $Cr^{6+}$ ,  $Cr^{2+}$ ,  $Mn^{2+}$  and  $Ce^{4+}$  but the use of superoxide ion, halogen and hydrogen as mediators has also been reported (22).

Electrocatalytic reactions employing organic mediators have been studied in detail only in the last few years. The earliest example on the organic catalytic system was mentioned by Fry on the cathodic reduction of t-butyl chloride mediated by naphthalene (60). Since then, a large number of papers have been published and this research has become one of the main topics in organoelectrochemistry.

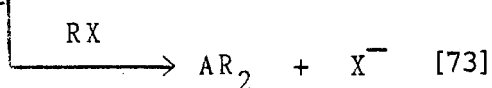
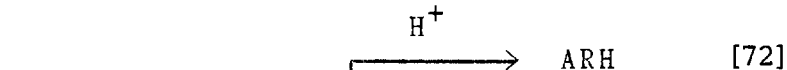
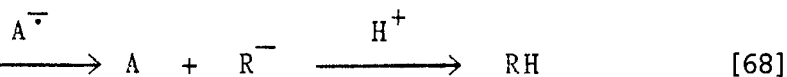
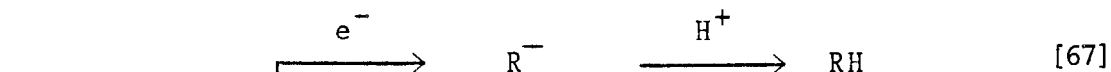
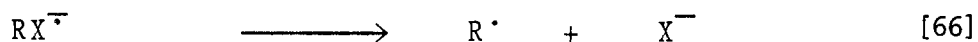
The electrocatalytic reduction of organic halides is perhaps

the most thoroughly investigated system (22,61). These compounds are particularly attractive because of the fast and irreversible cleavage of the resulting halide radical anion after the substrate receives one electron from the reduced mediator. This characteristic of the halide radical anion is important for obtaining high catalytic efficiency.

Lund and coworkers were among the first and the most active groups in this field. They (62-65) and several others (60,66) found that under aprotic conditions, a number of mono- and dihalogenated aromatic and aliphatic compounds were reduced by electrochemically generated radical anions and dianions of aromatic and heteroaromatic compounds, ketones, nitro compounds and esters. An increase in polarographic currents of the electron carriers was observed in the presence of substrates. On a preparative scale, reduction products were obtained in high yield, although the applied potential corresponded to the reduction potential of the mediators. In the absence of catalysts, electrolysis of halides at the same potential for the same period produced only negligible quantities of products. However, the analysis of the products obtained by the indirect electrolysis showed that while aromatic and benzylic halides were reduced to the corresponding hydrocarbons, coupling products were generally obtained from aliphatic compounds. For example, with anthracene as a catalyst, the indirect reduction of benzyl chloride produced toluene quantitatively (67) whereas the mediated reduction of t-BuCl gave alkylated dihydroanthracene in 60% yield (64). The results were interpreted on the basis of

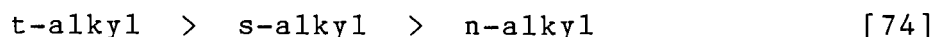


the following general mechanism for the indirect reduction of halides, where A is a mediator, RX is a halide and SH is solvent (61):

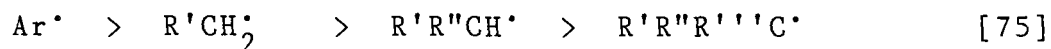


Eqs. [64], [65] and [66] are three basic reactions for a catalytic reduction of halides. Eqs. [67]—[73] describe pathways which the resulting radical R. may follow. The relative extent of these follow-up steps depends on the type of catalyst and substrate.

It was suggested that in the indirect reduction of aromatic and benzylic halides, aryl and benzylic radicals underwent reactions [67], [68], [69] and that [70] and [71] were not involved in the process. The reduction was purely catalytic and the mediator was fully regenerated. For aliphatic halides RX, the catalytic reactions ([65] and [68]) competed with reactions [71], which removed the catalyst  $A^{\cdot-}$  from the reaction cycle by the formation of  $AR^{\cdot-}$ . By examining several halides with different alkyl groups, Lund found that the extent of the competitive reaction [71] was dependent on the nature of the hydrocarbon chains and decreased in the order:



The dependence of the relative extent of reaction [71] on structure of halides was explained on the basis of electron affinity of the corresponding radicals (65). It was proposed that the electron affinity of radicals decreases in the following order (62):



Since the rate of reactions [67] and [68] increases with increasing electron affinity of radicals whereas the rate of

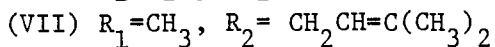
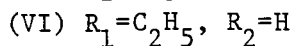
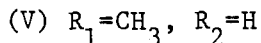
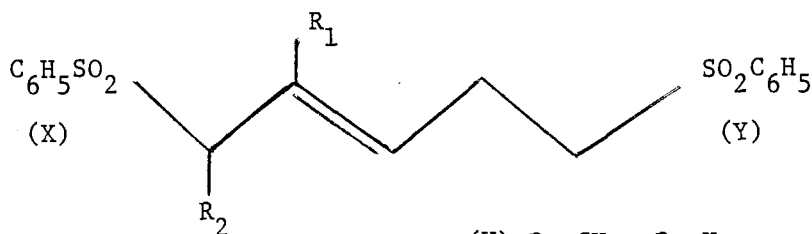
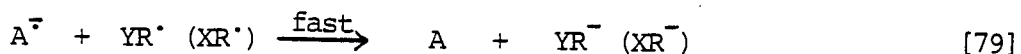
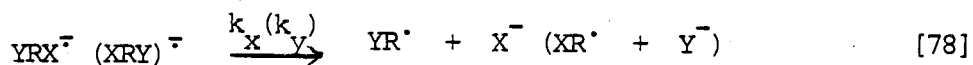
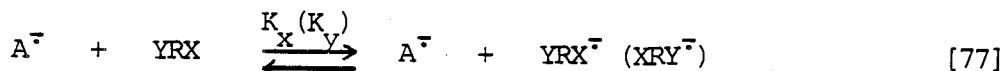
coupling reaction [71] is presumably less dependent on the structure of alkyl groups, reaction [71] would be most favored for tertiary alkyl halides and least favored for aromatic ones.

From the catalytic point of view, coupling reactions between a catalyst and substrates are not desirable because the catalyst is consumed in the reaction cycle. However, these reactions may produce compounds which are not readily accessible by other means and thus may present a new synthetic route.

Lund et al. also demonstrated that compounds which are not readily reduced at an electrode may be reduced by catalytic means. For example, the reduction of 2-chloropyridine in LiCl/DMF solution is not feasible because the polarographic wave of  $\text{Li}^+$  masks the cathodic reaction of the chlorinated compound. However, with the use of anthracene as a mediator, the reduction of 2-chloropyridine produced pyridine in 85% yield (64).

The catalytic reduction of substrates other than halides has also been reported. These include activated olefins (62), cyclopropanes (68), epoxides (69), triorganohalogermanes (70), bianthrone (71) and disulfides (72).

For molecules possessing two electroactive centers XRY slightly different in redox potentials, it is difficult to reduce one group selectively by a direct technique on a preparative scale because of the nonuniformity in current distribution and in electrode potential. However, Lund and Simonet showed that if a proper catalytic reagent was chosen so that  $K_x k_x \gg K_y k_y$ , X could be cleaved preferentially ( $K_{x(y)}$  and  $k_{x(y)}$  are the equilibrium constant and the rate constant of eqs. [77] and [78],



respectively). This was demonstrated by the reduction of the disulfones (V) - (VII) where the reduction potentials of the two sulfonyl groups are separated by 150 mV (73). With anthracene as a mediator, the cleavage occurred mainly on the allylic sulfonyl group whereas in the direct technique, removal of this group was accompanied by substantial cleavage of the other center.

Mediated reduction was also applied successfully in the reduction of biological macromolecules. Direct reduction of these compounds often encountered problems such as a low rate of substrate diffusion to the electrode, frequent adsorption on the electrode surface, steric hindrance imposed on the active centers and decrease of enzymatic activity. Lund reported the successful electrolysis of  $\text{NAD}^+$ , cytochrome C, hemoglobin, insulin and some

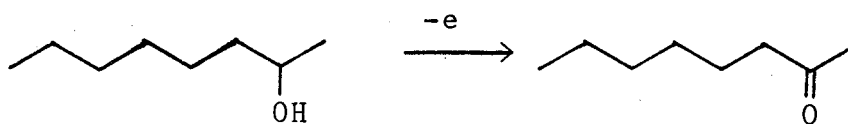
other proteins by using several reversible redox couples containing the pteridine nucleus as mediators (74,75). The technique possessed some advantages such as rapid reaction and high enzymatic activity of the products.

Steckhan and coworkers were the first to examine electrocatalytic oxidation. It was shown that several n-alkyl carboxylates underwent anodic reaction rapidly at a glassy carbon electrode in  $\text{CH}_3\text{CN}$ , with tris-(p-bromophenyl)amine as an electron carrier (75-78). The oxidation was followed by the decarboxylation of the resulting acyloxy radicals, yielding alkyl radicals. Fragmentation of the chain, hydrogen abstraction from solvent and competitive coupling reactions yielded a mixture of products.

Shono et al. reported the electrocatalytic oxidation of a number of secondary alcohols to ketones with thioanisole as mediator (79,80). Quantitative yields were obtained in most cases. It was demonstrated that further reduction of the overpotential for the oxidation of alcohols could be achieved by employing two mediators in combination (81). As seen from Table 10, organosulfur catalysts alone did not reduce the potential necessary for the oxidation of various alcohols to less than 1.6 V. With  $\text{Br}^-$  as a co-mediator, the oxidation could be carried out at 1.1 V, producing ketones in high yield.

The use of an electron carrier in the electrochemical reaction was also applied successfully in removing protecting groups in peptide synthesis. Mairanovsky demonstrated that 4-nitrobiphenyl, biphenyl, anthracene, pyrene, methyl benzoate,

Table 10: Catalytic Oxidation of 2-Octanol



Mediator ( $E_{ox}$ vs. SCE)	Supporting Electrolyte	Electrode Potential (V vs. SCE)	Yield (%)
none	Et <sub>4</sub> NOTs	>2.5	0
PhSCH <sub>3</sub> (1.60V)	Et <sub>4</sub> NOTs	1.6	85
PhSCH <sub>3</sub>	ET <sub>4</sub> NOTs	1.1	0
RSCH <sub>3</sub> <sup>b)</sup> (1.95V)	ET <sub>4</sub> NOTs	1.6	trace
RSCH <sub>3</sub> <sup>b)</sup>	ET <sub>4</sub> NBr	1.1	75
none	ET <sub>4</sub> NBr	1.1	0

a) Ts = tosyl

b) R = n-octyl

stilbene and 1-methylnaphthalene acted as effective mediators in removing a number of amine and alcohol protecting groups such as benzyloxycarbonyl, toluenesulfonyl and benzyl (82). Schmidt and Steckhan studied the oxidative removal of p-methoxybenzyl ether and of 1,3-dithiane groups by a homogeneous electron transfer reaction with  $(\text{BrC}_6\text{H}_4)_3\text{N}^+$  (83) and  $(\text{p-MeC}_6\text{H}_4)_3\text{N}^+$  (84), respectively. Although the electro-deprotection was carried out

at the oxidation potential of the catalysts, quantitative yields were obtained.

The present work explored the homogeneous electrocatalytic technique in the electroreduction of polychlorinated benzenes and biphenyls (PCB's), using benzophenone and anthracene as mediators. This study was attractive for two reasons. First, the investigation of these homogeneous systems may serve as a prelude for a further study of catalytic reactions at electrodes coated with films of polyvinylbenzophenone. Second, it can be reasonably expected from the studies of the indirect reduction of monohalides that the mediated reduction of polychlorinated benzenes and biphenyls will lead to the dechlorination of these compounds. Decomposition of polychlorinated aromatic molecules such as PCB's has received much interest in past several years since they are recognized as widespread environmental pollutants (85-88). These compounds, however, are thermally and chemically stable, and their decomposition by conventional means such as thermal and chemical methods requires extreme conditions (85,88). For example, incineration of PCB's should be performed at temperatures higher than  $1100^{\circ}\text{C}$ , whereas chemical dechlorination requires the use of highly active reagents such as  $\text{LiAlH}_4$ ,  $\text{BuLi}$ , Grignard reagents and sodium metal. The success of the electrocatalytic dehalogenation of PCB's thus may present a new technique of detoxification of these compounds.

## II.2. EXPERIMENTAL

### II.2.1. Chemicals

The purification of TEAP and DMF has been described in section I.2.1.

Chlorobenzene and 1,2,4-trichlorobenzene were dried over activated alumina.

p-Dichlorobenzene, 1,2,4,5-tetrachlorobenzene, benzophenone and anthracene were purified by zone refining and subsequently dried in vacuum for several days.

The PCB's (Aroclor 1242) obtained from Analabs were analyzed as C 55.0%, H 2.64% and the average number of Cl atoms per PCB molecule was estimated to be 3.1 (lit. 3.1 (85)). The compounds were dried over activated alumina.

### II.2.2. Electrochemistry

#### a) Cyclic Voltammetry

Electrodes, electrolytic cell and electronic equipment for voltammetric measurements have been described in section I.2.4.. Experiments were performed using solutions of 0.1M TEAP in DMF. The scan rate was  $0.05 \text{ Vs}^{-1}$  unless otherwise indicated.

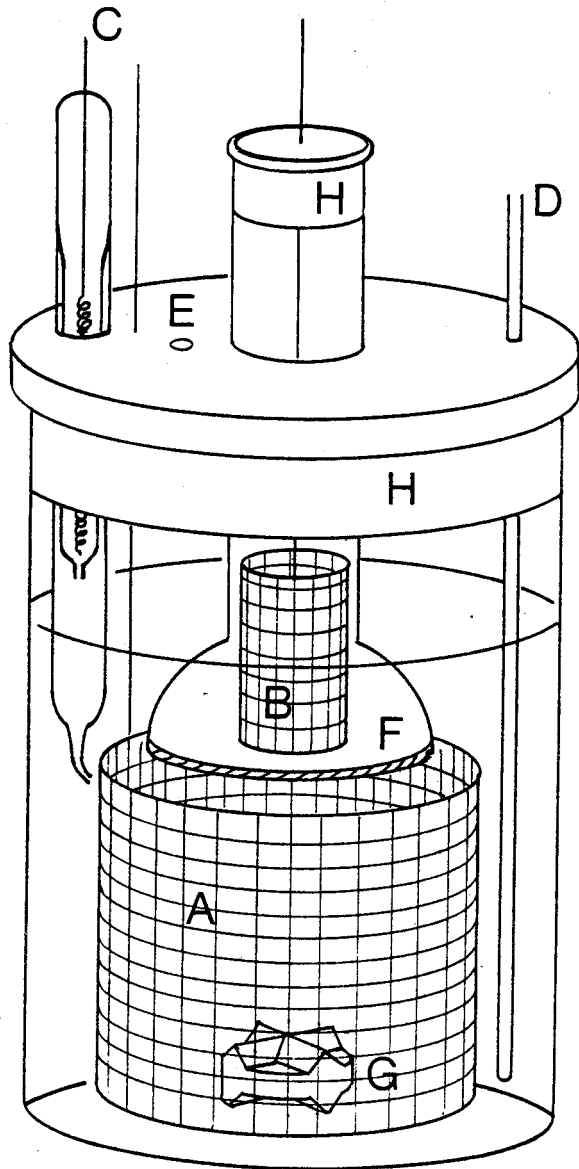
#### b) Preparative Controlled-Potential Electrolysis

A three-compartment cell as illustrated in figure 23 was employed. A sintered-glass disk of fine porosity separated the counter and working compartments. The working electrode was a Pt gauze. A Pt counter electrode was positioned above the working electrode to obtain a uniform potential distribution. The



Figure 23: ELECTROCHEMICAL CELL FOR PREPARATIVE ELECTROLYSIS.

- A) Working Electrode
- B) Counter Electrode
- C) Reference Electrode
- D) Argon Inlet
- E) Argon Outlet
- F) Fritted Glass
- G) Magnetic Bar
- H) Teflon Caps



solution levels in the two compartments were equalized. An Ag/AgNO<sub>3</sub> reference was positioned close to the working electrode through a Luggin capillary.

A Princeton Applied Research EG&G 175 programmer, a EG&G 173 potentiostat and a EG&G 179 coulometer were employed. All experiments were performed with IR compensation.

Preparative-scale electrolysis and analysis of the products were carried out as follows. A 24.5 mL sample of 3 mM durene/0.1M TEAP/DMF solution was placed in the working electrode compartment of the cell. A small amount of the same solution was added to the counter electrode compartment until the solution levels were equalized. Durene (1,2,4,5-tetramethylbenzene) was employed as the internal standard for the gas chromatography analysis. The presence of this compound did not have any effect on the electrochemistry of the systems.

The solution in the working compartment was deaerated with argon gas while being stirred vigorously. Pre-electrolysis was carried out until the background current became negligible. 0.5 mL of a 0.15 M stock solution containing the chlorinated compounds or catalysts (i.e., benzophenone and anthracene) was injected into the working compartment and a 0.5 mL sample of the electrolysis solution was withdrawn and saved for chromatographic analysis. The electrolysis was then allowed to proceed at a given potential. 0.5 mL of the test solution was withdrawn at time intervals and subsequently analyzed.

The 0.5 mL electrolysis sample was added to 2.5 mL distilled water and the resulting mixture was extracted with three 2.5 mL

portions of distilled ether. The ether extract was dried over anhydrous magnesium sulphate powder and concentrated to about 200 ul before being analyzed. A Hewlett-Packard 5790 A Series gas chromatograph containing a OV-1 capillary column (12.5 m x 0.2 mm) and a FID detector was employed. A Hewlett-Packard 3390 A Integrator was employed to record chromatograms and to integrate the peaks. The injection temperature was 250°C, the detection temperature was 250°C, the oven temperature was programmed at 110°C for 2 min. to 230°C for 12 min. at a rate of 13°Cmin<sup>-1</sup>. The helium carrier gas was flowed at 30 mLmin<sup>-1</sup>. Identification of the chromatographic peaks was made by comparison with those of the authentic compounds. The identification was further confirmed by GC-MS analysis.

All the chlorobenzenes were separated and quantitated as indicated by the g.c. retention times and responses given in Table 11. The g.c. retention times and the relative detector responses of the chlorobenzenes, benzophenone, anthracene and durenene were determined from the gas chromatograms of an ether extract of a 0.1M TEAP/DMF solution containing equimolar concentrations of these compounds. The analysis of PCB's was not attempted because this material is a mixture of several dozen compounds and the authentic compound for each component is not available.

Table 11: Retention times and relative responses of chlorobenzenes, benzophenone, anthracene and durene.

Compound	Retention time (min.)	Relative response
PhCl	1.21	0.321
1,4-C <sub>6</sub> H <sub>4</sub> Cl <sub>2</sub>	2.00	0.593
Durene	2.96	1.0
1,2,4-C <sub>6</sub> H <sub>3</sub> Cl <sub>3</sub>	3.54	0.603
1,2,4,5,-C <sub>6</sub> H <sub>2</sub> Cl <sub>4</sub>	5.24	0.643
Benzophenone	8.20	1.432
Anthracene	9.79	1.691

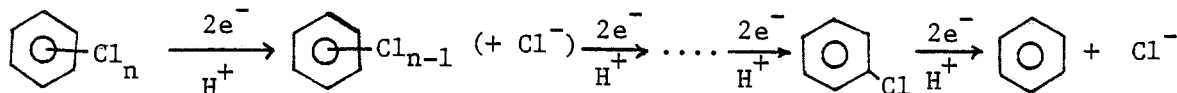
### II.3. RESULTS AND DISCUSSION

The main objective of this work was the investigation of the possibility of dechlorinating PCB's by electrocatalytic techniques. However, because commercial PCB's contain various isomers and compounds of differing chlorination degrees, most experiments were performed with chlorobenzenes as model reactions

#### II.3.1. Direct reduction of chlorobenzene (PhCl),

p-dichlorobenzene (C<sub>6</sub>H<sub>4</sub>Cl<sub>2</sub>), 1,2,4-trichlorobenzene (C<sub>6</sub>H<sub>3</sub>Cl<sub>3</sub>), 1,2,4,5-tetrachlorobenzene (C<sub>6</sub>H<sub>2</sub>Cl<sub>4</sub>), p-chlorobiphenyl and PCB's

Although the electroreduction of mono- and dihalogenated aromatic compounds has been investigated extensively, the reduction of polychlorinated molecules received little attention. Previous works were confined to a few papers (89-91). Farewell et al. examined the cathodic reduction of polychlorinated benzenes, -naphthalenes and -biphenyls at Hg electrodes in TEABr/DMSO solution. The results showed that the reduction of these compounds proceeded by a stepwise mechanism with the successive removal of chlorine atoms as shown in the following scheme:



Since there are no reports on the reduction of polychlorinated benzenes and PCB's at a Pt electrode in 0.1M TEAP/DMF solution, their direct reduction in these conditions was examined in order to provide a basis of comparison for the catalytic reactions.

The cyclic voltammograms of several chlorinated benzenes are shown in Figure 24 and the data are summarized in Table 12. The *i*-E response of PhCl shows an irreversible peak at -2.75 V. The reduction of  $p\text{-C}_6\text{H}_4\text{Cl}_2$  produces an irreversible peak at -2.48 V and an irreversible peak at -2.75 V. The latter is identical to that found in the reduction of PhCl. The voltammogram of  $1,2,4\text{-C}_6\text{H}_3\text{Cl}_3$  shows three irreversible peaks: -2.25 V, -2.48 V and -2.75 V. The last two peaks are identical to those observed in the reduction of  $\text{C}_6\text{H}_4\text{Cl}_2$ . The reduction of  $1,2,4,5\text{-C}_6\text{H}_2\text{Cl}_4$  yields four irreversible peaks: -2.03 V, -2.25 V, -2.48 V and -2.76 V, the last three of which are similar to those of  $1,2,4\text{-C}_6\text{H}_3\text{Cl}_3$ . In other words, the reduction of  $\text{C}_6\text{H}_{6-n}\text{Cl}_n$  compounds consists of *n* irreversible peaks, the second reduction potential of which is identical to the first of  $\text{C}_6\text{H}_{7-n}\text{Cl}_{n-1}$  molecules.

It can be seen from Figure 24 that all peak currents obtained by cyclic voltammetry of solutions of identical concentration of  $\text{C}_6\text{H}_{6-n}\text{Cl}_n$  (*n* = 1 - 4) are of the same magnitude. As PhCl has been reported to undergo a two-electron reduction (92), it was concluded that each reduction peak of  $\text{C}_6\text{H}_{6-n}\text{Cl}_n$  compounds is also a two-electron transfer.

Figure 24: CYCLIC VOLTAMMETRY OF 3mM SOLUTIONS OF

a) PhCl

b) 1,4-C<sub>6</sub>H<sub>4</sub>Cl<sub>2</sub>

c) 1,2,4-C<sub>6</sub>H<sub>3</sub>Cl<sub>3</sub>

d) 1,2,4,5-C<sub>6</sub>H<sub>2</sub>Cl<sub>4</sub>

Scan rate 0.05 Vs<sup>-1</sup>, in 0.1M TEAP/DMF



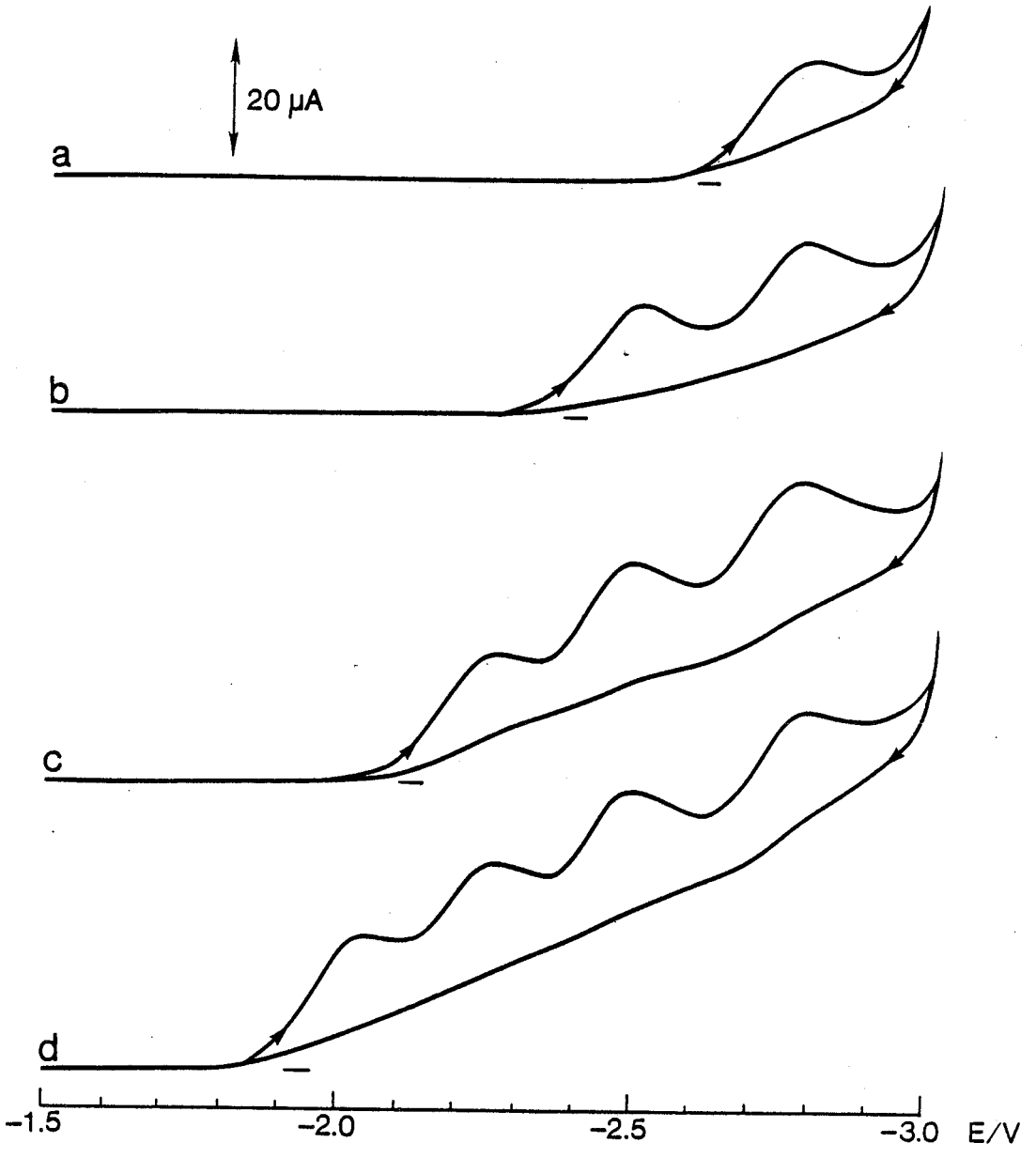


Table 12: Peak Potentials of Mediators and Substrates. <sup>a)</sup>

Compounds	Peak Potential (V vs. SCE)	$E_{pc}^1$	$E_{pa}^1$	$E_{pc}^2$	$E_{pa}^2$	$E_{pc}^3$	$E_{pa}^3$	$E_{pc}^4$
Benzophenone		-1.80	-1.73	-2.44				
Anthracene		-1.99	-1.91	-2.56				
Biphenyl		-2.64	-2.56					
PhCl		-2.75						
1,4-C <sub>6</sub> H <sub>4</sub> Cl <sub>2</sub>		-2.48		-2.75				
1,2,4-C <sub>6</sub> H <sub>3</sub> Cl <sub>3</sub>		-2.25		-2.48		-2.75		
1,2,4,5-C <sub>6</sub> H <sub>2</sub> Cl <sub>4</sub>		-2.03		-2.25		-2.48		-2.76
p-Chlorobiphenyl		-2.27		-2.64	-2.56			
PCB's		-2.18		-2.31		-2.65	-2.56	

a) 0.1M TEAP/DMF, 0.05 Vs<sup>-1</sup>, SCE

From these results, it was concluded that the electroreduction of polychlorinated benzenes at a Pt electrode in 0.1M TEAP/DMF solution proceeds by a stepwise mechanism similar to that reported by Farewell et al., leading to the formation of molecules of lower degrees of chlorination.

Cyclic voltammograms of chlorinated biphenyls are shown in Figure 25. The reduction of p-chlorobiphenyl produced an irreversible peak at -2.27 V and a reversible peak at -2.64 V (Figure 25b). The latter is identical to that of biphenyl (compare Figure 25a to 25b) and is assumed to be due to the reduction of biphenyl which was generated during the reduction of p-chlorobiphenyl by a mechanism similar to that proposed for polychlorobenzenes:

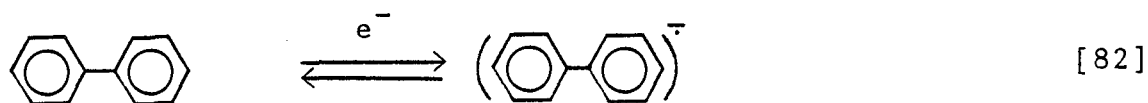
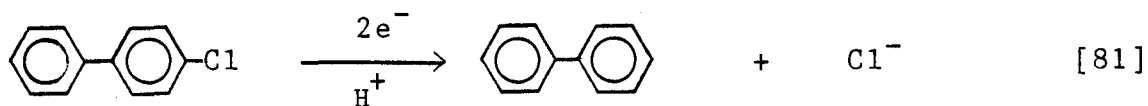
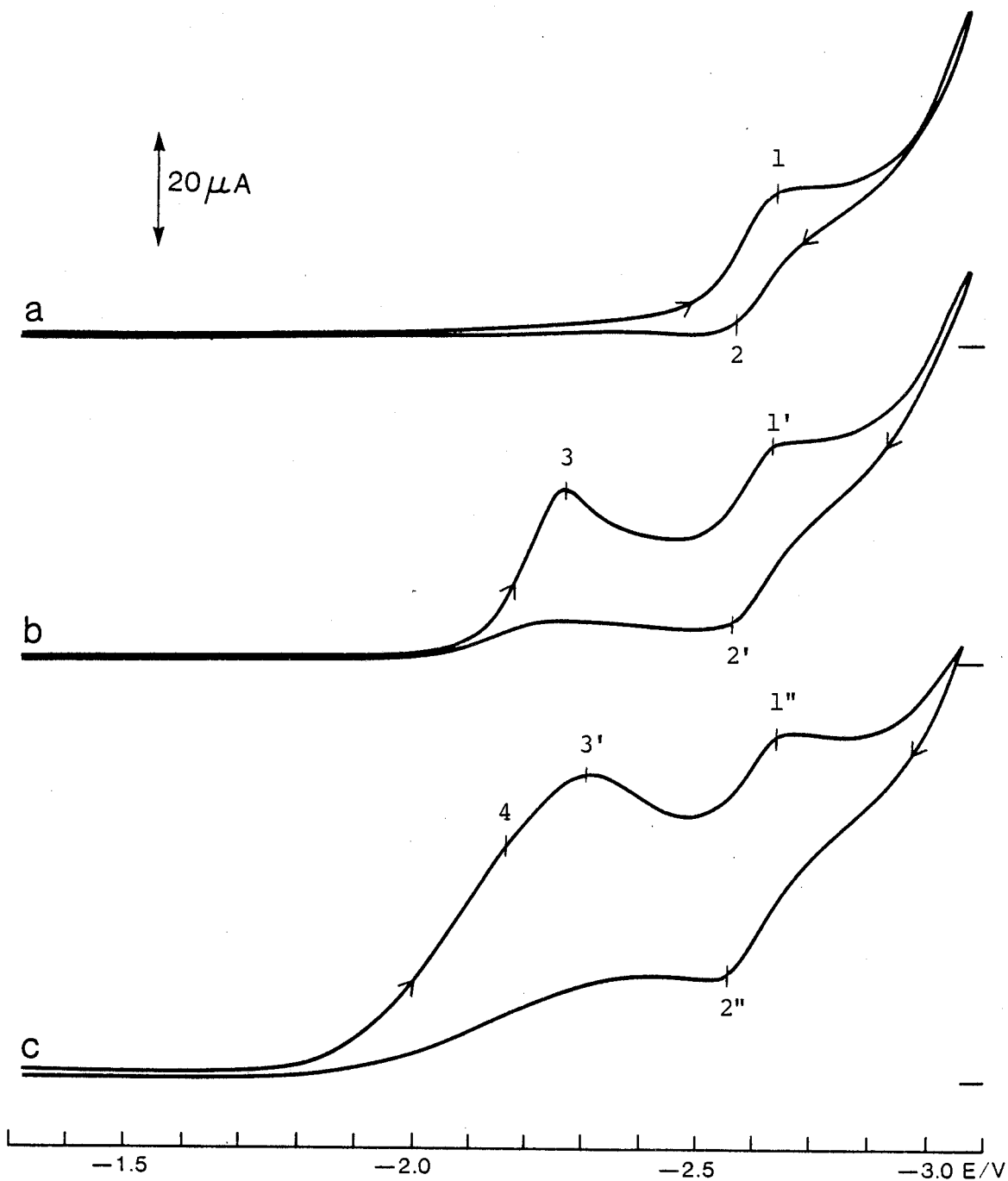


Figure 25: CYCLIC VOLTAMMETRY OF 3mM SOLUTIONS OF

- a) Biphenyl
- b) p-Chlorobiphenyl
- c) PCB's

Scan rate  $0.05 \text{ Vs}^{-1}$ , in 0.1M TEAP/DMF



This scheme is consistent with the observation that the diffusion current of the first peak is twice as high as that of the second peak, because the dehalogenation of p-chlorobiphenyl requires two electrons while the reduction of biphenyl is a one-electron process.

The reduction of PCB's produced an irreversible and broad peak at -2.18 V (peak 4), an irreversible peak at -2.31 V (peak 3') and a reversible peak at -2.65 V (peaks 1" and 2"). Inasmuch as peaks 3', 1" and 2" are identical with those of p-chlorobiphenyl (Figure 3c), they are assumed to be due to the reduction of p-chlorobiphenyl which was formed in the reduction of PCB's. Peak 4 is assigned to the reduction of the highly chlorinated compounds to the monochlorinated molecule.

These results indicate that chlorinated biphenyls undergo a reduction process similar to that of chlorinated benzenes. The more halogenated compounds are reduced more readily and the product of the reaction is a molecule containing fewer chlorosubstituents.

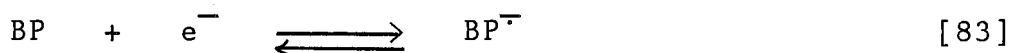
### II.3.2. Electrocatalytic Reduction of Polychlorinated Benzenes and Biphenyls with Benzophenone and Anthracene as Mediators

#### a) Benzophenone as Mediator

##### i) Voltammetric Studies

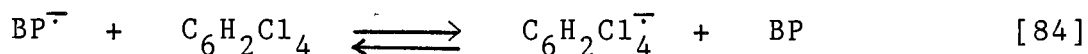
The electrocatalytic effect of BP on the reductions of polychlorinated compounds was examined by comparing the cyclic voltammetry of BP in the absence and in the presence of the substrates. In the potential range from -1.20 V to -2.05 V, the

voltammetry of BP produced a reversible wave, which corresponds to the following reaction (Figure 26):



The addition of  $\text{C}_6\text{H}_3\text{Cl}_3$  into the BP solution did not have any effect on the voltammetry of the latter. Similar observations were also found for  $\text{C}_6\text{H}_4\text{Cl}_2$  and  $\text{PhCl}$ . This implies that BP does not mediate the reduction of  $\text{C}_6\text{H}_3\text{Cl}_3$ ,  $\text{C}_6\text{H}_4\text{Cl}_2$  and  $\text{PhCl}$ .

The addition of an equal amount of  $\text{C}_6\text{H}_2\text{Cl}_4$  increased the cathodic peak current of BP by a factor of 1.73 and diminished the oxidation peak (Figure 26). This indicates that electron transfer occurred from  $\text{BP}^-$  to  $\text{C}_6\text{H}_2\text{Cl}_4$  with the generation of BP as shown in the following equation:



The absence of the anodic peak suggests that in this experimental time scale, most BP radical anions produced in the reduction of BP had reacted with  $\text{C}_6\text{H}_2\text{Cl}_4$  so that little  $\text{BP}^-$  was available for the reoxidation on the reverse scan.

The effect of scan rate on the cyclic voltammetry of a mixture of BP and  $\text{C}_6\text{H}_2\text{Cl}_4$  is shown in Figure 27. At scan rates less than  $0.02 \text{ Vs}^{-1}$ , the anodic peak of BP is totally suppressed but it appears at higher scan rates. Increased scan rates reduced the time available for the  $\text{BP}^-$  to react with  $\text{C}_6\text{H}_2\text{Cl}_4$  and therefore, a fraction of  $\text{BP}^-$  was reoxidized.

The catalytic reduction of  $\text{C}_6\text{H}_2\text{Cl}_4$  by BP was further evidenced in the voltammetry of a  $\text{BP}/\text{C}_6\text{H}_2\text{Cl}_4$  solution where the

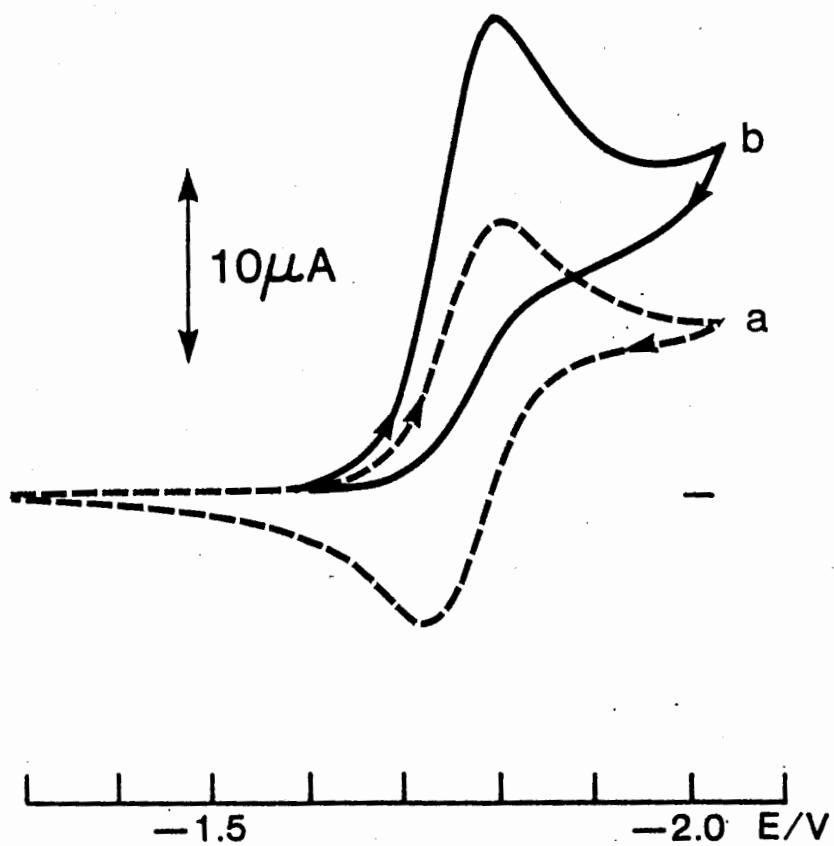


Figure 26: CYCLIC VOLTAMMETRY OF SOLUTIONS OF

a) 3mM Benzophenone

b) 3mM Benzophenone + 3mM  $C_6H_2Cl_4$

Scan rate  $0.05 \text{ Vs}^{-1}$ , 0.1M TEAP/DMF



Figure 27: CYCLIC VOLTAMMETRY OF A SOLUTION OF  
3mM BP + 3mM  $C_6H_2Cl_4$  AT VARIOUS SCAN RATES.

Scan rate:

a)  $0.50 \text{ Vs}^{-1}$

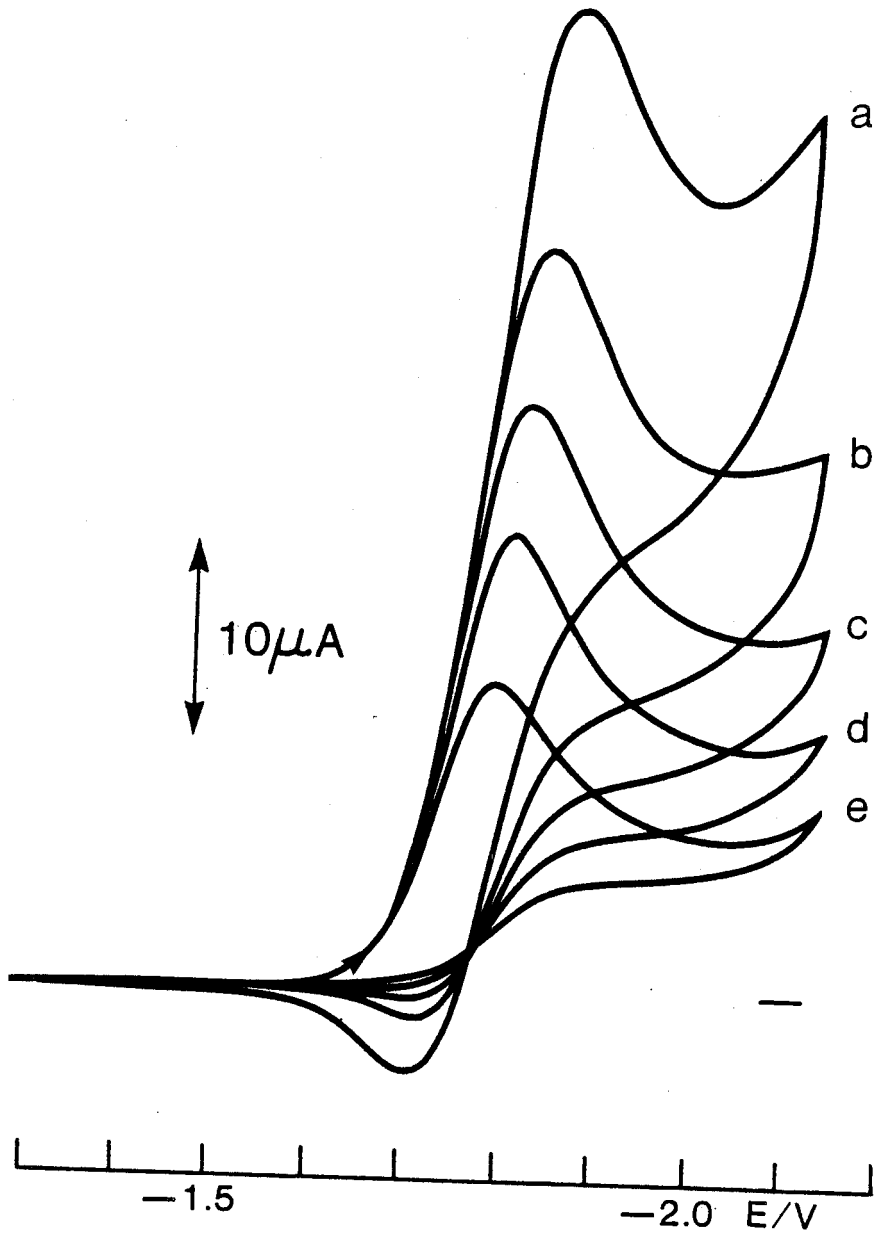
b)  $0.20 \text{ Vs}^{-1}$

c)  $0.10 \text{ Vs}^{-1}$

d)  $0.05 \text{ Vs}^{-1}$

e)  $0.02 \text{ Vs}^{-1}$

in 0.1M TEAP/DMF



potential scan was extended to -3.0 V (Figure 28). A comparison of the voltammograms of solutions of  $C_6H_2Cl_4$  (Figure 28a) and of  $BP+C_6H_2Cl_4$  (Figure 28c) revealed that in the presence of BP, the first reduction peak of  $C_6H_2Cl_4$  (peak 5) disappeared whereas the last three peaks remained unchanged. (Note that peak 7' is an overlap of peaks 7 and 10). Clearly, the catalytic reduction of  $C_6H_2Cl_4$  had depleted its concentration in the solution region close to the electrode surface and thereby, no  $C_6H_2Cl_4$  was available for the direct reduction.

Peaks 6, 7 and 8 are due to the direct reduction of  $C_6H_3Cl_3$ ,  $C_6H_4Cl_2$  and  $PhCl$ , respectively, which were formed in the reduction of  $C_6H_2Cl_4$ . The fact that these peaks were not affected by the addition of BP indicates that BP did not catalyze the reduction of these halides; otherwise, the catalytic reactions would compete with the direct reductions and these peaks would be diminished. The results are thus in agreement with those obtained in experiments where BP was added directly to solutions of these substrates.

BP also catalyzed the reduction of PCB's (Figure 29). However, the catalytic enhancement factor  $R^*$  was low (=1.3).  $R^*$  is defined as the ratio of the cathodic peak current of the mediator in the presence and absence of substrates. In addition, a small anodic peak was observed corresponding to the reoxidation of  $BP^{\cdot-}$  to BP. These results suggest that the electron exchange between  $BP^{\cdot-}$  and PCB's is not as fast as that between  $BP^{\cdot-}$  and  $C_6H_2Cl_4$ .

Figure 30 illustrates the cyclic voltammograms of PCB's and

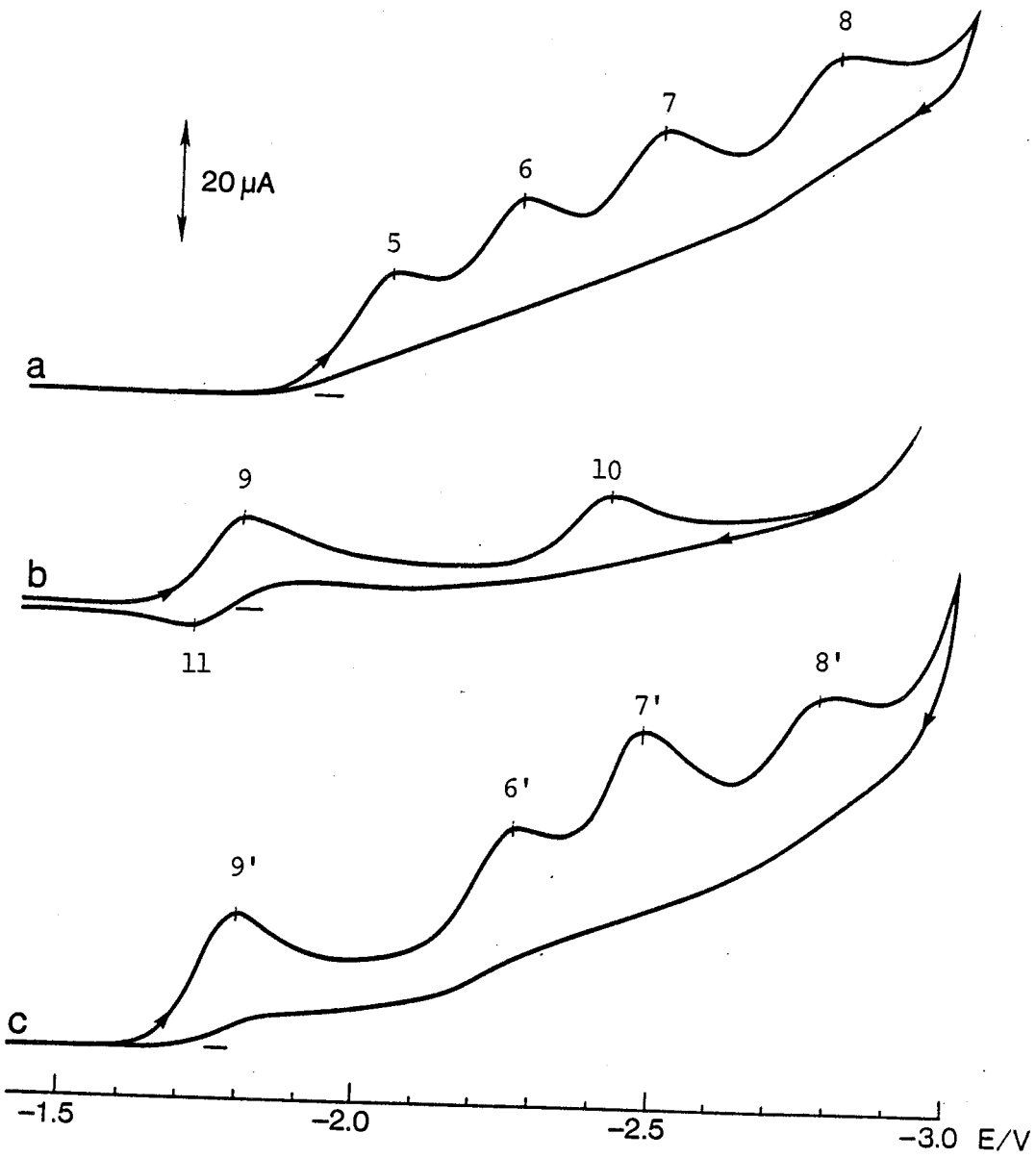
Figure 28: CYCLIC VOLTAMMETRY OF SOLUTIONS OF

a) 3mM  $C_6H_2Cl_4$

b) 3mM Benzophenone

c) 3mM Benzophenone + 3mM  $C_6H_2Cl_4$

Scan rate  $0.05 \text{ Vs}^{-1}$ , in 0.1M TEAP/DMF



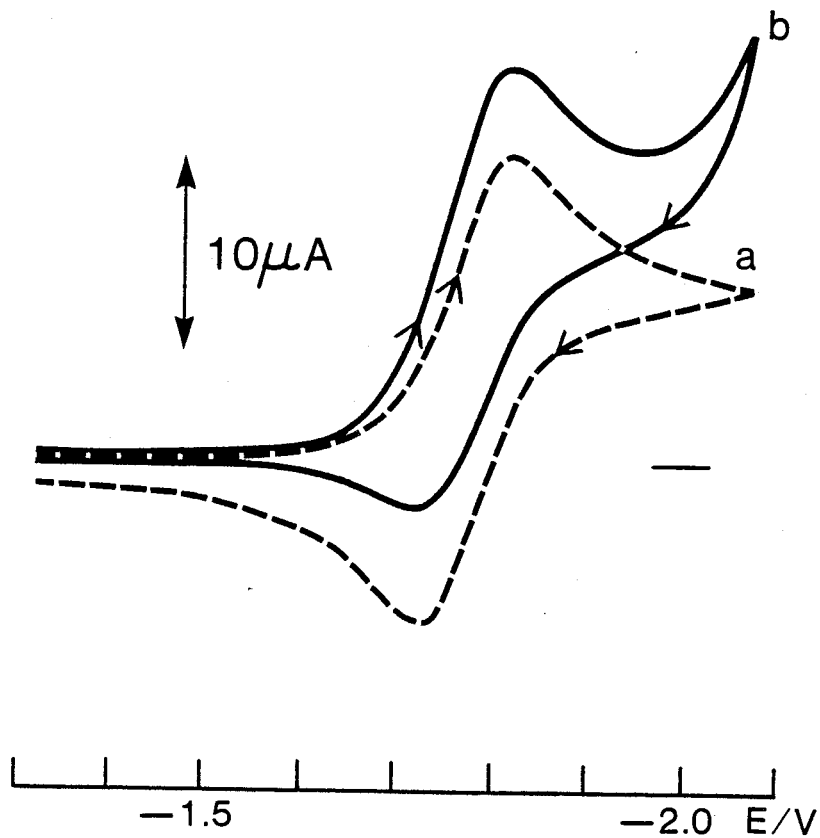


Figure 29: CYCLIC VOLTAMMETRY OF

a) 3mM Benzophenone

b) 3mM Benzophenone + 3mM PCB's

Scan rate  $0.05 \text{ Vs}^{-1}$ , 0.1M TEAP/DMF

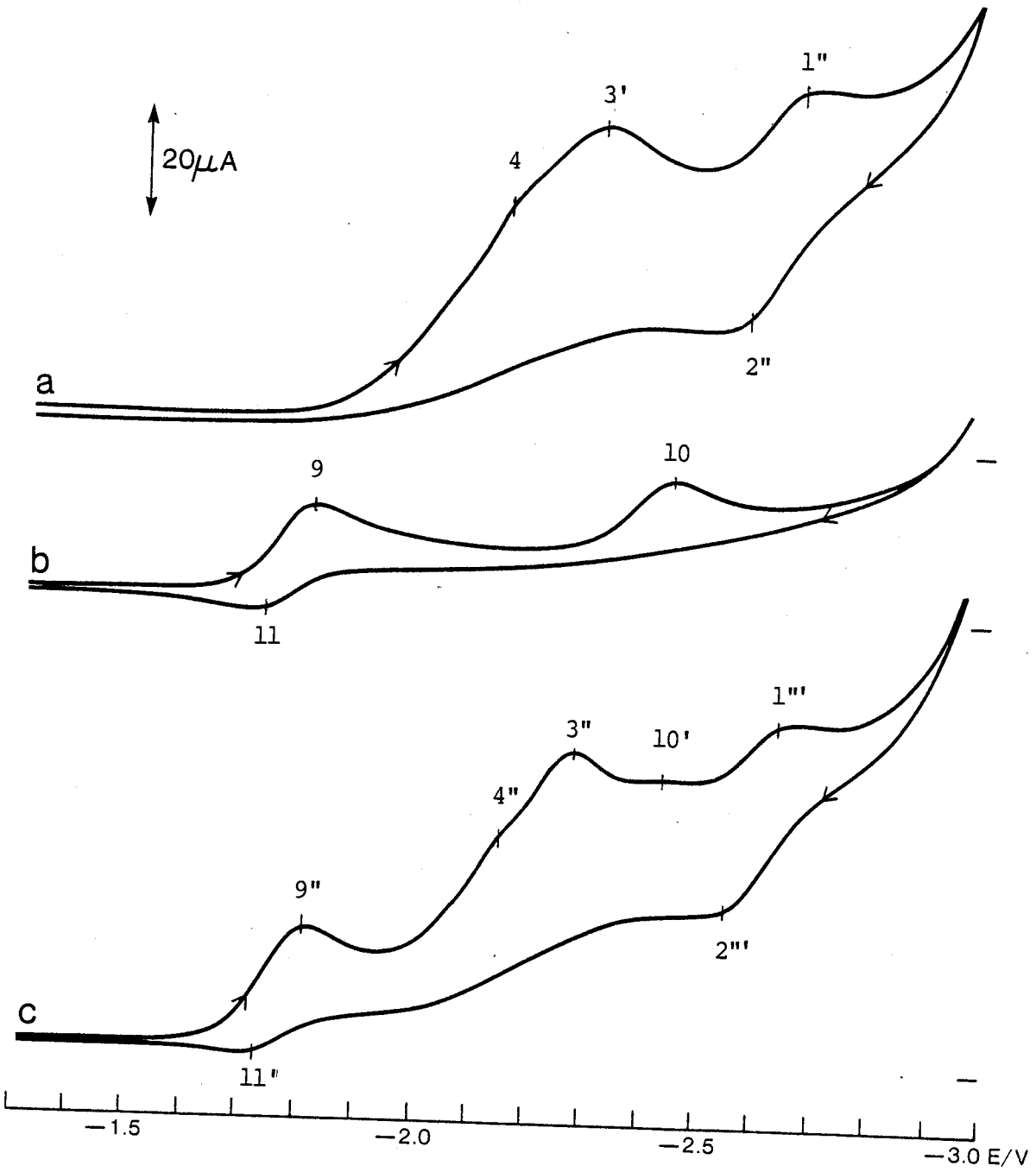
Figure 30: CYCLIC VOLTAMMETRY OF SOLUTIONS OF

a) 3mM PCB's

b) 3mM Benzophenone

c) 3mM Benzophenone + 3mM PCB's

Scan rate  $0.05 \text{ Vs}^{-1}$ , in 0.1M TEAP/DMF

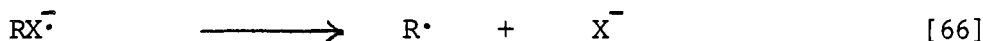
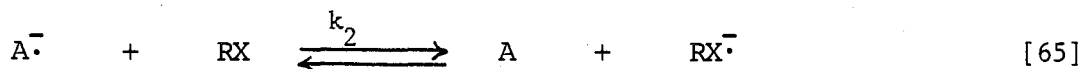
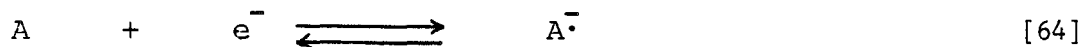


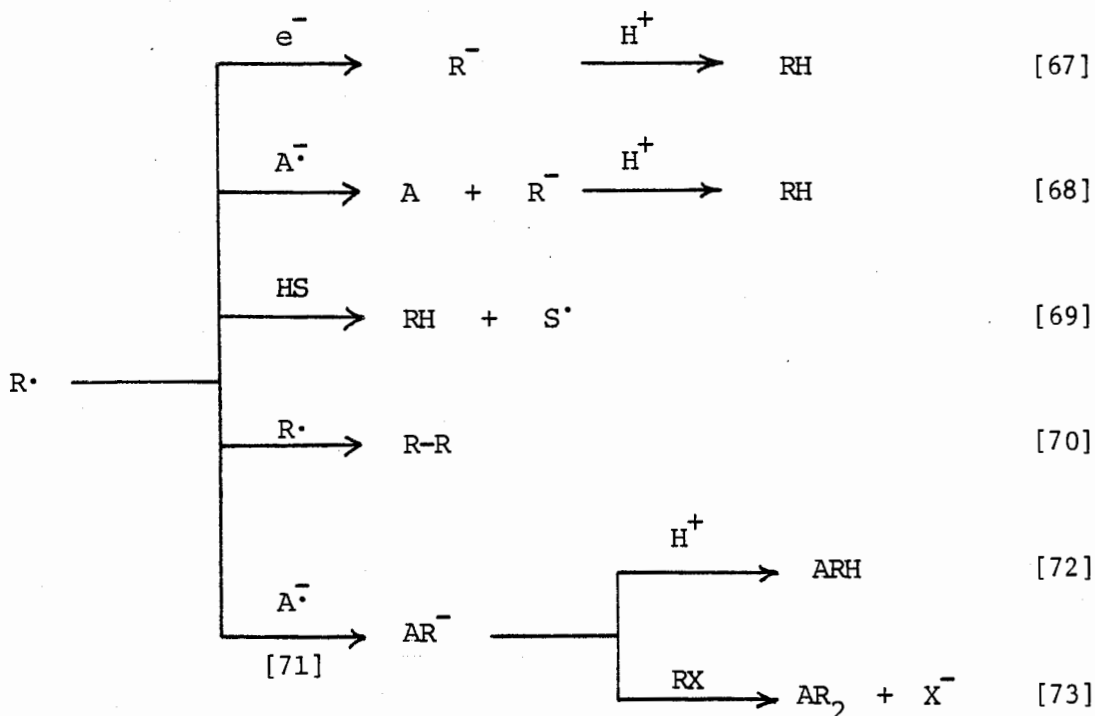


of BP in the absence and in the presence of PCB's, where the electrode potential was extended to -3.0 V. The addition of BP slightly reduced the magnitude of peak 4 whereas peaks 3', 1" and 2" were almost unchanged. This indicates that BP mediated the dehalogenation of PCB's to chlorobiphenyl but not further in the reaction chain. The results are consistent with voltammetric experiments with a BP + p-chlorobiphenyl mixture, where the i-E response is merely the sum of the voltammograms of the two individual components.

ii) Mechanism of the Electroreduction Mediated by BP of C<sub>6</sub>H<sub>2</sub>Cl<sub>4</sub> and PCB's

The voltammetric characteristics of the C<sub>6</sub>H<sub>2</sub>Cl<sub>4</sub>+BP and the PCB's+BP solutions give a clue to the reaction mechanism. Generally, the mechanism for the electrocatalytic reduction of halides can be expressed in the following scheme:





The resulting radical  $R^\cdot$  may undergo further reduction at the electrode [67] or by  $A^-$  [68], hydrogen abstraction from the solution [69], dimerization [70] or coupling with the catalyst [71]. The relative extent of these subsequent reactions ([67]-[71]) depends on the type of catalyst and substrate. It was shown that with aromatic hydrocarbons as catalysts, reactions [70] and [71] were not involved in the scheme when aromatic and benzylic halides were used as substrates, but in the indirect reduction of aliphatic halides, coupling reactions between the catalysts and substrates ([71] and [73]) occur to a great extent (20,62).

The electroreduction of BP in the presence of alkyl halides has been investigated by several authors (93-95). The results showed that mono- and di-alkylated benzophenones were produced exclusively and this is indicative of the occurrence of reactions [71] and [73]. Similar results were also reported for reactions

of alkyl halides with the alkali metal adducts of benzophenone (96,97).

Electrocatalytic reduction of aromatic halides by BP has not been reported but analogous reactions were investigated by Avny and Moshonov (32), who studied reactions of bromobenzene with radical anions and dianions of the lithium adducts of BP and PVBP-St copolymers. They found that bromobenzene did not react with radical anions of BP and PVBP-St, but reacted with  $\text{BP}^{2-}\text{Li}_2^+$  to give benzene (13%) and alkylated compounds (triphenylcarbinol (55%) and p-phenylbenzophenone (36%)). On the other hand, the reaction of bromobenzene with dianions of PVBP-St (VBP content =73%) yielded benzene (75%) and biphenyl (30%). The difference in the results found for BP and PVBP-St was attributed to the steric hindrance of the polymers which is not favorable to reactions [71] and [73].

In this work, it appears that the dimerization reaction [70] and the coupling between the catalyst and the substrate ([71] and [73]) did not proceed to any appreciable extent. This is inferred from the following observations:

- 1) In Figure 28, peak 6' is of comparable magnitude with peak 6. This implies that  $\text{C}_6\text{H}_3\text{Cl}_3$  was produced quantitatively in the catalytic reduction of  $\text{C}_6\text{H}_2\text{Cl}_4$ . If the reactions [70], [71] and [73] had occurred, the yield of  $\text{C}_6\text{H}_3\text{Cl}_3$  would have been decreased and therefore, peak 6' would have become smaller.

- 2) Products formed in reactions [70],[71] and [73] are polychlorinated compounds and should undergo further direct reduction at the electrode in the potential range investigated.

However, as seen from Figure 28c, cathodic peaks corresponding to the direct reduction of these compounds are not observed.

On the basis of this analysis, it is possible to conclude that reactions [70], [71] and [73] do not occur to any considerable extent in the electroreduction of  $C_6H_2Cl_4$ . A similar conclusion can also be made for the PCB's+BP system from its voltammetric characteristics. Comparing these results with those reported for BP + alkyl halide solutions, it can be seen that the extent of the reactions [71] and [73] is significant with alkyl halides but not with aromatic halides. This behavior is thus similar to that reported for systems using aromatic hydrocarbons as mediators.

iii) Preparative Controlled-Potential Electrolysis

Controlled potential electrolysis on a preparative scale followed by analysis of the products provides an alternative method to prove the catalytic reduction process. If benzophenone mediates the cathodic reaction of  $C_6H_2Cl_4$ ,  $C_6H_3Cl_3$  will only be formed in the presence of BP, when a voltage corresponding to the reduction potential of the latter is applied.

The results of macroelectrolysis of  $C_6H_2Cl_4$  with and without BP as catalyst are shown in Table 13. In all experiments, a potential of -1.80 V was applied, corresponding to the cathodic peak potential of BP. In the absence of BP, no formation of  $C_6H_3Cl_3$  was detected (entry 1). A small value of charge recorded was presumably due to the electrolysis of impurities, most likely

Table 13: Preparative Electrocatalytic Reduction of  $C_6H_2Cl_4$

Entry	BP (mM)	$C_6H_2Cl_4$ (mM)	t (min.)	Q		Yield (%)	
				(C)	(Fmol <sup>-1</sup> )	$C_6H_3Cl_3$	$C_6H_4Cl_2$
1	-	3	6.0	1.24	0.17	-	-
2	3	3	5.5	7.4	1.0	18 <sup>b)</sup> (36) <sup>c)</sup>	-
3	3	3	8.7	11.2	1.6	32 (40)	-
4	3	3	12.5	14.8	2.1	38 (36)	-
5	3	3	21.4	18.5	2.6	42 (33)	0.9

a) Applied Potential -1.80 V vs. SCE

b) Based on the initial amount of  $C_6H_2Cl_4$

c) Coulombic yield

the residual water in the solution. In the presence of BP, the current increased greatly, and after a similar electrolysis period, a charge of 7.4 C (or 1.0 Fmol<sup>-1</sup>) was passed (entry 2). Chromatographic analysis of the reaction solution showed that  $C_6H_3Cl_3$  was formed in 18 % yield. The yield increased with the charge passed. Surprisingly, after a charge equivalent to 2.6 Fmol<sup>-1</sup> was consumed,  $C_6H_4Cl_2$  was obtained in addition to  $C_6H_3Cl_3$  although the yield was small (0.9 %). This suggests that BP might also catalyze the reduction of  $C_6H_3Cl_3$  but the catalytic efficiency was so small that the reaction could not be detected by cyclic voltammetry.

iv) Reaction of BP Radical Anions With  $C_6H_2Cl_4$

The catalytic characteristics of BP were also examined

by analysis of the products of the reaction of  $\text{BP}^{\cdot-}$  with  $\text{C}_6\text{H}_2\text{Cl}_4$ . The reaction was performed by complete electrolysis of BP to  $\text{BP}^{\cdot-}$ , followed by the addition of  $\text{C}_6\text{H}_2\text{Cl}_4$ . Difficulties were encountered when attempts were made to reduce BP completely. Although the solution was carefully dried, deaerated, and preelectrolysed,  $\text{BP}^{\cdot-}$  deactivated rapidly. A dark blue color which is characteristic of the BP radical anion developed at the beginning of the electrolysis but faded rapidly. At the end of the electrolysis, the solution was light green, which indicates that a significant fraction of  $\text{BP}^{\cdot-}$  had been deactivated.

In order to maintain a high concentration of  $\text{BP}^{\cdot-}$ , it was necessary to minimize the electrolysis time. Thus, to reduce 3 mM BP in a short time, a solution with a three-fold increase in concentration was employed, but a charge only equivalent to 3 mM was passed. In this way, the electrolysis time was reduced to one tenth, and the solution maintained the dark blue color. Upon the addition of  $\text{C}_6\text{H}_2\text{Cl}_4$ , the blue color disappeared instantaneously. The reaction mixture was stirred for 5 minutes and then analyzed by chromatography. Analysis showed that  $\text{C}_6\text{H}_3\text{Cl}_3$  was formed in 30% yield. No formation of  $\text{C}_6\text{H}_4\text{Cl}_2$  was detected.

The results presented above indicate that benzophenone catalyzes the reduction of  $\text{C}_6\text{H}_2\text{Cl}_4$  and PCB's but not of other compounds. It has been recognized that for a given substrate, the smaller the difference in reduction potential between catalyst and substrate ( $\Delta E$ ), the more effective the catalyst is as a mediator (71,82). In fact, high efficiency has been reported only for systems with  $\Delta E$  less than 0.3 ~ 0.5 V (71). Thus, the

fact that BP does not catalyze the reduction of  $C_6H_3Cl_3$ ,  $C_6H_4Cl_4$ , PhCl and p-chlorobiphenyl can be attributed to the large difference in the redox potentials. If these substrates are to be catalytically reduced, one would have to employ a redox couple whose reduction potential is slightly more positive than that of the substrates. Anthracene, which has been widely used as a mediator for the indirect reduction of many aliphatic and aromatic halides, is reduced at a potential 170 mV more negative than benzophenone, and thus appears to be a good candidate for this purpose. The catalytic reduction of polychlorinated compounds with anthracene as mediator is described in the following section.

#### b) Anthracene as Mediator

Anthracene catalyzed the reduction of  $C_6H_3Cl_3$ , p-chlorobiphenyl and PCB's but not of  $C_6H_4Cl_2$  and PhCl. In Figure 31, it can be seen that the addition of an equimolar amount of  $C_6H_3Cl_3$  increased the first reduction peak of anthracene by a factor of 2.2 and diminished the corresponding anodic wave on the reverse scan. In the presence of anthracene, the direct reduction of  $C_6H_3Cl_3$  (peak 12) was totally suppressed while peaks 13 and 14 were unaffected. These results indicate that electron transfer was possible from the anthracene radical anion to  $C_6H_3Cl_3$ , but not to the dichloro- or monochlorobenzene. This was in agreement with experiments in which anthracene was added directly to solutions of the individual model compounds.

The results obtained from cyclic voltammetry were confirmed

Figure 31: CYCLIC VOLTAMMETRY OF SOLUTIONS OF

a) 3mM  $C_6H_3Cl_3$

b) 3mM Anthracene

c) 3mM Anthracene + 3mM  $C_6H_3Cl_3$

Scan rate  $0.05 \text{ Vs}^{-1}$ , in 0.1M TEAP/DMF



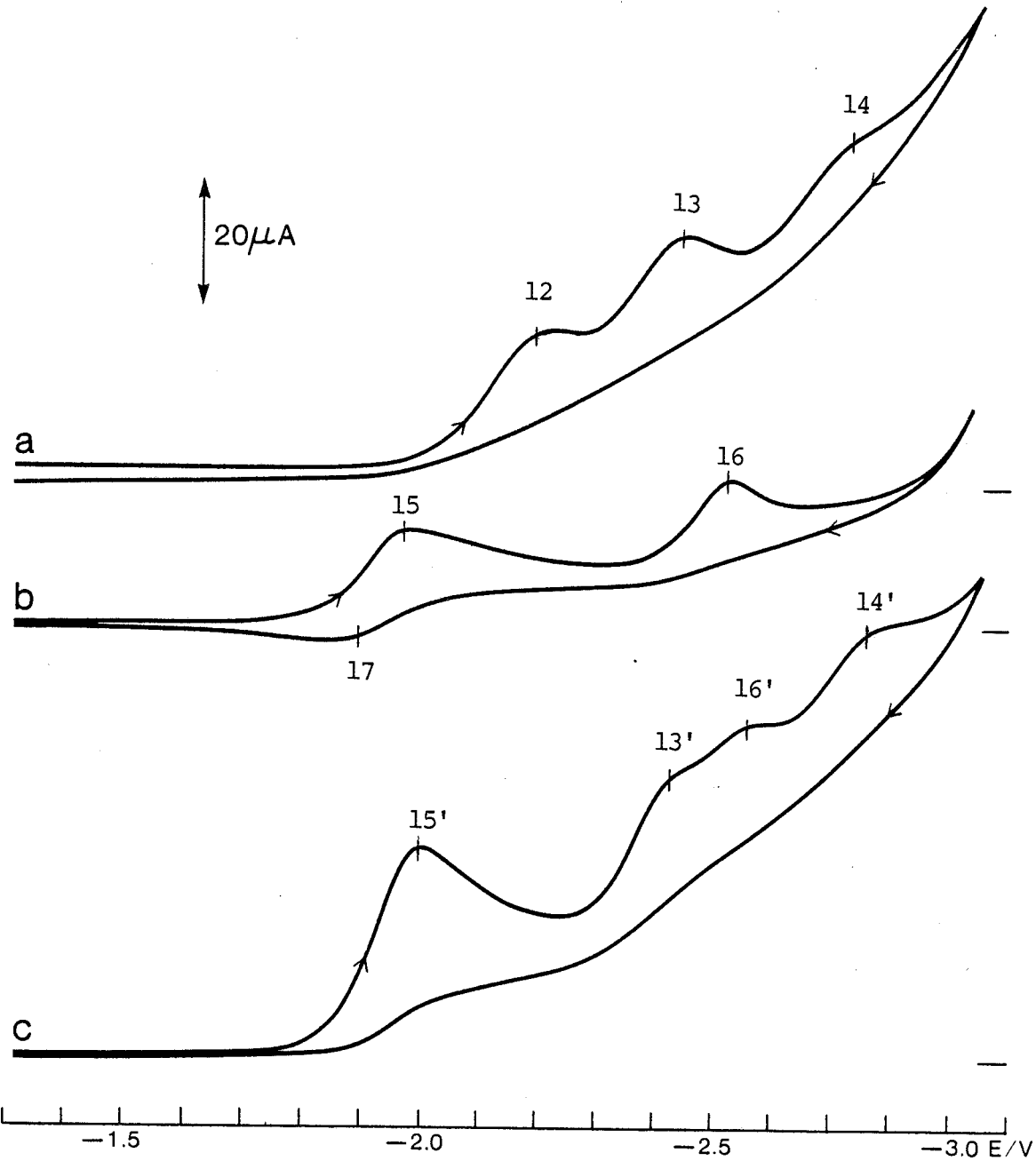


Table 14: Preparative Electrocatalytic Reduction of  $C_6H_3Cl_3$ <sup>a)</sup>

Entry	Anthracene (mM)	$C_6H_3Cl_3$ (mM)	t (min.)	Q		Yield of $C_6H_4Cl_2$ (%)
				(C)	( $Fmol^{-1}$ )	
6	-	3	8.0	0.9	0.12	-
7	3	3	7.5	7.3	1.0	21 <sup>b)</sup> (42) <sup>c)</sup>
8	3	3	14.8	11.0	1.5	39 (51)
9	3	3	19.5	14.6	2.0	57 (56)
10	3	3	25.5	17.3	2.4	66 (56)

a) Applied Potential -1.95 V vs. SCE

b) Based on the initial amount of  $C_6H_3Cl_3$

c) Coulombic yield

by controlled potential electrolysis experiments, the results of which are shown in Table 14. The electrolysis of  $C_6H_3Cl_3$  at -1.95 V in the absence of anthracene produced no  $C_6H_4Cl_2$ . In the presence of anthracene and with the same electrolysis period,  $C_6H_4Cl_2$  was obtained at 21% yield (entry 7). The yield of  $C_6H_4Cl_2$  increased with charge passed. No PhCl was formed, even at high yields of  $C_6H_4Cl_2$ . This indicates that anthracene catalyzes the reduction of  $C_6H_3Cl_3$  but not of  $C_6H_4Cl_2$ , and the results were consistent with those obtained from voltammetric experiments.

Using p-chlorobiphenyl as the substrate, a catalytic

enhancement factor of 1.09 was obtained. The anodic peak corresponding to the reoxidation of the anthracene radical anion decreased slightly (Figure 32). These results were indicative of slow electron exchange between the catalyst radical anion and p-chlorobiphenyl.

While this work was in progress, Rushling and Connors reported the indirect reduction of 4,4'-dichlorobiphenyl with anthracene as the mediator (98,99). Preparative electrolysis at the reduction potential of anthracene showed that chlorobiphenyl and biphenyl were formed with the latter as the major product. This suggested that anthracene catalyzed the reduction of chlorobiphenyl which was produced in the indirect reduction of 4,4'-dichlorobiphenyl. Their results were thus in accordance with our observations in voltammetric experiments.

When PCB's were employed as substrates, the height of the first reduction peak of anthracene was increased by a factor of 2.7 (Figure 33). The anodic peak due to the reoxidation of anthracene radical anion was totally suppressed in the sweep range investigated ( $0.01 \sim 0.5 \text{ Vs}^{-1}$ ). In the presence of anthracene, peak 4 of the PCB's was virtually eliminated. These results indicate that, as expected, anthracene is a more effective catalyst than benzophenone for the reduction of PCB's.

### II.3.3. Conclusion

This work has demonstrated that BP catalyzes the reduction of  $\text{C}_6\text{H}_2\text{Cl}_4$  and PCB's but not of other compounds whereas

anion  
of

Figure 32: CYCLIC VOLTAMMETRY OF SOLUTIONS OF

a) 3mM Anthracene

b) 3mM Anthracene + 3mM p-Chlorobiphenyl

Scan rate  $0.05 \text{ Vs}^{-1}$ , in 0.1M TEAP/DMF

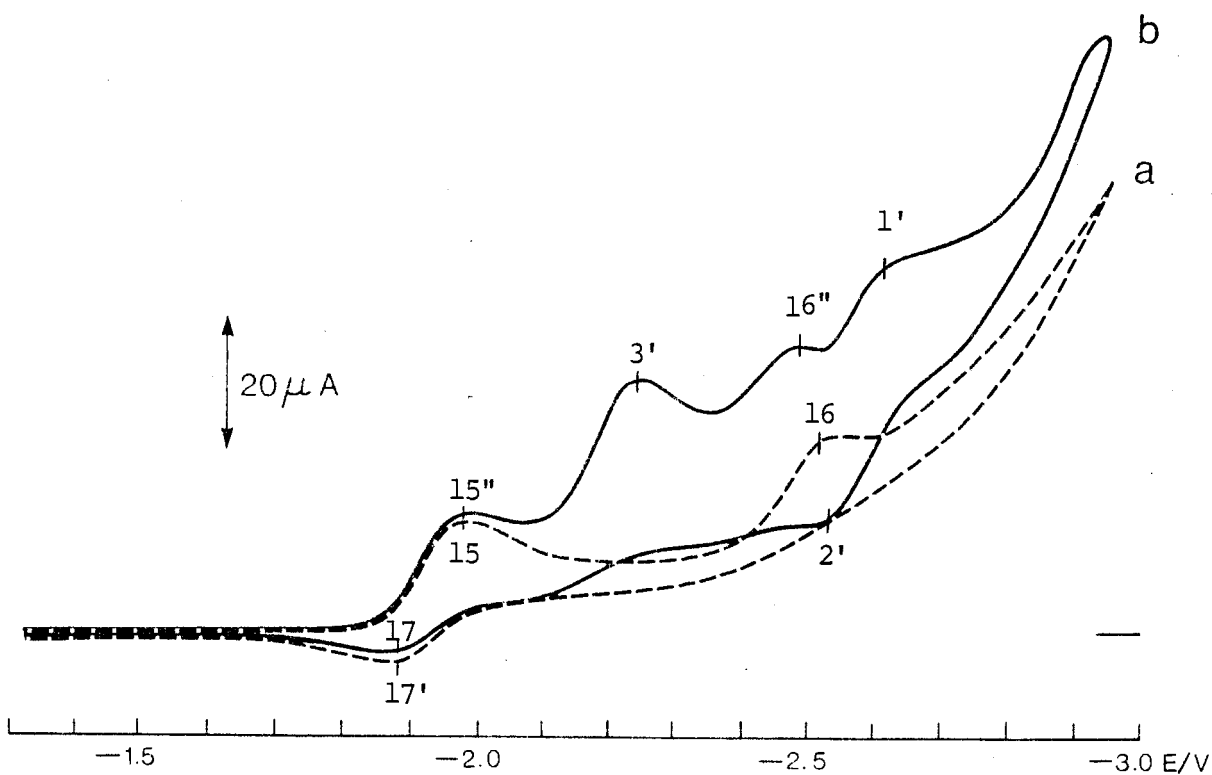


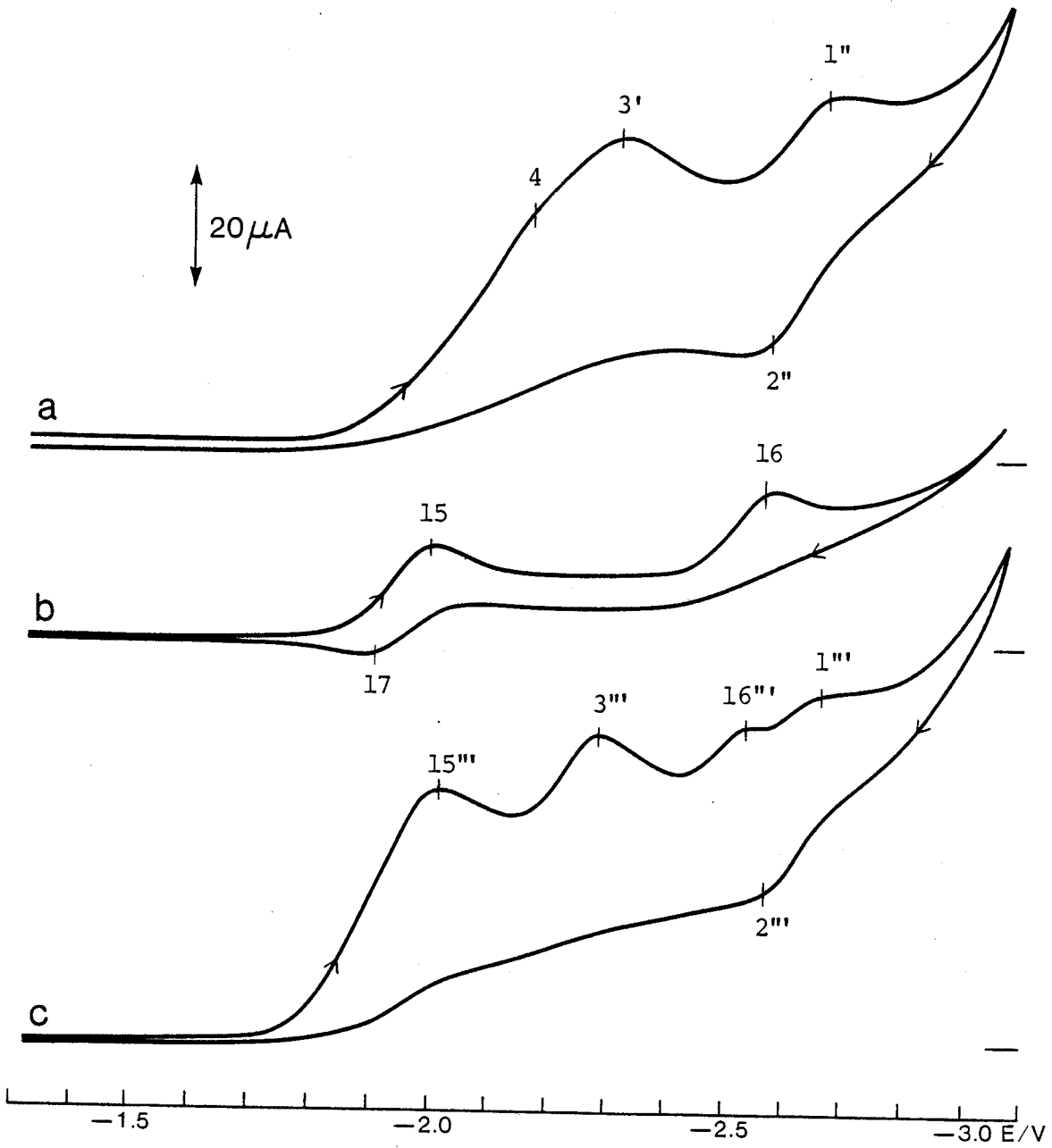
Figure 33: CYCLIC VOLTAMMETRY OF SOLUTIONS OF

a) 3mM PCB's

b) 3mM Anthracene

c) 3mM Anthracene + 3mM PCB's

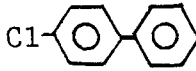
Scan rate  $0.05 \text{ Vs}^{-1}$ , in 0.1M TEAP/DMF



anthracene is a good mediator for the reduction of  $C_6H_3Cl_3$ , PCB's and p-chlorobiphenyl. The results are summarized in Table 15. For a given substrate, a higher catalytic efficiency is obtained with anthracene, which has a more negative reduction potential.

Coupling reactions between radicals of the substrates or between the substrates with the catalysts do not occur to a significant extent in these electrocatalytic reduction reactions.

Table 15: Difference in Peak Potentials of Mediators and Substrates ( $E^{Med} - E^{Sub}$ ) (in volts) and Catalytic Enhancement Factor ( $R^*$  in brackets) . a)

Substrate Mediator	$C_6H_2Cl_4$	PCB's	$C_6H_3Cl_3$	Cl- 	$C_6H_4Cl_2$	PhCl
BP	0.23 (1.73)	0.38 (1.3)	0.45 (1.0)	0.47 (1.0)	0.68 (1.0)	0.95 (1.0)
Anthracene	0.04	0.19 (2.7)	0.26 (2.2)	0.28 (1.09)	0.49 (1.0)	0.76 (1.0)

a) Substrate 3 mM, mediator 3 mM,  $0.05 \text{ Vs}^{-1}$ , 0.1M TEAP/DMF



C H A P T E R     I I I

ELECTROCHEMICAL STUDIES OF POLYMER-MODIFIED ELECTRODES

III.1. INTRODUCTION

III.1.1. General Remarks

A modified electrode is one in which the surface is deliberately altered usually to enhance its performance for a specific purpose. Prior to the research interest in electrode modification, adsorption of a solute on an electrode surface during the course of electrolysis had often been observed. Such occurrences were considered undesirable and no attempt was made to apply the phenomena.

The first deliberate modification of electrodes was reported in 1973 by Lane and Hubbard (100,101). They found that olefinic compounds adsorbed strongly on a platinum surface when the metal was soaked in a solution of the organic compounds. By using olefins with different terminal groups, a variety of surface functional groups was obtained. In 1975, Miller and coworkers prepared "chiral electrodes" by linking optically active amino acids to carboxylic acid sites on air-oxidized graphite (102). These electrodes were shown to yield optically active electrolysis products from inactive starting materials. The work was the first to demonstrate that electrode reactions could be made to follow selected pathways by surface modification, opening a new area in organic electrochemistry. In the same year, Murray et al. published the first of a series of papers on the general

strategy for electrode modification by covalent attachment (103). The approach was to bind organosilanes to surface hydroxyl groups present on pretreated metal oxide electrodes, in analogy to the derivatization of silica by silanization. Desired functional groups were immobilized at electrode surfaces via coupling reactions with silanes either prior to or after the silanization procedure.

Since the publication of these works, the study of modified electrodes has grown increasingly popular. The interest in this field is reflected in the considerable number of reviews which have appeared in the last few years (4-15).

The study of modified electrodes is particularly attractive for several reasons. The ability to synthetically manipulate the molecular composition of electrode surfaces offers new freedom in the design and construction of electrodes with particular characteristics. For example, redox species which catalyze certain types of reactions, can be attached to produce a surface with catalytic characteristics (18,19). A variety of applications have been proposed for modified electrodes. These include electrocatalysis (18,19), electrosynthesis (104-109), photoelectrocatalysis (13), electroanalysis (110), protection of semiconductor electrodes against photocorrosion (13), solar energy conversion (14,15), and electrochemical devices (storage batteries (111-113), electrochromic display devices (114-116), reference electrodes (117), pH sensors (118) and potentiometric sensors (119)).

Modified electrodes also provide convenient means for the

investigation of electrochemical characteristics of immobilized species and kinetic studies of electron transfer between them. Based on appropriate theoretical models (120-125), one can examine the interaction between surface reactants, the rate constant of a heterogeneous reaction between attached moieties and solution species and the diffusive parameters of the latter within the coating.

### III.1.2. Methods of Modifying Electrodes

There are several ways to modify an electrode surface. In general, the techniques employed can be categorized as chemisorption, covalent bonding and polymer deposition.

Chemisorption is strong or irreversible adsorption of small molecules in solution onto an electrode surface. Many organic compounds, such as olefins and polycyclic aromatic molecules, tend to adsorb from aqueous solution on Pt and carbon electrode surfaces (100,101,106). The technique is simple but lacks a control of the number of absorbed molecules. In addition, desorption of adsorbates may occur when they become charged and the surface coverage is low, which is equivalent to at most a monolayer.

Covalent bonding technique takes advantage of the fact that metal and oxide surfaces contain hydroxyl groups and that carbon surfaces possess a variety of functionalities such as carboxyl and quinoidal moieties. Bonding to the electrode is achieved by a reaction between these functional groups with a reactive organic species, such as silanes, cyanuric chlorides or acid chlorides

(4-13). The major advantage of this technique is that the bonding is so stable that the derivatized surfaces can be exposed to various solvents without loss of the reagent through dissolution. Disadvantages include the difficult and complex procedure, and low surface coverage.

Polymer deposition is a recently developed technique for modifying electrodes. The technique produces polymer films, the thickness of which may vary from a few to several thousand monolayer equivalents. Common methods of preparing polymer electrodes are based on physical adsorption, such as dip-coating, spin-coating, droplet evaporation, electrodeposition, electropolymerization and plasma polymerization (4-13). A few examples in which the polymer is chemically attached to the electrode surface have also been reported (127-129).

The polymer deposition technique has several advantages. The modification procedure is simple and requires mild conditions. The technique is non-specific, allowing modification of virtually any electrode surface. The electrical response may be higher due to a better surface coverage and a multilayer structure of the coating. The number of active centers can easily be regulated by varying the copolymer composition or film thickness. Various types of catalytic species can be immobilized onto a single surface for multimediation-reaction purpose by derivatizing electrodes with a copolymer or a homopolymer mixture.

However, the polymer deposition method has a fundamental limitation in that the modified electrodes cannot be used in

solvents which may dissolve or desorb the polymer film. Experiments are therefore restricted to media in which the polymer is insoluble. Even under these conditions, the loss of reactant may occur because the solubility of the polymer may increase as the film becomes charged. Nevertheless, the ease of the modification procedure, coupled with other advantageous characteristics of a polymer film have made the polymer deposition technique the most frequently used for electrode modification.

### III.1.3. Studies of Polymer-Modified Electrodes

#### a) Early Works

When this study was initiated, the large majority of modified electrodes reported were prepared by chemisorption and covalent attachment techniques. Literature on electrodes derivatized with polymeric materials consisted of only a few papers describing preliminary results. Among the first to report on this subject was Miller's group who dip-coated Pt surfaces with films of poly(p-nitrostyrene) (130,131). Cyclic voltammetry of these coated electrodes produced a reversible wave with a formal potential similar to those of molecular nitrobenzene in solution. The coated electrodes suffered loss of some chargeable material on the surface due to desorption and chemical instability of charged polymer. The polymer films in the neutral state inhibited the electrochemistry of dissolved ferrocene, but when negatively charged, catalyzed the reduction of oxygen, carbon tetrachloride (130) and meso-1,2-dibromo-1,2-

diphenylethane (131).

Bard et al. prepared polyvinylferrocene-coated electrodes by anodic deposition and by dip-coating techniques (132). The resulting polymer films apparently consisted of the equivalent of at least 20 monolayers of ferrocene. These coated electrodes exhibited a voltammetric behavior characteristic of ferrocene moieties, and were stable for a number of redox cycles. The group also covalently attached poly(methacrylchloride) to a silanized  $\text{SnO}_2$  surface and subsequently binded hydroxymethylferrocene to the polymer (127). The electrode thus obtained was considerably more stable than an analogous electrode prepared by dip-coating the same ferrocene polymer.

Pyrolytic graphite electrodes were coated with polyvinylpyridine and polyacrylonitrile by Oyama and Anson (133, 134). Metal complexes, such as  $\text{Ru}^{\text{III}}\text{EDTA}$  and  $\text{Ru}(\text{NH}_3)_5\text{OH}^{2+}$  were then coordinately incorporated to the polymer films. Cyclic voltammetry of the coated electrodes revealed that these coating were fairly stable and that the surface concentrations of the attached ruthenium complexes were about fifty times higher than that expected for a monolayer.

Murray (120) and Wrighton (129) inadvertently obtained electrodes chemically modified with ferrocene polymers during the course of covalent attachment of ferrocene moities on Pt surface with organosilanes. A multilayer coating was obtained as a result of polymerization of silanes which was induced by traces of moisture. The electrodes were very durable and could be used over hundreds of potential cycles with slight loss of modifying

material.

From the research presented above, it can be seen that electroactive polymers show potential as agents for derivatizing electrode surfaces. Detailed discussion on advantages of modification techniques using polymeric materials over the other methods has been presented in section III.1.2..

We have previously prepared several polymers containing electroactive groups such as benzophenone, benzoquinone, and anthraquinone, and investigated their electrochemical properties in solution (see chapter I). These polymers, with the exception of PVBQ homopolymer, are reduced reversibly at potentials similar to those found for the corresponding monomeric analogues. Active groups in polymer chains were shown to behave independently and to follow the theoretical prediction for non-interacting centers.

The electrochemical characteristics of these polymers, along with many important aspects of modified electrodes and the advantageous use of electroactive polymers as modifying agents had led to the exploration of the potential application of these polymers in modifying electrodes. Polymer films were formed by solvent evaporation from a Pt electrode surface and subsequently stabilized by a photolytic crosslinking reaction. The electrochemical behavior of polymer coatings was examined and compared with that of the same polymer in solution. The effect of experimental variables such as film thickness and scan rate on the voltammetric performance of coated electrodes was investigated in order to gain insight into the kinetics of

charge transport in the films. The effect of film morphology was studied by using various solvents. The application of polymer films in electrocatalysis was also examined.

While the present work was in progress, a large number of papers on polymer-modified electrodes were published. Since several excellent reviews have been written (4-15), it is unnecessary to provide comprehensive documentation here.

b) Studies of Polymer-Modified Electrodes

i) Type of Polymer Films

Polymer films on electrode surfaces can be grouped into four general classes: non-electroactive polymers, conducting polymers, ionic redox polymers and organic redox polymers.

Non-electroactive polymers are exemplified by polypeptide and polyester (135,136), poly(o-phenylenediamine) (137), and polymers of phenol and its derivatives (137,138). Films of these polymers do not undergo electron transfer reactions with electrodes and therefore cannot relay electrons between electrodes and solution species. Normally, non-electroactive polymer films hinder the electrochemistry of dissolved molecules because the diffusion of the latter to electrode surface is retarded. However, some unusual effects have been reported. Oyama et al. found that electrodes coated with polymers of some phenol and amino-aromatic compounds allowed a selective permeability to various ions in solution. It was demonstrated that these electrodes could be used for electroanalytical purpose (137). Recently, Nonaka and coworkers reported that electrodes modified



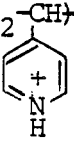
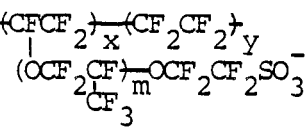
with films of some polypeptides were useful for asymmetric synthesis (106-109). For example, oxidation of phenylcyclohexyl sulfide at a poly-L-valine coated Pt electrode gave sulfoxide in 93.4% optical yield (109).

Conducting polymers are characterized by a delocalized band structure, by which electrons are transported through the bulk of polymers. Conducting polymer films are obtained by electropolymerization of heterocyclic aromatic compounds such as pyrrole, thiophene, aniline, carbazole, furan, azulene and many derivatives of these (139-141). Generally, the polymers are non-conducting in neutral state, but become highly conducting when positively charged. Depending on doping condition, conductivity can be as high as  $100 \text{ Scm}^{-1}$  (142).

Ionic redox polymers are a class of materials, in which ionic redox groups are electrostatically bound to a polyelectrolyte chain or coordinately incorporated to a macromolecule bearing ligand groups. Some important polymer films are presented in Table 16. Coated electrodes are reversibly oxidized and reduced at potentials appropriate for the electrochemical reaction of attached redox centers.

Organic redox polymers have organic redox couples covalently attached to a polymer backbone. Redox couples which have received much attention are ferrocene (143-144), quinones (145-146), dopamine (147), nitrophenyl (130-132), azobenzene (148), viologens (149,150), thionine (151,152), tetrathiafulvalene (153,154), porphyrins (155,156) and pyrazoline (153,157). Since polymers studied in this thesis fall into this category,

Table 16: Ionic Redox Polymers.

Polymer Backbone	Redox Ions
$\langle \text{CH}_2 - \text{CH} \rangle$ 	$\text{Fe}(\text{CN})_6^{3-}$ , $\text{IrCl}_6^{3-}$ , $\text{W}(\text{CN})_8^{4-}$ , $\text{Mo}(\text{CN})_8^{4-}$
$\langle \text{CF}_2\text{CF}_2 \rangle_x \langle \text{CF}_2\text{CF}_2 \rangle_y$ $\langle \text{OCF}_2\text{CF}_2 \rangle_m \text{OCF}_2\text{CF}_2\text{SO}_3^-$  (Nafion)	$\text{Co}(\text{bpy})_3^{3+}$ , $\text{Ru}(\text{bpy})_3^{2+}$ , $\text{MV}^{2+}$ $\text{Ru}(\text{bpy})_3^{2+}$ , $\text{CpFeCpCH}_2\text{N}(\text{CH}_3)_3^+$ , $\text{Os}(\text{bpy})_3^{2+}$

MV = viologen

$\text{CpFeCp}$  = ferrocene

bpy = bipyridine

discussion on modified electrodes will be focussed on those derivatized with redox polymers.

## ii) Theoretical Studies

### Monolayer

Cyclic voltammetry is a convenient technique to examine electrochemical properties of modified electrodes. For an electrode derivatized with a monolayer of a non-interacting, Nernstian redox species, the voltammetric current is related to

electrode potential by (149):

$$i = \frac{n^2 F^2 \Gamma A \exp(E - E^{0'})}{RT[1 + \exp(E - E^{0'})]^2} \quad [85]$$

and the peak currents are given by:

$$i_{pc} = i_{pa} = \frac{n^2 F^2}{4RT} \Gamma A \quad [86]$$

$\Gamma$  is the integrated peak area which is equivalent to the amount of material on the electrode surface, and the other terms have their usual meanings.

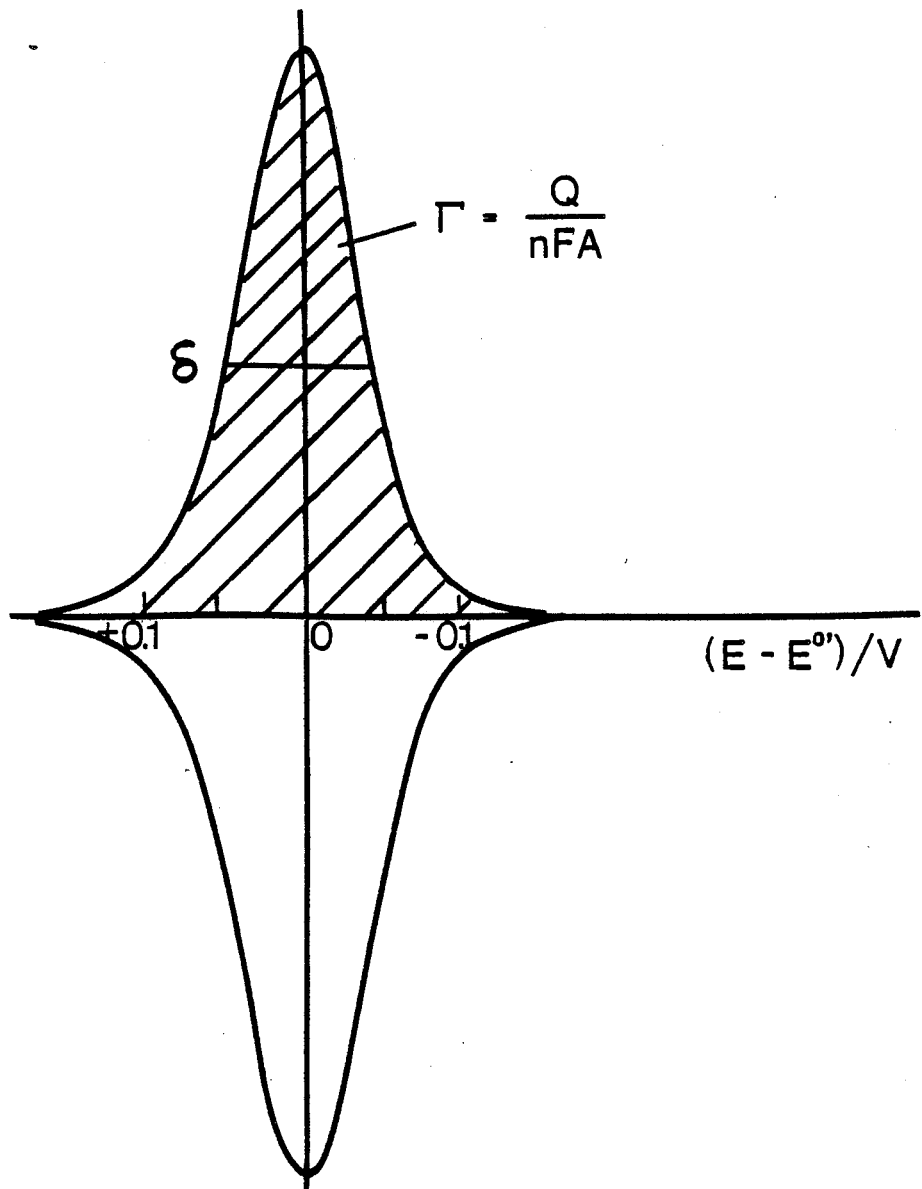
The linear relationship between peak current and scan rate differs from the  $v^{1/2}$  dependence observed for dissolved species because the attached reactant is oxidized and reduced without diffusion limitations. The absence of mass transfer also results in the coincidence of the peak potentials on forward and reversed sweeps, ie.  $E_{pc} = E_{pa} = E^{0'}$ , and the rapid decrease of current after the maximum is reached as shown in figure 34. The cyclic voltammogram is symmetrical with respect to both the zero current and formal potential axes. The peak width at half-maximum  $\delta$  is given by:

$$\begin{aligned} \delta &= 3.53 RT/nF \\ &= 90.6 \text{ mV (for } n=1 \text{ at } 25^\circ\text{C)} \end{aligned} \quad [87]$$

### Polymer Films

For polymer-coated electrodes, where the coating consists of multilayers, the situation is much more complex: the majority of

Figure 34: CYCLIC VOLTAMMOGRAM OF A REVERSIBLE MONOLAYER COATING.



active centers are not in contact with the electrode surface; the transmission of electrons through layers is necessary to reduce moieties remote from the surface; the transport of counter ions and associated solvent molecules through the film is needed to balance charges; the coating may not be uniform; the polymer morphology may change following oxidation-reduction and the presence of a thick film on an electrode surface may impose a higher resistance.

Theoretical treatments for the kinetics of electron transfer within a redox polymer film have been developed (120-122,159). The studies employed a multilayer model in which the polymer film is divided into  $p$  layers of thickness  $\Delta x$  ( $\Delta x = l/p$  where  $l$  is the film thickness). The model proposed that reduction occurs in the first (innermost) sublayer and other sublayers are subsequently charged by electron exchange between the inner and the next outer layers, as shown in figure 35. Assuming the concentration of active centers in the film is uniform, and that there are no interactions between them, the rate of electron exchange from one layer to the next can be written as:

$$\frac{dC_{R_j}}{dt} = k\Gamma\Delta x^2[(C_{R_{j-1}} - 2C_{R_j} + C_{R_{j+1}})/\Delta x^2] \quad (1 < j < p) \quad [88]$$

$$\text{and } \frac{dC_{R_p}}{dt} = k\Gamma(C_{R_p} - C_{R_{p-1}}) \quad (j=p) \quad [89]$$

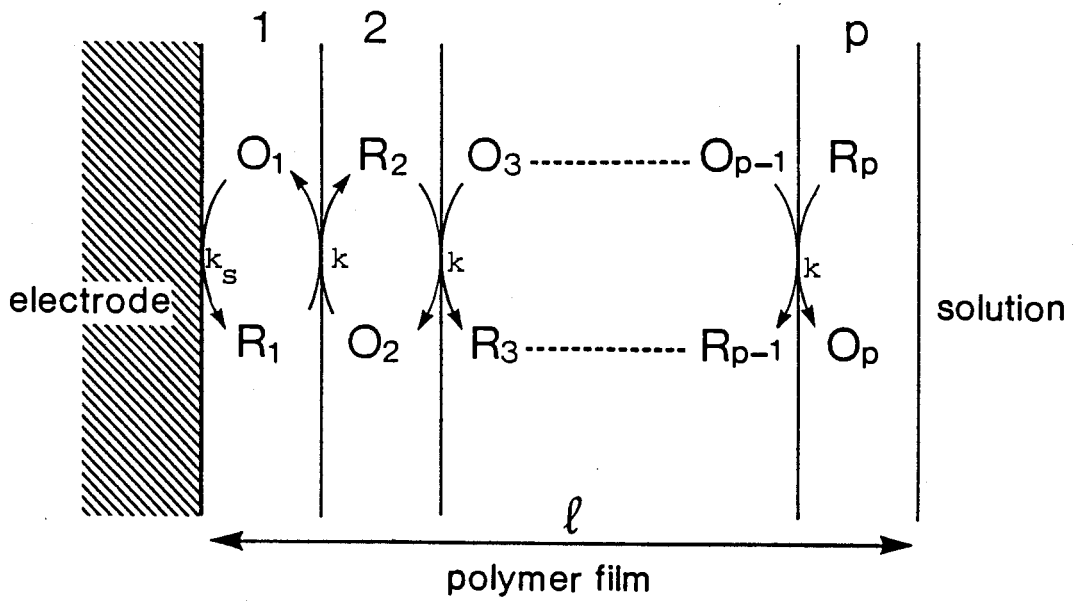


Figure 35: A MULTI-LAYER MODEL.

$C_{Rj}$  denotes the volume concentration of species R in the  $j^{\text{th}}$  layer, and  $\Gamma$  is the initial surface concentration of species O,  $k$  ( $\text{cm}^2 \text{mol}^{-1} \text{s}^{-1}$ ) is the surface rate constant of the electron self-exchange reaction between active centers. The bracketed terms of equation [88] is the finite difference expression of  $\frac{\partial^2 C_R}{\partial x^2}$ , and the above equation can be rewritten as:

$$\frac{\partial C_R}{\partial t} = D_{CT} \frac{\partial^2 C_R}{\partial x^2} \quad [90]$$

where  $D_{CT} = k \Gamma \Delta x^2 = k' \Gamma \Delta x$  ( $k'$ =volume rate constant) [91]

Equations for the first layer are

$$\frac{C_{O_1}}{C_{R_1}} = \exp \left[ \frac{nF}{RT} (E - E^{O'}) \right] \quad [92]$$

for a Nernstian behavior of the O/R couple,

$$\begin{aligned} \text{and } \frac{dC_{R_1}}{dt} = k_s [C_{O_1} \exp^{-\frac{\alpha nF}{RT} (E - E^{O'})} - C_{R_1} \exp[(1-\alpha) \frac{nF}{RT} (E - E^{O'})] \\ - k(C_{O_2} C_{R_1} + C_{O_1} C_{R_2}) \end{aligned} \quad [93]$$

for a quasi-reversible electron transfer ( $\alpha$  = transfer coefficient,  $k_s$  = heterogeneous standard rate constant).

The total current is given by:

$$i = nFA\Delta x \sum_{j=1}^p \frac{dC_{R_j}}{dt} \quad [94]$$



Linear potential sweep voltammograms were analyzed based on equation [94]. The results show that the shape and characteristics of the curves depend on the rate of electron exchange between the electrode and the first layer, the rate of electron exchange in the film and experimental variables such as scan rate and film thickness.

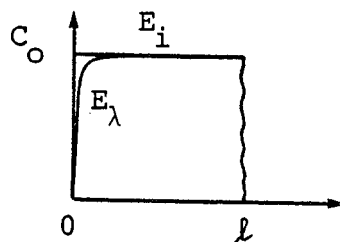
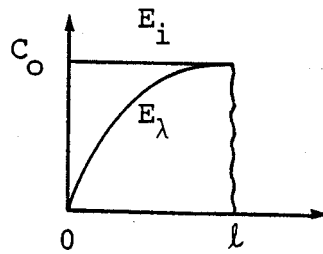
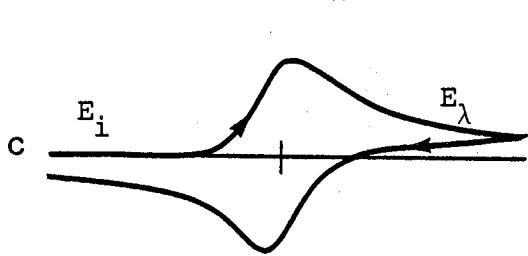
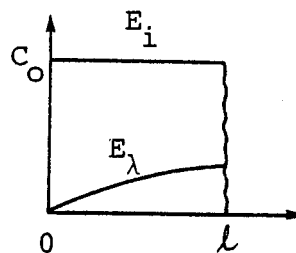
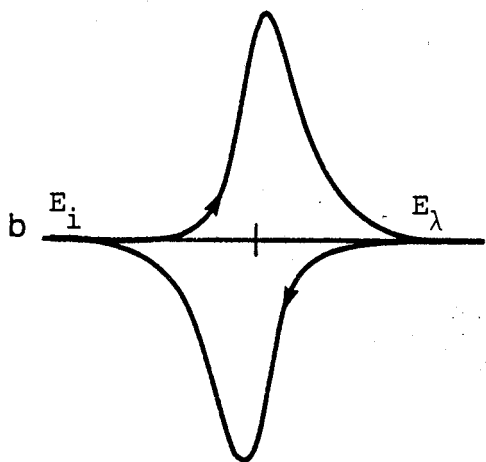
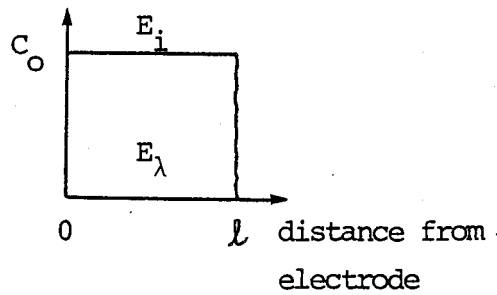
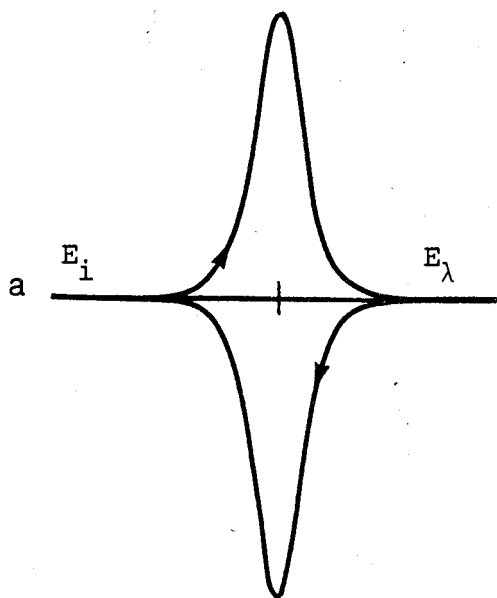
Figure 36 illustrates the variations of the cyclic voltammogram and of the concentration profile of species 0 in the film as a function of the dimensionless parameter  $\mu = RTk'/nFv$  in the Nernstian case. When  $\mu \rightarrow \infty$ , ie. the electron transfer in the film is fast and/or the scan rate is slow, there is enough time for the equilibrium to be established in any part of the coating. The  $i$ - $E$  response has the shape and characteristics identical to those of a reversible monolayer. The film is completely reducible, and the charge given by the area of the cathodic peak ( $\Gamma_{obs}$ ) corresponds to the total number of attached electroactive sites ( $\Gamma_{cal}$ ). As  $\mu$  decreases, ie.  $k'/v$  decreases, the current tends to tail as for a diffusion-controlled process. This is because the transmission of electrons in the film is slow on the experimental scale so that it continues to take place over longer times. The cathodic and anodic waves are no longer identical, the peaks become broader ( $\delta > 90.6$  mV), the peak currents are not proportional to the scan rate ( $i_{pc} \propto v^x$  with  $0.5 < x < 1$ ) and only a fraction of species 0 is reducible ( $\Gamma_{obs} < \Gamma_{cal}$ ). When  $\mu \rightarrow 0$ , the peak tends towards a reversible monolayer peak again because the transmission of electrons in the film is very slow and the reaction tends to be confined in the

Figure 36: THEORETICAL VOLTAMMOGRAMS AND CONCENTRATION-DISTANCE  
PLOTS FOR OXIDIZED SITES FOR A REDOX POLYMER FILM  
WITH FAST ELECTRON-TRANSFER WITH THE ELECTRODE.

$n = 1, p = 10, \mu =$

- a)  $\infty$
- b) 20
- c) 3
- d) 0.01

(Ref. 159)



first layer.  $\Gamma_{\text{obs}}$  corresponds to the number of active centers in the innermost layer.

The thickness of polymer films also has an influence on the voltammetry of coated electrodes (159). As shown in Figure 37, when the film is so thin that the transmission of electrons up to the last layer takes place rapidly, all active sites in the film are in equilibrium with the electrode potential, and the voltammetric behavior is like that of a reversible monolayer. As the film thickness increases, the peak height increases moderately but a diffusional tailing appears: a potential scan has traversed the wave before electrons propagate to the outermost layer, and a semi-infinite charge diffusion condition prevails. This is similar to the case where  $k'/v$  is small (Figure 36c). A further increase in the film thickness produces a more pronounced tailing for the same reason. However, there is no change in the peak height. This is because at the peak potential, the number of active centers being reduced has reached a limiting value.

Figure 38 shows the effect of the electrochemical irreversibility of immobilized redox species on the voltammetric behavior of a polymer film. When  $k_s(RT/FvD_{\text{CT}})^{1/2}$  decreases, i.e. the scan rate increases, the cathodic and anodic peaks are shifted significantly toward negative and positive potentials, respectively, and are no longer symmetrical (121,159).

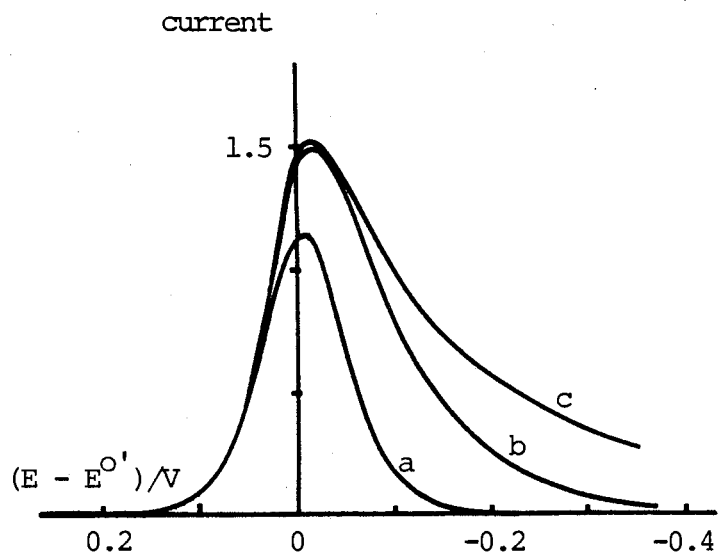
Figure 37: THEORETICAL VOLTAMMOGRAMS FOR REDOX POLYMER FILMS OF VARIOUS THICKNESSES (FAST ELECTRON-TRANSFER WITH THE ELECTRODE). (Ref. 159)

$n = 1$ ,  $\mu = 10$ ,  $P =$

a) 5

b) 10

c) 15



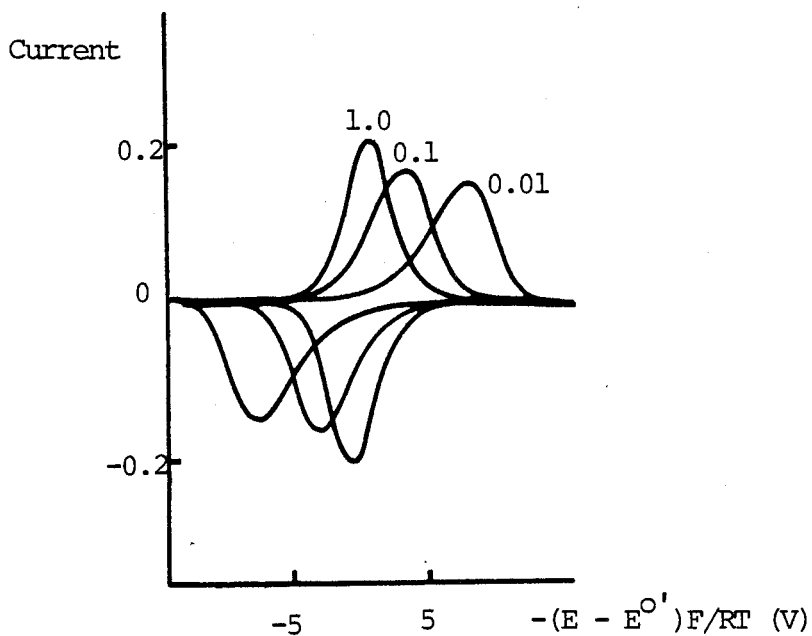


Figure 38: THEORETICAL VOLTAMMOGRAMS FOR A REDOX POLYMER FILM WITH A QUASI-REVERSIBLE ELECTRON TRANSFER WITH THE ELECTRODE. (Ref. 121)

The numbers on each curves are the values of the parameter  $k_s (RT/FDv)^{1/2}$   
 $1/(Fv/RTD_{CT})^{1/2} = 1.05$

iii) Electrochemical Studies

In most cases, literature on polymer electrodes shows that the redox centers in the coating exhibit formal potentials similar to those of analogous species in solution. However, very often, the voltammogram shape differs from that characteristic of a reversible, non-interacting monolayer. Films thicker than a few hundred angstroms usually show a kinetic limitation of charge transport (143,144). The  $i$ - $E$  response shows tailing at the peak edges, large peak separation (120-160 mV) and  $i_p$  varying with scan rate in a less than linear fashion. Voltammograms of symmetrical shape with  $i_p$  proportional to  $v$  may be obtained with films that are sufficiently thin ( $<100 \text{ \AA}$ ) (160), but they often exhibit a non-zero peak-to-peak separation and peak widths at half-height greater than 90.6 mV. For some polymers, such as those containing dopamine (146,147) or azobenzene (148), the transmission of electrons in the film is so slow that the reaction is confined only to the innermost layer.

Other changes of peak-shape have been observed. In the study of polyvinylferrocene films, Bard et al. observed voltammograms with multi-wave shapes although the films consist of only one type of redox center. Similar behavior was reported for poly-p-nitrostyrene (130) and polyvinylpyridine incorporated with  $\text{Ru}^{\text{III}}$ -EDTA (133,134). The results were ascribed to the existence of electrochemically non-equivalent sites, which possess different formal potentials. When polymer films are poorly swollen in the test solution, or when attractive interactions between active centers exist, peaks become narrow (161).



Polymer films containing redox groups may be rendered electrochemically inactive when studied in non-solvents (162, 163). The low permeability of solvent and electrolyte into the film was considered responsible for this behavior.

"Break-in" is another unusual feature of some polymer films. It was reported that in the cyclic voltammetry of tetrathiafulvalence polymers (153,154), peak currents grew considerably with repeated scans. When these films were maintained in the neutral state for a short period of time, the original structure of the films was restored. This effect was attributed to film swelling, increased electrolyte permeability in a charged film, and a slow polymer chain reorganization process.

From the brief review above, it can be seen that the electrochemical behavior of redox polymer films may be different in many ways from that of a monolayer coating and is generally more complex.

#### iv) Charge Transport

The kinetics of charge transport in a polymer film can be examined quantitatively by evaluating the  $D_{CT}$  value. The transmission of electrons in the coating has been proposed to occur by an "electron hopping" mechanism, ie. electron self-exchange between oxidized and reduced sites (153,154). This is analogous to a diffusion process, in which electrons diffuse from the electrode surface towards the polymer film/solution interface (reduction) or vice versa (oxidation) with an apparent electron diffusion coefficient  $D_{CT}$ . Indeed, this has been

shown mathematically by equation [90], in which the charge transport coefficient  $D_{CT}$  is expressed in the form of a diffusion equation. Murray experimentally demonstrated that the hopping process follows Fick's diffusion laws, and that transient techniques used to determine diffusion coefficients of solution species can also be applied to estimate  $D_{CT}$  (143,161). The most common method employed is chronoamperometry, in which the potential is stepped from the point where no reaction occurs to the value where the reduction is complete. Under semi-infinite conditions, where the depletion layer does not exceed the film outer boundary, the current decay follows the Cottrell equation:

$$i = nFAD_{CT}^{1/2}C(\pi t)^{1/2} \quad [95]$$

where  $C$  is the volume concentration of active centers in the film.

$D_{CT}$  can be calculated from the slope of a  $i$  vs.  $t^{-1/2}$  plot. Since it was introduced by Murray's group, the method has been widely applied to determine  $D_{CT}$  of a number of polymer films. The results were documented in a recent review, and show that  $D_{CT}$  values span over several orders of magnitude ( $10^{-7} \sim 10^{-13}$   $\text{cm}^2\text{s}^{-1}$ ) (9).

## III.2. EXPERIMENTAL

### III.2.1. Chemicals

Chemicals and their purification are the same as those described in section I.2.

### III.2.2. Film Preparation

A measured volume of a polymer solution in toluene (0.05 - 1.0 w/v %) was placed on the surface of the working electrode and the solvent was allowed to evaporate slowly. The electrode was subsequently dried in vacuo for 5 minutes. The film thickness was estimated from the quantity of polymer initially present in the solution.

The films were crosslinked by irradiating the coated electrodes immersed in isopropanol with light from a 100 W Hg lamp (Engelhard Hanovia). The electrode was then dried in vacuum for 10 minutes.

### III.2.3. Electrochemistry

A three compartment cell as shown in figure 5 was employed. The working electrodes were Pt disks sealed in soft glass. The Pt diameters were 1.25, 2.5 and 5.0 mm for experiments with PVBP, PVBQ and PAQ, respectively. The electrodes were polished successively with SiC 600, 3  $\mu$ m diamond paste, 2  $\mu$ m and 0.05  $\mu$ m alumina on polishing cloth and subsequently sonicated in distilled water for 10 min.. Before each set of runs, the polymer from the previous experiment was removed with tissue paper and

the electrode was cleaned chemically and electrochemically as described in the literature (164).

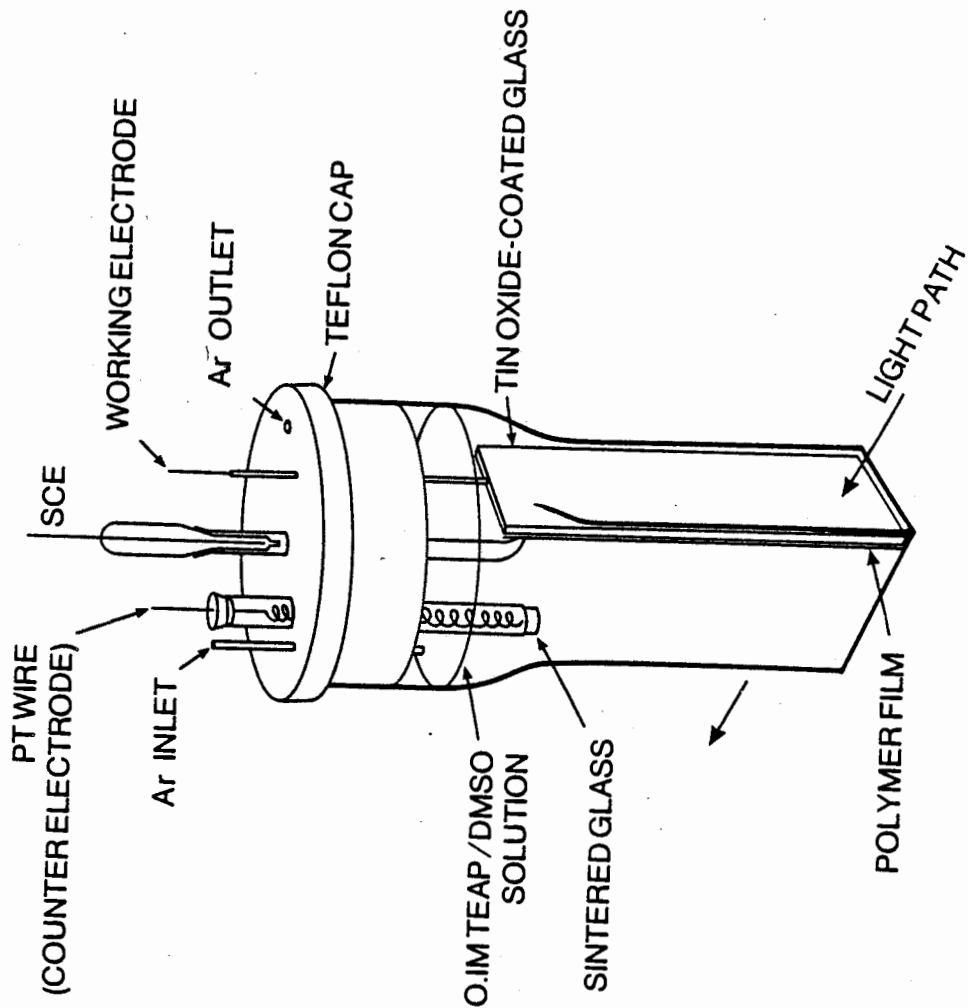
A Pt wire was used as the counter electrode. For the PVBP system, where the absence of trace water was essential, a Ag/AgNO<sub>3</sub> reference was employed, whereas a SCE with salt bridge was used for the PVBQ and PAQ systems. All potentials are reported relative to a SCE electrode.

The solutions were flushed with Ar, and an Ar atmosphere was maintained during the voltammetric measurements. A PAR 170 electrochemical system with IR compensation was employed. An Apple II microcomputer based data acquisition system was employed for step function Cottrell experiments. The integration of the voltammograms was made by "copy, cut and weigh" technique after subtracting the background current.

#### III.2.4. Spectroelectrochemistry

A 1x1x4 cm square cross section optical cuvette was connected to a 1.2 $\phi$  cm x 5 cm tube by a quartz to glass seal. The tube was fitted with a teflon cap with ports for a SCE, a miniature counter electrode and Ar inlet, as shown in Figure 39. The working electrode was a sheet of tin oxide-coated glass (VWR Scientific) on which the polymer sample was deposited. Electrical connections were made with silver dag (Electrodag), which was subsequently covered with epoxy resin. Visible spectra were recorded on a Unicam SP 8000 spectrophotometer.

Figure 39:           SPECTROELECTROCHEMICAL CELL.



### III.3. RESULTS AND DISCUSSION

This chapter describes electrochemical studies of electrodes modified with PVBP, PVBQ and PAQ. The study of each polymer will be presented separately in each section, with emphasis being on PAQ polymers because of their remarkable chemical and physical stabilities.

#### III.3.1. Studies of Electrodes Modified with Polyvinylbenzophenone

##### a) Stability of Polymer Films

The ability of a modified electrode to retain its electrochemical activity after several oxidation-reduction cycles is necessary for its practical use and kinetic studies. It has been reported that electrodes coated with an adsorbed polymer film often suffer loss of some modifying material due to desorption dissolution of the polymer (130,132). In this section, the durability of PVBP films was examined and an approach to increase their adherence to electrode surface by a photolytic crosslinking reaction is presented.

The voltammetry of PVBP films adsorbed on a Pt surface in a 0.1M TEAP/DMF solution is shown in figure 40. An electrode modified with a 1000 Å PVBP film without UV irradiation treatment did not exhibit any well-defined voltammogram in the potential range of -1.0 V ~ - 2.5 V vs. SCE (Figure 40a). Even for a thicker film (5000 Å), no improvement was observed. Since DMF is a good solvent for PVBP, it was believed that the polymer film had dissolved completely before voltammograms were recorded.

Figure 40: CYCLIC VOLTAMMETRY ON SUCCESSIVE SCANS OF  
ELECTRODES COATED WITH

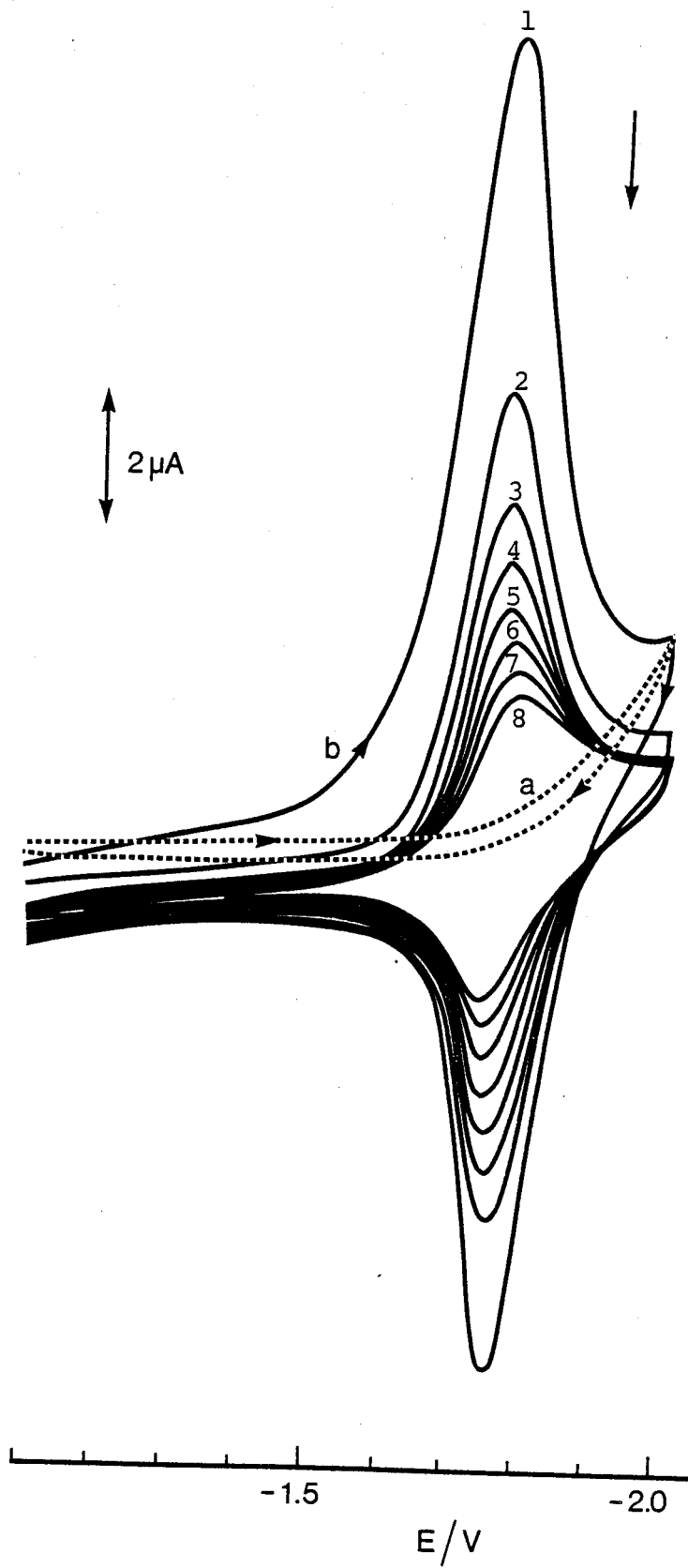
a) A non-irradiated PVBP film

b) An irradiated PVBP film

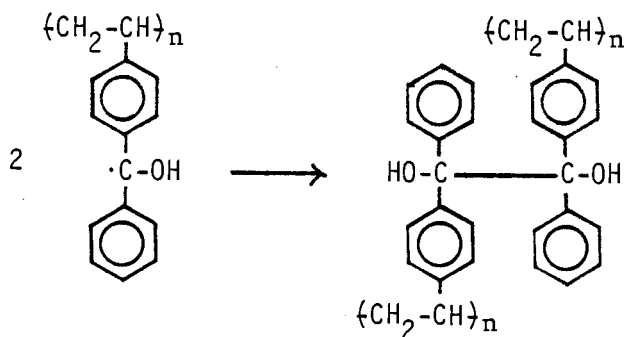
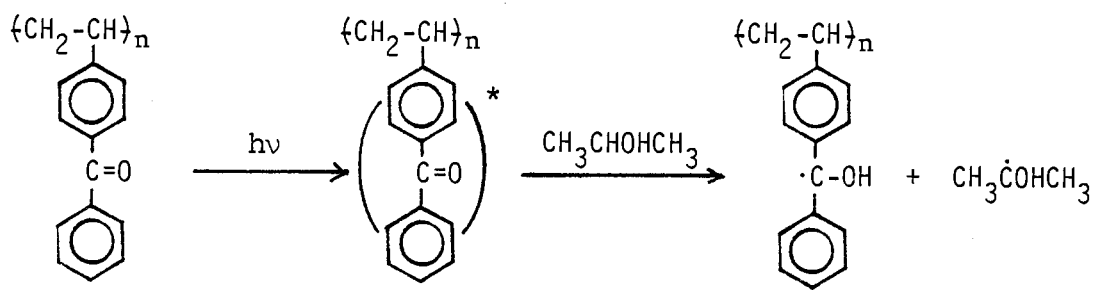
Film thickness 1000 Å, scan rate 0.1 Vs<sup>-1</sup>,  
in 0.1M TEAP/DMF.

The number on each curve is the number of cycle.





One method to prevent the dissolution of polymers is to crosslink them. It has been reported that PVBP polymers can be readily insolubilized by irradiation at 365 nm in i-PrOH (165). Intermolecular recombination between the resulting pendant BP radicals leads to a crosslinking reaction as shown in the following scheme:



[96]

A typical cyclic voltammogram of a PVBP-coated electrode after 10 min. exposure to UV light is shown in Figure 40b. As expected, a reversible wave was observed at -1.77 V, and was assigned to the BP/BP<sup>-</sup> couple in the film. The results thus indicate that UV irradiation had increased the physical stability of the film.

The peak current diminished continuously on successive scans. Since the BP radical anion is known to be reactive with water to form non-oxidizable product, the continuous decrease in peak currents is attributed to the protonation of BP<sup>-</sup> by residual water, rather than to the dissolution of polymer. This interpretation is supported by the fact that the variation of the length of time that the coated electrode was soaked in the test solution had little effect on the current magnitude. In addition, the longevity of the film was dependent on the dryness of the solution; the electroactivity of the film was retained longer in a more carefully purified solution.

An alternative method to increase the physical stability of the film is to conduct experiments in a solvent in which the polymer is insoluble. Acetonitrile was used for such a study. Figure 41a shows the cyclic voltammogram of a non-crosslinked PVBP film. A cathodic wave which corresponds to the reduction of PVBP to PVBP<sup>-</sup> is obtained. However, on the reverse scan, no corresponding anodic peak is observed. On successive scans, the reduction peak totally disappears. These observations can not be ascribed to the dissolution of polymer since a similar result was also obtained with a crosslinked film (Figure 41b). It is

Figure 41: CYCLIC VOLTAMMETRY OF

a) A non-irradiated PVBP film

b) An irradiated PVBP film

— First scan

---- Second scan

Film thickness 1000 Å, scan rate 0.1 Vs<sup>-1</sup>,  
in 0.1M TEAP/CH<sub>3</sub>CN

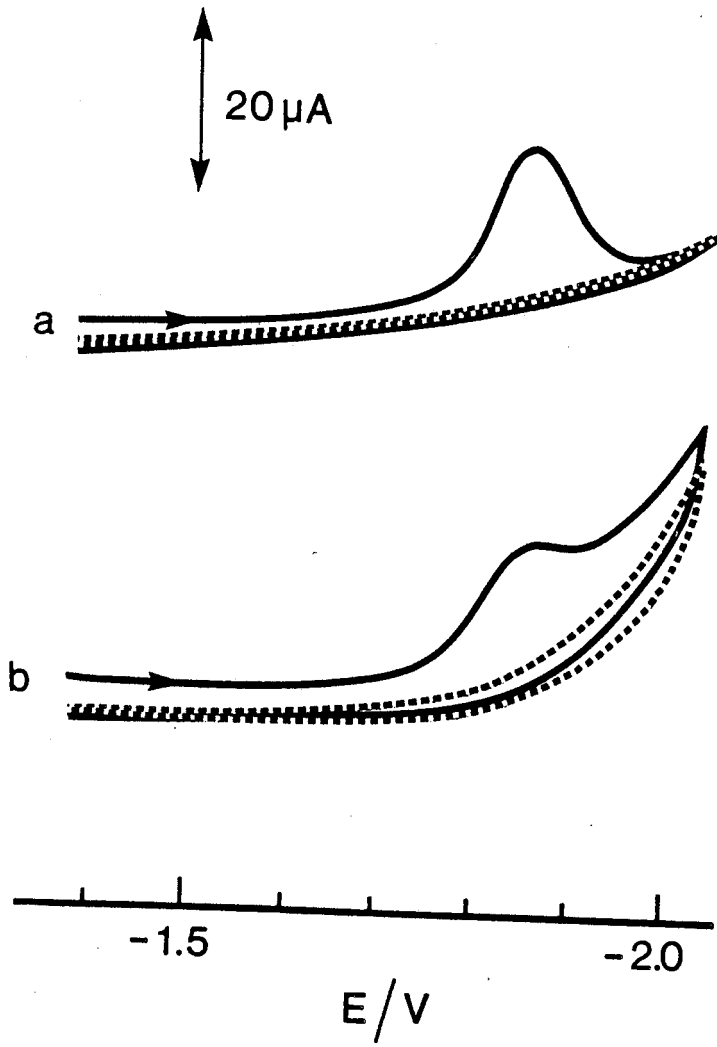


Table 17: Voltammetric Characteristics of PVBP in Solution and Coated on an Electrode Surface <sup>a)</sup>

Compounds	$E_{1/2}$ (V)	$\Delta E$ (mV)
PVBP Solution	-1.78	67
PVBP Film <sup>b)</sup>	-1.77	12

a) 0.1M TEAP/DMF, 0.05 Vs<sup>-1</sup>, SCE.

b) Film thickness 1000 Å, U.V. irradiation time 10 min.

known that radical anions have a shorter lifetime in  $\text{CH}_3\text{CN}$  than in DMF, because the former does not form a hydrogen bond with residual water (166). This is probably responsible for the rapid deactivation of benzophenone radical anions in the film in  $\text{CH}_3\text{CN}$ .

Since DMF appears to be a better solvent than  $\text{CH}_3\text{CN}$  from a chemical stability point of view and U.V. irradiation enhanced the physical stability of the film, further experiments with crosslinked PVBP-modified electrodes were conducted in DMF.

The effect of the U.V. irradiation period on the cathodic peak current was investigated in order to optimize the properties of the film. The results in Figure 42 show that a maximum was obtained after a 10 minute exposure. An excess of irradiation had led to destruction of electroactive centers and excessive crosslinking of chains, whereas insufficient irradiation resulted in dissolution of the film. The optimum condition of U.V. irradiation was thus determined, and was chosen for all film preparations reported here.

#### b) Voltammetric Studies

Voltammetric characteristics of PVBP films are summarized in Table 17. For scan rates up to  $0.2 \text{ Vs}^{-1}$ , the behavior of films of  $1000 \text{ \AA}$  thickness closely follows that expected for surface-confined redox species (120-122,159). The peak separation was small (12 - 16 mV), the wave shape was almost symmetrical about the  $E_p$  axis and the cathodic peak current varied linearly with scan rate (Figure 43). However, the peak width at half-height was 152 mV, compared to the theoretical value of 90.6 mV.

Figure 42: EFFECT OF TIME OF U.V. IRRADIATION ON THE  
CATHODIC PEAK CURRENT OF PVBP-COATED ELECTRODES.

Film thickness 1000 Å, scan rate 0.1 Vs<sup>-1</sup>,  
in 0.1M TEAP/DMF



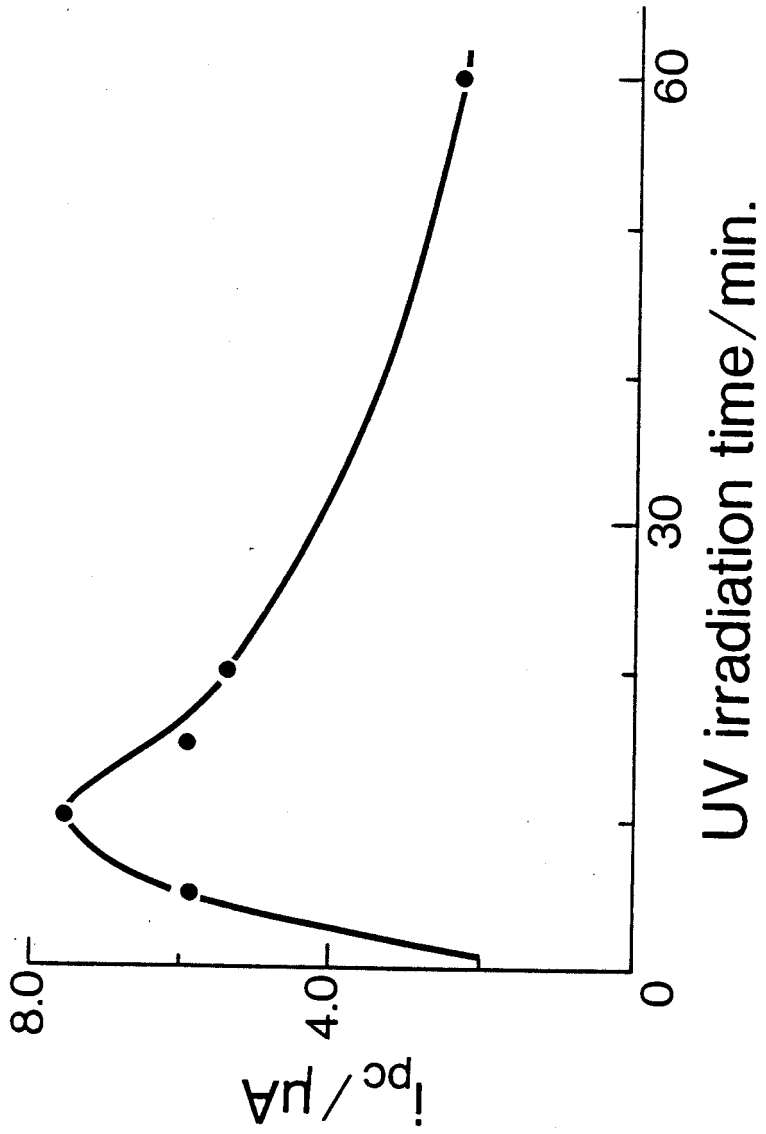


Table 18: Voltammetric Characteristics of PVBP Films<sup>a)</sup>

Thickness (x1000 Å)	Scan rate (Vs <sup>-1</sup> )	ΔE (mV)	δ (mV)	Γ <sub>obs</sub> (nmolcm <sup>-2</sup> )	$\frac{\Gamma_{obs}}{\Gamma_{cal}}$ (%)
1	0.02	16	152	4.42	9.5
1	0.05	12	152	4.55	9.7
1	0.10	16	152	4.53	9.7
1	0.20	16	152	4.42	9.5
1	0.50	56	196	4.23	9.1
5	0.10	48	184	1.39	3.0

a) 0.1M TEAP/DMF, U.V. irradiation time 10 min., Data obtained in the first scan.

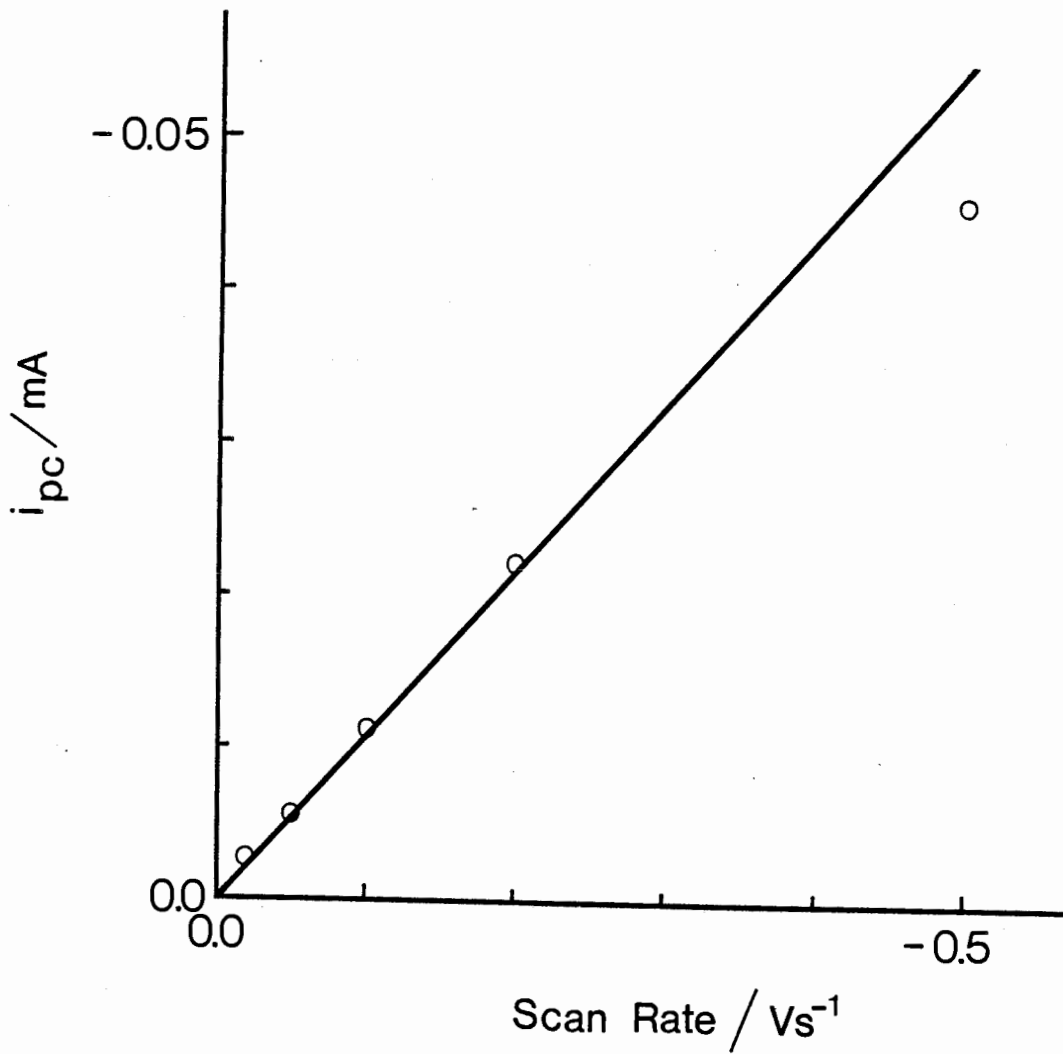
Integration of the cathodic peak yielded a surface coverage of 4.42 - 4.55 nmolcm<sup>-2</sup>.  $\Gamma_{obs}$  is surprisingly low compared to the number of BP groups initially present ( $\Gamma_{cal} = 46.9$  nmolcm<sup>-2</sup>) on the Pt surface. This indicates that only a small fraction of electroactive centers in the film was reduced.

At higher scan rates, e.g. 0.5 Vs<sup>-1</sup>, peaks became broader, cathodic and anodic peaks became more separated and peak currents varied with scan rate in a less than linear fashion. These are indicative of a kinetic limitation of charge transport in the film. Similar characteristics were also obtained with thicker films.

Theoretical studies of the voltammetric behavior of redox polymer films based on a multilayer model have been recently reported and the results were briefly presented in section III.1.3.b) ii). Although the treatment does not take into account factors such as the inhomogeneity of electrode, the non-equivalence of redox sites, the non-uniformity of the coating, the change of film morphology upon charging, the resistance effects and the permeability of ions and solvent, the results of the studies have been widely employed to interpret experimental observations of many redox polymer films. The PVBP system in the present work may present a more complicated situation since the film is crosslinked and a chemical reaction interferes with the electrochemical process. However, the voltammetric data shown in Table 17 appear to be qualitatively interpretable on the basis of the multilayer model.

Figure 43: CATHODIC PEAK CURRENT VS. SCAN RATE PLOT  
FOR PVBP FILMS.

Film thickness 1000 Å, U.V. irradiation time  
10 min., in 0.1M TEAP/DMF



On the basis of this theory, the symmetrical wave shape, the small peak separation potential and the linear dependence of  $i_{pc}$  on scan rate for 1000 Å films at  $v \leq 0.2 \text{ Vs}^{-1}$  are indicative of fast electron transfer at electrode, and the results are thus in accordance with the reversible behavior of PVBP in solution. With the exception of the large peak width  $\delta$  and small  $\Gamma_{obs}$ , the small peak separation potential  $\Delta E$ , the absence of diffusional tailing and the linear dependence of  $i_{pc}$  on scan rate suggest that the charge transport in the film may be either very fast or very slow on the experimental time scale. Theoretically, in the former case,  $\Gamma_{obs}$  should be comparable to  $\Gamma_{cal}$ , the total number of BP groups in the film, whereas in the latter situation, should correspond to the amount of BP in a monolayer. Surface coverage of a monolayer is generally about  $1 \times 10^{-10} \text{ molcm}^{-2}$  (129).  $\Gamma_{obs}$  obtained with a 1000 Å PVBP film at scan rate  $\leq 0.2 \text{ Vs}^{-1}$  is thus equivalent to 40 - 50 monolayers. From this result, it is believed that the charge propagation in 1000 Å PVBP films on this time scale is relatively fast (case b in Figure 36). The low  $\Gamma_{obs}$  value is presumably due to a reaction of BP radical anions with residual water during the course of electron transport. As a consequence, charge could not be transmitted throughout the film.

Voltammograms with peak width  $\delta$  larger than the theoretical value are not unique in this system, and have indeed been noted in many other modified electrode systems. For instance, a  $\delta$  value of  $\sim 150 \text{ mV}$  has been reported for films of polymers containing ferrocene (143,144), porphyrins (155,156) and p-nitrostyrene (130,131), respectively. However, other voltammetric

characteristics of these polymer films conformed to the theoretical prediction, ie. the linear dependence of peak current on scan rate and the symmetrical wave shape. There are two different explanations for this phenomenon. Bard (127) and Kuwana (156) attributed the large value to the existence of active centers at different environment sites at different energy whereas Laviron (159), Anson (133,134) to name but a few, interpreted the observation as a consequence of repulsive interaction between redox groups. Since the study of PVBP polymer solutions has shown that each benzophenone group behaves as independent moiety, the explanation by Bard and Kuwana is presumably more appropriate for PVBP films.

c) Electrocatalytic Reduction of  $\text{PhCl}_4$  by PVBP Films

An important application of modified electrodes is mediated oxidation or reduction of solution substrates by immobilized redox reagents. Catalysis at a modified electrode has advantages over homogeneous catalysis in that smaller quantities of mediator are required and that cumbersome separation problems are avoided. Coatings consisting of electroactive polymers are particularly attractive because they combine the advantage of an attached catalyst with the dimensional distribution of catalytic centers prevailing in homogeneous catalysis. A number of examples have been reported concerning with electrocatalytic reactions at polymer-modified electrodes (18,19).

In section II.3.2. b) i), it has been demonstrated that benzophenone is an effective catalyst for the electroreduction of

$C_6H_2Cl_4$ . This has led us to explore the potential application of PVBP-coated electrodes in electrocatalytic reduction of  $C_6H_2Cl_4$ .

Figure 44a shows the voltammogram of a 3mM  $C_6H_2Cl_4$ /0.1M TEAP /DMF solution at a bare Pt electrode, in a potential range of -1.2 V to -2.0 V. The  $i$ - $E$  response of the same electrode coated with a 1000 Å PVBP film in a solution containing no  $C_6H_2Cl_4$  is shown in Figure 44b. The voltammetric curve of the polymer film is symmetrical with  $i_{pa} = i_{pc}$ . When  $C_6H_2Cl_4$  was added into the solution, the cathodic peak current of the polymer film was greatly enhanced and the anodic current entirely suppressed (Figure 44c). Since the reduction of  $C_6H_2Cl_4$  on a clean Pt electrode yielded a negligible current at the polymer peak potential, the increase in the cathodic peak current of the polymer film is attributed to the mediated reduction of  $C_6H_2Cl_4$  by the PVBP film. However, the film was rapidly deactivated. On the second scan, the peak height of the film decreased substantially and the peak totally disappeared on successive scans.

#### d) Conclusion

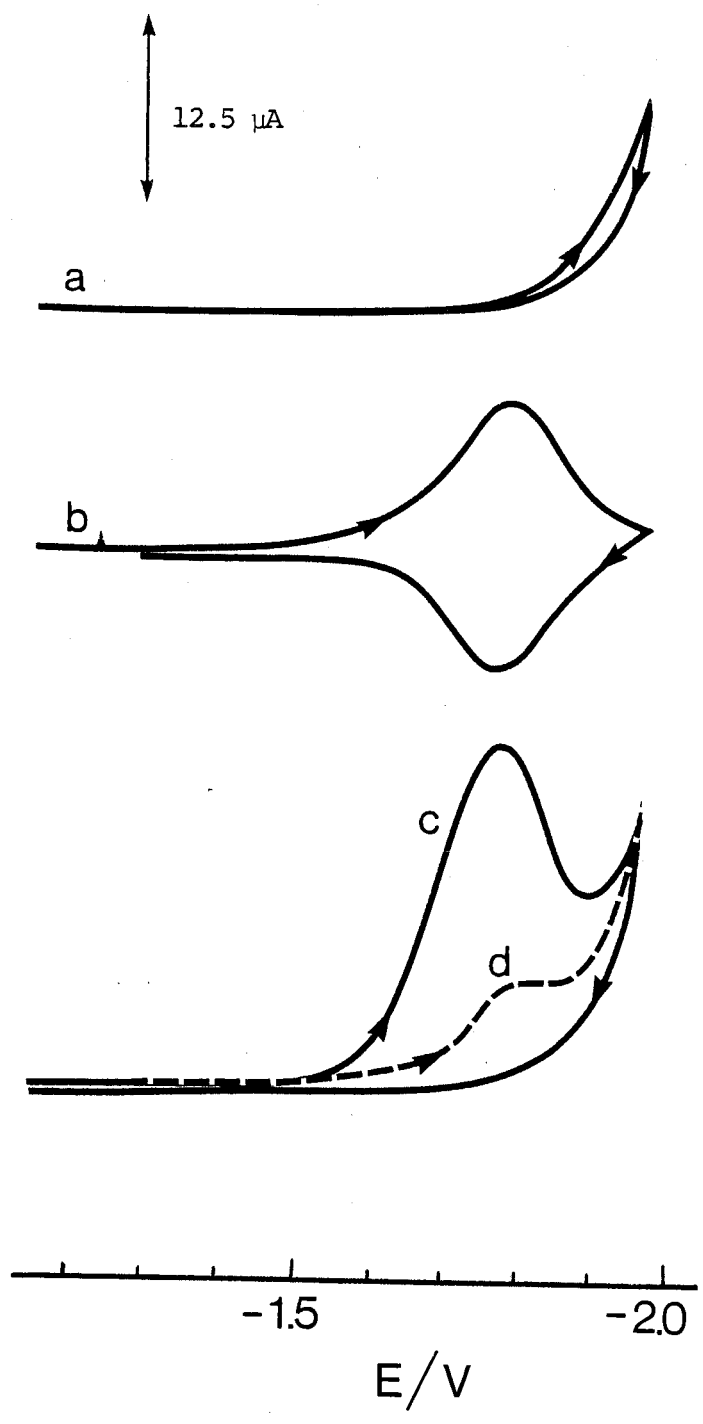
This study has demonstrated that benzophenone groups can be immobilized on an electrode surface by coating it with benzophenone polymers. In  $CH_3CN$ , polymer films adhered on electrode surface but the latter was rapidly deactivated after the polymer was reduced to the radical anion. In DMF, a good solvent of PVBP, the film dissolved rapidly. The physical stability of the film was enhanced by U.V. irradiation, which induced a crosslinking reaction.



Figure 44: CYCLIC VOLTAMMETRY OF

- a) 3 mM  $C_6H_2Cl_4$  at a bare electrode
- b) A PVBP coated electrode (film thickness 1000 Å)
- c) 3 mM  $C_6H_2Cl_4$  at the same coated electrode in b),  
first scan
- d) As c) but second scan

Scan rate  $0.05 \text{ Vs}^{-1}$ , in 0.1M TEAP/DMF



The polymer film underwent a fast electron transfer reaction with electrode and was reduced at a potential similar to that found for an analogous, homogeneous solution. Films of less than 1000 Å thickness exhibited characteristics of a fast film charging process whereas thicker films showed a kinetic limitation of charge transport in the films.

The transmission of electrons in polymer coatings was interfered with by a chemical reaction between attached benzophenone radical anions and residual water. This resulted in a continuous decrease in electrochemical activity on successive scans, and in a small fraction of reducible groups. The polymer films catalyzed the reduction of  $C_6H_2Cl_4$  but were rapidly deactivated.

III.3.2. Electrochemical Characteristics of Electrodes Coated With Films of Poly(vinyl-p-benzoquinone) and Its Copolymers With Styrene

a) Film Stability

Figure 45 illustrates the voltammograms of a Pt electrode coated with a 5000 Å PVBQ-St (VBQ=24.5%) copolymer film in 0.1 M TEAP/DMSO solution. The electrode exhibited reversible behavior with  $E_{pc} = -0.56$  V and  $E_{pa} = -0.49$  V, which are close to values for MeBQ and PVBQ-St dissolved in solution (see section I.3.2. a)). This suggests that quinone groups attached in a polymer film undergo electrochemical processes similar to their analogues in solution. The peak currents, however, diminished significantly with scanning cycles, and stabilized after about 20 scans. This stability was attained more rapidly at high sweep rates.

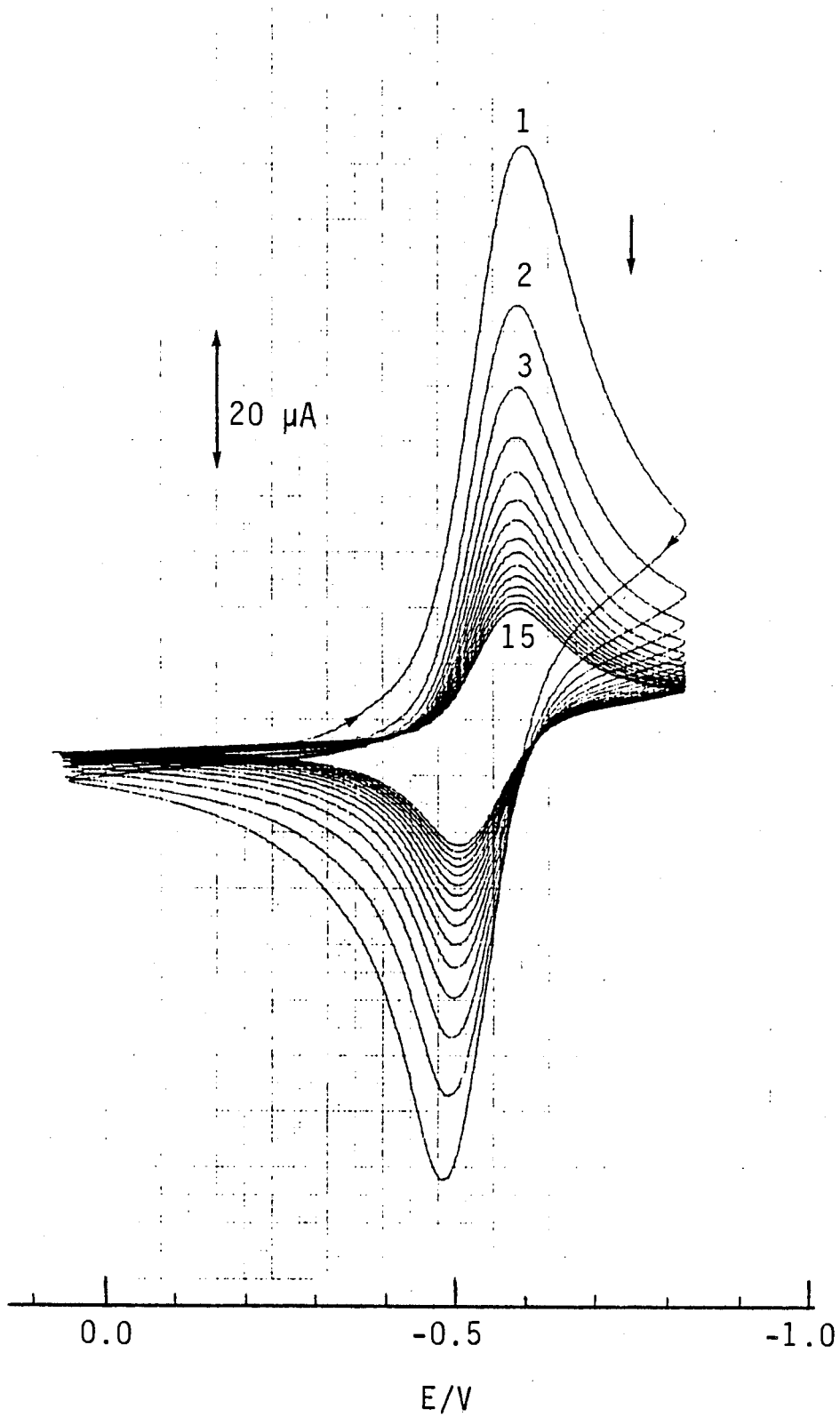
The scanning effect on the stability of the coating has been also reported for electrodes coated with polyvinylferrocene (132) and benzo(c)cinnoline (159), and the initial instability was attributed to the desorption of absorbate. In the study of electrodes modified with dopamine containing polymers, Miller et al. ascribed the continuous decrease of peak current with repeated cycling to the intervening chemical reaction involving the redox centers (146,147).

In the present work, both polymer desorption and chemical interaction may be responsible for the diminution of the current magnitude. Desorption is evidenced by the fact that a coated electrode which had been soaked in a TEAP/DMSO solution for 10 minutes prior to the voltammetric experiment showed a

Figure 45: CYCLIC VOLTAMMETRY IN 0.1M TEAP/DMSO OF  
A 5000 Å PVBQ-St FILM (VBQ% = 24.5) ON  
SUCCESSIVE SCANS.

Scan rate  $0.05 \text{ Vs}^{-1}$ , in 0.1M TEAP/DMSO.

The number on each curve is the number of cycles.



featureless voltammogram. This indicates that the electrode had lost all of its absorbed material. The data shown in Figure 45a imply that electrochemical treatment improved the adherence of the film. The reason for this increased stability is not clear, but one possible explanation is the occurrence of the coupling reaction involving BQ radical anions, resulting in the crosslinking of the film. However, the enhancement of the film stability upon cycling has also been obtained with some systems, such as benzo(c)cinnoline (159), where a crosslinking reaction is unlikely to occur. Presumably, repeated charging and discharging processes have also caused a change in the orientation of the absorbate in such a way that the physical interaction increased between the electrode surface and the absorbate.

It was reported that the photolysis of benzoquinones leads to coupling reactions. Cookson et al. found that the irradiation of BQ and MeBQ with light from a medium-pressure Hg lamp or from the sun produced insoluble polymers (167). Gold and Ginsburg obtained a dimer of BQ, using a high pressure Hg lamp (168). This is in agreement with our observation that the exposure of PVBQ and PVBQ-St polymers to ambient light for several days yielded insoluble materials. This suggests that a PVBQ-St film on an electrode may be stabilized by the photolysis technique. Irradiation of a PVBQ-St coated electrode was carried out with a medium pressure Hg lamp for 10 - 60 min. However, contrary to expectation, improvement in the film stability was not obtained. Presumably, the coupling reaction was slow, and on this time scale, did not produce sufficient crosslinking to insolubilize

the film.

b) Voltammetric Studies of Electrodes Coated with PVBO-St Films

The voltammetric data for 1000 Å and 5000 Å PVBO-St films at various scan rates are presented in Table 19 and Figure 46. Experiments with thinner films were also performed but were unsuccessful because of the rapid desorption of the polymers.

Films with an initial, dry thickness of 1000 Å appeared to exhibit the kinetic limitation of the charge transport process (Figure 46b). The peak separation potential was 16 ~ 48 mV for scan rates of 0.02 ~ 0.5 Vs<sup>-1</sup>, whereas the peaks should coincide for a fast charge transport in the film. The peak width at half-height was 180 ~ 210 mV in contrast to 90.6 mV predicted for a reversible monolayer. The current was proportional to  $v^{0.77}$  (Note: the voltammograms shown in Figure 46 were recorded after the film stability was established, ie. after the current dropped to about 60% of the initial value. Thus, the actual film thickness might be much smaller than originally estimated). The kinetically limiting features were more pronounced at higher scan rates; for  $v$  greater than 0.1 Vs<sup>-1</sup>, a diffusional tailing was clearly observed.

Diffusion controlled characteristics were also pronounced in thicker films. A 5000 Å film produced an  $i$ - $E$  response with the shape and properties very similar to those obtained with species dissolved in solution. The voltammogram was no longer symmetrical,  $\Delta E$  was 56 ~ 168 mV, depending on scan rate, and the



Figure 46: CYCLIC VOLTAMMETRY OF A PVBQ-St FILM  
(VBQ% = 24.5) AT VARIOUS SCAN RATES.

Scan rate:

- a)  $0.50 \text{ Vs}^{-1}$
- b)  $0.20 \text{ Vs}^{-1}$
- c)  $0.10 \text{ Vs}^{-1}$
- d)  $0.05 \text{ Vs}^{-1}$
- e)  $0.02 \text{ Vs}^{-1}$

Initial film thickness  $1000 \text{ \AA}$  , in  $0.1\text{M TEAP/DMSO}$

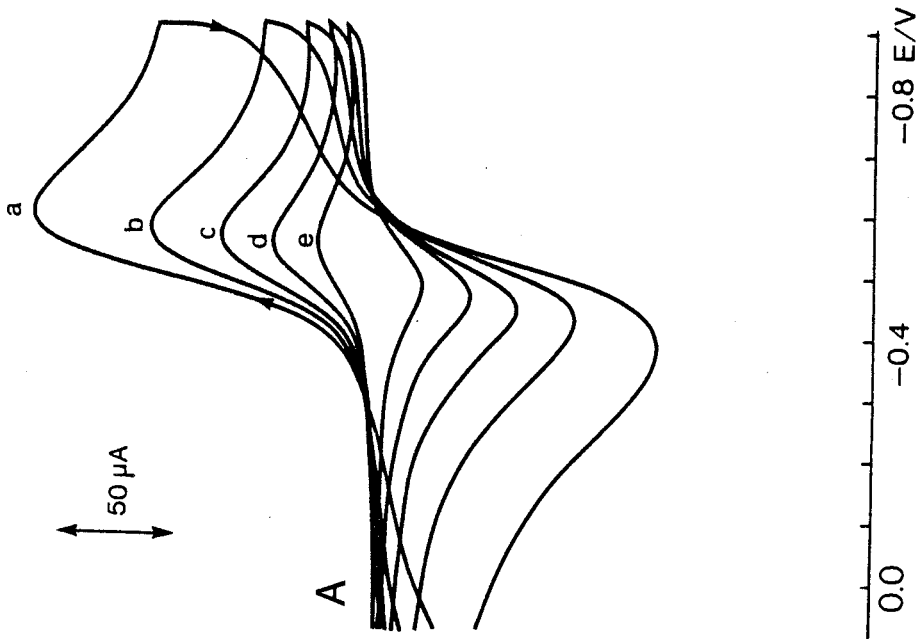
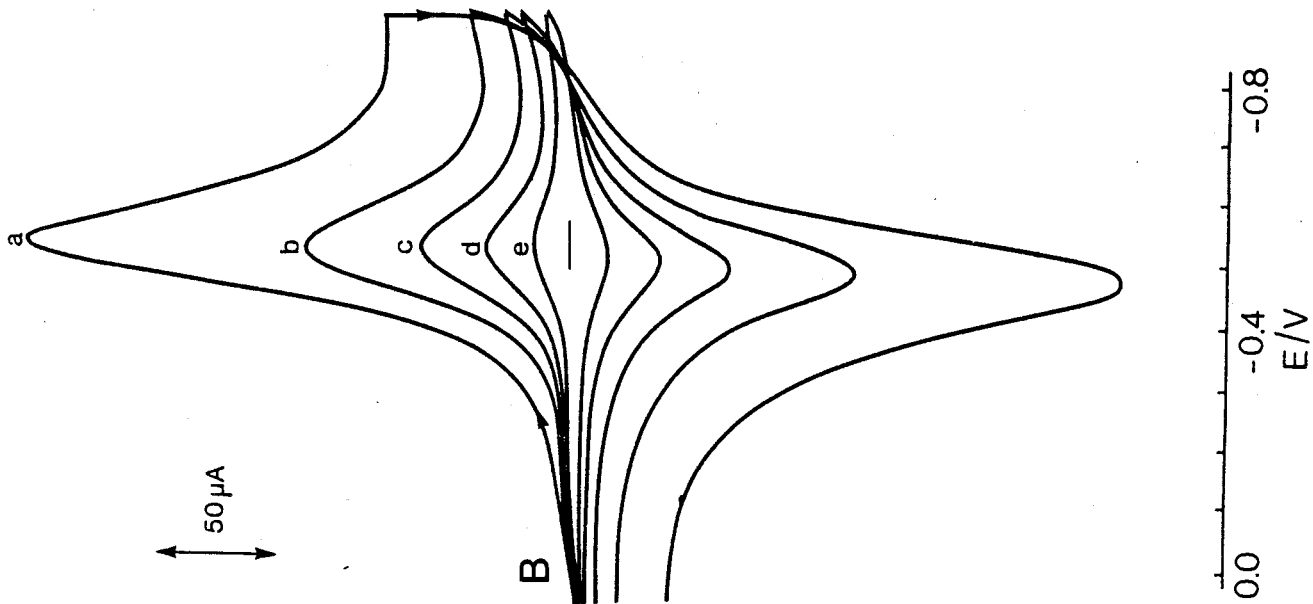


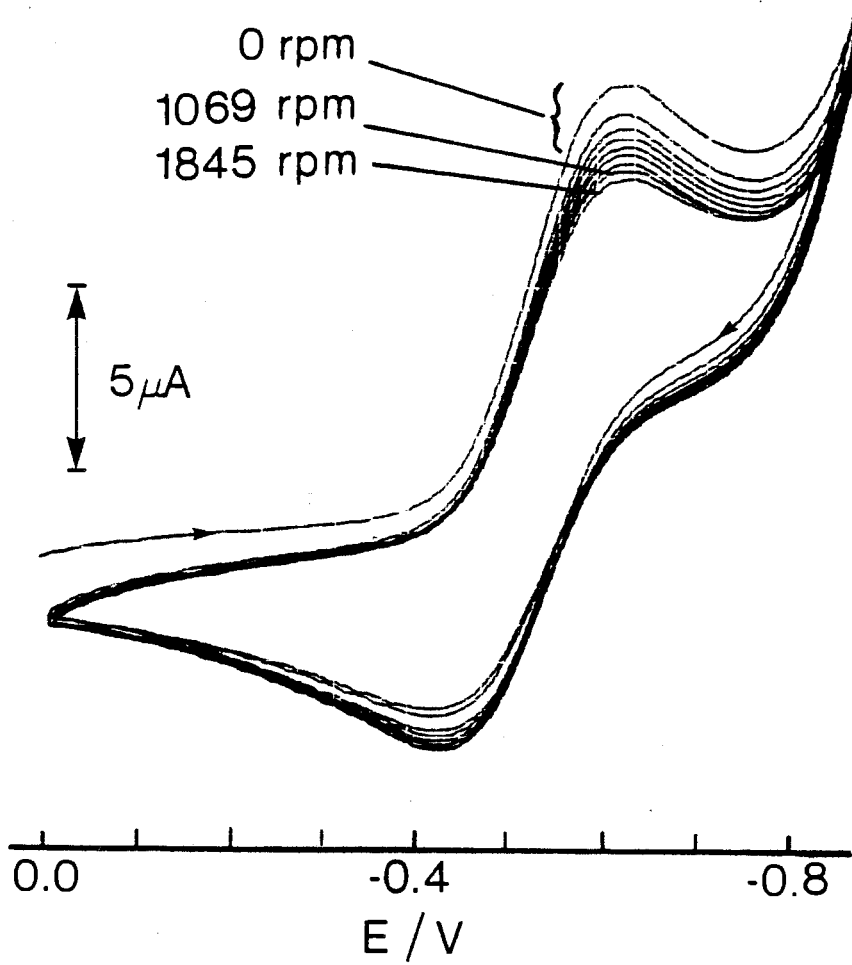
Table 19: Voltammetric Characteristics of PVBQ-St Films<sup>a)</sup>

Thickness (x 1000 Å)	Scan Rate (Vs <sup>-1</sup> )	ΔE (mV)	δ (mV)
1	0.02	16	180
1	0.05	24	184
1	0.10	32	196
1	0.20	36	200
1	0.50	48	210
5	0.02	56	
5	0.05	71	
5	0.10	100	
5	0.20	128	
5	0.50	168	

a) PVBQ-St 5 (VBQ%=24.5), 0.1M TEAP/DMSO. Voltammograms were recorded after polymer films became stabilized.

Figure 47: CYCLIC VOLTAMMETRY OF A PVBQ-St FILM  
(VBQ% = 24.5) AT VARIOUS ROTATION RATES.

Initial film thickness 5000 Å, in 0.1M TEAP/DMSO



symmetrical,  $\Delta E$  was 71 mV, and the current varied with  $v^{0.5}$ . To confirm that the observed voltammogram was not due to the dissolved polymer in solution, the characteristics of a coated rotating disk electrode were examined. At various rotation rates, a cyclic voltammogram-type pattern was obtained in contrast to the asymptotic limiting current expected for entities in solution (Figure 47). Clearly, the voltammograms observed were due to the reduction-oxidation of the films, and the diffusional shape of the curve indicates that the kinetics of the film charging process were limited by the propagation of electrons in the film.

The number of BQ groups reduced ( $\Gamma_{\text{obs}}$ ) was calculated from the area of the cathodic peak of the first scan. For a 1000 Å film,  $\Gamma_{\text{obs}}$  was estimated to be  $5.2 \text{ nmolcm}^{-2}$ .  $\Gamma_{\text{obs}}$  represents only 10% of the total amount of BQ initially deposited on the Pt surface. However, the percentage of reducible groups may be higher because of the partial desorption of the polymer prior to the voltammetric experiments. Since the loss of the polymer is unknown, a discussion based on the  $\Gamma_{\text{obs}}$  value was not attempted.

PVBQ-St films seem to be porous in 0.1 M TEAP/DMSO solution because the presence of the films on the electrode surface did not inhibit the electrochemistry of ferrocene in solution. This is expected since DMSO is a good solvent of the polymers, and it is believed that the film is highly swollen in this solvent.

c) Comparative Voltammetric Studies of PVBQ-St Films and PVBQ Films

Figure 48 compares the voltammetry of a PVBQ film and of a PVBQ-St film. In contrast to the reversible behavior of the copolymer film, the homopolymer coating yielded an asymmetric curve with the oxidation peak greatly suppressed. On successive scans, no significant faradaic current was obtained in either the cathodic or the anodic process. The rapid deactivation of the PVBQ film cannot be attributed solely to the loss of polymer. On the basis of the results obtained in the electrochemical studies of polymers in solution (Chapter I, section I.3.2. b)), it is believed that an intervening chemical reaction between neighboring groups is responsible for this observation.

d) Effect of Solvent

In an attempt to enhance the physical stability of the films, experiments were performed in water and acetonitrile, which are poor solvents for PVBQ-St polymers. Unexpectedly, a major change in the film behavior was observed.

Figure 49 compares the electrochemical characteristics of a PVBQ-St film in DMSO and in H<sub>2</sub>O solutions. In the organic medium, the copolymer film produced a reversible wave as shown in Figure 49a. When the solvent was replaced with water, the peaks disappeared completely and a featureless voltammogram was obtained. If the electrode was reimmersed in the DMSO solution, the original peak shape was again observed. These results indicate that morphological changes and kinetic limitations were occurring rather than desorption or chemical deactivation.

Figure 48: CYCLIC VOLTAMMETRY OF A Pt ELECTRODE COATED WITH

a) PVBQ

b) PVBQ-St (VBQ% = 24.5)

Scan rate  $0.05 \text{ Vs}^{-1}$ , in 0.1M TEAP/DMSO



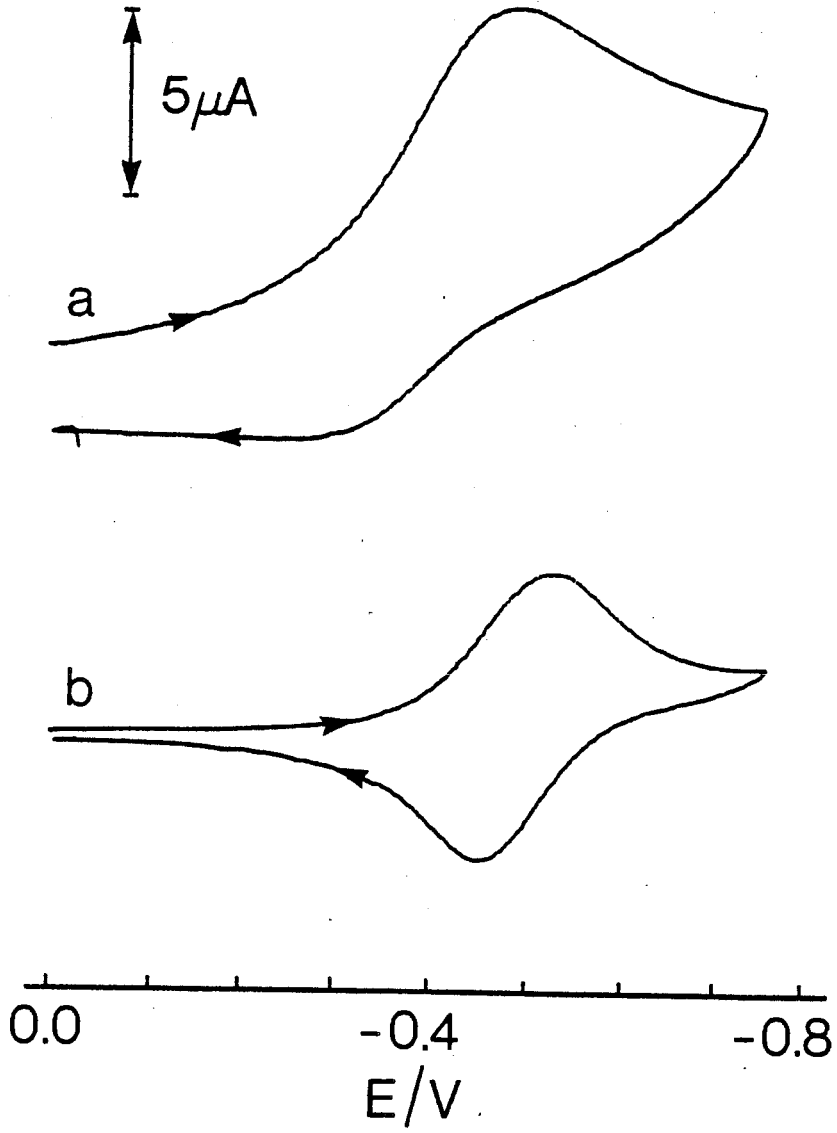
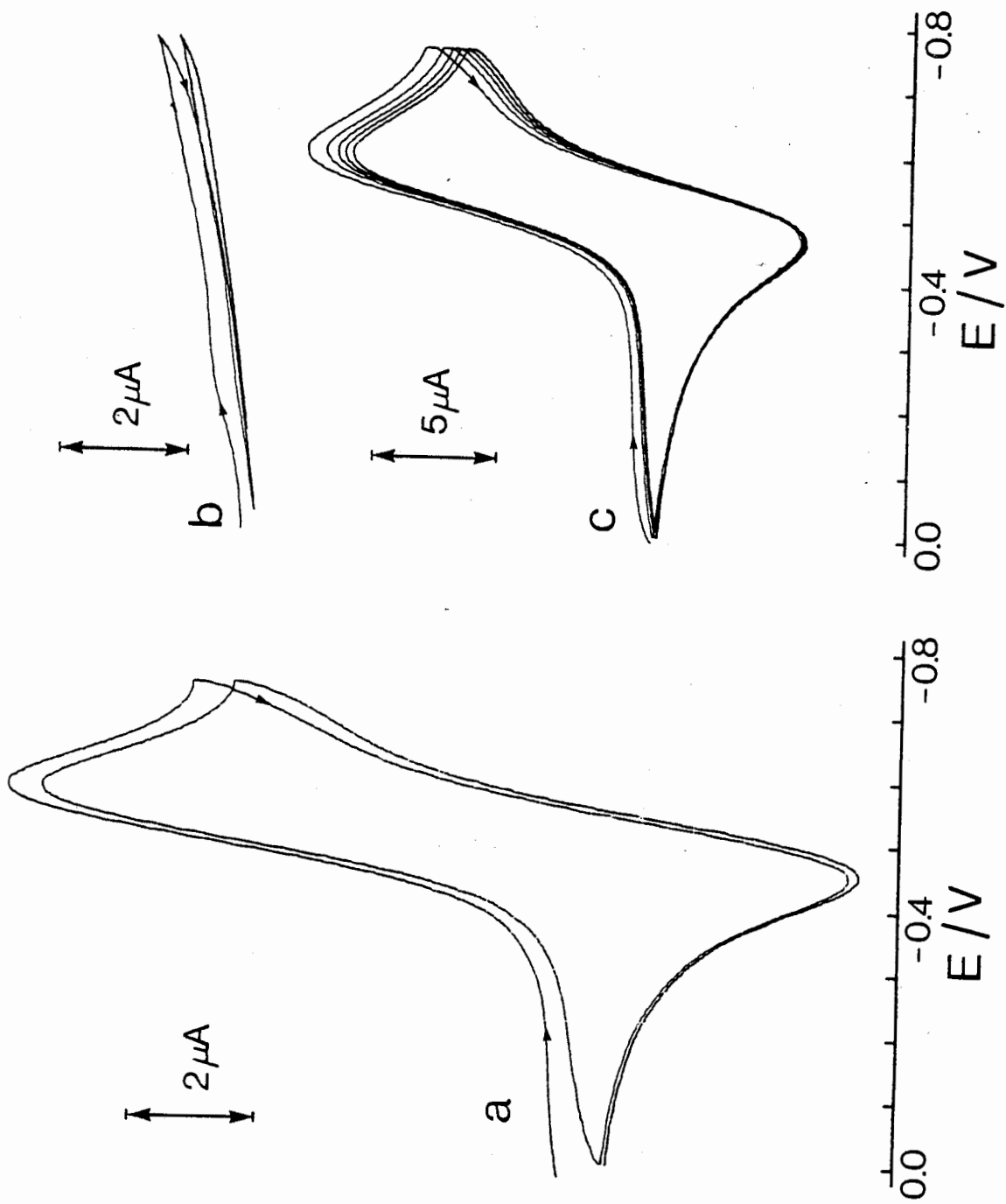


Figure 49: CYCLIC VOLTAMMOGRAMS OF A PVBQ-St  
(VBQ% = 24.5) COATED ELECTRODE

- a) in 0.1M TEAP/DMSO
- b) the same electrode in 0.1M TEAP/H<sub>2</sub>O
- c) the same electrode in 0.1M TEAP/DMSO again

Scan rate 0.05 Vs<sup>-1</sup>



The behavior of the film in  $\text{CH}_3\text{CN}$  solution was also striking. The peak current dropped steadily on continuous scans, but recovered to approximately 90% of the initial value after 15 min. standing (Figure 50). This implies that the degradation of the peak height was not due to irreversible chemical reactions or a desorption process. A further comparison of the anodic and the cathodic peak currents showed that  $i_{pa}$  is smaller than  $i_{pc}$ , but is essentially equal to  $i_{pc}$  of the following scan. Thus, some of  $\text{BQ}^-$  groups produced in the forward scan were not reoxidizable on the reverse sweep, but most of the reoxidized units were reducible in the following cycle.

The effect of solvents on the electroactivity of BQ groups attached in a polymer film is similar to that on the electrochemical reaction of solution species at a PVBQ-St coated electrode. In DMSO and  $\text{CH}_3\text{CN}$  solutions, coating a Pt surface with a polymer film did not have any effect on the electrochemistry of dissolved ferrocene. However, in an aqueous solution, the presence of the film completely impeded the electrode reaction of ferrocene in solution.

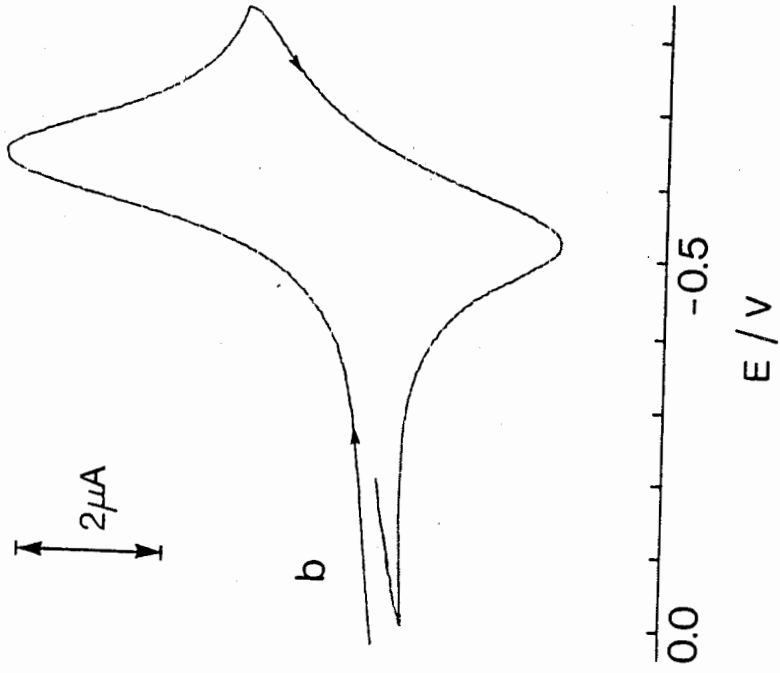
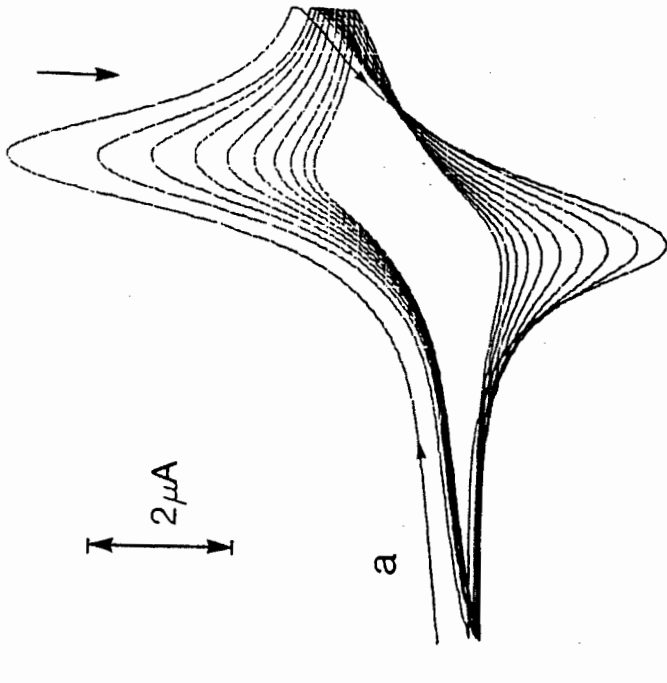
The complete loss of electroactivity of the PVBQ-St film in an aqueous solution can be explained on a morphological basis. In a "good" solvent, such as DMSO, the polymer chain will be extended and a greater permeability to ions and solvent is expected. In water, this hydrophobic polymer cannot provide such permeability and the ionic conductivity is considerably reduced. The inhibition of an electrode reaction of ferrocene in aqueous solution by a polymer film strongly supports the view that the

Figure 50: CYCLIC VOLTAMMOGRAMS OF A PVBQ-St  
(VBQ% = 24.5)-COATED ELECTRODE

a) on successive scans (—→)

b) 15 min. after the last scan in a)

Scan rate  $0.05 \text{ Vs}^{-1}$ , in  $0.1\text{M TEAP/CH}_3\text{CN}$



solution species does not penetrate through the film.

The effect of solvents on the performance of polymer films has been investigated by several authors (161-163). Usually, a pronounced change in the film property was observed when the medium was changed from polar to non-polar, or from aqueous to non-aqueous, and vice versa. A behavior similar to that of PVBQ-St films was reported for a plasma-polymerized vinylferrocene film electrode (163). Anson et al. found that poly(vinylpyridine) films incorporated with Ru<sup>III</sup>EDTA exhibited very high activity in water, but were totally inactive in CH<sub>3</sub>CN and DMSO solutions (162). This observation appears to be in contrast with the results shown in Figure 49, but is quite understandable because their polymers were highly hydrophilic. Miller et al. examined the behavior of films of several polymers containing hydroquinone (146-147) and anthraquinone groups (145), and reported that those films were electroactive in an aqueous solution. Again, the hydrophilic nature of those polymers is no doubt the main reason for the difference between the present work and theirs.

An unusual feature found in this study was that the current decreased on successive scans and the initial current amplitude recovered when the electrode was left to stand in a CH<sub>3</sub>CN solution. Only Bard reported similar characteristics for a Nafion film incorporated with Ru(2,2'-bipyridine)<sup>2+</sup> but he did not attempt to explain the results (169).

It has been recognized that charging a polymer film usually results in a morphological change of the film due to a change in

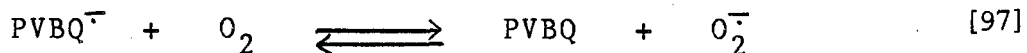
polymer solubility or repulsion between charged groups (153,154, 161). This was the basis for the explanation of the "break-in" phenomenon, in which the peak height increases continuously with cycling until the film exhibits a maximal activity. The decrease in current magnitude on discharging scans observed for PVBQ-St films may likewise reflect morphological changes in polymer which result from variations in conformation of the chains when electroactive groups become charged. The exact nature of changes in film morphology is not clear. Presumably, the reduction of the film leads to a more open structure where the spacing between active centers is increased and the site-to-site collision is decreased. Changes in chain conformation may also reduce the accessibility to the Pt surface of electroactive groups in the vicinity of the electrode.

The kinetics of physical structure changes in the polymer, involving main chain dislocation and movement, may not be the same during a reduction-oxidation cycle in the film. In the study of polyvinylferrocene films, Murray suggested that the rate of structural reorganization of the polymer upon discharging may be slower than in the charging process (161). It appears that PVBQ-St films follow this pattern and the results are compatible with the time scale of the recovery processes encountered.

An alternative explanation for the recovery phenomena observed on successive scans invokes a chemical rather than a physical process. If the oxidation rate is slower than the reduction rate, successive scans will yield lower currents, as some of the units reduced initially will still be in the reduced



state and cannot be reduced again. Chemical oxidation may occur on standing due to traces of O<sub>2</sub> in the polymer film or because of O<sub>2</sub> permeating through the film. By analogy to BQ, the reaction



would lead to regeneration of neutral polymer.

e) Conclusion

A Pt electrode can be coated with benzoquinone-containing polymers to produce a surface with benzoquinone functionality. The electrochemistry of polymers films is in good agreement with that of polymer solutions; ie. films prepared from PVBQ-St copolymers behave reversibly whereas homopolymer coatings exhibit irreversible voltammograms. Benzoquinone groups in polymer films are reduced at potentials similar to those found for methyl-p-benzoquinone in solution. Polymer films do not adhere well to a Pt surface but their physical stability is enhanced by repeated cycling of electrode potential. The electrochemistry of polymer films is profoundly affected by solvent type and this is attributed to the variation in permeability and in polymer chain conformation.

III.3.3. Studies of Electrodes Modified With Poly[p-(9,10-anthraquinone-2-carbonyl)styrene]-co-styrene

a) Film Stability

The voltammetry of the polymer films and of the model compound (EBAQ) in solution is shown in Figure 51 and the data are summarized in Table 20. A cyclic voltammogram of the model compound at a bare Pt electrode shows two well defined Nernstian peaks. An electrode coated with a PAQ film not exposed to U.V. light produced successive peaks which decreased in magnitude due to desorption of the polymer, and deviated from Nernstian behaviour.

Table 20: Voltammetric Characteristics of a EBAQ Solution and of a PAQ-Coated Electrode.<sup>a)</sup>

Compounds	$E_{1/2}^1$ (V)	$\Delta E^1$ (mV)	$E_{1/2}^2$ (V)	$\Delta E^2$ (mV)
EBAQ Solution	-0.69	63	-1.26	63
PAQ 200(2) Film <sup>b)</sup>	-0.71	16	-1.25	16

a) 0.1M TEAP/DMSO, 0.05 Vs<sup>-1</sup>, SCE.

b) Film thickness 1000 Å, U.V. irradiation time 10 min.

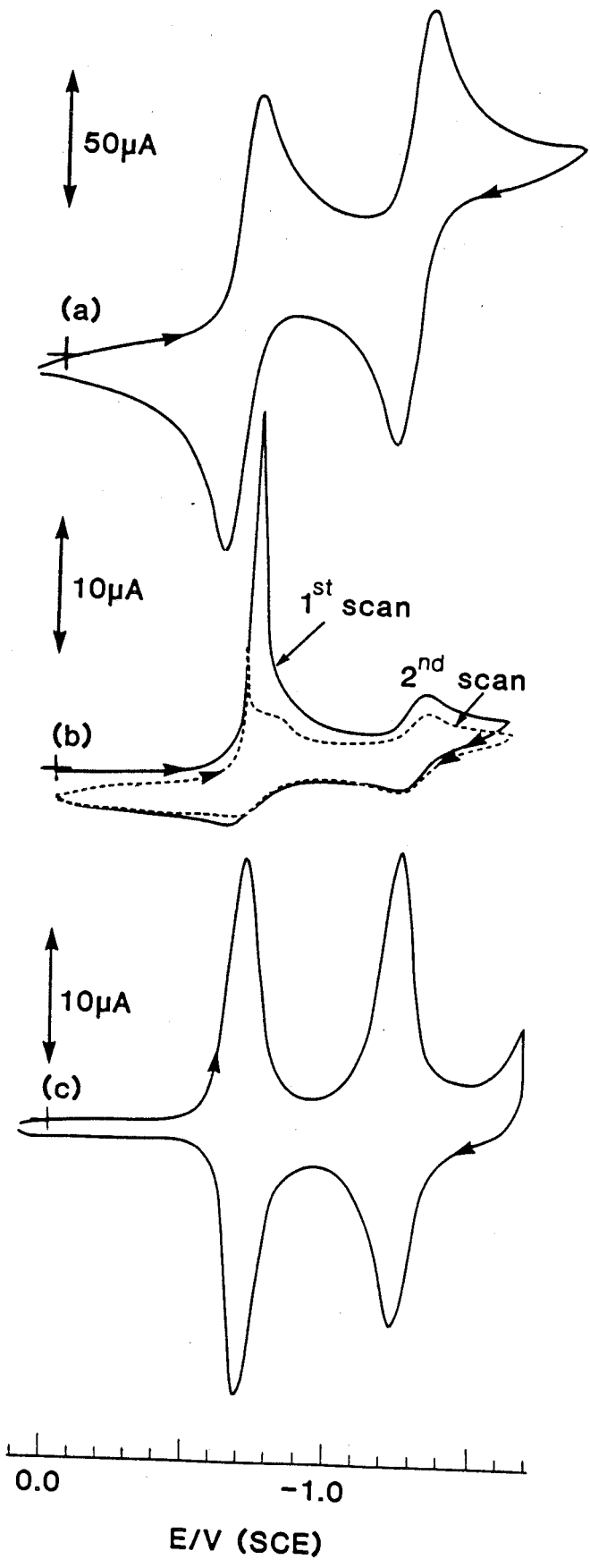
$E_{1/2}^i$  (i=1,2): half-wave potential of the i<sup>th</sup> reduction

$\Delta E^i$  (i=1,2): peak separation potential of the i<sup>th</sup> reduction

Figure 51: CYCLIC VOLTAMMOGRAMS OF

- a) EBAQ in solution
- b) unirradiated PAQ-coated electrode
- c) irradiated PAQ-coated electrode

Film thickness 1000 Å, scan rate 0.05 Vs<sup>-1</sup>,  
in 0.1M TEAP/DMSO



The electrode could be stabilized through exposure to UV irradiation. Figure 51c shows the effect of 10 minutes of irradiation. A voltammogram was obtained with the first and second reduction potentials essentially identical to those of the model compound. A remarkable improvement in stability was noted. Scanning potential between 0.0 V and -1.6 V 50 times resulted in less than 1% loss in coverage  $\Gamma_{obs}$ . Even after the electrode had been soaked in the test solution for several days, the electrochemical activity remained almost unchanged. Obviously, U.V. irradiation had induced a crosslinking reaction between polymer chains, although the nature of the reaction is not clear. The excellent reproducibility of the  $i$ - $E$  response on successive scans also indicates that PAQ films are chemically stable.

The effect of varying the period of U.V. irradiation is shown in Figure 52. Maximum peak currents were obtained after 10 minute exposure. Therefore, all PAQ films were prepared with this period of irradiation, unless otherwise indicated.

#### b) Voltammetric Studies

The effect of film thickness on the electrochemical performance of PAQ-coated electrodes in 0.1 M TEAP/DMSO is shown in Table 21. Typical voltammograms of films of 3 different thicknesses, i.e. 100 Å,  $5 \times 10^3$  Å and  $3 \times 10^4$  Å, are illustrated in Figure 53. For a 100 Å film, the positions of cathodic and anodic peaks coincide as theoretically expected for a reversible, absorbed reactant. The peak width at half-height is 98 mV, which is in good agreement with the theoretical value of 90.6 mV. The curve is symmetrical through the  $E = E_{pc}$  axis, and no diffusional

Figure 52: EFFECT OF TIME OF U.V. IRRADIATION ON THE  
CATHODIC PEAK CURRENT OF PAQ 200(2)-COATED  
ELECTRODES.

Film thickness 1000 Å; scan rate 0.05 Vs<sup>-1</sup>,  
in 0.1M TEAP/DMSO.

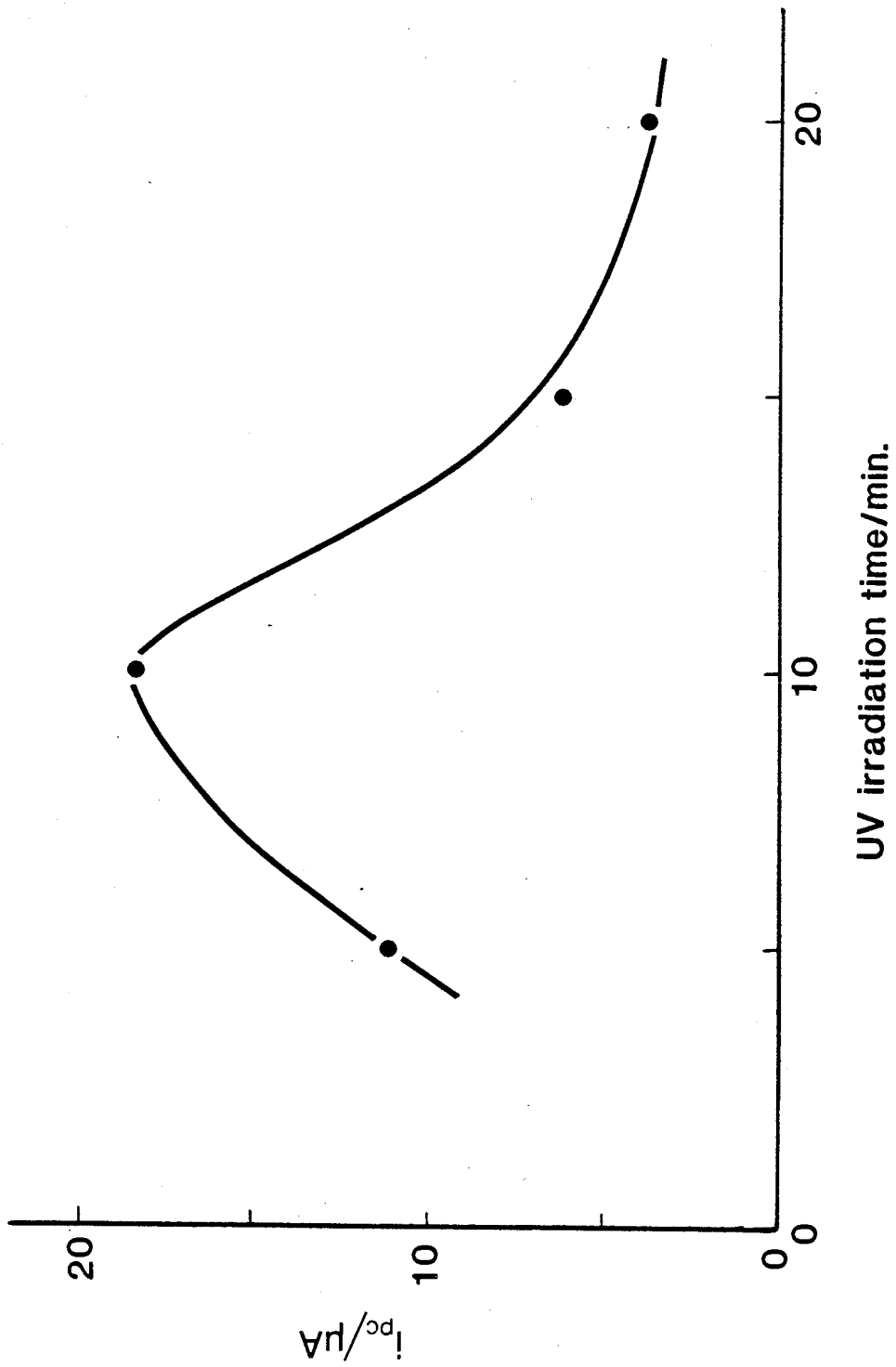


Table 21: Voltammetric Characteristics of PAQ Films<sup>a)</sup>

Thickness (x1000 Å)	$\Delta E$ (mV)	$\delta$ (mV)	$i_{pc}$ ( $\mu A$ )	$\Gamma_{obs}$ ( $nmolcm^{-2}$ )	$\frac{\Gamma_{obs}}{\Gamma_{cal}}$ (%)	$x^{b)}$
0.1	0	98	8.1	1.3	79	1.0
0.5	0	110	12.2	1.9	22.6	0.99
1	16	112	18.4	2.7	16.4	0.93
5	16	112	72	9.7	11.8	0.87
10	16	112	110	14.9	9.0	0.84
15	20	112	156	21.0	8.3	0.82
20	25	116	174	23.4	7.1	0.80
30	32	112	184	24.8	5.0	0.79

a) PAQ 200(2), 0.1M TEAP/DMSO, 50  $mVs^{-1}$ , U.V. irradiation time 10 min.

b)  $x$  is the exponential parameter in the  $i_{pc} = kv^x$  ( $k =$  constant) relationship.



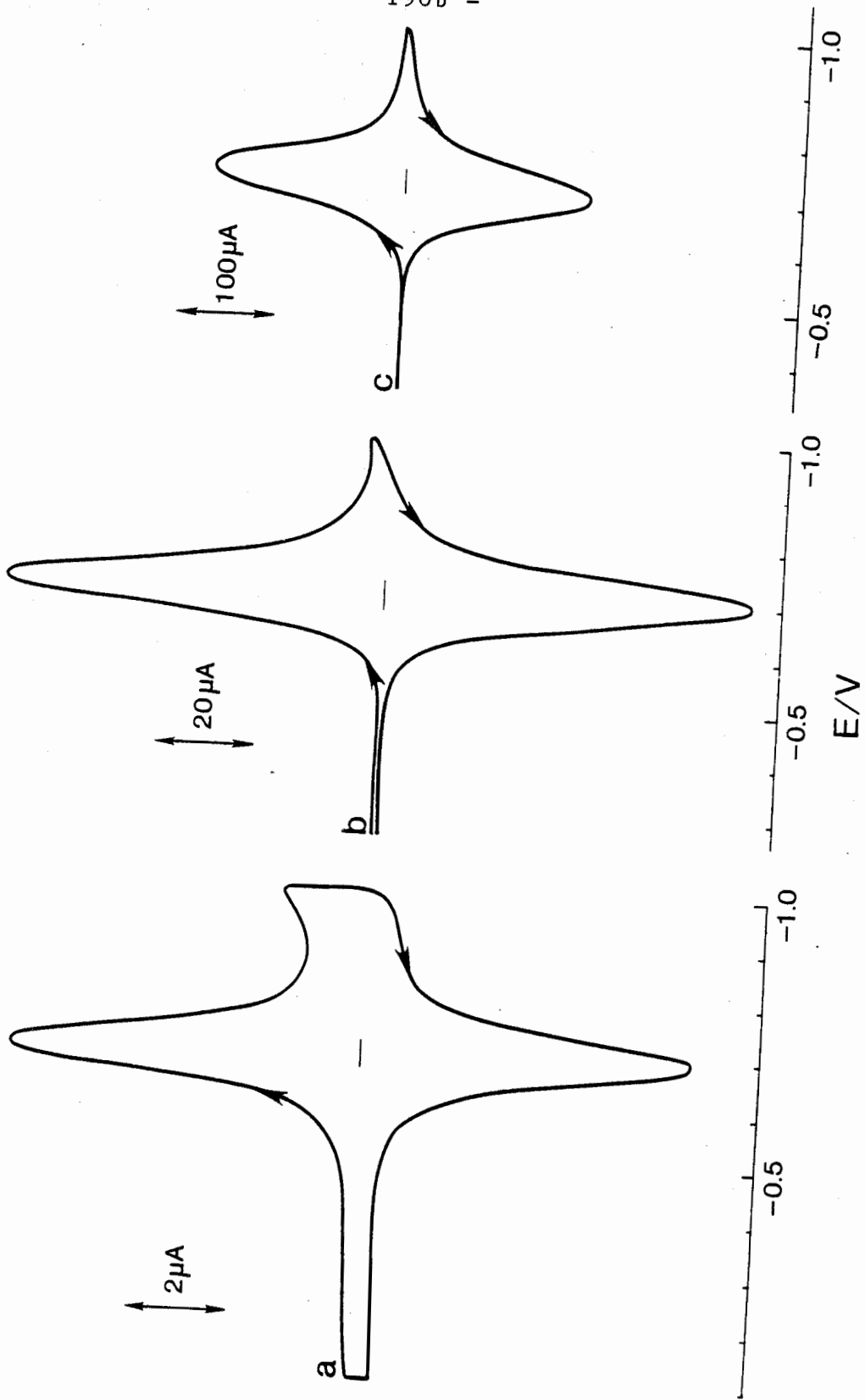
Figure 53: CYCLIC VOLTAMMOGRAMS OF PAQ 200(2) FILMS OF  
DIFFERING THICKNESSES.

Film thickness:

- a) 100 Å
- b)  $5 \times 10^3$  Å
- c)  $3 \times 10^4$  Å

Scan rate  $0.05 \text{ v s}^{-1}$  , 0.1M TEAP/DMSO

- 190b -



tailing is observed. Integration of the peak area yielded a surface coverage of  $1.3 \text{ nmolcm}^{-2}$ , which corresponds to 78% of the value estimated from the amount of polymer deposited. Taking into account the fact that some AQ groups may have been destroyed through the crosslinking process, it is possible to postulate that the electroactive centers in the film were quantitatively reduced. These results indicate that on the voltammetric time scale, the rate at which electrons are transported through the film is very fast. The ratio of oxidized and reduced sites in the film remains in Nernstian equilibrium with electrode potential during the potential scan.

An increase in the film thickness produced a larger current and did not lead to major deviations in the curve shape. Even a several hundred-fold increase in the thickness to  $\sim 3 \times 10^4 \text{ \AA}$  caused only a small peak separation (16 - 32 mV) and a slightly larger peak width (112 - 116 mV). The  $\Gamma_{\text{obs}}/\Gamma_{\text{cal}}$  ratio, however, decreased sharply with increasing thickness. For instance, the percentage of AQ groups which could be reduced dropped from 79% to 22.6% for a five fold increase in film thickness from 100  $\text{\AA}$  to 500  $\text{\AA}$ . This indicates that more active centers were reduced in thick films but the ratio of the reducible groups to the total amount of AQ residues present in the film was small.

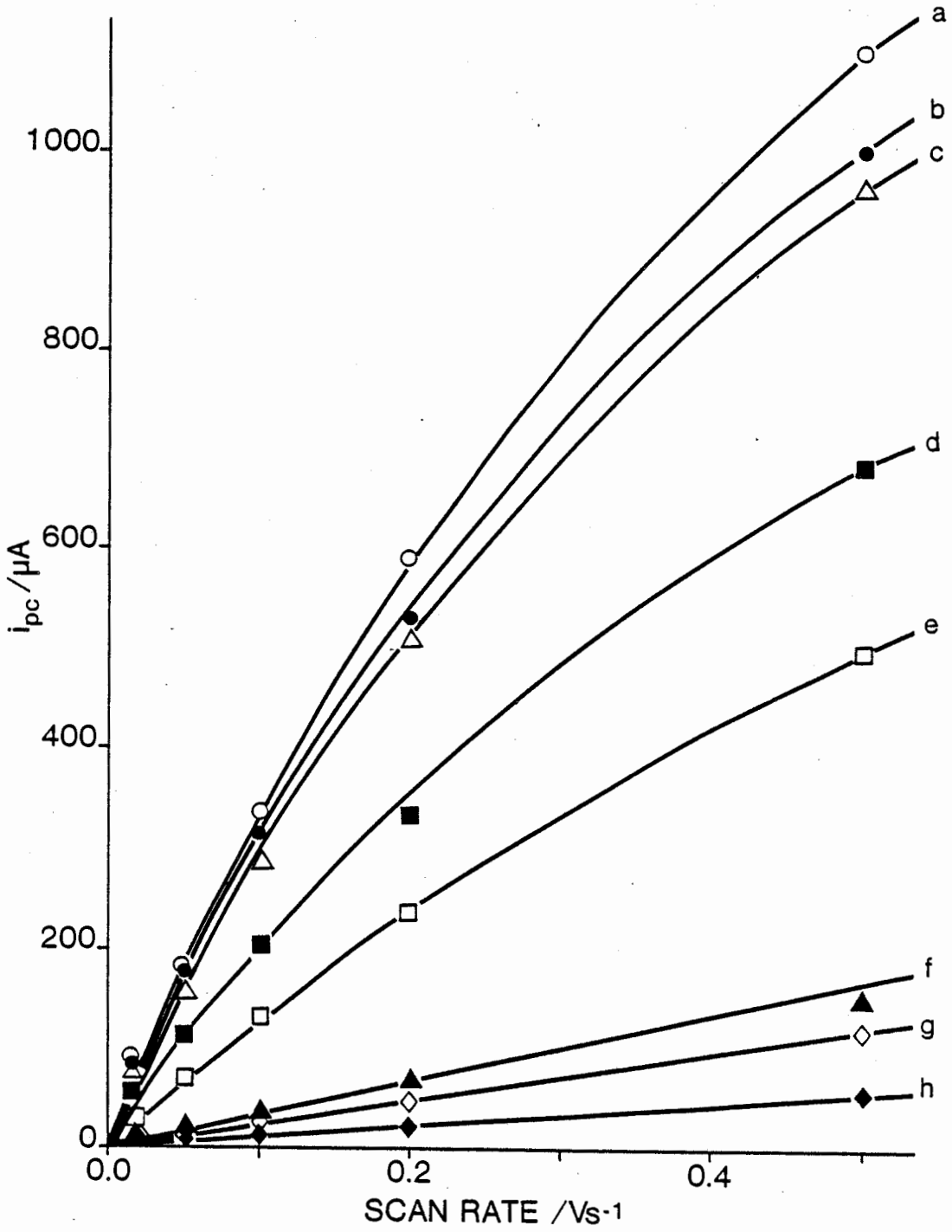
The dependence of peak current on scan rate for films of various thickness is shown in Figure 54. A linear relationship is obtained for films up to 1000  $\text{\AA}$  thick. With thicker films, peak current increased with scan rate in a less than linear fashion. Plots of  $\log i_{\text{pc}}$  vs.  $\log v$  yield straight lines, the slopes of

Figure 54: EFFECT OF SCAN RATE FOR PAQ 200(2) FILMS  
OF VARIOUS THICKNESS.

Film thicknesses:

- a)  $3 \times 10^4 \text{ \AA}$
- b)  $2 \times 10^4 \text{ \AA}$
- c)  $1.5 \times 10^4 \text{ \AA}$
- d)  $1 \times 10^4 \text{ \AA}$
- e)  $5 \times 10^3 \text{ \AA}$
- f)  $1 \times 10^3 \text{ \AA}$
- g)  $5 \times 10^2 \text{ \AA}$
- h)  $1 \times 10^2 \text{ \AA}$

in 0.1M TEAP/DMSO.



which show that the currents are proportional to a power of 0.79 - 0.87 of the scan rate (Table 21). The peak potential separation  $E$  increases with scan rate in contrast to the small, constant values found for thin films. For example, for a  $3 \times 10^4 \text{ \AA}$  film,  $\Delta E$ 's of 56 mV and 144 mV are observed at scan rates of 0.1 and  $0.5 \text{ Vs}^{-1}$ , respectively. This indicates that in these thick films, the rate of film charging was not fast on the experimental time scale and was controlled by the rate of electron transfer through the coating.

It is not common to observe voltammograms with near ideal shape for polymer films as thick as  $1000 \text{ \AA}$ . Most polymers reported in the literature show incipient kinetic control of the rate of film charging when film thicknesses exceed a few hundred angstroms. For example, polyvinylferrocene (143,144), poly(p-nitrostyrene) (130,131) and polytetrathiafulvalene (153, 154) exhibited a  $\delta$  value of 150 - 200 mV and  $\Delta E$  of 50 - 100 mV even when the surface coverages were only  $1 - 10 \text{ nmolcm}^{-2}$ . An  $i$ - $E$  response as ideal as that observed for the  $100 \text{ \AA}$  PAQ film has been reported only for covalently modified electrodes, where the film is equivalent to a monolayer (160). The results in this work indicate that PAQ films in DMSO solutions represent one of the most ideal polymer-coated electrode system reported to date. The above characteristics of PAQ films have some significance, considering the desirability of fast charge transport for the various applications of polymer electrodes.

While electron hopping may be a mechanism for charge transport in the film, a number of factors other than the

intrinsic rate of electron self-exchange between redox sites in the proper juxtaposition can constitute the rate controlling event for overall charge transport. These include the movement of counterions and co-ions into and out of the film to preserve electroneutrality, the degree of swelling, and the segmental motions of polymer chains needed to bring about the site-site collisions. Thus, solvent has a great influence on the electrochemical response of the film. In this work, the crosslinking of PAQ films allowed experiments to be performed in DMSO in which the polymer swells to a great extent. In contrast, most polymer-modified electrodes reported in the literature were examined in poor solvents in order to minimize the dissolution of polymers. The proper choice of solvent may be one of the reasons for the more ideal behavior observed with PAQ films.

That PAQ films with thickness up to several thousand angstroms exhibit voltammograms with almost ideal shape indicates that charge transport in these films is very fast and that equilibrium is rapidly established throughout the film within the time scale of experiment. For such a mechanism, one would expect a  $\Gamma_{\text{obs}} / \Gamma_{\text{cal}}$  ratio close to unity, and a linear increase in peak current with increasing film thickness. However, the percentage of reducible groups drops sharply when the film thickness exceeds 100 Å and the peak current does not vary linearly with the total AQ content in the coating. If the reduction occurs by slow progression through successive layers, a limiting thickness would be encountered beyond which further reaction would not occur (see Figure 36c). Such a model should not show an increase of current

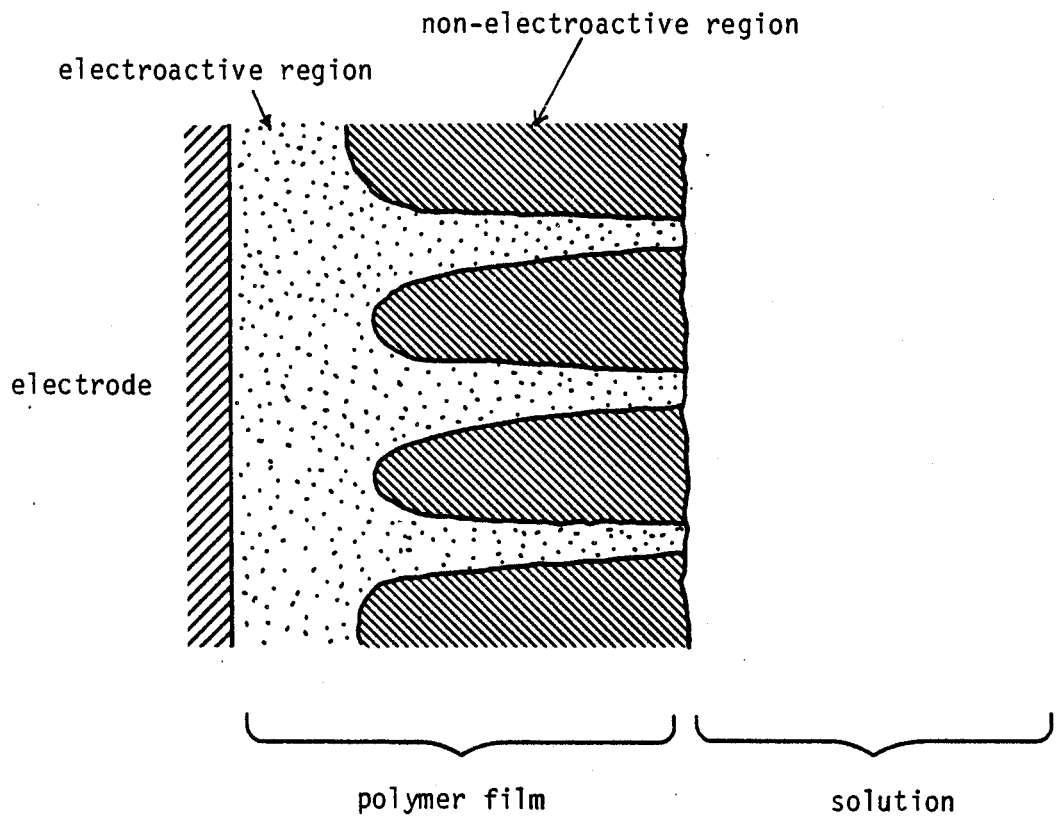
with thickness as shown in Figure 54. In addition, the voltammogram would exhibit the distinctive "diffusion tail" with large  $\Delta E$ , and a  $x$  value (where  $i_{pc} \propto v^x$ ) close to 0.5, as exemplified by PVBQ-St and some other reported systems (170).

The low  $\Gamma_{obs} / \Gamma_{cal}$  ratio found for thick films cannot be viewed as a consequence of chemical interference as ascribed to PVBP films. The PAQ radical anion is chemically stable in DMSO solution, and repeated cycling of the coated-electrodes did not cause any significant decrease in the peak height of the voltammograms.

It is suggested that the orientation of the polymer chains in the film may lead to preferred pathways or channels for electrical conductivity. It is recognized that long chain molecules can be oriented by stretching and that such orientation results in higher crystallinity and regioregularity in the polymer. Such orientation of polymeric chains may favor electron hopping in certain channels in the coating as shown in Figure 55. Thus, for films thicker than 100 Å, some regions may be completely reduced in channels extending from the electrode to the solution interface, while other regions may only be reduced in the thin layer close to the electrode surface. Such a model is consistent with the finding that films of greater thickness yield currents whose increase is not proportional to the total AQ content, although the voltammetric characteristics are suggestive of a fast film charging process.



Figure 55: A PROPOSED STRUCTURE FOR PAQ FILMS



c) Determination of Charge Transport Coefficient

The stability of PAQ films enabled the determination of the charge transport coefficient  $D_{CT}$ . Chronoamperometry was employed for such a study and the results were analyzed on the basis of the Cottrell equation for a semifinite diffusion condition:

$$i = nFAD_{CT}^{1/2}C(\pi t)^{-1/2} \quad [95]$$

where  $i$  is the magnitude of current at time  $t$  and  $C$  is the volume concentration of electroactive species in the film.

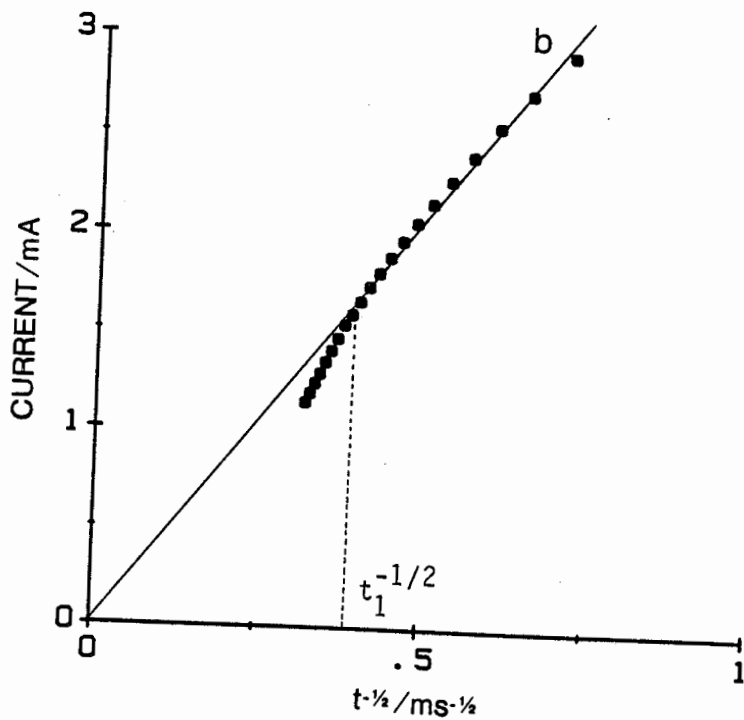
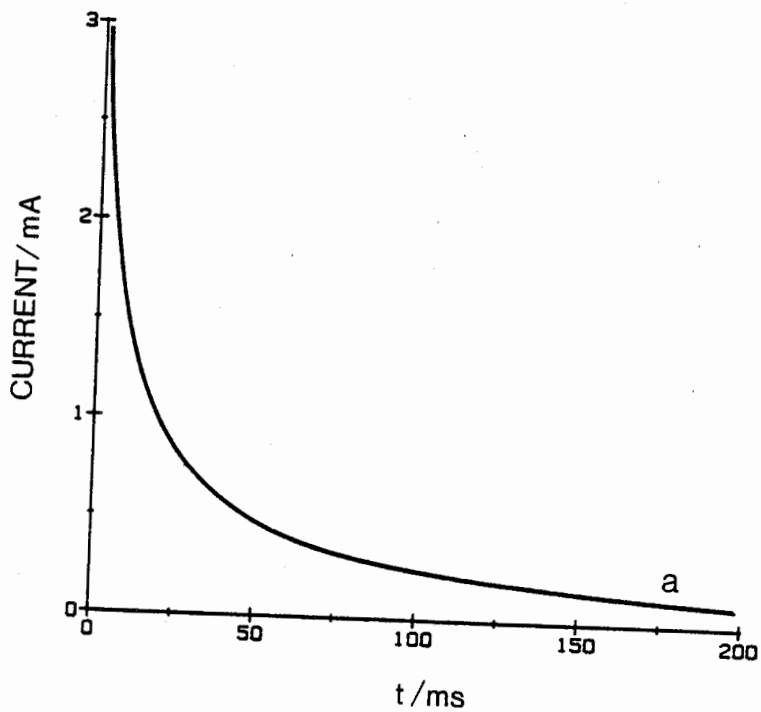
The electrode potential was stepped from  $-0.2$  V to  $-0.9$  V to produce the reduction to the radical anion. The time-dependent current decay and the corresponding Cottrell plot for a  $1000 \text{ \AA}$  film are shown in Figure 56. The current decreased linearly with  $t^{-1/2}$  at the beginning as predicted by the Cottrell equation, but dropped rapidly at longer times. A similar observation has been reported for many other polymer films (171-174). Murray postulated that at sufficiently short times, the diffusion layer does not reach the outer boundary of the film, and the propagation of electrons follows the infinite diffusion laws, i.e. the Cottrell equation. At longer times, the depletion layer reaches the film/solution interface, and the "supply" of redox groups becomes limited by the finite thickness of the film.

The interpretation given by Murray is applicable only to systems where all active centers can be reduced. If the electrochemical charging reaction is confined in the first few layers, departures from the  $i$  vs.  $t^{-1/2}$  linearity would occur earlier than expected for a completely reduced film. For PAQ

Figure 56: CHRONOAMPEROMETRY OF A 1000 Å PAQ 200(2) FILM

a) Current-time plot

b) Cottrell plot



films, it has been proposed that within a thickness of approximate 100 Å, most AQ groups are accessible to the reduction reaction, but in more remote areas, the electron hopping process proceeds only in "preferred pathways". It is believed that the onset of the deviation from the linear region of the  $i$  vs.  $t^{-1/2}$  plot shown in Figure 56 marks the time when the depletion layer of AQ sites reaches the thickness within which the polymer was completely reduced. Beyond this layer, AQ centers available for the reduction were confined in the preferential channels and consequently, the current fell more rapidly than anticipated from the Cottrell equation.

From the slope of the linear portion of the  $i$  vs.  $t^{-1/2}$  plot shown in Figure 56, a  $D_{CT}^{1/2}C$  value of  $11.8 \times 10^{-9} \text{ mol cm}^{-2} \text{ s}^{-1/2}$  was obtained. Assuming the dry polymer density to be  $1 \text{ g cm}^{-3}$ , the volume concentration of AQ units in the film is estimated to be 1.65 M. Substituting the value of  $C$  in  $D_{CT}^{1/2}C$ ,  $D_{CT} = 5.1 \times 10^{-11} \text{ cm}^2 \text{ s}^{-1}$ . In fact  $D_{CT}$  may be higher since the concentration  $C$  may be smaller than estimated because of the crosslinking reaction and the swelling of the film when dipped in DMSO solution.

Charge transport coefficients of a number of polymer films have been reported, and vary over several orders of magnitude ( $10^{-7} \sim 10^{-13} \text{ cm}^2 \text{ s}^{-1}$ ) (9). The  $D_{CT}$  value for PAQ films is smaller than examples quoted from literature although the films exhibit a more ideal behavior and should have a higher  $D_{CT}$  value. The results can be ascribed to two reasons.

Firstly, in the calculation of  $D_{CT}$  from the product  $D_{CT}^{1/2}C$ , most authors used a  $C$  value estimated from the relation:

$$C = \Gamma_{\text{obs}}/l \quad [98]$$

where  $l$  is the film thickness (171,172).

The concentration thus determined may be in considerable error because the calculation assumes a spatially uniform dilute concentration of reducible (or oxidizable) sites. In practice, a large proportion of the redox centers may not be electroactive on the experimental time scale. The film may consist of regions lacking in electroactivity interspersed with those fully active. For such films, the calculation based on equation [98] would yield a  $C$  value much smaller than the concentration of reducible centers. Consequently, the charge transport coefficient, which is derived from  $(\text{slope}/C)^2$ , would be much greater. For example, if the concentration of AQ groups is calculated by equation [98], a value of 0.15 M would be obtained for a  $1 \times 10^4 \text{ \AA}$  film, and the corresponding  $D_{\text{CT}}$  is  $6.2 \times 10^{-9} \text{ cm}^2 \text{ s}^{-1}$ , which is much higher than the value it should be.

Secondly, most systems which exhibit  $D_{\text{CT}}$  higher than that of PAQ films are ionic redox polymer films, where active centers are electrostatically or coordinately attached to a polymer chain (9). As pointed out by Buttry and Anson (175), in this type of polymers, reduction or oxidation of redox ions in the film may occur by two mechanisms. Active groups may diffuse to the electrode surface and undergo an electrode reaction, and electrons may propagate between redox ions by an electron hopping process. Thus the measured charge transport coefficient  $D_{\text{CT}}$  is the sum of those contributed by the diffusional motion of redox groups  $D_{\text{S}}$ , and by the electron self-exchange  $D_{\text{ET}}$ :

$$D_{CT} = D_S + D_{ET} \quad [99]$$

In some cases of ionic redox polymer films,  $D_S$  is the dominant contributor to  $D_{CT}$ . For example, a Nafion film incorporated with  $\text{Co}(\text{bipyridine})^{2+}$  ions exhibits a  $D_{CT}$  value of  $1.5 \times 10^{-9} \text{ cm}^2 \text{ s}^{-1}$  while  $D_{ET}$  was estimated to be  $5 \times 10^{-18} \text{ cm}^2 \text{ s}^{-1}$  (175). However, the diffusional motion of active groups is much more restricted when covalently attached to a polymer backbone and  $D_S$  can be considered negligible.

The  $D_{CT}$  value can be used to calculate the thickness of diffusion layer  $d$  in the film at time  $t$  using the following equation (176):

$$d = (2D_{CT}t)^{1/2} \quad [100]$$

If  $t_1$  is the time at which deviation from  $i$  vs.  $t^{-1/2}$  linearity appears,  $d$  should correspond to the thickness beyond which reducible AQ groups are no longer uniformly distributed in the film. From Figure 56,  $t_1$  was estimated to be 6.5 ms, and a  $d$  value of 86 Å was obtained. This value is close to the expected value of 100 Å. If the postulates of Murray were applicable, a  $d$  value comparable to the film thickness, ie. 1000 Å, would have been obtained. The results again support the charge-transport model proposed.

#### d) Effect of AQ Content

The electron hopping mechanism implies that an increase in the volume concentration of electroactive centers will enhance the overall conductivity of the polymer film as electron exchange



between neighboring sites is facilitated. Thus it was expected that faster charge transport and a higher fraction of reducible groups would be observed with films of polymers of higher AQ loadings.

Figure 57 illustrates the  $i$ - $E$  responses of PAQ films of identical thickness but with three different AQ contents, i.e. 19.5%, 28.0% and 47.4%. The voltammetric characteristics are summarized in Table 22. No substantive changes in reversibility or peak shape are apparent. Peak current increased with the concentration of active units, but the  $\Gamma_{\text{obs}}/\Gamma_{\text{cal}}$  ratio remained

Table 22: Effect of AQ Content on Voltammetric Characteristics of PAQ Films

Polymers	AQ%	$\Delta E$ (mV)	$\delta$ (mV)	$i_{\text{pc}}$ ( $\mu\text{A}$ )	$\Gamma_{\text{obs}}$ ( $\text{nmolcm}^{-2}$ )	$\Gamma_{\text{obs}}/\Gamma_{\text{cal}}$ (%)	$D_{\text{CT}} \times 10^{-11}$ ( $\text{cm}^2\text{s}^{-1}$ )
200(1)	19.5	16	116	15.0	2.2	19.2	6.8
200(2)	28.0	16	112	18.4	2.7	16.4	5.1
200(3)	47.4	36	116	29.2	4.3	15.4	5.4

0.1M TEAP/DMSO, 0.05  $\text{Vs}^{-1}$ , 1000 Å thick, U.V. irradiation time 10 min.

Figure 57: CYCLIC VOLTAMMETRY OF PAQ FILMS OF VARIOUS  
AQ CONTENTS.

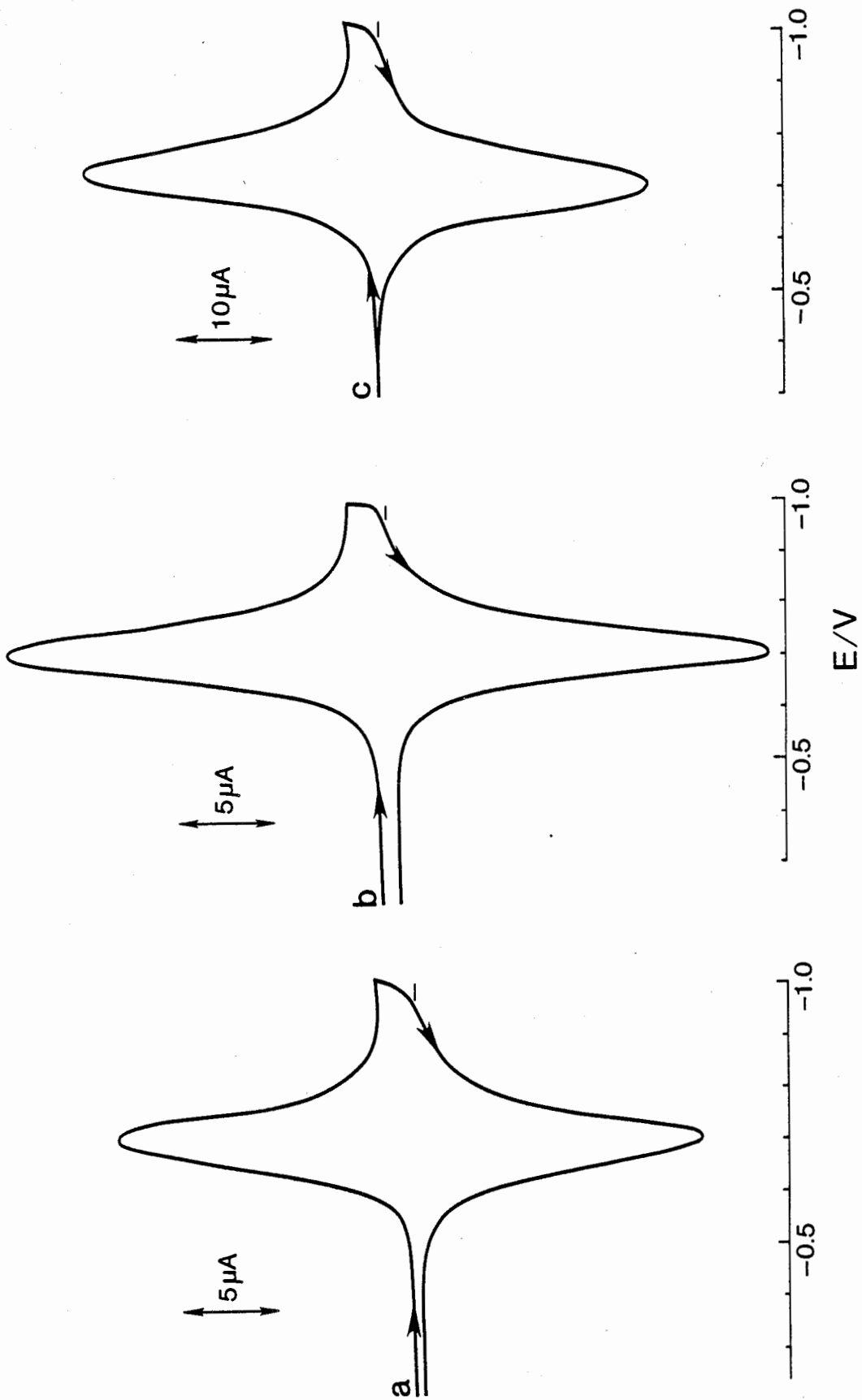
AQ %:

a) 19.5

b) 28.0

c) 47.4

Film thickness 1000 Å, scan rate 0.05 Vs<sup>-1</sup>,  
0.1M TEAP/DMSO.



essentially insensitive to AQ content.  $D_{CT}$  for each polymer was determined and similar values were obtained. These results indicate that the closer spacing between redox groups did not facilitate the propagation of electrons in the film. The similarity in the shape of voltammograms of these three polymers is also indicative of the lack of interaction between neighboring groups.

The effect of volume concentration of redox centers on the electrochemical performance of polymer films has been reported for some polymer systems (145,148,153,154,174,175,177-179). While an increase in concentration of active groups enhanced  $D_{CT}$  of vinylferrocene-siloxane copolymers (174), a decrease in the reversibility and symmetry of voltammograms were observed for polystyrene functionalized with tetrathiafulvalence groups (153, 154) and polymers containing azobenzene (148) and anthraquinone (145) groups. Bard et al. (177,178) and Buttry and Anson (175) found  $D_{CT}$  for  $Ru(bipyridine)_3^{2+}$  in a Nafion film to be independent of concentration. For a given polymer system, the concentration dependency of charge transport may also vary, depending on the concentration of active sites. Murray observed that  $D_{CT}$  of Os and Ru containing copolymers was constant at moderate concentrations, but increased in the high and low concentration regions (179).

The investigation of the effect of AQ concentration on the electron transfer process in the films by the variation of AQ loading in a polymer chain may be an oversimplification. A number of opposing effects might arise when the composition of copolymers was changed. While an increase in AQ content may

facilitate the "site-to-site" reduction process, the former greatly reduces the solubility of the polymers and thus the flexibility of the chain. The U.V. irradiation of the films may lead to enhanced crosslinking at higher AQ compositions. The failure to observe an increase in  $D_{CT}$  and in the  $\Gamma_{obs}/\Gamma_{cal}$  ratio indicates that these competing effects may balance out the expected enhancement in electron transport. As pointed out by Murray (179), each site removed in a dilution process, or replaced in a loading process, should be comparable in size, polarity, solubility, etc. Only in such a case, can one ensure that the change in distance between active groups rather than in chain conformation is the dominant factor.

e) Effect of Solvents

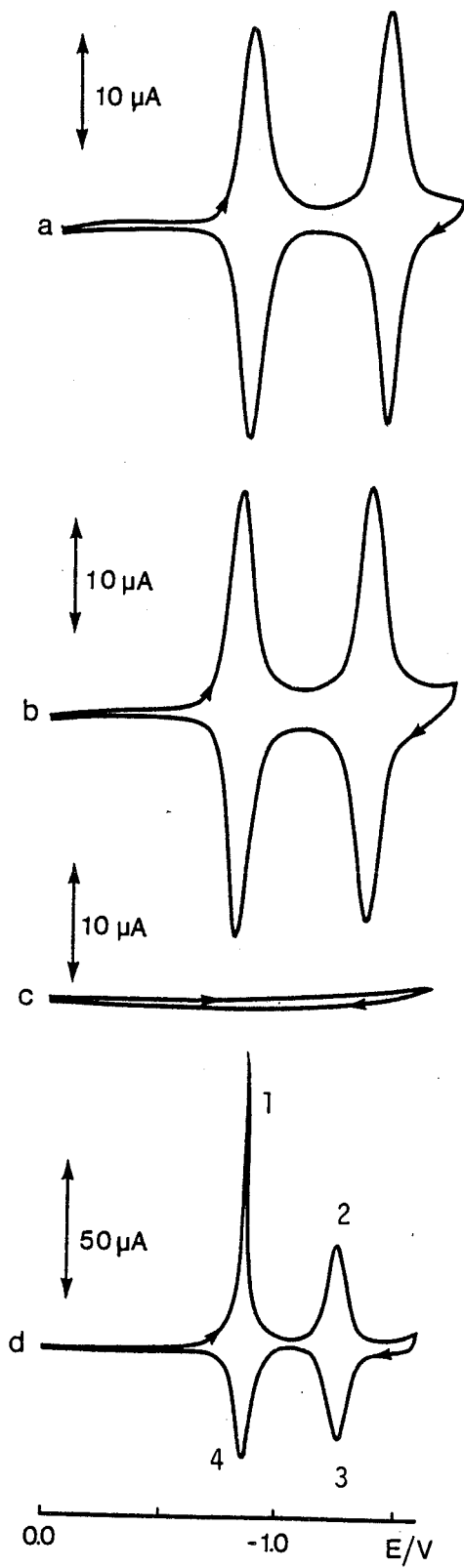
In the study of PVBQ-St coated electrodes, it was found that solvents exert a significant influence on the film behavior. Therefore, it was interesting to examine the effect of solvents on the electrochemical characteristics of PAQ films.

Figure 58 presents the voltammograms of an electrode coated with a 1000 Å PAQ film in four different solvents: DMSO, DMF, H<sub>2</sub>O and CH<sub>3</sub>CN, with 0.1M TEAP supporting electrolyte. In DMSO and DMF solutions, the i-E responses are very much identical in shape and size. The voltammetry produced almost ideally shaped, cathodic and anodic peaks for both the first and second reduction. Transferring the electrode into an aqueous solution rendered the film virtually electroinactive. The effect, however, was reversible. When the electrode was returned to the DMSO or DMF solution, voltammograms with original peak shape and peak

Figure 58: CYCLIC VOLTAMMETRY OF PAQ 200(2) FILMS IN:

- a) 0.1M TEAP/DMSO
- b) 0.1M TEAP/DMF
- c) 0.1M TEAP/H<sub>2</sub>O
- d) 0.1M TEAP/CH<sub>3</sub>CN

Film thickness 1000 Å, scan rate 0.05 Vs<sup>-1</sup>,  
0.1M TEAP/DMSO.



height were observed.

The electrochemical characteristics of PAQ films in  $\text{CH}_3\text{CN}$  solution differed substantially from those observed in DMSO or DMF solutions. The effect was most pronounced in the reduction of the film from the neutral state to the radical anion state. The cathodic peak produced in this process was narrow and sharp (Fig. 58d, peak 1). The peak current did not vary linearly with scan rate and the peak potential shifted more negatively as scan rate increased (Fig. 59, curve 1). In contrast, the second reduction peak and the two oxidation peaks on the reverse scan had a shape similar to that obtained in DMSO or DMF (Fig. 58d, peaks 2,3,4). For these peaks, the currents are proportional to scan rate and  $E_p$ 's vary little with scan rate (Fig. 59, curves 2,3,4).

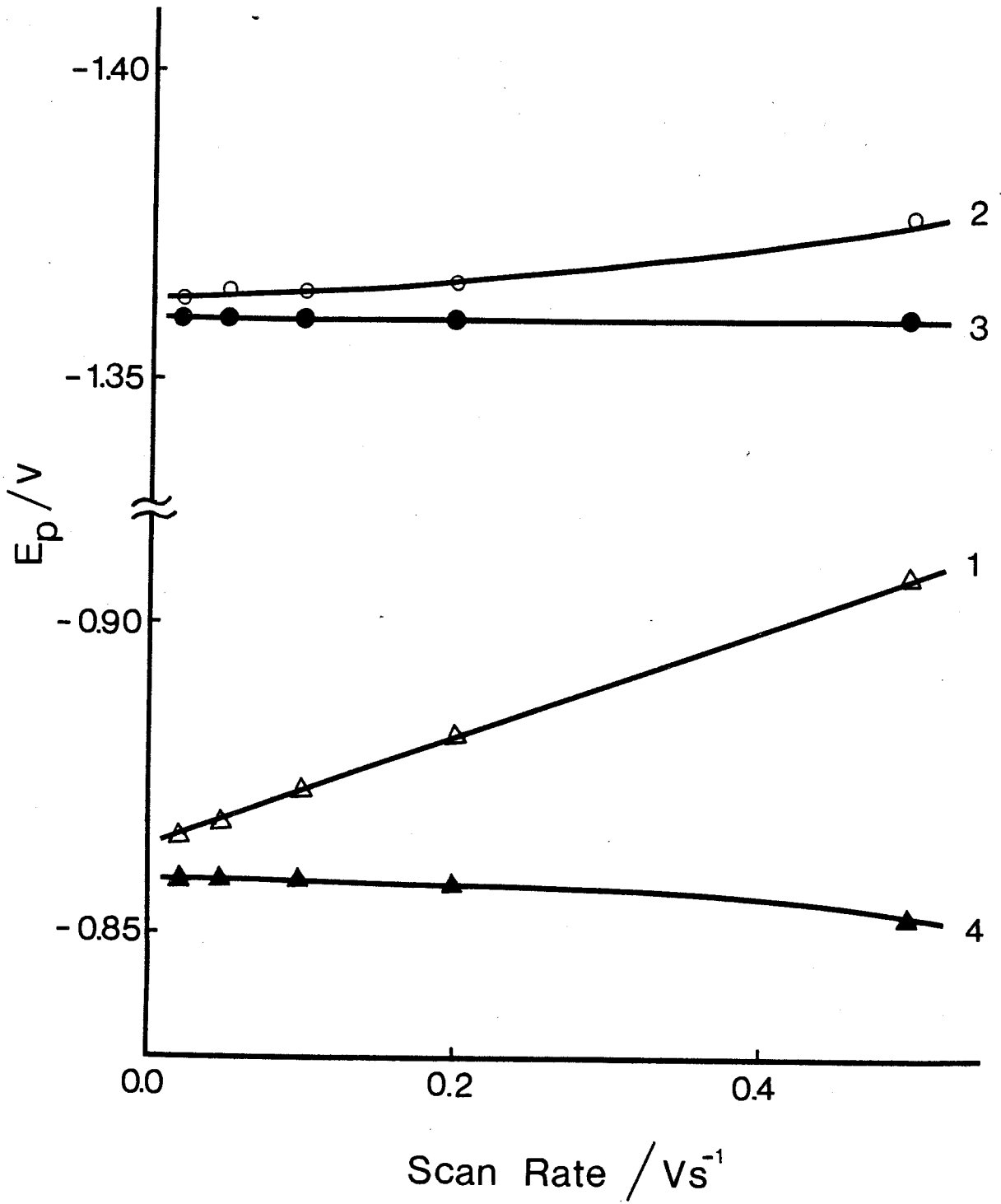
The effect of solvents on the electrochemical performance of PAQ films can be attributed to the variation in permeability arising from changes in chain conformation in analogy to electrodes coated with PVBQ-St polymers. In DMSO and DMF; the polymer swells to a greater extent and thus counter ions and solvent molecules permeate more easily. In aqueous solution, the hydrophobic polymer film may be so compact that the permeation of electrolytes is impeded. The polymer chain may also lack adequate flexibility needed for the "site-to-site collision" between active centers.

The voltammetric behavior of PAQ films in  $\text{CH}_3\text{CN}$  may be explained as a possible consequence of a swelling/deswelling process occurring during a redox cycle. A neutral film is poorly swollen in this solvent and thus has a large ohmic resistance due



Figure 59: DEPENDENCE OF PEAK POTENTIALS ON SCAN RATE  
OF A 1000 Å PAQ FILM IN 0.1M TEAP/CH<sub>3</sub>CN.

Curves 1,2,3,4 correspond to peaks 1,2,3,4  
in Figure 58d, respectively.



to a low ambient internal electrolyte concentration. The actual potential at the Pt/polymer film interface is less than that applied by the product of current and the film resistance. As scan rate increases, the peak current increases and consequently the amount of potential loss increases, and this accounts for a large shift in the peak potential (Fig. 59, curve 1).

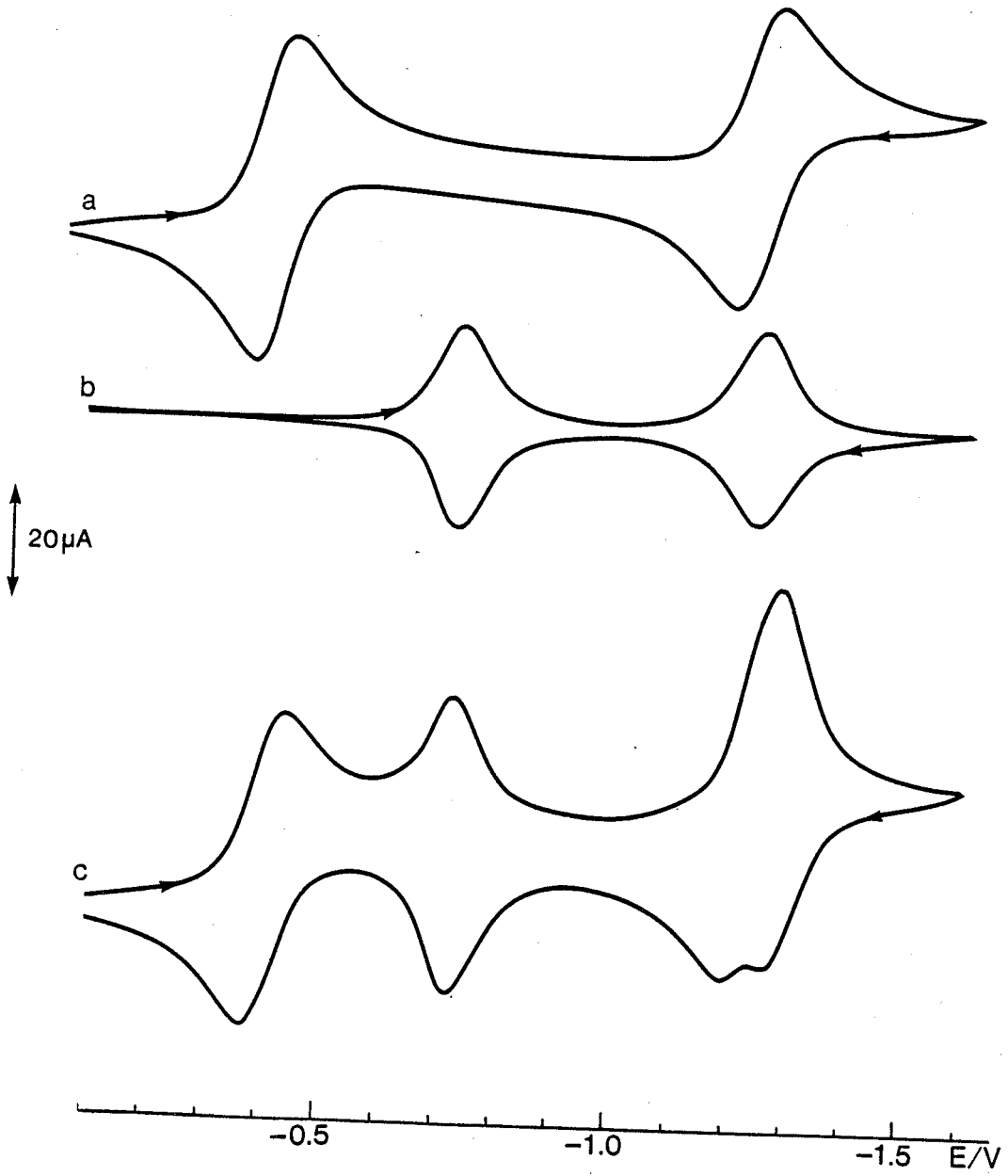
Once completely charged, the polymer network rapidly swells and a more open structure allows more facile penetration of electrolytes through the film. Consequently, the voltammetry of the charged film, ie. the second reduction and the two anodic reactions, closely resembles that observed in DMSO. After a complete cycle, the film becomes neutral and shrinks to the original state. The reversibility of the swelling-deswelling process produced voltammograms on successive scans similar to that yielded in the initial sweep.

To obtain more evidence of the variations in the swelling tendencies of polymers in different solvents, the reduction of p-benzoquinone (BQ) at a bare and at PAQ-coated electrodes in DMSO, H<sub>2</sub>O and CH<sub>3</sub>CN solutions was examined. The results in DMSO are shown in Figure 60. As expected, the presence of PAQ film on the Pt surface did not have any effect on the electrode reaction of the solution species. The reduction of BQ occurred essentially at the same potentials with the same current magnitudes as at a bare electrode. Curve c is merely a sum of curves a and b. Similar results were also obtained for films with much higher thickness, eg. 15000 Å. Since the reduction of BQ takes place at a more positive potential than AQ, it is unlikely that the cathodic reaction of BQ was mediated by the polymer film.

Figure 60: VOLTAMMOGRAMMETRY OF

- a) 1 mM benzoquinone solution at a bare electrode
- b) an electrode coated with a 1000 Å PAQ 200(2) film
- c) as a) but at the coated electrode

Scan rate  $0.05 \text{ Vs}^{-1}$ , 0.1M TEAP/DMSO



Instead, it is believed that the film was so porous that BQ easily diffused through the film to the locus of the reaction at the electrode surface.

When the same electrode was transferred into an aqueous solution of BQ, the reduction of the latter was greatly impeded, as shown in Figure 61. This indicates that BQ did not penetrate easily into the film, and only a small amount of BQ reached the electrode surface.

In BQ/TEAP/CH<sub>3</sub>CN solution, a profound effect was observed. The reduction of BQ at the modified electrode was shifted to more negative potential with the current greatly diminished (Figure 62). The cathodic peak corresponding to the reduction of PAQ to PAQ<sup>-</sup> increased in magnitude. A close examination revealed that the total area of peaks 3 and 4 is equal to that of 1 and 2. At more negative potential, the second reduction of BQ and the corresponding oxidation reaction occurred as observed at a bare Pt electrode. It was surprising to note the absence of the peak corresponding to the reoxidation of BQ<sup>-</sup> to BQ on the reverse scan.

These observations can be explained on the basis of the swelling-deswelling process of the film. At the potential where the reduction of BQ is to take place, the polymer film is neutral and poorly swollen. The effect on the reduction of BQ is thus similar to that found in aqueous solution. As the reduction of the polymer proceeds, the film swells and the open structure allows more BQ to penetrate into the film. The simultaneous reduction of the fresh BQ in the film results in an enhancement

Figure 61: VOLTAMMOGRAMS IN 0.1M TEAP/H<sub>2</sub>O OF:

- a) 1 mM benzoquinone solution at a bare electrode
- b) as a) but at an electrode coated with a 1000 Å  
PAQ 200(2) film

Scan rate 0.05 Vs<sup>-1</sup>

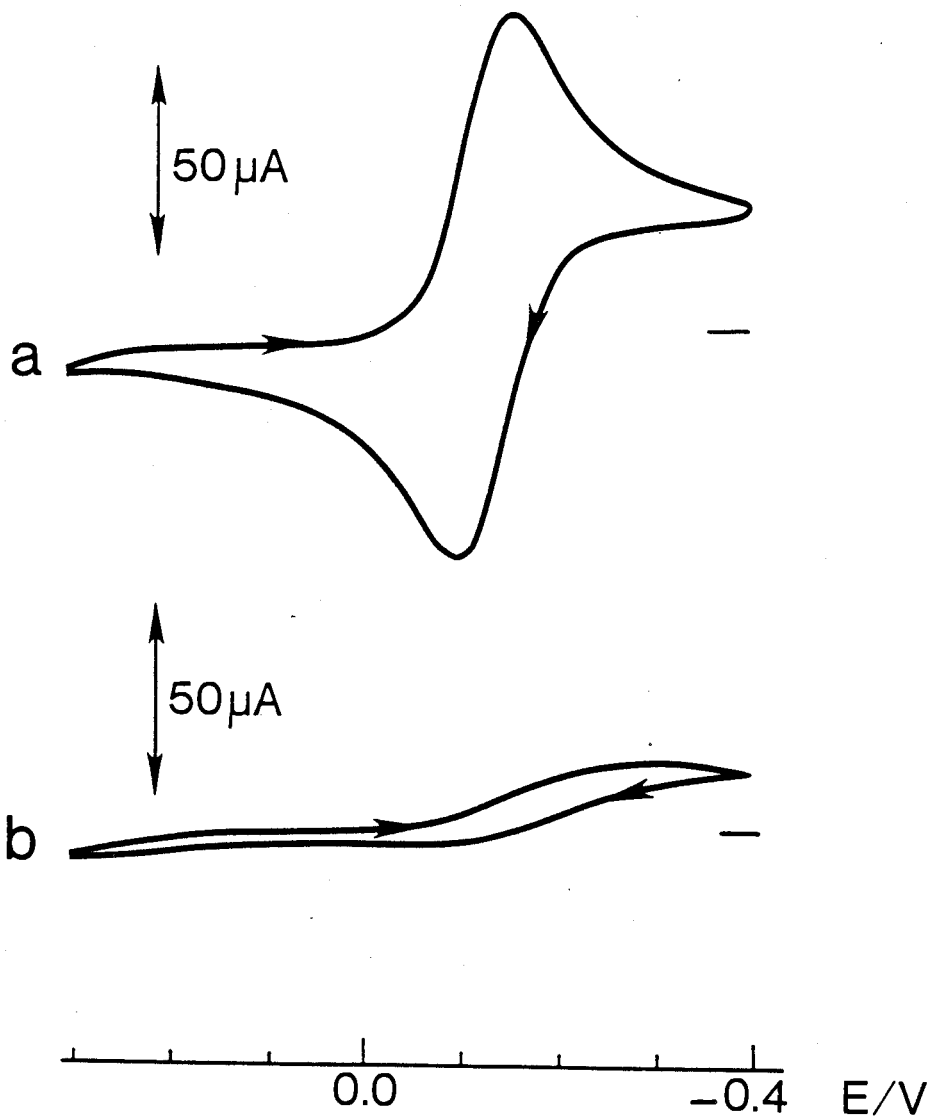
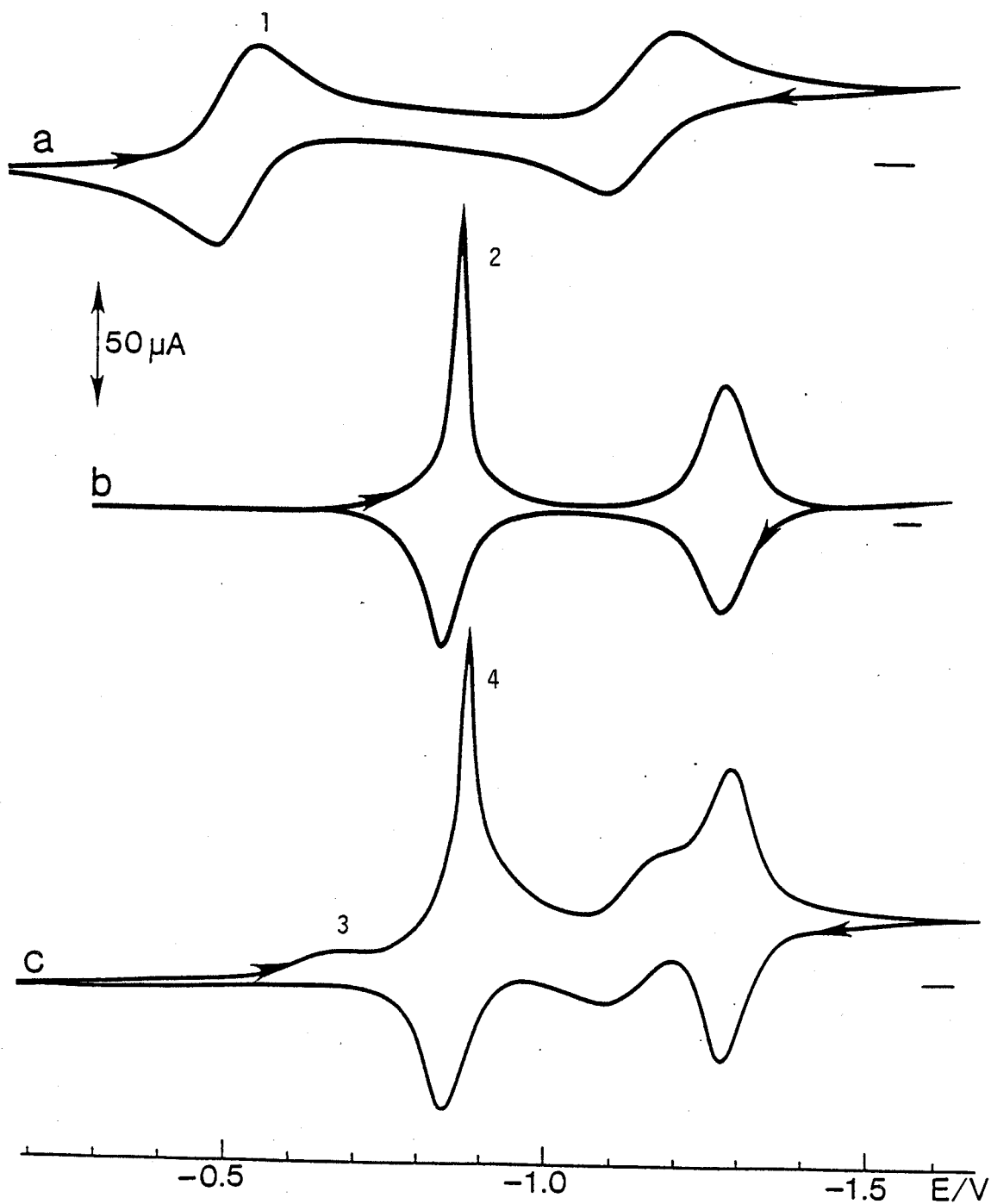




Figure 62: VOLTAMMOGRAMS IN 0.1M TEAP/CH<sub>3</sub>CN OF

- a) 1 mM benzoquinone solution at a bare electrode
- b) an electrode coated with a 1000 Å PAQ 200(2) film
- c) as a) but at the coated electrode

Scan rate 0.05 Vs<sup>-1</sup>



of PAQ/PAQ<sup>-</sup> peak. After being fully charged, the film becomes porous so that the second reduction of BQ and the corresponding oxidation reaction occur as at a bare electrode. At -0.7 V on a positive direction sweep, the film is reoxidized to the neutral state and the shrinking of the polymer expels BQ<sup>-</sup> out of the film before the oxidation of BQ<sup>-</sup> can take place.

The reduction of BQ at a PAQ-coated electrode in various solvents is thus closely related to the reduction of AQ groups attached in the film. In solvents where the permeation of BQ through the coating is impeded, ions and solvent would presumably also be unable to penetrate the film. In this condition, the immobilized active centers exhibit little or no electroactivity. For most applications of polymer electrodes, facile charge transport throughout the film is desired such that the film is fully electroactive and has rapid response time. The use of "good" solvents for experiments with polymer-modified electrodes is thus important.

#### e) Spectroelectrochemistry

During voltammetric measurements of PAQ films, it was observed that reduction of the films led to a change in color. The transparent, slightly yellow films became green upon reduction to PAQ<sup>-</sup> and then blue upon further reduction to PAQ<sup>2-</sup>. The spectroelectrochemistry on successive reduction cycles was examined in order to characterize the films, to probe their stability and reversibility, and to correlate the results with voltammetric data.

Polymeric films were deposited on conducting glass in the apparatus shown in Figure 39. The films were biased at a chosen potential until maximum optical absorption was exhibited. The results are presented in Figure 63. Below  $-0.7$  V, no effect is obtained. Between  $-0.7$  V and  $-1.2$  V, a strong band and two weak absorptions develop at 690, 415 and 392 nm, respectively. These correspond to the formation of PAQ radical anions. Further increase to  $-1.3$  V and more cathodic values produces a new peak at 595 nm, ( $\text{PAQ}^{2-}$ ) and a decrease in the 690 nm, 415 nm and 392 nm peaks. The process was reversible and reproducible, and similar intensities were obtained on successive cycles.

Plots of absorbance at 690 nm and 595 nm wave lengths as a function of potential are illustrated in Figure 64. Curve b shows that the first reduction of PAQ commences at  $-0.6$  V and reaches the full extent at  $-0.9$  V  $\sim$   $-1.1$  V. This corresponds well to the first wave of the voltammogram shown in the inset figure of Figure 63. At more negative potentials, the curve falls off, but does not drop down to the original value. This is because the band with  $\lambda_{\text{max}}$  at 595 nm is quite broad and extends into 695 nm region. Curve a, which represents the dependence of  $\text{PAQ}^{2-}$  absorbance on potential, exhibits two increases. The first one is due to the weak absorption of  $\text{PAQ}^{\cdot-}$  at 595 nm wave length. The second increase, which starts at  $-1.2$  V and becomes saturated at  $-1.5$  V, corresponds to the reduction of  $\text{PAQ}^{\cdot-}$  to  $\text{PAQ}^{2-}$ . Any further increase in the electrode potential does not have effect as the film has become fully charged.

The relationship between electrode potential E and

Figure 63: SPECTROELECTROCHEMISTRY OF A PAQ 200(2) FILM  
IN 0.1M TEAP/DMSO.

SPECTROELECTROCHEMISTRY OF  
ANTHRAQUINONE POLYMER  
FILM IN 0.1M TEAP / DMSO

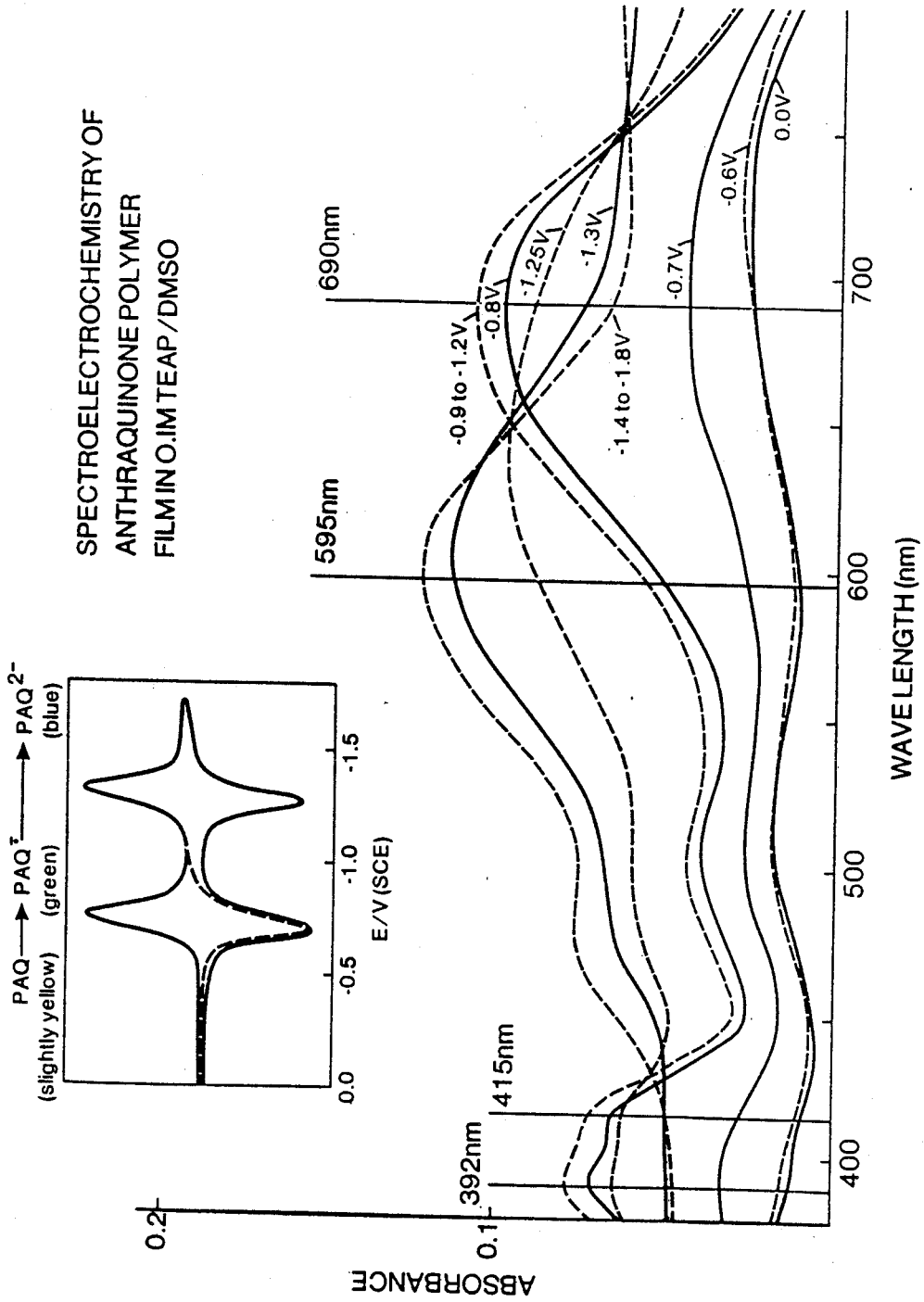
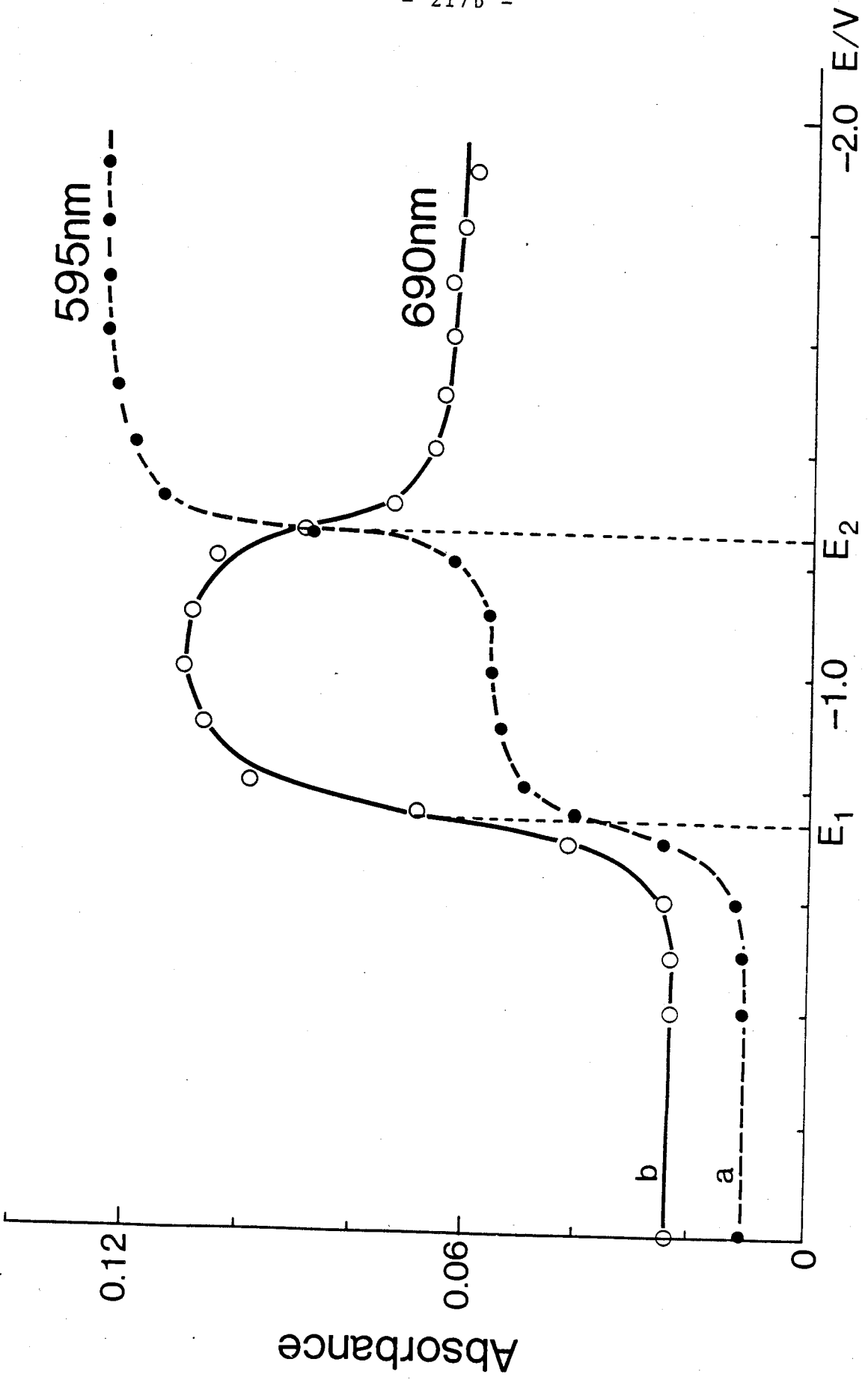


Figure 64: POTENTIAL DEPENDENCE OF ABSORBANCES OF  
A PAQ FILM IN 0.1M TEAP/DMSO AT

a) 595 nm

b) 690 nm





absorbance  $A$  of a redox couple has been derived for the thin-layer electrochemical technique and is given by (180):

$$E = E_{1/2} + 0.059 \log \frac{A_{\text{Red}} - A}{A - A_{\text{Ox}}} \quad [101]$$

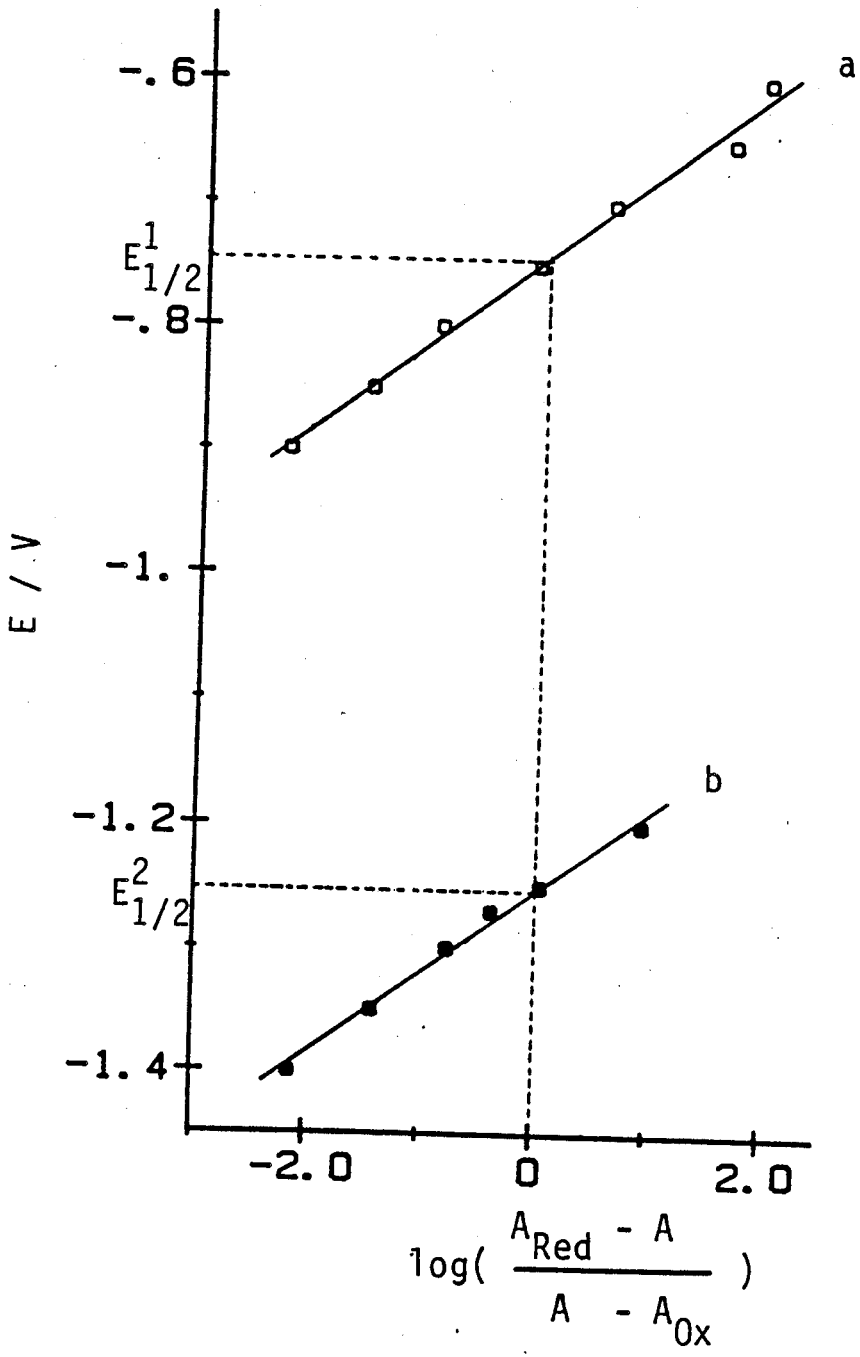
where  $E_{1/2}$  is the half-wave potential, and  $A_{\text{Red}}$  and  $A_{\text{Ox}}$  are the absorbances of the solution in its completely reduced and oxidized states, respectively.

A polymer-modified electrode has reactants and products confined to a very thin layer near the electrode surface. Therefore, it can be considered as a thin layer cell and eq.[101] can also be applied. Thus, a plot of  $E$  vs.  $\log\left(\frac{A_{\text{Red}} - A}{A - A_{\text{Ox}}}\right)$  should give a straight line with a slope of 59 mV/n an intercept of  $E_{1/2}$ . Nernstian plots from curves a and b in Figure 64 are shown in Figure 65. As expected, the plots are linear with a slope of 65 mV for both lines. This value is consistent with that expected for one-electron transfer process. The half-wave potentials for the first and second reductions are determined from intercepts as -0.74 V and -1.25 V, respectively. These results are in good agreement with values of -0.71 V for  $\text{PAQ}/\text{PAQ}^-$  and -1.25 V for  $\text{PAQ}^-/\text{PAQ}^{2-}$  estimated by cyclic voltammetry.

Determination of the  $E_{1/2}$  value(s) of an electroactive polymer film by this method may have some advantages over the linear sweep voltammetric technique. Since the measurements are not made until the film is in equilibrium with electrode potential, the results are less affected by the electrode kinetics, the large film resistance, the slow rate of charge transport in the film and the variation of this rate in a

Figure 65: NERNSTIAN PLOTS FOR ABSORBANCES OF A PAQ FILM  
IN 0.1M TEAP/DMSO AT:

- a) 690 nm (first reduction)
- b) 595 nm (second reduction)



reduction process vs. an oxidation process.

Compounds which change color when reduced or oxidized electrochemically are interesting for use in display devices. Reports on electrochromism of low molecular weight molecules such as tungsten oxide (181), hydrous nickel oxide (182,183), phosphotungstic acid (184), lutetium phthalocyanine (185) and viologens (186) have appeared over the last few years. Recently, few polymers, such as polyviologens, polypyrrole, polythiophene and polyaniline (139-141) were reported to exhibit electrochromic properties. For use in display devices, it is desirable to have electrochromic materials immobilized on an electrode surface; otherwise, their diffusion from the positions of utility to other areas will result in a color fog or stain. From this point of view, polymers are more attractive than low molecular weight compounds because the attachment of the former on electrode surface is easier. It is also desirable that the materials be chemically stable in both oxidized and reduced forms so that their optical properties are retained after several switching cycles. PAQ films are physically and chemically stable and exhibit a sharp change in color with reduction state, and thus are promising for this application.

g) Electrocatalytic Reduction of  $O_2$

The electrocatalytic reduction of  $O_2$  is perhaps one of the most intensively studied reactions at modified electrodes (9). The attraction of this reaction stems from the fact that efficient and inexpensive catalytic electrodes would be of great value for applications in fuel cells and electroanalytical

sensors. Much work has employed electrodes modified with metalloporphyrins and phthalocyanins (9,19). Reduction of oxygen at electrodes coated with organic polymers such as polyacrylonitrile and poly(p-nitrostyrene) was also studied, and a potential gain of 200 mV was reported (130).

It has been known that dihydroquinones are capable of reducing  $O_2$  to  $H_2O_2$  in aqueous solution. Dihydroanthraquinones have been used as catalysts for the production of  $H_2O_2$  from  $O_2$  on a large scale (187,188). Recently, Wrighton and coworkers covalently attached naphthoquinones to surfaces of Pt, semiconductors and oxides for electrochemical and photoelectrochemical reduction of  $O_2$  (189,190). It was reported that the catalytic reduction of  $O_2$  was diffusion controlled with >90% current efficiency in neutral solutions (pH 7.0 - 7.2). Very recently, Degrand employed an absorbed film of an anthraquinone polymer with an amine backbone for electrocatalytic reduction of  $O_2$  (191). The catalytic reaction was diffusion controlled at pH>8 and the reaction rate diminished as pH was decreased.

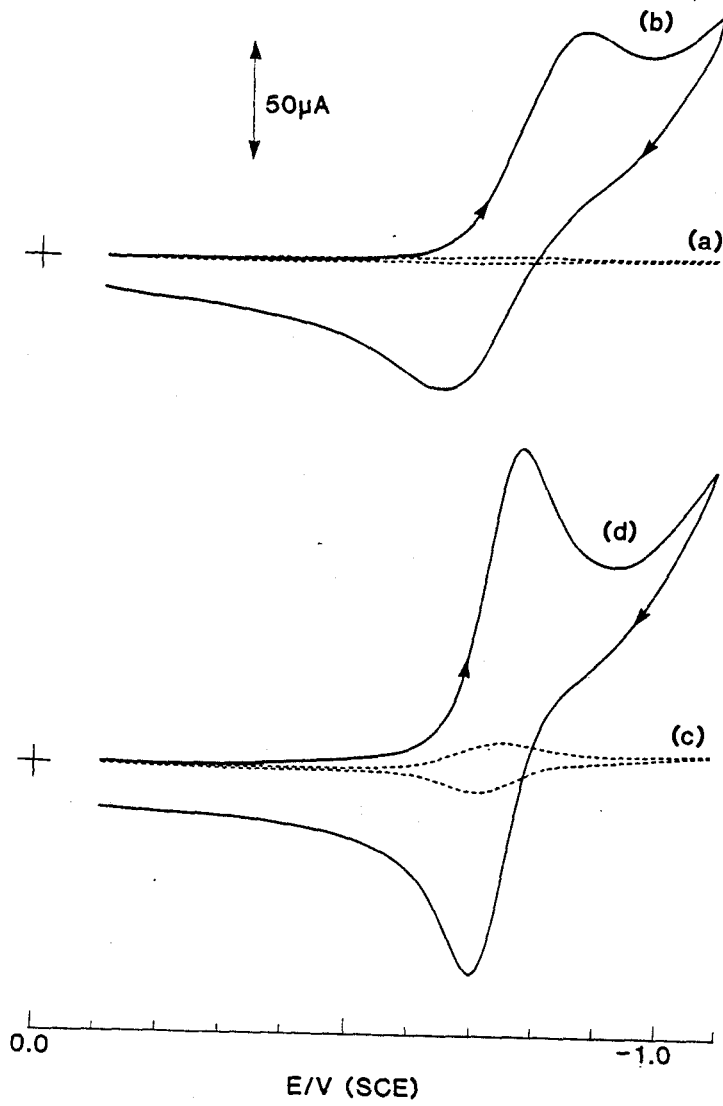
This section describes the study of electroreduction of  $O_2$  at PAQ-coated electrodes. Cyclic voltammetry and rotating disk electrode techniques were employed to examine the catalytic properties of polymer films. Determination of the rate constant of the electron exchange reaction between  $O_2$  and polymer films was attempted but was unsuccessful because the reaction was too fast for a kinetic study.

Figure 66 shows the reduction of  $O_2$  in 0.1M TEAP/DMSO

Figure 66:                    REDUCTION OF O<sub>2</sub>

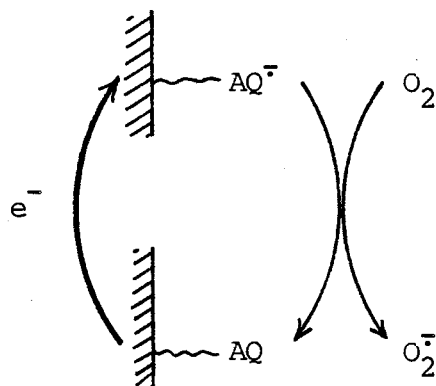
- a) Pt electrode under N<sub>2</sub>
- b) as a) but O<sub>2</sub> saturated
- c) PAQ 200(2)-coated electrode (film thickness  
100 Å) N<sub>2</sub> saturated
- d) as c) but O<sub>2</sub> saturated

Scan rate 0.05 Vs<sup>-1</sup>, 0.1M TEAP/DMSO.



solution at a bare Pt surface and at the same electrode coated with a 100 Å PAQ film. At the bare electrode, a quasi-reversible curve is obtained with  $E_{pc} = -0.88V$  and  $E_{pa} = -0.66V$  vs. SCE. The large peak separation potential,  $\Delta E = 222$  mV, indicates that the heterogeneous electron transfer is not fast, and the results are consistent with those reported by Sawyer and Roberts (192).

At the PAQ coated electrode, the smaller peak separation ( $\Delta E = 68$  mV,  $E_{pc} = -0.78$  V and  $E_{pa} = -0.71$  V) indicates improved reversibility. Of greater interest is the 98 mV positive shift of the cathodic peak. This indicates the catalytic reduction of  $O_2$  by PAQ/PAQ<sup>-</sup> couple as shown in the following scheme and implies that the electron transfer from Pt to  $O_2$  in solution via the PAQ film is faster than the direct electron transfer from the electrode.



[102]

In Figure 66d, a peak at  $-0.88$  V which corresponds to the direct reduction of  $O_2$  at the Pt surface is not observed. This cannot be ascribed to the blocking effect of the PAQ film because it has been demonstrated in section III.3.3.e) that in DMSO



solution, the film was so porous that solution species could diffuse easily into the film. Furthermore, the thickness of the film used in this experiment was only one-tenth of that described in section III.3.3.e). It is instead believed that at this potential, there is little  $O_2$  present at the electrode surface because it has all been reduced at more positive potentials by the polymer film. This is in keeping with the view that the electron transfer from  $AQ^{\cdot-}$  moieties to oxygen molecule is very fast.

The effect of scan rate on the cyclic voltammetry of  $O_2$  is shown in Figure 67. At a naked electrode, the reduction peak shifted cathodically, the oxidation peak shifted anodically and the peaks became more separated as scan rate increased. In contrast, when the electrode was coated with a PAQ film, the positions of the cathodic and anodic peaks were almost insensitive to scan rate. Clearly, oxygen is reduced more reversibly at PAQ-coated electrodes due to the catalytic effect of PAQ films.

Figure 68 presents the reduction of an  $O_2$ -saturated solution at a bare and at a coated rotating electrode. The polymer film caused a positive shift in reduction potential and a sharpening in the shape of the voltammogram. As rotation rate increased,  $E_{1/2}$  values for the reduction at the bare electrode shifted more negatively, whereas  $E_{1/2}$  remained unchanged at the coated electrode. Plots of  $(E - E_{1/2})$  vs.  $\log\left(\frac{i_1 - i}{i}\right)$  are linear for both voltammograms recorded at the bare and at the coated electrode. However, the slopes for data obtained at the later are

Figure 67: VOLTAMMETRY OF A SATURATED O<sub>2</sub> SOLUTION IN 0.1M TEAP/DMSO AT VARIOUS SCAN RATES AT

A) a PAQ 200(2)-coated electrode (film thickness 100 Å)

B) a bare Pt electrode

Scan rates: a) 0.5 Vs<sup>-1</sup>  
b) 0.2 Vs<sup>-1</sup>  
c) 0.1 Vs<sup>-1</sup>  
d) 0.05 Vs<sup>-1</sup>  
e) 0.02 Vs<sup>-1</sup>  
f) 0.01 Vs<sup>-1</sup>

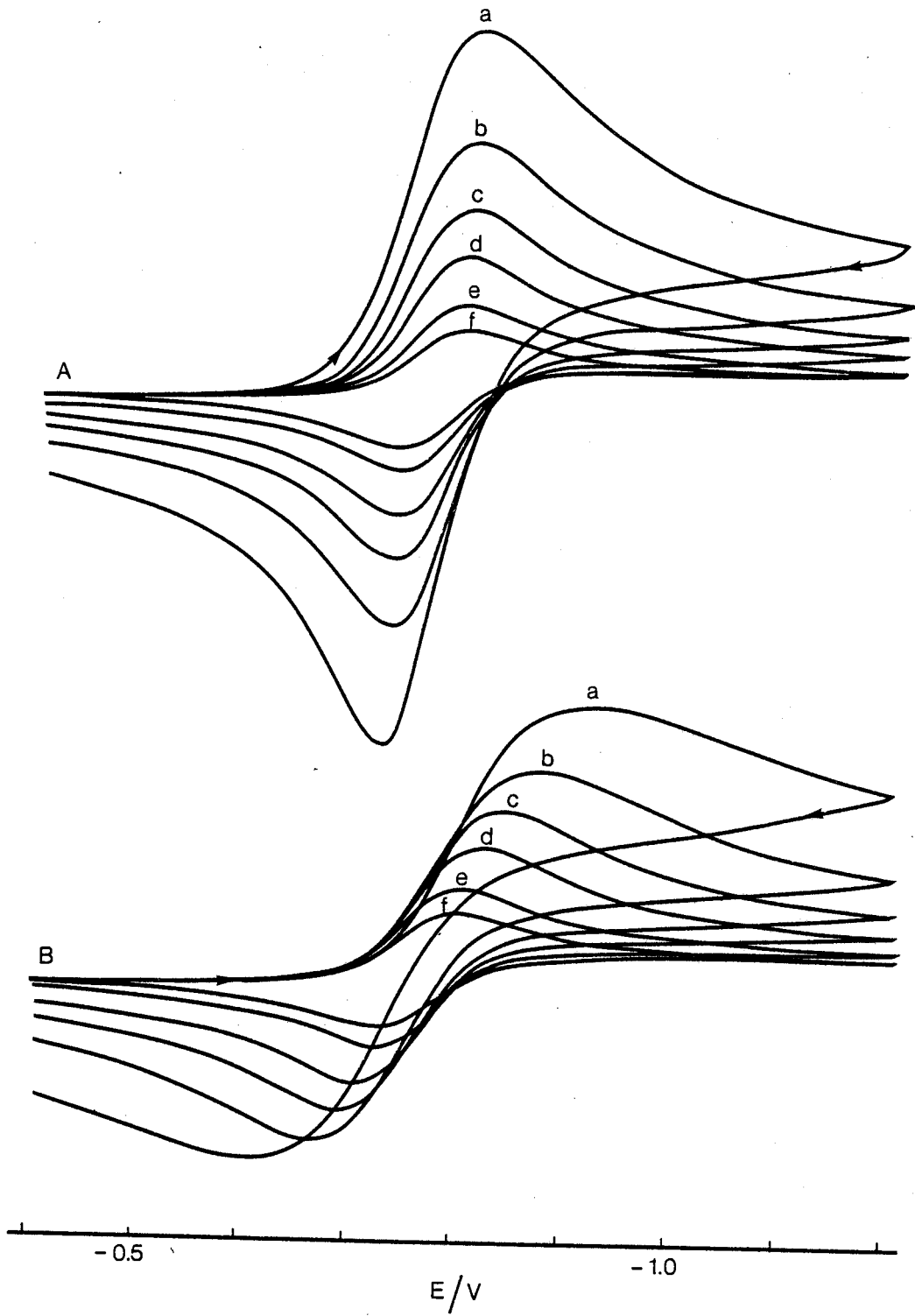
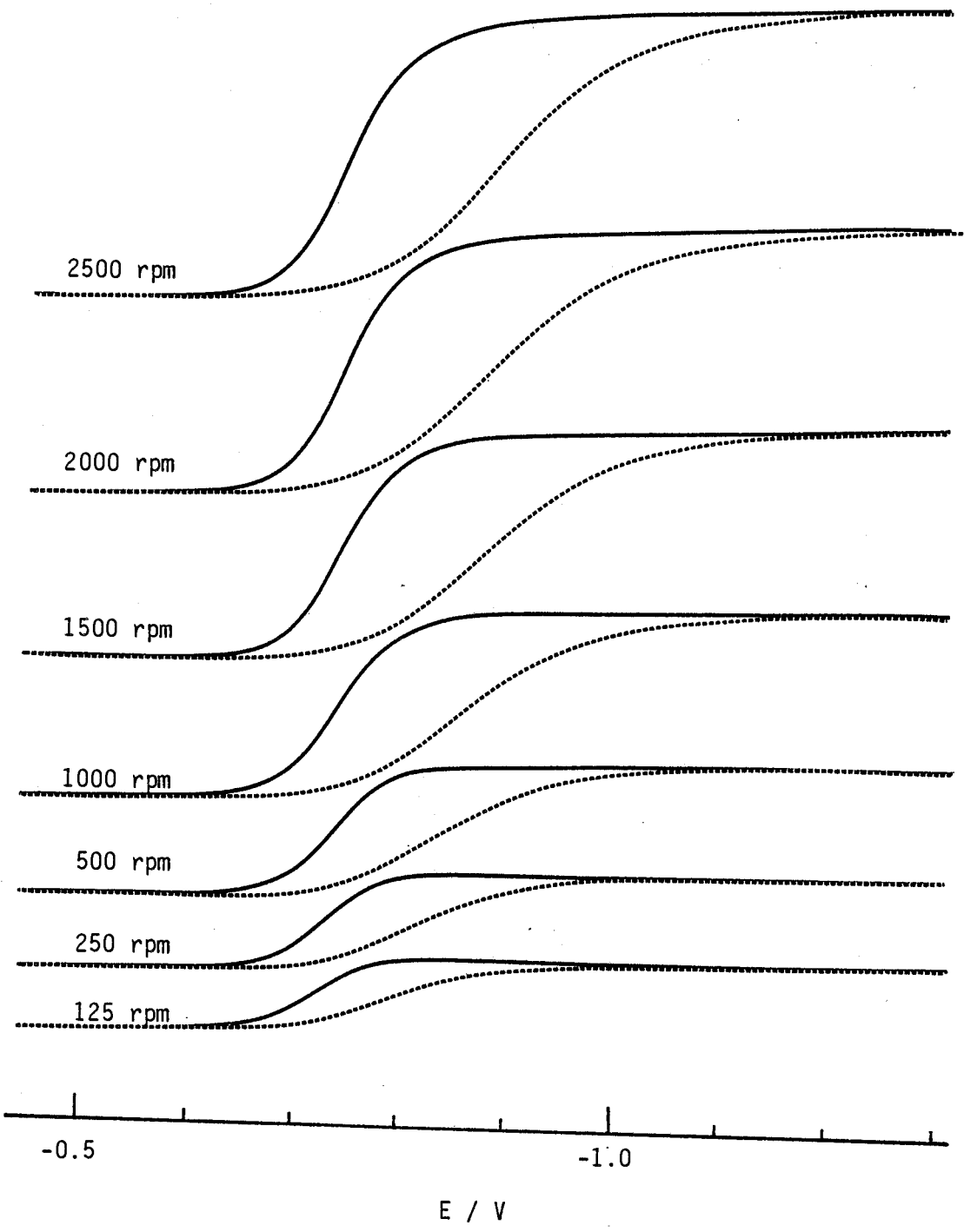


Figure 68: RDE VOLTAMMOGRAMS OF  $O_2$  AT A BARE ELECTRODE (----) AND AT A PAQ-COATED ELECTRODE (FILM THICKNESS 100 Å) (——) AT VARIOUS ROTATION RATES IN 0.1 TEAP/DMSO.



much closer to that expected for an ideal Nernstian behavior (Figure 69) (The slopes are 63 mV and 128 mV for a coated and for a bare electrode, respectively). Again, this is indicative of catalytic reduction of  $O_2$  by the PAQ film, and the results are consistent with those obtained at a stationary electrode.

Quantitative analysis of the current-potential curves revealed that the limiting currents are essentially equal to their value on the uncoated electrode and vary linearly with (rotation rate)<sup>1/2</sup> up to the highest rotation velocity available. The effect of film thickness is shown in Figure 70 and it appears that the magnitude of the limiting current and the shape of the voltammograms are invariant to the thickness of the film.

Several theories have been reported dealing with kinetics of mediated electrolysis at a rotating electrode coated with a polymer film (9,123-125,193). The overall process is considered to consist of five individual steps:

i) The hydrodynamic mass transport of the substrate from solution to the polymer film surface.

ii) The permeation of the substrate into and within the polymer film.

iii) The electron transfer reaction between the catalyst and the substrate.

iv) The transport of charge from the electrode through the film to regenerate catalytic sites in the film.

v) The heterogeneous electron transfer between the electrode and active centers at the film-electrode interface.

The rate of the overall mediated electron transfer process will be governed by the kinetics of the rate-limiting

Figure 69: NERNSTIAN PLOTS FOR REDUCTION OF  $O_2$  AT

a) a bare Pt electrode

b) a PAQ-coated electrode (film thickness 100 Å)

Rotation rate 1500 rpm, 0.1M TEAP/DMSO

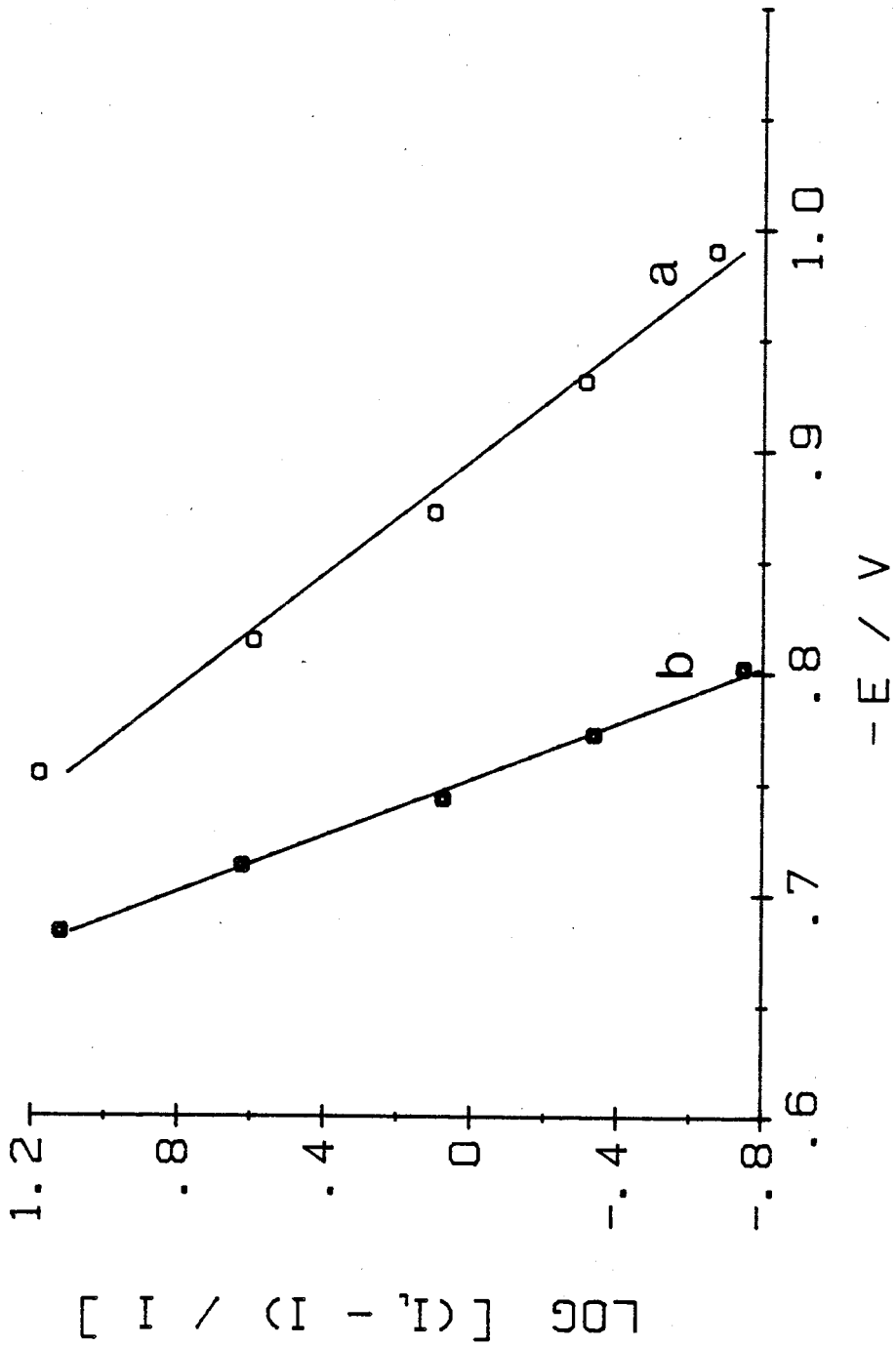




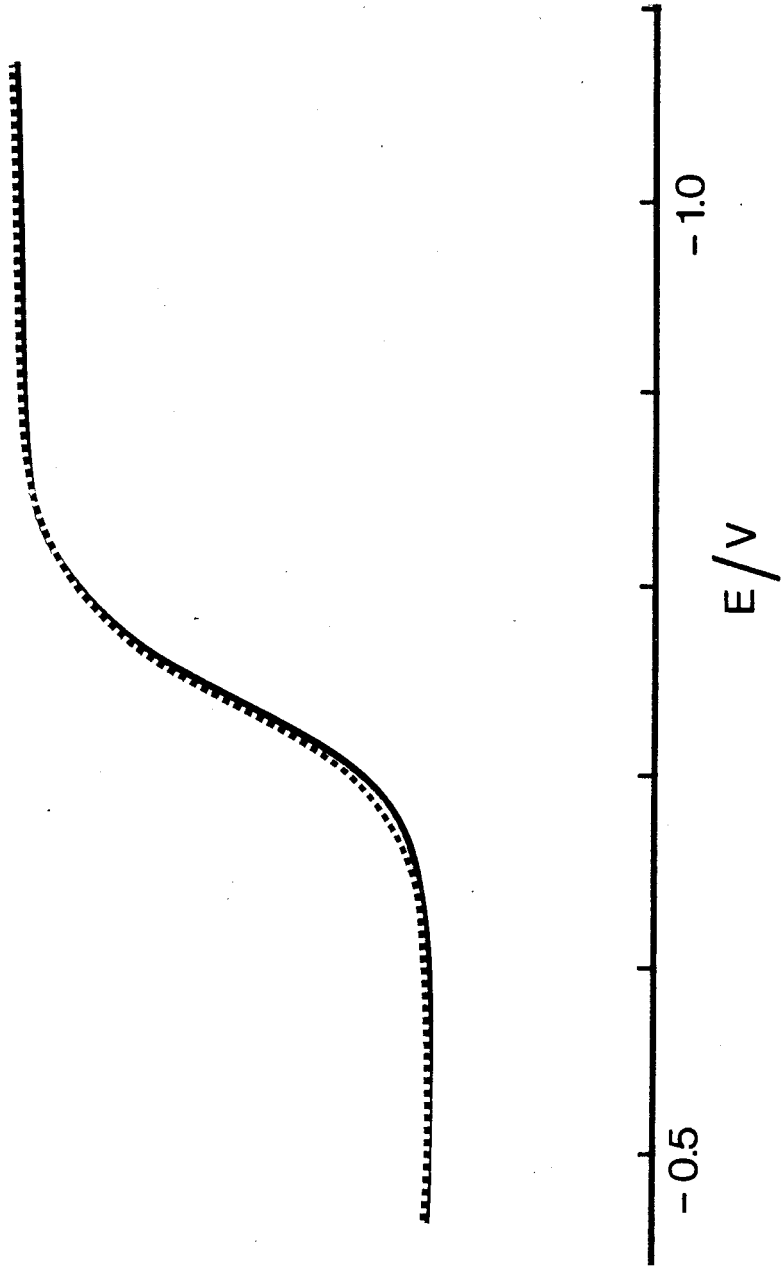
Figure 70: RDE VOLTAMMETRY OF A  $O_2$  SATURATED SOLUTION AT ELECTRODES COATED WITH PAQ FILMS OF DIFFERING THICKNESSES.

Film thickness:

a) 100 Å      -----

b) 1000 Å     \_\_\_\_\_

Rotation rate 1500 rpm, 0.1M TEAP/DMSO.



process(es). Savéant (123), Murray (193), Alberly (9) and Anson (124) have derived equations for the catalytic limiting currents for various limiting cases. It was shown that when the rate of the overall process is determined by the rate of supply of the substrate to the polymer film-solution interface, the catalytic limiting current  $i_1$  is equal to the limiting current obtained at a bare electrode, and the current-potential relationship is given by (193):

$$E = E_{1/2}^{\text{cat}} - \frac{RT}{nF} \ln\left(\frac{i_1 - i}{i}\right) \quad [103]$$

where  $E_{1/2}^{\text{cat}}$  is the half-wave potential of catalytic species.

For other limiting situations,  $i_1$  is a function of the rate of the associated limiting process(es).

In the present work, the reduction of  $O_2$  at a PAQ-coated electrode produced a voltammetric wave having the shape predicted by equation [103] (Figure 69) and  $i_1$  identical to that obtained at a naked electrode (Figure 68). This behavior indicates that the rate of the overall process is determined by that of the mass transport of  $O_2$  to the film-solution interface. This is further supported by the fact that the catalytic limiting current is independent of film thickness. Otherwise, the catalytic current should decrease with increasing thickness because the rates of processes ii), iii) and iv) are inversely proportional to thickness (123-125,193).

Finally, in order to examine the chemical stability PAQ films following prolonged use in electrocatalysis, cyclic voltammetry of a polymer film was examined in an Ar-saturated

solution, before and after a series of experiments described in Figure 68. The polymer film showed only 15% loss in activity, indicating that the film was quite durable.

h) Conclusion

PAQ films formed by droplet evaporation from an electrode were not adequately stable for long periods. Desorption of the polymer occurred and peak currents diminished rapidly with time. The films were stabilized by inducing crosslinking of the polymer film by exposing it to U.V. irradiation. The optimum irradiation condition was determined and the resulting films remained physically and chemically stable for the full period of investigation.

Electrochemical reductions of polymer films to the radical anion and to the dianion were reversible and occurred at potentials similar to those found for the model compound in solution. Films thinner than 1000 Å exhibited a behavior which is suggestive of fast reduction of polymer films. Voltammetric peaks were symmetrical, peak currents varied linearly with scan rate and peak widths at half-height were comparable with that predicted for a reversible monolayer. For thicker films, some deviations from the ideal behavior were observed.

Coulometry showed that 78.8% of the AQ groups present in the film were reduced and oxidized in each potential cycle for a 100 Å film. For thicker films, the peak current increased but was not proportional to film thickness, and only a small fraction of active centers were reacted. It was proposed that in thick films,

there are regions devoid of electroactivity interdispersed with those completely electroactive.

Charge transport coefficient  $D_{CT}$  of polymer films was determined as  $5.1 \times 10^{-11} \text{ cm}^2 \text{ s}^{-1}$  by chronoamperometry.  $D_{CT}$  was apparently insensitive to the content of AQ groups on a polymer chain.

As with PVBQ-St films, solvent had a profound effect on the electrochemistry of PAQ coatings. The polymer films showed a high electroactivity in good solvents and were inactive in non-solvents. This effect was attributed to the variation of film morphology in different solvents.

Polymer films changed color with reduction states. The transition to the green radical anion and to the blue dianion was spectrophotometrically examined. A spectroelectrochemical method was presented, which may be used to obtain thermodynamic data of redox groups in an electrochromic film.

PAQ films catalyzed the reduction of oxygen. A positive shift of about 98 mV in the cathodic peak potential was noted. The electron exchange reaction between attached  $AQ^{\cdot -}$  moieties and dissolved oxygen molecules was very fast and the rate of the catalytic process was diffusion controlled.

REFERENCES

1. T. W. Smith, J. E. Kuder and D. Wychick, J. Polym. Sci. Polym. Chem. Ed., 14, 2433 (1976).
2. T. Saji, N. F. Pasch, S. E. Webber and A.J. Bard, J. Phys. Chem., 82, 1101 (1978).
3. J. B. Flanagan, S. Margel, A. J. Bard and F. C. Anson, J. Am. Chem. Soc., 100, 4248 (1978).
4. K. D. Snell and A. G. Keenan, J. Chem. Soc. Chem. Soc. Rev., 259(1979).
5. W. R. Heineman and P. T. Kissinger, Anal. Chem., 50, 166R (1978).
6. W. R. Heineman and P. T. Kissinger, Anal. Chem., 52, 138R (1980).
7. R. W. Murray, Acc. Chem. Res., 13, 135 (1980).
8. T. Osa "Kagaku Zokan", Vol 86, T. Osa, T. Shono and K. Honda (Ed.), Kagaku Dojin, Kyoto, 1980, Chap. 2.
9. W. J. Albery and A. R. Hillman, Chem. Soc. Ann. Rep. Progr. Chem., Sec. C, 78, 377 (1982).
10. M. D. Ryan and G. S. Wilson, Anal. Chem., 54, 20R (1982).
11. D. C. Johnson, M. D. Ryan and G. S. Wilson, Anal. Chem., 56, 7R (1984).
12. L. R. Faulkner, Chem. Eng. News, 62, 28 (1984).
13. R. W. Murray in "Electroanalytical Chemistry", Vol 13, A. J. Bard (Ed.), Marcel Dekker, New York, 1984, p. 191.
14. H. D. Mettee in "Polymers in Solar Energy Utilization", Am. Chem. Soc., 1983, Chap. 29.
15. K. Kaneto, "Advances in Polymer Science", Vol. 55, Springer-Verlag, Berlin Heidelberg, 1984, p. 1.
16. S. W. Mayer, C. Park and D. E. McKenzie, U.S. Patent 3,185,590 (1965).
17. D. L. Klass, U.S. Patent 3,300,342 (1967).
18. M. Noel, P. N. Anatharaman and H. V. K. Udupa, Trans. SAEST, 15, 49 (1980).

19. J. Zak and T. Kuwana, *J. Electroanalytical. Chem.*, 150, 645 (1983).
20. H. Lund, *Denki Kagaku Oyobi Kogyo Butsuri Kagaku*, 45, 2 (1977).
21. H. Lund in "Kagaku Zokan", Vol 86, T. Osa, T. Shono and K. Honda (Ed.), *Kagaku Dojin*, Kyoto, 1980, Chap. 6.
22. J. Simonet in "Organic Electrochemistry", M. M. Baizer and H. Lund, Ed., Second Ed., Marcel Dekker, New York, 1983, Chapter 26.
23. H. Wendt, *Electrochim. Acta*, 29, 1513 (1984).
24. A. S. Lindsey, M. E. Peover and N. S. Savill, *J. Chem. Soc.*, 193, 4558 (1962).
25. S. E. Hunt, A. S. Lindey and N. S. Savill, *J. Chem. Soc.*, 791 (1967).
26. G. M. Brown, T. J. Meyer, D. O. Cowan, C. LeVanda, K. Kaufman, P. V. Roling and M. D. Rausch, *Inorg. Chem.*, 14, 506 (1975).
27. C. LeVanda, K. Beckgard, D. C. Cowan and M. D. Rausch, *J. Am. Chem. Soc.*, 99, 2964 (1977).
28. W. H. Morrison, Jr., S. Krogsrud and D. N. Hendrickson, *Inorg. Chem.*, 12, 1998 (1973).
29. W. T. Yap and R. A. Durst, *J. Electroanal. Chem.*, 130, 3 (1981).
30. Y. Morishima, Y. Itoh and A. Koyagi, *J. Polym. Sci. Polym. Chem. Ed.*, 21, 953 (1983).
31. S. Wawzonek and A. Gundersen, *J. Electrochem. Soc.*, 107, 537 (1960).
32. Y. Avny and A. Moshonov, *Eur. Polym. J.*, 13, 99 (1977).
33. J. Q. Chambers in "The Chemistry of The Quinonoid Compounds", S. Patai (Ed.), Wiley, London, 1974, p.737.
34. R. E. Moser, H. Kamogawa, H. Hartmann and H. G. Cassidy, *J. Polym. Sci.*, Part A, 2, 2401 (1964).
35. S. Piekarski and R. N. Adams in "Physical Methods of Chemistry, Part IIA Electrochemical Methods", Vol. 1, A. Weissberger and B. W. Rossiter (Ed.), Wiley, New York, 1971, Chapter 7.

36. W. J. Albery and M. L. Hitchman, "Ring-Disk Electrodes", Oxford University Press, London, 1971.
37. A. Secvik, Collection Czech. Chem. Commun., 13, 349 (1948).
38. J. E. B. Randles, Trans. Faraday Soc., 44, 327 (1948).
39. R.S. Nicholson and I. Shain, Anal. Chem., 36, 706 (1964).
40. A. J. Bard and L. R. Faulkner, "Electrochemical Methods. Fundamentals and Applications.", Wiley, New York, 1980, p. 224.
41. V. G. Levich, "Physicochemical Hydrodynamics", Prentice-Hall, Englewood Cliffs, N. J., 1962.
42. R. N. Adams, "Electrochemistry at Solid Electrodes", Marcel Dekker, New York, 1969, 214.
43. C. Tanford, "Physical Chemistry of Macromolecules", Wiley, New York, 1961, p. 346.
44. H. V. Drushel and J. F. Miller, Anal. Chem., 29, 1456 (1957).
45. Ref. 43, p. 349.
46. G. Meyerhoff and G. V. Schulz, Makromol. Chem., 7, 294 (1952).
47. Ref. 40, p. 390.
48. P. C. Miller and D. Banerjee, J. Indian Chem. Soc., 9, 375 (1932).
49. K. Uno, M. Ohara and H. G. Cassidy, J. Polym. Sci., Part A-1, 6, 2729 (1968).
50. G. Odian, "Principles of Polymerization", Second Ed., Wiley, New York, 1981, p. 246.
51. A. A. Yassin and N. A. Risk, Polymer, 19, 57 (1978).
52. A. A. Yassin and N. A. Risk, J. Polym. Sci. Polym. Chem. Ed., 16, 1475 (1978).
53. B. R. Eggins and J. Q. Chambers, J. Electrochem. Soc., 117, 186 (1970).
54. D. A. Holden and J. E. Guillet, J. Polym. Sci. Polym. Chem. Ed., 18, 565 (1980).
55. B. L. Funt and L. C. Hsu, J. Polym. Sci. Polym. Chem. Ed.,



- 18, 1957 (1980).
56. R. Brdicka and C. Tropp, *Biochem. Z.*, 289, 301 (1937).
  57. R. Brdicka and K. Wiesner, *Naturwiss.*, 31, 247 (1943).
  58. S. G. Mairanovskii, "Catalytic and Kinetic Waves in Polarography", B. M. Fabuss and P. Zuman (Tranl.), Plenum Press, New York, 1968.
  59. A. P. Tomilov, S. G. Mairanovskii, M. Y. Fioshin and V. A. Smirnov, "Electrochemistry of Organic Compounds", J. Schmorak (Tranl.), Halsted Press, Jerusalem, 1972, p. 537.
  60. A. J. Fry, "Synthetic Organic Electrochemistry", Harper & Row, New York, 1972, p. 67-68.
  61. "Encyclopedia of Electrochemistry of The Elements", Vol. XIV, A. J. Bard and H. Lund (Ed.), Marcel Dekker, New York, 1980, p. 133.
  62. H. Lund and J. Simonet, *J. Electroanal. Chem.*, 65, 205 (1975).
  63. H. Lund, M. A. Michel and J. Simonet, *Acta Chem. Scand.*, B28, 900 (1974).
  64. H. Lund, M. A. Michel and J. Simonet, *Acta Chem. Scand.*, B29, 217 (1975).
  65. J. Simonet, M. A. Michel and H. Lund, *Acta Chem. Scand.*, B29, 489 (1975).
  66. J. W. Sease and R. C. Reed, *Tetrahedron Lett.*, 6, 393 (1975).
  67. L. A. Avaca, E. R. Gonzalez and E. A. Ticianelli, *Electrochim. Acta*, 28, 1479 (1983).
  68. K. Boujlet, J. Simonet, J. P. Barnier, C. Girard and J. M. Conia, *J. Electroanal. Chem.*, 117, 161 (1981).
  69. K. Boujlet, P. Martigny and J. Simonet, *J. Electroanal. Chem.*, 144, 437 (1983).
  70. G. Dabosi, M. Martineau and J. Simonet, *J. Electroanalytical. Chem.*, 139, 211 (1982).
  71. D. H. Evans and X. Naixian, *J. Electroanal. Chem.*, 133, 367 (1982).
  72. L. Griggio, *J. Electroanal. Chem.*, 140, 155 (1982).
  73. J. Simonet and H. Lund, *Acta Chem. Scand.*, B31, 909

(1977).

74. S. Kwee and H. Lund, *Bioelectrochem. Bioenerg.*, 1, 87 (1974).
75. S. Kwee and H. Lund, *Bioelectrochem. Bioenerg.*, 2, 231 (1975).
76. W. Schmidt and E. Steckhan, *J. Electroanal. Chem.*, 89, 215 (1978).
77. W. Schmidt and E. Steckhan, *J. Electroanal. Chem.*, 101, 123 (1979).
78. S. Dopferheld and E. Steckhan, *Angew. Chem.*, 94, 785 (1982).
79. T. Shono, Y. Matsumura, J. Hayashi and M. Mizoguchi, *Tetrahedron Lett.*, 2, 165 (1979).
80. T. Shono, Y. Matsumura, J. Hayashi and M. Mizoguchi, *Tetrahedron Lett.*, 21, 1867 (1980).
81. T. Shono, Y. Matsumura and H. Hamaguchi in "Kagaku Zokan", Vol 86, T. Osa, T. Shono and K. Honda (Ed.), Kagaku Dojin, Kyoto, 1980, Chap. 5.
82. V. G. Mairanovsky, *Angew. Chem. Int. Ed. Engl.*, 15, 281 (1976).
83. W. Schmidt and E. Steckhan, *Angew. Chem. Int. Ed. Engl.*, 17, 673 (1978).
84. M. Platen and E. Steckhan, *Tetrahedron Lett.*, 21, 511, (1980).
85. O. Hutzinger, S. Safe and Zitko, "The Chemistry of PCB's", CRC Press, Cleveland, OH, 1974.
86. R. E. Hatton in "Encyclopedia of Chemical Technology", Third Ed., Vol. 5, 1979, p. 844.
87. T. C. Cairns and E. G. Siegmund, *Anal. Chem.*, 53, 1183A (1981).
88. D. G. Ackerman, L. L. Scinto, P. S. Bakshi, R. G. Delumyea, R. J. Johnson, G. Richard, A. M. Takata and E. M. Sworzyn, "Destruction and Disposal of PCBs by Thermal and Non-Thermal Methods", Noyes Data, New Jersey, 1983.
89. S. O. Farwell, F. A. Beland and R. D. Geer, *J. Electroanal. Chem.*, 61, 303 (1975).
90. S. O. Farwell, F. A. Beland and R. D. Geer, *J. Electroanal.*

- Chem., 61, 315 (1975).
91. S. O. Farwell, F. A. Beland and R. D. Geer, Anal. Chem., 47, 895 (1975).
  92. E. Brillas, J. M. Costa and I. Gallardo, An. Quim., Ser. A, 77, 409 (1981). Chem. Abs. 97: 46404r
  93. H. Lund and J. Simonet, Bull. Soc. Chim. Fr., 1843 (1973).
  94. L. H. Kristensen and H. Lund, Acta Chem. Scand., B33, 735 (1979).
  95. C. Degrand, P. L. Compagnon, F. Gasquez and G. Belot, Electrochim. Acta, 29, 625 (1984).
  96. E. Hebert, J. P. Mazaleyrat and Z. Welwart, Nouv. J. Chim., 7, 55 (1983).
  97. J. F. Garst and C. D. Smith, J. Am. Chem. Soc., 98, 1520 (1976).
  98. J. F. Rusling and T. F. Connors, Anal. Chem., 55, 776 (1983).
  99. T. F. Connors and J. F. Rusling, J. Electrochem. Soc., 130, 1120 (1983).
  100. R. F. Lane and A. T. Hubbard, J. Phys. Chem., 77, 1401 (1973).
  101. R. F. Lane and A. T. Hubbard, J. Phys. Chem., 77, 1411 (1973).
  102. B. F. Watkins, J. R. Behling, E. Kariv and L. L. Miller, J. Am. Chem. Soc., 97, 3549 (1975).
  103. P. R. Moses, L. Wier and R. W. Murray, Anal. Chem., 47, 1882 (1975).
  104. T. Matsue, M. Fujihira and T. Osa, J. Electrochem. Soc., 126, 500 (1979).
  105. T. Matsue, M. Fujihira and T. Osa, J. Electrochem. Soc., 128, 1473 (1981).
  106. S. Abe, T. Nonaka and T. Fuchigami, J. Am. Chem. Soc., 105, 3630 (1983).
  107. S. Abe and T. Nonaka, Chem. Lett., 1541 (1983).
  108. T. Komori and T. Nonaka, Chem. Lett., 509 (1984).
  109. T. Komori and T. Nonaka, J. Am. Chem. Soc., 106, 2656

- (1984).
110. J. F. Price and R. P. Baldwin, *Anal. Chem.*, 52, 1940 (1980).
111. J. Caja, R. B. Kaner and A. G. MacDiarmid, *J. Electrochem. Soc.*, 131, 2744 (1984).
112. K. Kaneto, K. Yoshimo and Y. Unuishi, *Jpn. J. Appl. Phys.*, 22, L567 (1983).
113. J. H. Kaufman, J. W. Kaufer, A. J. Heeger, R. B. Kaner and A. G. MacDiarmid, *Phys. Rev. B*, 26, 2327 (1982).
114. F. B. Kaufman, A. H. Schroeder, E. M. Engler and V. V. Patel, *Appl. Phys. Lett.*, 36, 422 (1980).
115. H. Akahoshi, S. Toshima and K. Itaya, *J. Phys. Chem.*, 85, 818 (1981).
116. T. Kobayashi, H. Yoneyama and H. Tamura, *J. Electroanal. Chem.*, 161, 419 (1984).
117. P. J. Peerce and A. J. Bard, *J. Electroanal. Chem.*, 108, 121 (1981).
118. I. Rubinstein, *Anal. Chem.*, 56, 1135 (1984).
119. W. R. Heineman, H. J. Wieck and A. M. Yacynych, *Anal. Chem.*, 52, 345 (1980).
120. E. Laviron, *J. Electroanal. Chem.*, 112, 1 (1980).
121. C. P. Andrieux and J. M. Saveant, *J. Electroanal. Chem.*, 111, 377 (1980).
122. P. J. Peerce and A. J. Bard, *J. Electroanal. Chem.*, 114, 89 (1980).
123. C. P. Andrieux, J. M. Dumas-Bouchiat and J. M. Saveant, *J. Electroanal. Chem.*, 131, 1 (1982).
124. F. C. Anson, *J. Phys. Chem.*, 84, 3336 (1980).
125. R. W. Murray, *Philos. Trans. R. Soc. Lon.*, A302, 253 (1981).
126. A. P. Brown and F. C. Anson, *Anal. Chem.*, 49, 1589 (1977).
127. K. Itaya and A. J. Bard, *Anal. Chem.*, 100, 1487 (1978).
128. R. Nowak, F. A. Schultz, M. Umana, H. Abruna and R. W. Murray, *J. Electroanal. Chem.*, 94, 219 (1978).

129. M. S. Wrighton, R. G. Austin, A. B. Bocarsly, J. M. Bolts, O. Haas, K. D. Legg, L. Nadjó and M. C. Plazzotto, J. Electroanal. Chem., 87, 429 (1978).
130. M. R. Van Der Mark and L. L. Miller, J. Am. Chem. Soc., 100, 3223 (1978).
131. J. B. Kerr and L. L. Miller, J. Electroanal. Chem., 101, 263 (1979).
132. A. Merz and A. J. Bard, J. Am. Chem. Soc., 101, 3222 (1978).
133. N. Oyama and F. C. Anson, J. Am. Chem. Soc., 101, 739 (1979).
134. N. Oyama and F. C. Anson, J. Am. Chem. Soc., 101, 3450 (1979).
135. L. L. Miller and M. R. Van Der Mark, J. Am. Chem. Soc., 100, 639 (1978).
136. L. L. Miller and M. R. Van Der Mark, J. Electroanal. Chem., 88, 437 (1978).
137. Y. Ohnuki, H. Matsuda, T. Ohsaka and N. Oyama, J. Electroanal. Chem., 158, 55 (1983).
138. M. C. Pham, J. E. Dubois and P. C. Placaze, J. Electroanal. Chem., 99, 331 (1979).
139. A. Diaz, J. M. Vasque Vallejo and A. M. Duran, IBM J. Res. Dev., 25, 42 (1981).
140. G. B. Street and T. C. Clarke, IBM J. Res. Dev., 25, 51 (1981).
141. G. Wegner, Angew. Chem. Int. Ed., 20, 361 (1981).
142. G. Tourillon and F. Garnier, J. Electroanal. Chem., 135, 173 (1982).
143. P. Daum and R. W. Murray, J. Phys. Chem., 85, 389 (1981).
144. D. R. Rolinson, M. Umana, P. Burgmayer and R. W. Murray, Inorg. Chem., 20, 2996 (1981).
145. C. Degrand and L. L. Miller, J. Electroanal. Chem., 117, 267 (1981).
146. M. Fukui, C. Degrand and L. L. Miller, J. Am. Chem. Soc., 104, 28 (1982).

147. C. Degrand and L. L. Miller, J. Am. Chem. Soc., 102, 5728 (1980).
148. C. Degrand and E. Laviron, J. Electroanal. Chem., 117, 283 (1981).
149. D. C. Bookbinder and M. S. Wrighton, J. Am. Chem. Soc., 102, 5123 (1980).
150. H. D. Abruna and A. J. Bard, J. Am. Chem. Soc., 103, 6898 (1981).
151. W. J. Albery, A. W. Foulds, K. J. Hall and A. R. Hillman, J. Electrochem. Soc., 127, 654 (1980).
152. W. J. Albery, M. J. Eddowes, H. A. O. Hill and A. R. Hillman, J. Am. Chem. Soc., 103, 3904 (1981).
153. A. H. Schroeder, F. B. Kaufman, V. Patel and E. M. Engler, J. Electroanal. Chem., 113, 193 (1980).
154. F. B. Kaufman, A. H. Schroeder, E. M. Engler, S. R. Kramer and J. Q. Chambers, J. Am. Chem. Soc., 102, 483 (1980).
155. R. D. Rocklin and R. W. Murray, J. Phys. Chem., 85, 2104 (1981).
156. A. Bettelheim, R. J. Chan and T. Kuwana, J. Electroanal. Chem., 110, 93 (1980).
157. F. B. Kaufman and E. M. Engler, J. Am. Chem. Soc., 101, 547 (1979).
158. Ref. 40, p. 522.
159. E. Laviron, L. Roullier and C. Degrand, J. Electroanal. Chem., 112, 11 (1980).
160. J. R. Lenhard, Ph.D. Thesis, University of North Carolina, 1979.
161. P. Daum and R. W. Murray, J. Electroanal. Chem., 103, 289 (1979).
162. N. Oyama and F. C. Anson, J. Electrochem. Soc., 127, 640 (1980).
163. M. F. Dautartas and J. F. Evans, J. Electroanal. Chem., 109, 301 (1980).
164. M. Sharp, M. Peterson and K. Edstrom, J. Electroanal. Chem., 95, 123 (1979).
165. C. David, W. Demartean and G. Geuskens, Polymer, 10, 21

- (1969).
166. J. R. Jezorek and H. B. Mark, Jr., *J. Phys. Chem.*, 74, 1627 (1970).
  167. R. C. Cookson, D. A. Cox and J. Hudec, *J. Chem. Soc.*, 4499 (1961).
  168. E. H. Gold and D. Ginsburg, *J. Chem. Soc. (C)*, 15 (1967).
  169. I. Rubinstein and A. J. Bard, *J. Am. Chem. Soc.*, 102, 6642 (1980).
  170. R. J. Nowak, F. A. Schultz, M. Umana, R. Lam and R. W. Murray, *Anal. Chem.*, 52, 315 (1980).
  171. P. Daum, J. J. R. Lenhard, D. Rolinson and R. W. Murray, *J. Am. Chem. Soc.*, 102, 4649 (1980).
  172. J. Facci and R. W. Murray, *J. Phys. Chem.*, 85, 2870 (1981).
  173. P. Denisevich, H. D. Abruna, C. R. Leidner, T. J. Meyer and R. W. Murray, 21, 2153 (1982).
  174. S. Nakahama and R. W. Murray, *J. Electroanal. Chem.*, 158, 303 (1983).
  175. D. A. Buttry and F. C. Anson, *J. Electroanal. Chem.*, 130, 333 (1981).
  176. Ref. 40, p. 129.
  177. H. S. White, J. Leddy and A. J. Bard, *J. Am. Chem. Soc.*, 104, 4811 (1982).
  178. C. R. Martin, I. Rubinstein and A. J. Bard, *J. Am. Chem. Soc.*, 104, 4817 (1982).
  179. J. S. Facci, R. H. Schmehl and R. W. Murray, *J. Am. Chem. Soc.*, 104, 4959 (1982).
  180. W. R. Heineman, F. M. Hawkridge and H. N. Blount in "Electroanalytical Chemistry", Vol. 13, A. J. Bard (Ed.), Marcel Dekker, New York, 1984, p. 1.
  181. B. W. Faughnan, R. S. Crandall and M. A. Lampert, *Appl. Phys. Lett.*, 27, 275 (1975).
  182. S. Gottesfeld and J. D. E. McIntyre, *Appl. Phys. Lett.*, 33, 208 (1978).
  183. J. L. Shay, G. Beni and L. M. Schiavone, *Appl. Phys. Lett.*, 33, 942 (1978).

184. B. Tell and S. Wagner, Appl. Phys. Lett., 33, 837 (1978).
185. M. M. Nicholson and R. V. Galiardi, U.S. NTIS, AD Rep. 1977, AD-A039596; Chem. Abstr., 87, 144073v (1977).
186. J. Bruinink, C. G. A. Kregting and J. J. Pointing, J. Electrochem. Soc., 124, 1854 (1977).
187. W. F. Schumb, C. N. Satterfield and R. L. Wentworth, "Hydrogen Peroxide", Reinhold, New York, 1955.
188. D. M. Considine (Ed.), "Chemical and Process Technology Encyclopedia", McGraw-Hill, New York, 1974.
189. G. S. Calabrese, R. M. Buchanan and M. S. Wrighton, J. Am. Chem. Soc., 104, 5786 (1982).
190. G. S. Calabrese, R. M. Buchanan and M. S. Wrighton, J. Am. Chem. Soc., 105, 5594 (1983).
191. C. Degrand, J. Electroanal. Chem., 169, 259 (1984).
192. D. T. Sawyer and J. L. Roberts, Jr., J. Electroanal. Chem., 12, 90 (1966).
193. T. Ikeda, C. R. Leiner and R. W. Murray, J. Electroanal. Chem., 138, 343 (1982).